



# **ASPECTS OF THE ENGINEERING GEOLOGY OF MAPUTO CITY, MOZAMBIQUE**

**By**

**ENOQUE MENDES VICENTE**

Submitted in fulfilment of the academic requirements for the Doctoral degree (PhD) in  
the

School of Geological Sciences

University of KwaZulu-Natal

Durban

**MARCH 2011**

## ABSTRACT

The geological formations of Maputo City, which are mainly unconsolidated materials with soil like properties, are described in terms of their engineering geological and geotechnical characteristics with relevance to their distribution patterns and spatial trends. Problematic conditions such as collapse potential characteristics, loose aeolian sand dune deposits and loose sand plains characterize many of the materials. The geological characteristics combined with anthropogenic interference such as intensive urbanization with inappropriate land use, construction in sensitive areas like steep sandy slopes has led to many problems including slope stability. Foundation problems with building settlement and gully erosion also occur. The aim of this research was to study the engineering geological characteristics and the geotechnical properties of the geological formations of Maputo City and various related problems. Special relevance has been given to the understanding of three specific problems: building damage, gully erosion and slope instability.

The geological formations are predominantly sandy (coarse to very fine sand) with very low clay content, are non-plastic and are classified as from the group SP-SM which are poorly-graded sand with silt. The majority of the materials are loose and normally consolidated with a high level of residual strength. Assessment of collapse settlement through double consolidation technique indicated soil compressibility and significant sensibility to collapse upon wetting. Truly collapsible soils that show full collapse of the soil structure were identified in 33% of the tested materials where the highest collapse behaviour reached values above 5%, predicted to cause moderate trouble in foundation design. Some of the bonded materials are bonded (evident in 67% of samples tested). Bonding was confirmed by comparing the compressibility of the undisturbed and remoulded samples. The remoulded samples showed a significantly higher compression than that of the bonded materials as part of the stress applied is carried by the bonds themselves, as the bonded material is stiffer than the same without bonds. The curves of the remoulded samples were used to establish the limit between the stable and meta-stable states of the material.

A qualitative evaluation of the erosion susceptibility was investigated by physical tests such as the crumb test, shear strength and chemical indicators while a quantitative evaluation of the erodibility characteristics was obtained using a flume test. Some correlations were found between the results of various methods. Almost all samples that were found to be dispersive with ESP were also dispersive with TDS vs. %Na and SAR. Results of the flume erodibility

test have very little correlation with the chemical properties related to dispersion revealing that the erosion susceptibility and gullying in Maputo City have more relation to the physical processes than to the dispersion related chemical properties of the soils. The positive identification of dispersive and erodible soils can only be carried out using a combination of various techniques. Therefore, a new rating system for erosion susceptibility of sandy soils combining the physical and chemical factors of dispersion is proposed including the flume test, crumb test, TDS/%Na, SAR and ESP. The proposed rating system was applied to the tested soils of Maputo City. Fifteen samples (83% of the rated samples) were classified with intermediate susceptibility to erosion while 3 samples (17%) were classified as having a low susceptibility to erosion. The highest rating scores were obtained by the same samples that showed dispersive behaviour with SAR, ESP and TDS/%Na. This group of samples was of intermediate erodibility in the flume test.

The slope instability mechanisms observed in Maputo City are predominantly rotational failures with a mass of soil sliding along a curved surface of rupture followed by sand flow at the toe as failure occurs in the presence of excess water. Four groups of factors account for the slope instability problems in Maputo City: geomorphological causes, physical and meteorological causes, geological and geotechnical properties of soils, and anthropogenic causes. The mechanism of failure is mostly due to the loss of matric suction of soils in the presence of rainwater and possibly from destruction of bonding agents. Factors of safety values indicate that the slopes are generally unstable with the control being the slope angle.

The slopes in the Polana-Caniço and Ferroviário Quarters show high factor of safety values but is the area most affected by slope instability. Slope failure in these areas is intrinsically caused by anthropogenic factors related to inappropriate land use planning. The gully sidewalls are unstable as the slope created is very steep. The slope at Friedrich Engels Avenue causes most concern due not only to the slope height and angle but also to the size and number of buildings constructed at the crest, mainly high rise buildings along the Julius Nyerere Avenue, the integrity of which could be threatened by a landslide event (this slope has recently been affected by active landslides).

## **PREFACE**

The research work described in this thesis was carried out in the School of Geological Sciences, University of KwaZulu-Natal from April 2004 to December 2009 under the supervision, first of Prof Deneys Schreiner from the School of Civil Engineering, Surveying and Construction and Prof Colin Jermy and in the last year under the supervision Dr Nick Richards.

This thesis represents original work by the author and has not otherwise been submitted in any form for any degree or diploma to any tertiary institution. Where use has been made of the work of others it is duly acknowledged in the text.

Enoque Mendes Vicente

11 March 2011



# **FACULTY OF SCIENCE AND AGRICULTURE**

## **DECLARATION 1 – PLAGIARISM**

I, **ENOQUE MENDES VICENTE**, declare that

1. The research reported in this thesis, except where otherwise indicated, is my original research.
2. This thesis has not been submitted for any degree or examination at any other university.
3. This thesis does not contain other persons' data, pictures, graphs or other information, unless specifically acknowledged as being sourced from other persons.
4. This thesis does not contain other persons' writing, unless specifically acknowledged as being sourced from other researchers. Where other written sources have been quoted, then:
  - a. Their words have been re-written but the general information attributed to them has been referenced
  - b. Where their exact words have been used, then their writing has been placed in italics and inside quotation marks, and referenced.
5. This thesis does not contain text, graphics or tables copied and pasted from the Internet, unless specifically acknowledged, and the source being detailed in the thesis and in the References sections.

Signed

.....

# FACULTY OF SCIENCE AND AGRICULTURE

## DECLARATION 2 – PUBLICATIONS

DETAILS OF CONTRIBUTION TO PUBLICATIONS that form part and/or include research presented in this thesis (include publications in preparation, submitted, *in press* and published and give details of the contributions of each author to the experimental work and writing of each publication)

**Publication 1: Vicente, E. M.;** Jermy, C. A. & Schreiner, H. D. (2006). Urban Geology of Maputo, Mozambique. Proceedings of the International Association of Engineering Geologists Congress. 8. Nottingham, 12 pp.

The candidate was the first author of this conference paper. This paper was a compilation of the research topic sent to the university during the application process for the PhD studies. The co-authors are the first supervisors of this research project. All the data, the field work in Maputo and laboratory testing at University of KwaZulu-Natal was done by the candidate as a part of this research.

**Publication 2: Vicente, E. M.;** Amurane, D. P. & Xerinda, L. (2006). Assessment of slope stability in Maputo City, Mozambique. Proceedings of the International Association of Engineering Geologists Congress. 8. Nottingham, 9 pp.

The candidate was the first author of this conference paper. All the data, the field work in Maputo and laboratory testing at the University of KwaZulu-Natal was done by the candidate as a part of this research. The co-authors were only involved in the field work.

Signed:

# LIST OF CONTENTS

|                                     |     |
|-------------------------------------|-----|
| <i>Abstract</i>                     | ii  |
| <i>Preface</i>                      | iv  |
| <i>Declaration 1 – Plagiarism</i>   | v   |
| <i>Declaration 2 – Publications</i> | vi  |
| <i>List of Figures</i>              | xi  |
| <i>List of Tables</i>               | xiv |
| <i>Acknowledgements</i>             | xvi |

## **CHAPTER ONE 1**

### **1 – INTRODUCTION 1**

|                                     |    |
|-------------------------------------|----|
| 1.1 – Background and Research Topic | 1  |
| 1.2 – Research Objectives           | 4  |
| 1.3 – Hypotheses to Be Tested       | 4  |
| 1.4 – Research Definition           | 6  |
| 1.5 – Future Research               | 11 |

## **CHAPTER TWO 13**

### **2 – LITERATURE REVIEW 13**

|  |    |
|--|----|
| 2.1 – Gully Erosion                              | 13 |
| 2.2 – Buildings Settlement and Collapsible Soils | 15 |
| 2.3 – Slope Instability                          | 17 |

## **CHAPTER THREE 20**

### **3 – RESEARCH METHODOLOGY 20**

|   |    |
|---|----|
| 3.1 – Sampling Methodology                                  | 20 |
| 3.2 – Laboratory Testing Process                            | 22 |
| 3.2.1 – Testing Physical Properties For Soil Classification | 23 |
| 3.2.1.1 – Particle Size Distribution                        | 23 |
| 3.2.1.2 – Consistency Limits (Liquid And Plastic Limits)    | 24 |
| 3.2.1.3 – Moisture Content                                  | 25 |
| 3.2.1.4 – Particle Density And Specific Gravity             | 26 |
| 3.2.1.5 – Organic Matter                                    | 26 |
| 3.2.2 – Determination Of Shear Strength                     | 27 |

|  |           |
|--|-----------|
| 3.2.2.1– Standard Shear Box  | 27        |
| 3.2.3 – Determination Of Consolidation Characteristics                                 | 27        |
| 3.2.3.1– Double Oedometer Test   | 27        |
| 3.2.4 – Determination Of Soil Erosion Susceptibility                                   | 28        |
| 3.2.4.1 – Crumb Test   | 28        |
| 3.2.4.2 – Pinhole Test   | 28        |
| 3.2.4.3 – Flume Test   | 29        |
| 3.2.4.4 – Exchangeable Sodium Percentage (ESP)   | 29        |
| 3.2.4.5 – Cation Exchange Capacity (CEC)   | 30        |
| 3.2.4.6 – Sodium Adsorption Ration (SAR)   | 30        |
| <b>CHAPTER FOUR</b>  | <b>31</b> |
| <b>4 – SITE SPECIFIC INFORMATION</b>   | <b>31</b> |
| 4.1 – Location And General Geographical Background                                     | 31        |
| 4.2 – Climate  | 31        |
| 4.3 – Geology Of Maputo City   | 34        |
| 4.4 – The Maputo Bay And Its Characteristics   | 39        |
| 4.5 - Hydrology  | 41        |
| 4.6 – Geomorphology Of Maputo City And Slope Development                               | 42        |
| 4.7 – Urban Land Use   | 44        |
| 4.8 – Problems Previously Encountered In Maputo City                                   | 47        |
| 4.8.1 – Gully And Coastal Erosion  | 47        |
| 4.8.2 – Building Settlement  | 51        |
| 4.8.3 – Slope Instability  | 54        |
| 4.8.4 – Flooded Areas  | 57        |
| <b>CHAPTER FIVE</b>  | <b>59</b> |
| <b>5 – ENGINEERING GEOLOGICAL CHARACTERISTICS AND GEOTECHNICAL PROPERTIES OF SOILS</b> | <b>59</b> |
| 5.1 – Introduction   | 59        |
| 5.2 – Description of Soil Types  | 61        |
| 5.3 – Physical Properties and Soil Classification                                      | 64        |
| 5.3.1 – Particle Size Distribution   | 64        |
| 5.3.2 – Consistency Limits and Moisture Content  | 68        |

|   |            |
|---|------------|
| 5.3.3 – Particles Density and Specific Gravity                      | 69         |
| 5.3.4 – Organic Matter  | 71         |
| 5.3.5 – Soil Permeability   | 71         |
| 5.3.6 – Soil Classification   | 75         |
| 5.4 – Shear Strength of Soils                                       | 76         |
| 5.4.1 – Introduction  | 76         |
| 5.4.2 – Shear Strength Characteristics                              | 78         |
| 5.5 – Consolidation Characteristics of Soils                        | 83         |
| 5.5.1 – Introduction  | 83         |
| 5.5.2 – Magnitude and Rate of Settlement of Soil of Maputo City     | 83         |
| 5.5.3 – Collapsible Soils Identification by Physical Properties     | 92         |
| 5.5.4 – Collapsible Soils Identification with Double Oedometer      | 96         |
| 5.5.5 – Partial Collapse: Presence and Influence of Bonding         | 100        |
| 5.6 – Collapse Settlement and Buildings Damage                      | 102        |
| 5.7 – Summary and Conclusions                                       | 103        |
| <b>CHAPTER SIX</b>  | <b>108</b> |
| <b>6 – SOIL EROSION SUSCEPTIBILITY</b>                              | <b>108</b> |
| 6.1 – Introduction  | 108        |
| 6.2 – Mechanism of Soil Erosion                                     | 109        |
| 6.3 – Physical Properties and Erosion Susceptibility                | 113        |
| 6.3.1 – Crumb Test  | 113        |
| 6.3.2 – Pinhole Test  | 116        |
| 6.3.3 – Atterberg Limits and Shear Strength                         | 116        |
| 6.3.4 – Flume Tests   | 117        |
| 6.4 – Chemical Determination of Erosion Susceptibility              | 121        |
| 6.4.1 – Exchangeable Sodium Percentage and Cation Exchange Capacity | 123        |
| 6.4.2 – Sodium Adsorption Ratio                                     | 127        |
| 6.4.3 – Total Dissolved Salts and Percentage of Sodium              | 128        |
| 6.4.4 – pH and Electrical Conductivity                              | 131        |
| 6.4.5 – Combination of Chemical Properties                          | 131        |
| 6.5 – Rating System for Sandy Soils                                 | 133        |
| 6.6 – Site Specific Characteristics and Erosion Problems            | 137        |
| 6.6.1 – Topography and Slope Steepness                              | 137        |
| 6.6.2 - Soil Type and Lithologic Controls                           | 139        |

|  |            |
|--|------------|
| 6.6.3 - Rainfall-Runoff Erosivity and Soil Water Conditions  | 139        |
| 6.6.4 - Land Use Pattern   | 139        |
| 6.7 – Summary and Conclusions  | 143        |
| <b>CHAPTER SEVEN</b>   | <b>147</b> |
| <b>7 – SLOPE STABILITY ANALYSIS</b>  | <b>147</b> |
| 7.1 – Introduction   | 147        |
| 7.2 – Mechanism of Slope Failure   | 147        |
| 7.3 – Causes of Slope Failure in Maputo City   | 150        |
| 7.3.1 – Geomorphological Causes  | 150        |
| 7.3.2 – Physical and Meteorological Causes   | 152        |
| 7.3.3 – Geological and Geotechnical Properties of Soils  | 153        |
| 7.3.4 – Anthropogenic Causes   | 154        |
| 7.4 – Slope Stability Analysis and Factor of Safety  | 155        |
| 7.5 – Probabilistic Analysis   | 161        |
| 7.6 – Sensibility Analysis   | 164        |
| 7.7 – Measures for Improving the Stability of the Slopes   | 165        |
| 7.8 – Summary and Conclusions  | 169        |
| <b>CHAPTER EIGHT</b>   | <b>171</b> |
| <b>8 – CONCLUSIONS</b>   | <b>171</b> |
| <b>REFERENCES</b>  | <b>177</b> |
| <b>APPENDIX A: Summary of the Engineering Geological Characteristics and Geotechnical Properties</b> | <b>192</b> |
| <b>APPENDIX B: Raw Chemical Data</b>   | <b>214</b> |
| <b>APPENDIX C: Graphs of Slope Stability Analysis</b>  | <b>216</b> |

## LIST OF FIGURES

|  |    |
|--|----|
| Figure 1.1 – Geographical location of Maputo City, Mozambique  | 2  |
| Figure 3.1 – Map of Maputo City showing sites of sample collection   | 21 |
| Figure 3.2 – Schematic representation of the location of the sampling point on the slopes  | 22 |
| Figure 3.3 – Straight flume apparatus with water circulated by a paddle-wheel and soil sample being tested in the flume apparatus                                | 29 |
| Figure 4.1 – Geographic location of Maputo City with the boundaries of Municipal Districts   | 32 |
| Figure 4.2 – Distribution of rainfall in the last 30 years in Maputo City  | 33 |
| Figure 4.3 – Geological Map of Maputo City   | 35 |
| Figure 4.4 – Google Earth image showing the geographic positioning of the Maputo Bay, the Inhaca Island and some rivers entering the bay                         | 40 |
| Figure 4.5 – Location of the main slopes in Maputo City  | 43 |
| Figure 4.6 – Distribution of urban form characteristics in Maputo City.  | 45 |
| Figure 4.7 – Gullying failure in a built up area of Polana-Canico Quarter in 2000  | 47 |
| Figure 4.8 – Location of gullying failure in Polana-Canico Quarter in 2000   | 48 |
| Figure 4.9 – Gully filled with solid waste with people searching for useful things.  | 49 |
| Figure 4.10 – Extremely large gully in Ferroviário Quarter (left) and remedial work at the beginning of the gully in Ferroviário Quarter (right)                 | 50 |
| Figure 4.11 – Gabion baskets filled with rhyolite used to support the slope at ONU Avenue .  | 50 |
| Figure 4.12 – Signs of coastal erosion in Maputo City  | 51 |
| Figure 4.13 – Measures undertaken to control coastal erosion in Maputo City  | 51 |
| Figure 4.14 – Site location of the problematic buildings covered in this study in Maputo City  | 52 |
| Figure 4.15 – Frontal view of a problematic building at Site 1 (left). Backward (eastern) displacement observed from the top of the building (right)             | 53 |
| Figure 4.16 – Cracks on a single story construction on the north hand side of a building on Site 1 as a result of backward and sideways rotation of the building | 53 |
| Figure 4.17 – Shallow landslide along ONU Avenue with a vertical displacement of 30-40 cm  | 55 |
| Figure 4.18 – Slump in coastal slope deposits marked by Gap of thick vegetation (30 m wide) in the slope along Friedrich Engels Avenue                           | 56 |
| Figure 4.19 – Evidence of movement at the top of the slope along Friedrich Engels Ave.   | 57 |
| Figure 4.20 – Flooded area in Inhagóia Quarter after the 2000 floods   | 58 |
| Figure 5.1 – Geological formations and Sampling sites in Maputo City   | 60 |
| Figure 5.2 – Typical grain-size distribution curves of the soils of Maputo City  | 65 |
| Figure 5.3 – Geographical trend on the distribution of grain size particles in the Ponta Vermelha Formation (TPv)  |    |

|   |     |
|---|-----|
|   | 67  |
| Figure 5.4 – Shear stress-horizontal displacement curve of direct shear tests of Sample 8   | 79  |
| Figure 5.5 – Stress–strain diagram of direct shear tests of the dense sand or bonded soils of Maputo City   | 80  |
| Figure 5.6– Vertical versus horizontal displacement curves for the tested soil of Maputo City   | 80  |
| Figure 5.7 – Shear stress vs. Normal stress for Sample 16 with the indication of the procedure to obtain the friction angle and cohesion  | 81  |
| Figure 5.8 – Typical consolidation voids ratio vs. vertical stress curve of the tested soils in Maputo City   | 84  |
| Figure 5.9 – Casagrande’s method of finding the preconsolidation stress   | 85  |
| Figure 5.10 – Collapsible and non collapsible soil using the Gibb (1962) criterion based on dry density and liquid limit  | 96  |
| Figure 5.11– Double consolidation test of Sample 1 showing full collapse of the soil structure of the saturated soil  | 97  |
| Figure 5.12 – Double consolidation test and adjustments of curves for normally consolidated soils   | 98  |
| Figure 5.13 – Collapse ranges for the collapsible soils of Maputo City  | 99  |
| Figure 5.14– Typical $e/\log \sigma_{v0}'$ curves from the double consolidation test performed on the soils of Maputo City showing the presence of the bonding material in the soil structure | 100 |
| Figure 5.15 – Typical compression curve in a normal scale of an oedometer test of the remoulded soil compared with the curve of a bonded soil occurring in Maputo City                        | 102 |
| Figure 6.1 – Rill erosion in Ferroviário Quarter, Maputo City. The rills preferentially follow the roads and footpaths  | 111 |
| Figure 6.2 – V-shaped gullies occurring in Ferroviário Quarter (left); U-shaped gully crossing the Polana-Caniço Quarter in Maputo City (right)   | 111 |
| Figure 6.3 – Tension crack development at a gully sidewall in Ferroviário Quarter and Soil fall of 1.80 m occurred on a gully sidewall in Polana-Caniço Quarter                               | 113 |
| Figure 6.4 – Surface gradient of Maputo City  | 121 |
| Figure 6.5 – Exchangeable Sodium Percentage of the tested soils of Maputo City  | 124 |
| Figure 6.6 – Correlation of ESP values and sodium adsorption ration (SAR) of the tested soils of Maputo City  | 125 |
| Figure 6.7 – Cation exchange capacity of the tested soils of Maputo City  | 126 |
| Figure 6.8 – Plot of the Maputo City soil samples on the ESP vs. CEC of Gerber & Harmse (1987)  |     |



|  |     |
|--|-----|
| showing the distribution on the different dispersivity classes   | 127 |
| Figure 6.9 – Distribution of SAR values in Maputo City   | 129 |
| Figure 6.10 – Percentage Sodium vs. TDS chart as proposed by Sherard <i>et al.</i> (1976a) for the identification of dispersive soils                          | 130 |
| Figure 6.11 – Strait line relationship between the total dissolved solids and the electrical conductivity of the tested soils of Maputo City                   | 132 |
| Figure 6.12 – Chemical evaluation to identify the dispersive soils (Harmse, 1980)  | 132 |
| Figure 6.13 – Slope gradient of Maputo City  | 138 |
| Figure 6.14 – Groundwater seepage in the Polana-Caniço Quarter gully   | 141 |
| Figure 6.15 – Gully initiating in the discharging point of concentrated water flow from the railway drainage system in Ferroviário Quarter, Maputo City        | 143 |
| Figure 7.1 – Shallow landslide along Nações Unidas Av with a vertical displacement of 30-40 cm. The crack is located only some meters above the ground surface | 149 |
| Figure 7.2 – Distribution of slope angle in Maputo City and the areas with prominent slope instability problems  | 151 |
| Figure 7.3 – Groundwater flow directions in Maputo City  | 152 |
| Figure 7.4 – Slope face exposure as a result of cultivation  | 156 |
| Figure 7.5 – Interaction of the components of Slide 5.0  | 158 |
| Figure 7.6 – Geometry and Factor of Safety calculations of the slopes for Site 10 in relation to the general natural slope angle of the area                   | 161 |
| Figure 7.7 – Geometry and Factor of Safety calculations of the slopes for Site 10 in relation to the slope angle created by the adjacent gullies               | 161 |
| Figure 7.8 – Convergence plot of the probability of failure analysis for Site 2  | 162 |
| Figure 7.9 – Histogram illustration the probability of failure for the slope on Site 9a  | 163 |
| Figure 7.10 – Typical graph of sensitivity analysis in relation to cohesion, friction angle and unit weight in the slopes of Maputo City                       | 164 |
| Figure 7.11 – Lateral view of the Maxaquene Barrier heavily vegetated giving stability to the slope  | 166 |
| Figure 7.12 – Gabion baskets filled with rhyolite constructed at the toe of the slope located at Nações Unidas Avenue  | 166 |
| Figure 7.13 – Surface slope drainage in front of Cardoso Hotel used with relative success as lack of maintenance limits its usefulness                         | 167 |
| Figure 7.14 – Some remedial measures undertaken on the slope of Friedrich Engels (Site 8) showing deficiencies of maintenance                                  | 168 |

## LIST OF TABLES

|   |    |
|---|----|
| Tabela 4.1 – Variation of population by Municipal District in Maputo City in the last 10 years  | 33 |
| Tabela 4.2 – Summary of the geological formations of Maputo City  | 31 |
| Tabela 5.1 – Details of the each sampling site  | 61 |
| Tabela 5.2 – Consistencies of non-cohesive soils  | 62 |
| Tabela 5.3 – Grain size analysis and the textural characteristics of the tested soil in Maputo City   | 65 |
| Tabela 5.4 – Consistency limits and moisture content of the tested soils in Maputo City   | 68 |
| Tabela 5.5 – Bulk density, specific gravity and organic matter content of the tested soils in Maputo City   | 70 |
| Tabela 5.6 – Coefficient of permeability results obtained by three different empirical methods  | 74 |
| Tabela 5.7 – Typical Values of Hydraulic Conductivity, $k$ , for saturated soils  | 74 |
| Tabela 5.8 – Soil classification of Maputo City according to the Unified Soil Classification System (1985)  | 75 |
| Tabela 5.9 – Shear strength characteristics (peak cohesion and friction angle) and plasticity index of the tested soils of Maputo City                            | 78 |
| Tabela 5.10 – Basic parameters obtained from the consolidation curves of the tested samples in Maputo City  | 86 |
| Tabela 5.11 – Typical compression index at various relative densities ( $D_r$ ) for the three types of normally consolidated sandy soils occurring in Maputo City | 87 |
| Tabela 5.12 – Classification of Soil Compressibility  | 88 |
| Tabela 5.13 – Coefficient of Compressibility and Coefficient of Volume Decrease of the tested soils in Maputo City at different loading stages                    | 90 |
| Tabela 5.14 – Coefficient of consolidation of the tested soils of Maputo City at different loading stages   | 92 |
| Tabela 5.15 – Criteria for identification of collapsible soils based on the physical properties   | 94 |
| Tabela 5.16 – Results of collapse identification based on the physical parameters   | 94 |
| Tabela 5.17 – Soils of Maputo City characterized according to their collapse behaviour using the different classification based on the physical parameters        | 95 |

|  |     |
|--|-----|
| Tabela 5.18 – Collapse Potential Values indicating the severity of problem for foundation design   | 99  |
| Table 6.1 – Crumb test, Atterberg Limits and Shear Strength results of the tested soil of Maputo City                                      | 114 |
| Table 6.2 – Guide to interpretation based on the level of reactions during the crumb test  | 115 |
| Table 6.3 – Results of the flume erodibility tested in samples collected in Maputo City  | 118 |
| Table 6.4 – Precipitation values during the 1999-2000 rainy season in Maputo City  | 120 |
| Table 6.5 – Chemical results of the soil samples collected in Maputo City  | 122 |
| Table 6.6 – Cation exchange capacity of different clay minerals  | 125 |
| Table 6.7 – New SAR grading for dispersivity suggested by Walker (1997) and Bell & Walker (2000)   | 128 |
| Table 6.8 – Rating system modified by Bell <i>et al.</i> (1998) and adopted by Bell & Walker (2000)  | 133 |
| Table 6.9 – New rating system for the susceptibility of the sandy soils to erosion   | 135 |
| Table 6.10 – Rating system for the susceptibility of the sandy soils to erosion applied to the soils of Maputo City                        | 136 |
| Table 7.1 – Input data for the determination of Factor of Safety with Slide 5.0 and the Factor of Safety of analysed slopes in Maputo City | 159 |
| Table 7.2 – Statistical data of the analysed slopes of Maputo City   | 162 |

## **ACKNOWLEDGEMENTS**

I would like to thank and acknowledge all people that direct or indirectly made efforts for this research. First I would like to thank my supervisors for their guidance during the 5 years of study. Prof Deneys Schreiner and Prof Colin Jermy for the advice given during conception and research definition and Dr Nick Richards, in the later stage of the research, for the advice given and for reading and making improvements to the thesis.

Many thanks to the academic and technical staff members of the School of Geological Sciences, UKZN for their assistance. Special thanks to the lab technicians Mark Davis at Geology and Mark Holder from the Civil Engineering laboratory for their assistance during laboratory testing. I would like to extend my thanks to my colleagues at Eduardo Mondlane University in Mozambique who assisted me during the field work, samples and data collection namely Mr Dionísio Amurane, Mr. Leonardo Xerinda, Ms Elisabeth Junior, Ms Natércia Macamo and Ms Helena Vaz.

To SIDA/SAREC (Swedish International Development Cooperation Agency) for the generous financial support through the research programme “The Role of Geological Sciences for Sustainable Development in Mozambique” based at the Eduardo Mondlane University in Mozambique.

Finally, I would like to thank my family and friends for their love, support and encouragement throughout my entire research. Special thank to my wife Elisa and to my daughter Jendaye for the patience during my long absence in your lives. Jendaye and Luana, my little ones, this is for you.

# CHAPTER 1

## INTRODUCTION

### 1.1 – BACKGROUND AND RESEARCH TOPIC

Geology has gained importance in the study or application to development and planning of urban centres as well as engineering work. This importance has been recognised repeatedly and is fundamental for the development of urban geology and Geotechnics (Boon Kong & Komoo, 1990; Mulder & Cordani, 1999). Geotechnics is a joint effort of engineering geology and geotechnical engineering which aims at the “*application of scientific methods and engineering principles to the acquisition, interpretation, and use of knowledge of materials of the Earth's crust and earth materials for the solution of practical civil engineering problems*” (Bates & Jackson, 1980). Instead of being largely qualitative, geology became factual, quantitative, and in engineering is applied in the search for more perfect adjustment of man's structures to nature's limitations and for greater safety in public works (Berkey, 1939; Bennett & Doyle, 1997).

Maputo (Figure 1.1), the capital city of Mozambique located in the southern part of the country on the east coast of Africa, has shown rapid development growth in the last 15 years which is observed through many construction projects such as housing development schemes and high-rise buildings spread around the city. These construction projects are a product of the economic development shown by the country during this same period.

Consistent with the size of each project some are preceded by detailed site investigation to characterise and predict ground conditions prior to detailed design and construction and are followed by geotechnical studies. Most of these studies are conducted by the Engineering Laboratory of Mozambique (LEM). While there have been many detailed subsoil investigations conducted in Maputo City, the geotechnical data are not concentrated in one place or readily accessible. Past site investigations are normally a valuable source of information from which lessons are learned, however much of this information is missing.



Most of the projects in Maputo City are developed without any site investigation. Design is based mainly on the builder's experience from past projects and problems arise in construction as a consequence of structural defects. This is linked to planning aspects which are also of great concern in Maputo City which are shown as informal settlements. Like other cities in developing countries, informal settlements in Maputo are being established in areas less suitable for development. These popular, unplanned settlements usually lack sewers, clean water supplies and good road access which are the basic aspects of a modern city. Low safety (construction on unsafe places like on flood-prone low areas, unstable slopes), aesthetics and environmental factors (Solid waste generation, greenbelts to reduce carbon dioxide levels in the area) are common in the suburban area of Maputo City.

The built up area of Maputo City lies on top of a sedimentary sequence of varying thickness and mineralogical composition, mostly of marine, fluvial and aeolian origin (Afonso *et al.*, 1998) grouped into formations of Tertiary and Quaternary age. They are dominated by dunes comprising red silty sand grading into yellow sandstone (Ponta Vermelha Formation), reddish coarse-to-fine grained sands (Malhazine Formation) and white, yellow and orange coarse-to-fine grained sands (Congolote Formation).

The study area is bordered by an extensive slope (20 to 60° angle) which separates the upper part of the town (more than 60 m height) from the downtown area (almost at sea level) in the east and south. Slope instability events occur on this slope which is assumed to be of tectonic origin by the geological map of Maputo of Momade *et al.* (1996).

Furthermore, Maputo City has shown urban and geotechnical related problems which need immediate solution in order to make the city sustainable in terms of physical environmental point of view. Many areas of Maputo City are associated with problematic soils and complex subsoil conditions such as collapsing soils, loose aeolian sand dunes deposits, loose sand plains and clay deposits. The geological characteristics combined with factors such as urbanization (unplanned high population density), construction in sensitive areas such as steep sandy slopes and inappropriate land use planning has led to many problems. Foundation problems with building damage, gully and coastal erosion and slope stability problems are constantly being reported. Maputo City is also usually affected by inundation in flood prone areas and flash floods which are related to the geomorphological setting, geological characteristics of the soils and urbanization with weak drainage systems. Another related problem is the relatively low life span of the roads in the city which can be linked to the road construction itself or to complex

soil and subsoil geological characteristics. All these aspects make this geotechnical and engineering geological study of the various soil types of Maputo City relevant.

This research aims to study the engineering geological characteristics, the geotechnical properties of the soils of Maputo City. Various hypotheses of significance for land use will be tested and the information obtained from this study can be used by planners for practical and comprehensive urban policy and land use planning and management.

## **1.2 – RESEARCH OBJECTIVES**

The objective of this research is to study the engineering geological characteristic and the geotechnical properties of the soils of Maputo City and its related problems. Special relevance will be given to the understanding of three specific problems: building damage, gully erosion and slope instability.

The specific objectives of this research project are:

- 1 – A study of the engineering geological characteristics and the geotechnical properties of the soils of Maputo City;
- 2 – A study of the erosion susceptibility of the soil types and relate it with the soil properties;
- 3 – The analysis of slope stability problems;
- 4 – An investigation of the collapse potential of the soils of Maputo City in order to understand the buildings settlement problems;

## **1.3 – HYPOTHESIS TO BE TESTED**

### **Engineering Geology and Geotechnical Characterization**

Several cases of building damages have been reported in Maputo City (described in Chapter 4, Section 4.8), which is also usually affected by inundation in the flood prone areas and flash floods. Other related problems are slope instability and gully erosion. These problems are probably related to the engineering geology and to the geotechnical characteristics of the soils and this hypothesis will be tested in this research.

In order to depict the geological material in relation to engineering requirements the study of the engineering geological characteristics of earth material will be developed in the city. Taking into consideration the new construction projects and the development of Maputo City, this



research will become more important because it will provide basic information which can be used for detailed geotechnical studies.

### **Gullying Erosion**

Gullying and coastal erosion is a major threat in most Mozambican cities with both economic losses and aesthetic impact. It is believed that the erosion in coastal areas is to a large extent controlled by the type of soils that dominate the area. This assumption will be tested. The dune sand deposits of Maputo are very prone to erosion by surface water which is also combined, in most cases, with anthropogenic influences such weak drainage systems used in urban development. Development in sand dune deposits reduces the percolation area and infiltration as the surfaces are paved. Paving prevents water from infiltrating into the ground, so a greater volume of surface water run off, increasing the risk of erosion (Coch, 1995). Other common human interference in Mozambican cities is the cultivation of slopes and removal of vegetation for fire wood.

Apart from the qualitative aspects, this research will also look at the quantitative features of erosion which are less investigated in Mozambique and relate to the type of soils that occur in Maputo City.

### **Building Damage**

Building settlement is another common problem occurring in Maputo City which results in tilting due to differential settlement. The affected buildings are generally the ones with 8-10 floors (25-40 m high), tilting 150 to 400 mm sideward when measured at the top. These buildings are located along the Julius Nyerere Avenue at the stretch of road closest to the coastal slope located on its eastern side (Section 4.8). At this point the slope has the greatest height. Common to the affected buildings is water leakage from water pipes or underground reservoirs.

Building damage can be linked to the interaction of geological processes that may have caused tilting. This research will test the hypothesis of building settlement be linked to geotechnical characteristics of the soils. The geological processes that might cause the observed damage will be investigated with special reference to collapse settlement of the soils structure. Water leakage creates different wetting conditions in the affected area allowing soil collapsing to occur causing settlement in the wet area. Because the wetting conditions are different in each area, differential settlement occurs causing the buildings to lean.

## **Slope Instability**

Landslides and slope instability problems have been identified in the south and east margins of Maputo City. They are associated with abandoned coastal slopes and to anthropogenic causes. In this research the causes of the problem and stability analyses will be investigated. The possible causes of landslides in many of the coastal Mozambican cities are:

- geological characteristics of the material;
- runoff at the top of the slopes and infiltration in extreme rainfall events altering the groundwater conditions;
- geometry of the slope (slope height, slope angle);
- inappropriate drainage systems in urbanised areas;
- loading of slopes (construction of buildings at or near the top of a slope)
- cultivation of slopes and vegetation removal.

### **1.4 – RESEARCH DEFINITION**

Soil is a natural aggregation of mineral grains disposed in layers (soil horizons) of variable thicknesses, and differs from the parent materials in their physical, chemical, morphological, and mineralogical characteristics. These mineral particles are the weathering products of rocks that have been altered by mechanical, chemical or chemical-biological and environmental processes including erosion (Birkeland, 1999; Spigolon, 2001).

The term “soil” in this research refers to the geological formations which are mainly unconsolidated materials. The nature of the geological formations which are unconsolidated sediments gives them soil-like properties and therefore defined in terms of soil properties and characteristics. The geological formations will be treated as soils throughout the document. The investigated material and sampled for the various laboratorial tests was the one that gave enough stiffness to obtain undisturbed samples.

The soil characteristics are associated with the main engineering geological and geotechnical problems common in Maputo City, namely gully erosion, collapse settlement and building damage, slope instability and flood prone areas. The magnitude of these problems is linked to other specific factors which are discussed in detail in the appropriate chapters. This research tries to understand these problems and relates them to the geological and geotechnical characteristics of the soils and to the common land use practices in the city.

Erosion is the most prominent problem due to the dimension of the affected area and the threat

to the sustainability of the affected residential areas. Soil erosion is the process of detachment and movement of solids, including soil, sediment, rock and other particles, in the environment by the action of flowing water, wind or ice and by mass movement of soil downslope under the influence of gravity (Coch, 1995; McGraw-Hill, 2003; Mayhew, 2004; Quartel *et al.*, 2007). It is shown as rills and gullies caused by surface water flow along the slopes and in the form of coastal erosion caused by the sea waves. An erodibility study quantifies the erosion susceptibility of the soils and determines its relationship with the topographic and geomorphological characteristics of the area and the historical land use practices (anthropogenic interference). Because dispersivity was suspected to occur in the soils of the study area, dispersion related tests were also carried out. In this study, soil dispersivity is assumed as an index of the likelihood of initiation of erosion. Dispersive soils are those in which the fine clay component goes into suspension in non-flowing water (Elges, 1985).

Physical and chemical properties of soils were determined to identify which have influence on the weakness of the soils controlling rill and gully erosion in the study area. The selected specialized analytical methods to study the soil erodibility are similar to those used by Gerber & Harmse (1987), Walker (1997), Bell & Walker (2000) and Rienks *et al.* (2000). Standard tests for soil classification were determined, namely liquid limit by cone penetrometer, particle size distribution by sieving and laser particle sizing, moisture content by oven drying method, linear shrinkage, and particle density by density bottles.

Soil properties affecting erodibility are sodium adsorption ratio (SAR), cation exchange capacity (CEC), and electrical conductivity (EC) determined from an extract of saturated soil paste and exchangeable sodium percentage (ESP) from exchangeable cations. The influence of these properties on soil erodibility is investigated. The sodium adsorption ratio (SAR) of the soil quantifies the role of sodium dispersion with respect to other free salts in the pore water. Gerber & Harmse (1987) established reference values for evaluating soil erodibility according to this chemical parameter. The cation exchange capacity (CEC) is due to the type and nature of clay minerals present. Clay minerals that tend to be associated with erodibility are smectites and other 2:1 phyllosilicates which are naturally swelling clays. The CEC of these minerals is in the range of 40 to 150 meq/100g clay. These minerals have also influence in the liquid and plastic limits of the soils because of their different reactivity. If these minerals are present in the clay fraction then the soils is likely to be erodible as CEC values greater than 40 meq/100g clay have good shrink-swell potential. Cycles of natural shrink-swell are able of loosening compacted soil horizons.

However, the CEC alone cannot be used to identify erodibility as other factors, such as high organic content, may contribute to high CEC values (Bell & Walker, 2000). Soil erodibility is also related to the chemical composition of the clay fraction. Erodibility correlates strongly with the dispersion potential classification, which is based on the cation exchange capacity (CEC) and exchangeable sodium percentage (ESP) (Bell & Walker, 2000). A threshold value of ESP of 10 % has been recommended by Harmse (1980), above which soils that have their free salts leached by seepage of relatively pure water are prone to erodibility (Gerber & Harmse, 1987). Soils with ESP above 15% are highly erodible. The results of this test are interpreted according to the proposal of Harmse (1980).

The pinhole test is widely considered to be one of the most reliable physical tests to determine erodibility because it simulates the action of water draining through a pipe in soil (Head, 1988). The test procedure is based on extensive trials and observational experience and the results are evaluated from the appearance of the collected water, the flow rate, and the final size of the hole in the specimen (Sherard *et al.*, 1976a). Pinhole test was designed for clay soils but although the study area is dominated by sandy soils, it was tested in this research to assess its workability for this type of soils. Due to the soil characteristics it did not work well. The Crumb test is one of the erodibility tests performed, which provides a very simple means of identifying dispersive soils and erodibility without requiring special equipment. The results depend on observations in accordance with the guide to interpretation which is based on the level of reactions occurred (Head, 1988). The Flume test was developed to assess the influence of flowing water on the gullies and determine the soil erodibility. The procedure followed by Rienks *et al.* (2000) was also adopted in this research. Undisturbed samples were positioned *in a flume* with horizontal water circulation by a paddle-wheel. Constant water depth was kept over every sample and the water speed was controlled during the 10 minutes of test (Rienks *et al.*, 2000). The amount of sediments eroded was then correlated to the area of the sample placed in the flume. The interpretation of the test results depends on the site specific situation that leads to erosion. In most cases of gully erosion it is not necessarily the susceptibility of the *in situ* soil but the runoff conditions created upslope that initiated erosion. Hydraulic erodibility of natural and engineered earth materials were evaluated in terms of a rational correlation between the rate of energy dissipation of flowing water (flow shear stress) and an “erodibility classification” of the soils (Annandale, 1995; Poesen *et al.*, 2003). The critical flow shear strength to initiate detachment of particles was calculated after transferring part of the laboratory conditions to the real environment using the surface gradient of Maputo City.

Differential settlement affecting buildings is another common problem in Maputo City. The affected buildings are those with 8-10 floors (25-40 m high), and tilting 150 to 400 mm when measured at the top. Common to all the affected buildings is water leakage from water pipes or underground reservoirs. This research finds out if buildings settlement is linked to unexpected geotechnical characteristics of the soils during foundation design or to construction faults. Buildings damage can be linked to the interaction of geological processes that may have caused tilting. The hypothesis to be tested in this topic is related to the geological processes that might cause the observed damage with special reference to collapse settlement of the soils structure.

The hypothesis of collapse settlement is investigated through the results of the following laboratory tests: specific gravity, dry density and void ratio, particle size analysis, permeability, double oedometer test and standard shear box test. Collapsible soils frequently show low dry density (GSEG, 1990 in the range of 900 to 1600 kg/m<sup>3</sup>). It is important to recognise that low dry density soil does not mean tendency to collapse or, vice versa, once many stable soils have very low dry densities (Jennings and Knight, 1957). The particle size distribution assists in identifying collapsible soils because problems with collapse are generally linked to silty or sandy soils with low clay content. In this case is also important not to assume all high clay content soils do not experience collapse. The double oedometer test is the widely used approach to determine the potential collapse settlement. Two similar undisturbed samples were tested in the consolidometer, one at natural moisture content and the other saturated. Correct interpretation of the test curves of normally consolidated and over-consolidated soils is important in order to predict the consolidation at natural moisture content and collapse settlement using normal consolidation theory (Schwartz, 1985).

The standard shear box test was developed to determine cohesion of particles ( $C_u$ ) and the angle of shear resistance ( $\phi$ ). It also provides the most direct means of relating  $\phi$  to the void ratio,  $e$ . The results of a shear strength test in a shear box were plotted graphically, and values of cohesion and angle of shear resistance were obtained directly from the strength envelopes (shear stress vs. Normal stress). The collapsibility of soils depends on several factors strongly affecting each other and it has been observed that soils which are susceptible to collapse are well-sorted, porous with relatively low cohesion (Rizkallah & Keese, 1989).

The shape of the shear stress/horizontal displacement and shear stress/normal stress curves given by the shear box test and logarithm of pressure/void ratio curve given by the double oedometer test were the basis for the interpretation of the collapse behaviour of the soils. The shape of the above curves can be influenced by the bonding between particles or by cementing.

The possible influence of these two factors was carefully analysed. Thus, the framework suggested by Vaughan *et al.* (1988) to use an engineering classification system based on initial void ratio to identify collapsible soils was followed. Such classification is based on the relationship between the *in situ* voids ratio and the boundary between the stable and meta-stable states for the soil given by the oedometer test of bonded and remoulded soil respectively.

A triaxial test was planned to be carried out under isotropic conditions and to be used as a subsidiary test to confirm that collapse is an intrinsic property of the soil if oedometer test indicate that the soil collapses on wetting. The loose character of the sandy soils of the study area made this test impossible to be carried out in most of the samples and the results of the few samples were not taken into account for this research.

Maputo City is divided in two distinct topographic areas: down town and upper town. Much of the city is on an elevated region above a slope formed as a consequence of tectonic activity (faulting) and a small part is on the lower level near the beach in the east and near the Maputo Estuary in the south. The difference in height between the two areas varies from 20 to 60 m. The overall slope angle is between 20 and 40°, but it can locally reach 60° or more. Parts of these slopes are unstable. A full slope stability study is undertaken in this research to test the hypothesis regarding the causes of the problem and the stability analysis. A systematic study of slope stability is developed involving (i) identification and description of the instable places, (ii) evaluation of the probability of occurrence of landslides, and (iii) assessment of the risk associated to them in order to recommend effective preventive measures (Anbalagan & Singh, 1996).

The present research is conducted on deposits composed of dune sands under partially saturated conditions presenting high shear strength when dry (appears cemented and stable) and low when saturated. Under partially saturated conditions a wide range of soil properties depend on the amount of water retained in the pore space, e.g., increased tensile strength of partially saturated granular materials, such as sand, compared to their saturated state (Lechman *et al.*, 2006). Thus, this study also tests the effect of loss of apparent cohesion (loss of matric suction) caused by rainwater infiltration on the stability of partly saturated slopes using the procedure recommended by Rao (1996).

The laboratory tests carried out for the slope stability analysis are dry density, standard shear box, moisture content and particle size distribution. Permeability information is generated from the other soil parameters and correlations as explained in Chapter 5. The soil density is an important property having many applications in soil engineering. Knowledge of the

permeability characteristics of soil was required because the use of a flow net analysis together with permeability data enables the modelling of the factor of safety under different groundwater conditions. In the analysis of slope stability, the weight of a slope provides the main force which is obtained from the soil density. Slope stability is also related to particle size distribution. Each soil material has its own equilibrium characteristics, which are related to particle size distribution which is in turn related to characteristics such as slope angle, types of failure and speed of failure. Therefore, this parameter controls the type of stability analysis. Many stability problems in soils are related to limiting conditions in which the mechanism of failure involves the sliding of a body of soil relative to the main soil mass. For slope stability analysis the shear box test was used for the determination of shear strength parameters cohesion and friction angle. From the results of geotechnical tests the present factor of safety was calculated, to give a more accurate assessment of the present hazard and to assist on the design of mitigation and remedial measures. Widely used computer software, Slide 5.0, was used in these calculations to simulate (model) the factor of safety in extreme water flowing and ground water conditions. The model allows also consideration of building loads (not used in this research) and is complimented by limit-equilibrium analysis. Recommendations for stabilization are made after the factor of safety calculations.

## **1.5 – FUTURE RESEARCH**

The results obtained in this research open space for the development of other topics, not only to complement but also to make a step further. Following are some of the recommended future research:

1. Investigate the hypothesis regarding internal erosion as a causal mechanism of building damage. It may be investigated by drilling and comparing the geotechnical properties of boreholes at the site of the problem and away (landward) of the problem where internal erosion is not expected to have taken place.
2. Find the original design plans of the problematic buildings so that they can be analysed and compared with those of adjacent buildings of greater height to see if there is a factor that explains why these buildings have failed and others have not. The problematic buildings are situated close to each other and have suffered very similar damage what implies a causal factor that is common to all (Forster, 2001). Since they are all similar in age, dimensions and design, it may be worth considering a common flaw in their design or construction. It is possible that taller buildings are founded at a greater depth, thus avoiding the problem (Forster, 2001).

3. To complement the erosion component of this research a coastal erosion study has to be done. The coastline around Maputo City is dynamic due to shifting of sand or its removal from a low-lying beach by longshore currents. It has moved tens of meters inland in the last two decades and shows clear signs of coastal erosion. Qualitative and quantitative analysis of coastal erosion has to be done through different methodologies. A study of the pattern of water currents in the Maputo Bay and the causes of the problems can be undertaken. Change detection represents the morphological changes coupled to periods of accretion or erosion, and thus provides a qualitative description. GIS and remote sensing based methodologies are presently used for change detection providing a qualitative description of beach erosion and instability. Satellite remote sensing data at different spatial, spectral, and temporal resolutions are presently an effective tool to monitoring coastal change and measuring erosion.
4. Many areas of Maputo City are prone to flooding. The causes of flooding in these areas are mainly of geological and topographic nature but associated to land use practices. The geological profile of these areas can be interpreted in comparison with the identification tests undertaken in the soil samples collected in the area and recommendations on the best measures to solve the problem drawn.
5. As most of the investigated problems are somehow geological hazards, vulnerability and risk analysis related to the natural disasters affecting this coastal city has to be investigated. Knowledge of the problems related to the main geohazards in the city (gullyng and coastal erosion, landslides, slope stability, groundwater pollution, sea level rise and salt water intrusion) can be well understood in order to define their solutions. Natural Hazards and Risk Maps with reference to these problems can be produced to serve as part of the vulnerability assessment and Natural Hazard Profiling of the city required for the planning process and the development of short and long-term local strategies for natural hazards management.



## **CHAPTER 2**

### **LITERATURE REVIEW**

The main engineering geological problems identified in Maputo City, namely gully erosion, soil collapse settlement and buildings damage, slope instability and flood prone areas, have received limited attention by researchers and little or nothing has been done to find a solution to them. Nevertheless, a number of corrective measures are taken, often without a scientific assessment of the problems. However, studies on similar problems have been undertaken in the Southern Africa region and in other parts of the world. The methodology and main findings of these different studies are revised in this chapter.

#### **2.1 – GULLY EROSION**

Soil erosion is the process of displacement and movement of solids, including soil, sediment, rock and other particles, in the environment by the action of flowing water, wind or ice and by mass movement of soil downslope under the influence of gravity (Coch, 1995; McGraw-Hill, 2003; Mayhew, 2004; Quartel *et al.*, 2007).

Although soil erosion is a naturally occurring and a normal geologic process associated with the hydrologic cycle, in many places it has been accelerated by human activities and poor land use planning, becoming much faster than under natural conditions (French, 1997; Thorpe, 2002). Poor land use practices include uncontrolled urbanization, poorly managed construction activity, road or trail building, destruction of natural vegetation, overgrazing or changes of the natural drainage system.

Geological erosion is a natural process resulting from the action of water flow, wind, ice and the influence of gravity which weaken the geological material creating conditions for weathering soil formation (Coch, 1995; McGraw-Hill, 2003, Quartel *et al.*, 2007). It occurs where soil is in its natural environment surrounded by natural vegetation. Natural erosion is a relatively slow

process, excluding some stream bank and shoreline erosion, and occurs continuously by thin surface sheet flow (Watson & Laflen, 1986; Bradford *et al.*, 1987; Kinnell, 2005; Assouline & Ben-Hur, 2006). Accelerated erosion is the increasing of the rate of erosion which occurs when the anthropogenic activity interferes with the natural process, for example, destruction of the protective natural vegetation or the natural drainage system (Plummer, *et al.*, 2007). Accelerated erosion is behind environmental problems, such as sedimentation in water leading to reduction of the dimension of water bodies, ecosystem damage and arable soil loss (Colosio *et al.*, 2007).

The velocity of water erosion is controlled by several factors, including the rainfall pattern in the region, the soil fabric, land use pattern, the terrain morphology, type density of vegetative cover and surface erosion. These factors are interrelated but it is expected that high-intensity and long lasting rainfall event, steep slopes, sandy soils, bare soils and inappropriate land use practices be the most erosive (Coch, 1995; Schmittner and Giresse, 1999).

Four types of water erosion can be found according to Plummer *et al.* (2007) and Duiker (2009): Interrill erosion, Rill erosion, Gully erosion and Streambank erosion.

1. *Sheet or interrill erosion* is the result of heavy rain on bare soil where water flows as a sheet down any gradient, removing soil particles in uniform layer. The primary mechanism for detachment of soil particles from the surface in this type of erosion is by the impact of raindrops on the soil surface. It results in loss of the most productive part of the soil profile and reduced plant growth. Deposition of eroded material frequently causes damage.
2. *Rill erosion* is the removal of soil by ephemeral concentrated water flow in closely-spaced small rivulets, streamlets or headcuts (Øygarden, 2003) which work as both source of sediment and sediment delivery systems for erosion. Rills are active where precipitation rates exceed soil infiltration rates and runoff begins to form small concentrated channels becoming faster-flowing channels of few centimeters or less (Øygarden, 2003; Watson & Evans, 1991).
3. *Gully erosion* occurs when concentrated flows of water scouring along flow routes cause sharp sided entrenched channels deeper than 30 cm (Carey, 2006). Channels come together into larger channels, increasing water velocity and volume resulting in land that is physically dissected, limiting its access. Excess draining and drying of depressions occur together with damage to roads and other public utilities.

4. Streambank erosion is a natural process, and occurs “particularly during peak storm flows and is part of an on-going cycle of sediment erosion and deposition within the stream system” (Ziebell, 1999; EB, 2009). Streambank erosion occurs when increased runoff from catchments places significant erosive stress on streams and when vegetation is removed from the stream-side. This vegetation removal can lead to extensive erosion when soils do not have enough strength to resist water erosion.

Rienks *et al.* (2000) investigated gully erosion in northern KwaZulu-Natal, South Africa. They concentrated on “*the physical and chemical properties of sediments exposed in a gully*” terrain and relate them to erodibility. The study was conducted on colluvial sediments and associated paleosols. Samples from this material were analysed and the properties controlling gully erosion were identified. Dispersion potential was identified through the dispersivity and erodibility tests, but the different dispersion tests showed poor correlation with Crumb Test and double pipette method but significant correlation with silt content (Rienks *et al.*, 2000). The flume test was well correlated with electrical conductivity and sodium adsorption ration (SAR), exchangeable sodium percentage (ESP) and Cation Exchange Capacity (CEC) values.

Bell & Walker (2000) also studied the erosion of dispersive soils of Natal, South Africa and found that the dispersive erosion is controlled by the clay chemistry and by the total dissolved salts (TDS) in the eroding water as well as the presence of exchangeable sodium on clay mineral surfaces. Bell & Walker (2000) also developed a rating system to aid the identification of dispersive soils. The parameters included in the rating system were selected through a discriminant analysis.

## **2.2 – BUILDINGS SETTLEMENT AND COLLAPSIBLE SOILS**

Buildings settlement in Maputo City is linked to water leakage from water pipes or underground reservoirs below the buildings foundations, indicating that water is the triggering factor. Collapse settlement is suspected to occur in the area of the affected buildings.

A collapsible soil may be defined as a soil which can withstand relatively large imposed stresses with small settlement at low *in situ* moisture contents but will exhibit a decrease in volume and associated settlement (which could be of large magnitude), with no increase in the applied stress, if wetting up occurs. The change in volume is associated with a change in soil structure (collapse of soil structure) (Schwartz, 1985; Jennings & Knight, 1957; GSEG, 1990). The collapse settlement may reach as high as twelve percent on the original thickness (El-Ruwaih & Touma, 1986). The collapsibility of soils depends on several factors strongly affecting each

other. A major effect is the internal fabric. It has been observed that soils which are susceptible to collapse are well-sorted, fine-grained clastic sediments as well as porous soils with relatively low cohesion (Rizkallah & Keese, 1989). These soils have high void ratio, stiff to very hard *in situ* consistencies while their natural densities are low.

The soil collapse potential is evaluated by methods that are primarily of qualitative nature or depend on idealized soil conditions. The following are the main approaches used in assessing the soil collapse potential according to El-Ruwaih & Touma (1986): (a) Approach based on the principle of effective stress. This approach depends on the application of the well known traditional effective stress concept to partially saturated soils. The main concern in this approach is on the prediction of the behaviour of partly saturated soils with changes in moisture content without considering the collapse of soil structure upon wetting. For that reason, the principle of effective stresses cannot be used for prediction of the soil collapse potential; (b) Approach based on physical properties. The approach based on physical properties uses qualitative methods to evaluate the soil collapse potential. Soil properties such as the Atterberg limits and plasticity index, grain size characteristics, voids ratio, natural moisture content and the degree of saturation are used on this approach. The disadvantage of this approach is in the fact that it does not take into account the influence of loading, types of minerals present in the soil or the nature of the soil structure and bonding between particles; (c) Approach based on oedometer tests. The approach based on oedometer test on natural soil samples provides not only qualitative prediction of the possibilities of collapse, but also quantitative information to allow estimates of the magnitude and rate of soil collapse. The well established methods developed on this basis are from Denisov (1951) and Jennings & Knight (1957). The Jennings & Knight (1957) method also called “double consolidometer” technique evaluates the effect of both saturation and loading at various levels. It involves performing two oedometer tests concurrently on identical undisturbed soil samples. The first oedometer test is performed on a sample at its natural moisture content and the second with water in the cell saturating the sample. Jennings and Knight (1957) suggest a geometrical method to superimpose the consolidation curves from both tests to evaluate the effect of saturation.

Jennings and Knight (1957) applied their theory to study the additional settlement of foundations due to collapse of sandy soils on wetting. Further studies on collapse settlement potential were undertaken in many places. Ferreira & Teixeira (1989) published the results of an investigation on collapsible soils in Pernambuco, Brazil where research on a practical case in construction was conducted. The behaviour of the collapse through laboratory and field tests was investigated. Single oedometer tests were carried out in soils moulded with dry apparent

specific gravity of 15, 17 and 19 KN/m<sup>3</sup> and humidity of 0, 1.5, 3 and 6 %. The pressures were applied in stages and the inundation was carried out when they reached 20, 40, 80, 160 and 320 kPa. Double oedometer tests were also performed but there is no indication of the procedure followed. They found that the majority of the samples moulded in the laboratory, under conditions similar to those in the field, presented collapse potential values smaller than those in the undisturbed samples. The difference was assumed to be mainly related to the differentiated form of the arrangement of the particles in each sample. A reduction in the collapse potential with increasing humidity and dry apparent specific gravity was observed.

Vaughan *et al.* (1988) proposed an alternative way for indexing the engineering properties of residual soils, which are normally weakly bonded and may have widely varying void ratios and a collapsible behaviour. They tested artificial material in the laboratory and found that their engineering behaviour depends on the bond strength and on the voids ratio of the soil. This makes the bonding together of the soil particles the dominant feature of residual soils (Vaughan *et al.*, 1988) and is used to describe the component of strength and stiffness occurring in addition to that due to the natural properties of the soil particles and their packing (Maccarini, 1987; Vaughan *et al.*, 1988; Maccarini *et al.*, 1989). Because bond strength is difficult to determine experimentally than initial void ratio, Vaughan *et al.* (1988) suggest that an engineering classification system based on initial void ratio is practical. The framework suggests that such a engineering classification, based on the relationship between the *in situ* voids ratio and the boundary between the stable and meta-stable states for the soil (given by the oedometer test of bonded and remoulded soil respectively) has shown to be practical (Maccarini *et al.*, 1989).

### 2.3 – SLOPE INSTABILITY

Slope instability problems in Maputo City were first observed in early 1990's and are associated with tropical storms and heavy rainfall. In fact, rainfall has been considered the cause of the “majority of slope failures and landslides that happened in regions experiencing high seasonal rainfalls” (Huat *et al.*, 2005; Li *et al.*, 2005) because most of them are registered following long-lasting or antecedent heavy rainfall.

The incidence and severity of landslides and slope instability problems was raised particularly in recent years as an increased lack of land has forced rapid urban development in hilly terrain (inherently unstable areas) above the neutral line of slides (construction of buildings at or near the top of a slope). In 2000, severe rainstorms in Maputo City triggered ground movements and slope instability on the sandy slopes causing damage to buildings. The loss of stability and

shallow and deep slides is attributed to the groundwater rising which reduced the effective stress and shear strength along the potential slip surface (Lumb, 1975; Wolle, 1985; Rouse, 1990; Mshana *et al.*, 1993; Rao, 1996). Water infiltration into the ground is associated to matric suction (negative pore-water pressure).

Matric suction is a pore-water pressure developed by the soil material that induces water to flow in unsaturated soil. This pore-water pressure is negative and is a consequence of the shared effect of adsorption and capillarity caused by the soil matrix. The higher matric suction is observed in a dry soil while the lower matric suction occurs on a wet soil. This negative pore-water pressure (or matric suction) plays a critical role in the stability of unsaturated soil slopes (Fredlund & Rahardjo 1993; Au, 1998). Saturation of the soil slopes starts to occur when the rainfall infiltrates into the slopes resulting on partial or complete disappearance of the matric suction at shallow depths (Li *et al.*, 2005), consequently, a slope failure may occur (Li *et al.*, 2005). The failure mechanism is associated to the loss of soil matric suction in the presence of rainwater and possibly from destruction of the bonding agents. The effect of water infiltration on soil suction is likely to be influenced by the soil porosity and permeability, the surface cover, the soil type and angle of the soil slopes (Huat *et al.*, 2005). Head loading (construction of buildings at or near the top of a slope) can also contribute to failure.

Although it has been recognized that negative pore-water pressure plays a crucial role in the instability of unsaturated soil slopes, its effect is often ignored in slope stability studies. The negative pore-water pressure is assumed to dissipate with rainfall infiltration, therefore it has been taken out in design considerations (Zhang *et al.*, 2004). However, soil suction can be maintained under certain conditions. A study by Zhang *et al.* (2000) “based on the theory of infiltration and seepage through a saturated–unsaturated soil system”, showed that under stable conditions, the maintenance of matric suction is mostly influenced by the extent of rainfall flux through the coefficient of permeability of soil (expressed as a percentage). The high soil permeability in the slopes in Maputo City allows quick dissipation of matric suction and these conditions are not likely to occur.

The shallow surface failure shown by slopes occurs in soils with high permeability and is probably controlled by its sandy composition. The shallow failures likely occur in slopes comprising sandy and gravelly soils, in contrast to those composed of clays and silts (Lee *et al.*, 1983). The soil grain size has been used to evaluate surficial stability which has normally a bias in relation to cohesion. With rainfall and water infiltration, the groundwater table rises and a decrease in the matric suction of the slope soils is observed. The topsoil becomes saturated

creating conditions for high pore water pressure and reduction of the soil shear strength (Abramson *et al.*, 2002; Eberhardt, 2003). The high soil weight and the low shear strength trigger failure and rainfall-induced landslide (Li *et al.*, 2005).

Additional factors can also be behind the slope failures in Maputo City, namely the existence of paved surfaces with a weak drainage system allowing water to flow uncontrolled to the slope, and loading of slopes (construction of buildings at or near the top of a slope).

## **CHAPTER 3**

### **RESEARCH METHODOLOGY**

#### **3.1 – SAMPLING METHODOLOGY**

The techniques by which the soil samples are obtained for laboratory testing vary greatly in the extent to which they disturb the natural fabric of the soil. For this research 21 test pits were excavated by hand to collect disturbed and undisturbed samples from horizons representative of the soils types at the site (Figure 3.1). The undisturbed samples were used to determine the undisturbed soil fabric, the behaviour of the soil fabric under stress and the compaction of soil. The disturbed samples were collected for the determination of the properties of disturbed soil and for soil classification.

Taking into account the marked increase in density with depth to at least 20 m on the geological formations in Maputo City, the test pits in the slopes were excavated at the middle of the face of slopes (Figure 3.2). The other sampling points were defined in order to have best distribution throughout the geological formations. The depth of sampling varied from 0.9 to 2.4 m measured from the ground level on the sampling point. It was decided according to the stiffness of the soil, being sampled when the soil was stiff enough to obtain undisturbed sample. The soils under investigation behave as “cohesive soils” during sampling due to the moisture and the bonding between particles. It was not possible to collect undisturbed samples at two of the sites due to the high content of gravelly material.

The block sampling from exposures in test pits is a method to obtain the highest quality intact samples (GSEG, 1990; Schwartz, 1985). Block samples were collected using a sampler with the dimensions 230x230x200 mm made from galvanized steel sheet, 1 mm thick to avoid bending when driven into the soil. The sampler had small holes in its top to avoid air trapping in the container. Sampling was decided according to the stiffness of the soil, being sampled when the soil was stiff enough to obtain undisturbed sample. The sampler was driven into the



bottom of the pit by hands and the surrounding soil was then cut away with a shovel. The samples were then immediately sealed against moisture loss with 15 mm paraffin wax, as recommended by Brink *et al.* (1982).

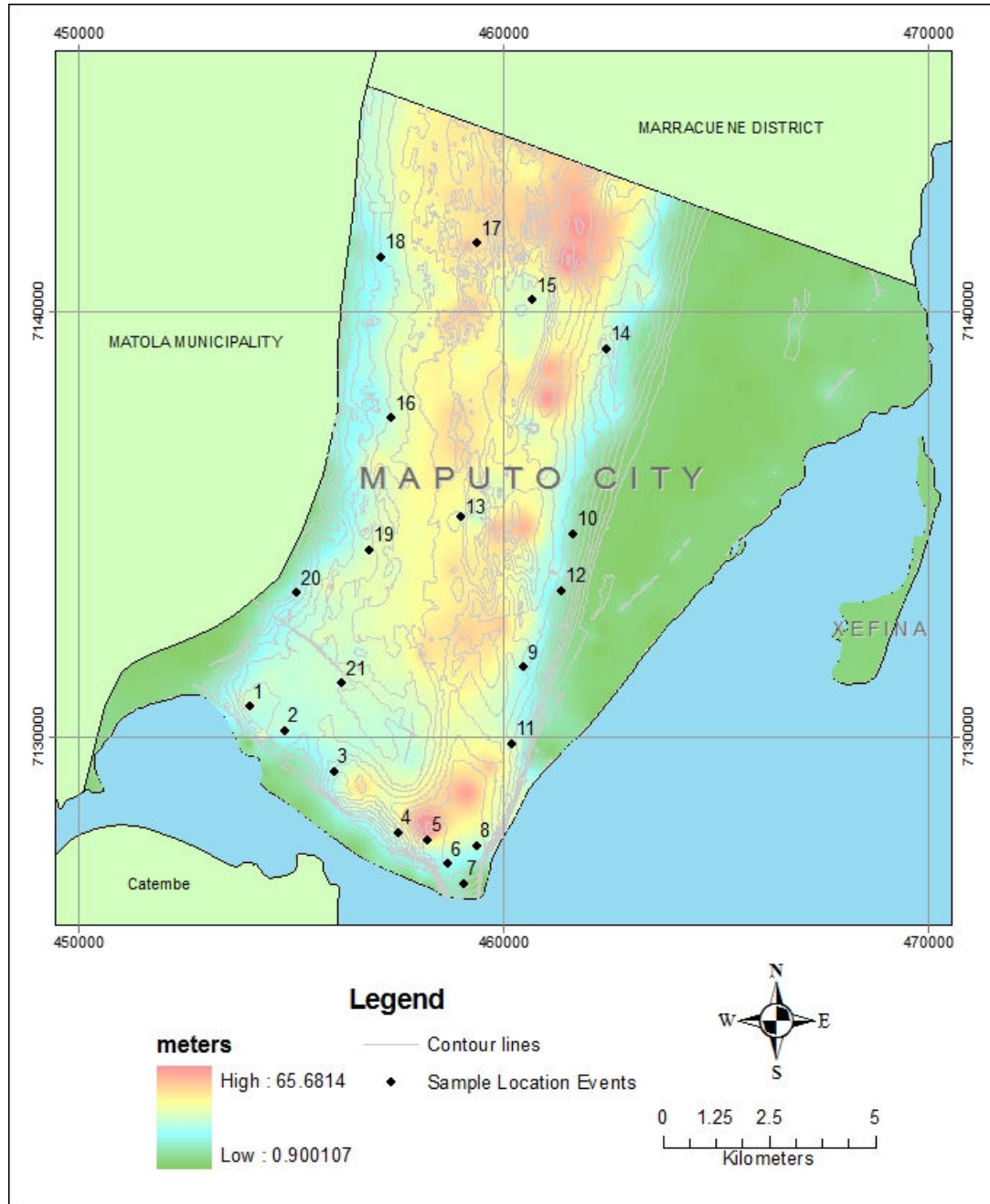


**Figure 3.1** – Map of Maputo City showing sites of sample collection

At the same depth of undisturbed sampling, approximately 20 kg of disturbed samples were collected at each site and immediately placed in polyethylene bags and sealed to prevent moisture loss. This methodology is recommended by Head (1984) and Brink *et al.* (1984) as it prevents uncontrolled moisture loss. Moisture loss has to be done at air temperature inside the

laboratory therefore the importance to seal the disturbed samples in polyethylene bags. Data on the sample location and depth, and surface elevation were taken in every sampling point.

A 100% undisturbed sample is not possible to obtain. However, all effort was made to keep the disturbance as minimum as possible. The 1mm thickness of the galvanized steel sheet was chosen to make the samplers because it is strong enough to avoid bending when driven into the soil, what would allow sample disturbance. Grease was used to reduce friction between the sampler and the soil. The unavoidable sample disturbance caused by friction of the surface with steel sheet was minimized as no re-sampling for laboratory testing was made in the vicinity of the wall samplers.

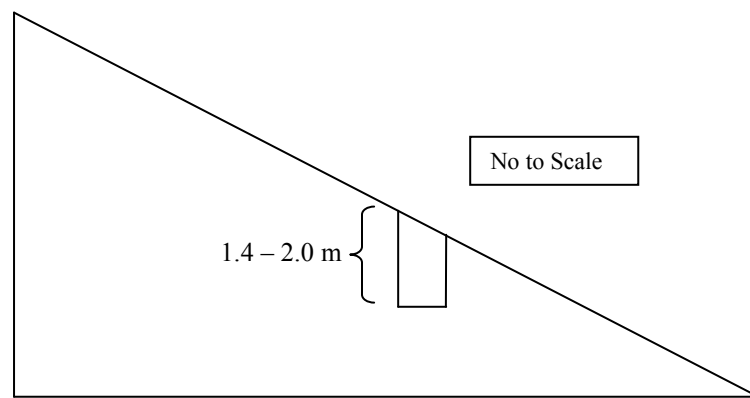


**Figure 3.2** – Schematic representation of the location of the sampling point on the slopes

At each sampling point, soils were examined and described in their natural state based on six characteristics recommended by the guidelines for soil and rock logging in South Africa (Brink & Bruin, 2002), namely moisture content, colour, consistency, soil structure, soil texture and soil origin.

Visual inspections of the vegetation cover, land use, erosion characteristics, groundwater seepage on the slope surface were done.

### **3.2 – LABORATORY TESTING PROCESS**

A number of specialized analytical tests have been developed in the laboratory to determine the engineering geotechnical and physico-chemical properties of the soils and in order to fulfil the research objectives. The geotechnical tests were undertaken at the laboratories of the School of Geological Sciences and School of Civil Engineering, Surveying and Construction. The chemical tests were done at the accredited laboratory of the South African Sugarcane Research Institute.

The geotechnical tests were carried out on disturbed and undisturbed samples and were conducted for soil classification, which indicate the general soil type and the engineering category to which it belongs, for the assessment of engineering and geotechnical properties (strength), and for the assessment of the soil erodibility, collapse settlement and slope stability. Soil samples were stored in cupboards inside the laboratories protected from extremes of heat and cold and were tested immediately after collection. Testing process lasted for 1 year.

The most important requirement for any test sample is that it be fully representative of the material from which it is taken. A representative disturbed test sample was obtained by riffle box method which is one of the recommended methods for subdividing a large sample of granular soil (Head, 1984).

Partial drying at moderate temperatures may change the index properties derived from plasticity, shrinkage and particle size tests, and the physical behaviour of tropical soils. Some of these changes are chemical and are not reversed when the soil is remixed with water (Fookes, 1997). For this reason, the classification tests were applied to natural soil with as little drying as possible. The desegregation of particles was done with care aiming to separate individual particles without crushing or splitting and was limited to that achievable by finger pressure. The test specimens of the undisturbed samples were prepared following the procedures recommended by Head (1984). The undisturbed samples were resealed soon after removal of material for testing to prevent loss of moisture and material.

The laboratory tests were conducted under strict controlled environmental conditions and using precise equipment to obtain accurate results and using step-by-step testing methodology. The procedures of the testing are fully described in Head (1984) when not otherwise stated. The accuracy of the test procedures were measured by getting the same results on repeating testing of the same material. Repeating testing is a normal procedure undertaken at the beginning of any laboratory campaign in order to make sure that the process followed is appropriate and to check if similar results can be obtained when testing the same sample at a later stage. This was done for one sample in every test undertaken. Results to demonstrate repeatability are available.

### **3.2.1 – Testing Physical Properties for Soil Classification**

#### **3.2.1.1 – Particle Size Distribution**

The particle size distribution aims at grouping the solid particles into separate size ranges and determine the relative proportions of each size range and to determine the relative proportions, by dry weight, of each size range (Brink *et al.*, 1984; Head, 1984, GSEG, 1990;). The particle

size distribution is important for engineering soil classification and to predict the soil behaviour. For example, the problems with collapse are generally associated with silty or sandy soils of low clay content, although high clay content does not necessarily mean that collapse will not occur (Jennings and Knight, 1957; El-Ruwaih & Touma, 1986). Particle size distribution will assist in identifying these soil types. Additionally, the particle size distribution is an important tool for slope stability analysis as each soil material has its own equilibrium characteristics, which are related to particle size distribution. Particle size determines the slope angle, type, speed and form of failure.

The particle size distribution was determined by Wet Sieving (BS 1377:1975, Test 7 (A)). The initial soil sample was weighed and a duplicate sample taken for moisture content determination so that the initial dry mass could be calculated. The sample was immersed in a dispersant solution of sodium hexametaphosphate for wet sieving (Head, 1984). After washing the material retained in the 63  $\mu\text{m}$  sieve was oven-dried for dry sieving. A “standard” set of sieves of the British Standards (15-mesh series from 8–0.063mm) was chosen which covers most requirements of apertures sizes for each particular soil and is sufficient to provide a reasonable grading curve.

The distribution of finer particles (passing the 63  $\mu\text{m}$  sieve) was obtained using a laser diffraction grain-size analyser (Malvern Mastersizer, Model APA2000). This new technology is able to produce more accurate distribution curve in a fraction of time of a standard test. A small sample was prepared and placed within a clean beaker of water circulating through the laser particle sizer. It performs three runs and displays the results if it finds three identical particle size distribution curves. The laser particle sizer measures the particle size distribution of the samples by volume, differently of the sieving test, which measures the samples by weight. A mathematical inversion was used to convert the particle size distribution by volume obtained in the laser diffraction grain size analyser to particle size distribution by weight.

### **3.2.1.2 – Moisture Content**

The moisture content is the most frequently determined soil characteristic which provides an extremely useful method for classifying soils and for assessing their engineering properties. The reasons for carrying out moisture content tests on soils fall into three categories: “(1) to determine the moisture content of the soil *in situ*, (2) to determine the plasticity index and shrinkage limits of soils, for which moisture content is used as the index, and (3) to measure the moisture content of samples used for laboratory testing” (Head, 1984). The moisture content was determined through the oven drying method (BS 1377:1975, Test 1(A)). It is usually

expressed as a percentage, always on the basis of the oven-dry mass of soil. A test sample is dried out in the oven to reach a constant mass. The percentage of moisture loss is then calculated.

### 3.2.1.3 – Consistency Limits (Liquid and Plastic Limits)

The consistency limits are useful indices for the identification and classification of soils. Particle size tests provide quantitative data on the range of sizes of particles and the amount of clay present, but say nothing about the type of clay. Clay particles are too small to be examined visually, but the Atterberg limits enable clay soils to be classified physically, and the probable type of clay minerals to be assessed.

The liquid limit is the water content at the boundary between the plastic and the liquid state on which soil begins to flow. In this state it has very low but measurable shear strength (about 1.7 kPa) (Head, 1984; Brink *et al.*, 1984). The Liquid Limit was measured by the cone penetrometer method (BS 1377:1975, Test 2(A)) and was carried out in the fraction of the air dried remoulded soil passing the 425  $\mu\text{m}$  sieve. The cone penetrometer method was chosen instead of Casagrande method because the results obtained by the cone method have been proved to be more consistent, and less liable to experimental and personal errors, than those obtained by the Casagrande method (Head, 1984). The cone method is based on the measurement of penetration into the soil of a standardised stainless steel cone of sharp point, length approximately 35 mm and mass of 80 g. The liquid limit corresponds to the moisture content that allows a cone penetration of 20 mm.

The plastic limit defines the boundary between the plastic and the solid state, and is the moisture content equivalent to the state where the soil mass begins to crumble when rolled into thin threads between the palm of the hand and a flat surface. In this condition it has a shear strength of about 170 kPa (Brink *et al.*, 1984). This test was determined through the BS 1377:1975, Test 3. The Plastic Limit can be carried out only on soils with some cohesion, on the fraction passing a 425  $\mu\text{m}$  sieve. Because the tested soils of Maputo City have very low clay content (Section 5.3.1), the determination of this limit was not possible in the majority of the samples.

The *Plasticity Index* is the moisture content *range* over which the soil remains in a plastic condition. It is calculated by the difference between the liquid and the plastic limit. The approximate estimate of the plasticity index of the soil in which the plastic limit was difficult to determine was obtained by the relationship with the Linear Shrinkage (Head, 1984).

The Linear Shrinkage test indicates the shrinkage capability and the activity of a soil (Head,

1984). It is the percentage decrease in length of a bar of soil near its liquid limit dried in an oven. This test also provides an approximate estimate of plasticity index for soils in which plastic limits are difficult to determine (equation 5.1), for example, soils of low clay content. The Linear Shrinkage was determined using the BS 1377:1975, Test 5.

#### **3.2.1.4 – Particle Density and Specific Gravity**

A soil consists of an accumulation of particles which may be of a single mineral type or more usually a mixture of a number of mineral types, each with a different specific gravity. For a soil consisting of a variety of minerals only the mean specific gravity of the mass as a whole is measured. The specific gravity of the soil particles is required in calculations of the void ratio, but it may also indicate the presence of unusual minerals. The density bottle method (BS 1377:1975, Test 6 (B)) was used in this research for the determination of specific gravity. It determines the mass of a volume of water equal to the volume of soil particles and calculates the specific gravity as the ratio of the mass of the solid particles to the mass of water (Head, 1984). De-aired distilled water was used as the density bottle fluid and care was taken to remove all the air from the voids between soil particles. This was possible by leaving the sample under vacuum overnight. Three replicate tests on 30 g sub-samples were carried out in each soil sample and the average taken as the sample specific gravity.

The particle density is an important property having many applications in soil engineering. It is required for determining the soil porosity or void ratio, which can be related to fabric structure, for example, collapsible fabric. Soils with a collapsible fabric often have a low dry density (in the range of 900 to 1600 kg/m<sup>3</sup>) but special attention has to be taken to the fact that not all soils with low dry density exhibit a tendency to collapse or, vice versa, that all soils with high dry density will not collapse. This is warned by Jennings & Knight (1957) because many stable soils have very low dry densities. Similar importance is given to the bulk density, very important in the analysis of slope stability as the weight of soil provides the main force. This weight is obtained from the soil density which is also significant in calculating the bearing capacity and settlement of foundations for other structures. The particles density was obtained from the outputs of the oedometer test.

#### **3.2.1.5 – Organic Matter**

Organic matter was determined by loss on ignition method. This method was designed to measure the amount of moisture or impurities lost when the soil material is subjected to specified high temperatures. All volatile substances are allowed to escape, until the soil mass ceases to change. With this method about 20 g of an oven-dried soil was placed in the muffle

furnace and heated to 800°C. The percentage of weight loss after the test is equivalent to the organic matter of the soil sample. The procedure followed in this test is recommended by the ASTM D7348 (Standard Test Methods for Loss on Ignition of Solid Combustion Residues).

### **3.2.2 – Determination of Shear Strength**

#### **3.2.2.1 – Standard Shear Box**

The shear box test is based on the relative movement of two halves of a square block of soil along a horizontal surface. Loads imposed on the soil which supports the foundations of every building or structure cause deformations of the soil by the slippage of soil particles, one on another, which may lead to the sliding or roll of soil past the surroundings mass. This process known as shear failure occurs when the stress exceeds the maximum shear resistance which the soil can offer. The standard shear box, for 60 mm square specimen, was used to measure the shear strength of the soil.

The shear box test is the simplest, the oldest and the most straightforward procedure for measuring the immediate or short-term strength of soils in terms of total stress (Head, 1988). This test was developed for the determination of the cohesion of particles ( $C_u$ ) and the angle of shear resistance ( $\phi$ ) which are necessary for the calculations of the stability of slopes. It also provides the most direct means of relating  $\phi$  to the void ratio,  $e$ , and of determining the critical void ratio (or critical density) of dry sands or of saturated sands which do not contain fine material in sufficient quantity to impair the drainage characteristics. This is important for the analysis of buildings tilting. The results of a shear strength test in a shear box are plotted graphically, and values of cohesion and angle of shear resistance are obtained directly from the graph. This test is not covered by the current 1975 British Standards but the consolidated-drained test is given in US standards under ASTM 3080.

Soils were tested on direct shear box in drained saturated condition and consolidated under normal pressures of 56, 139 and 250 kPa from which the strength envelope of the Mohr-Coulomb failure criterion was obtained, and cohesion ( $c$ ) and friction angle ( $\phi$ ) calculated.

### **3.2.3 – DETERMINATION OF CONSOLIDATION CHARACTERISTICS**

#### **3.2.3.1 – Double Oedometer Test**

The double oedometer test is the classical approach used for quantification of potential collapse settlement. Two undisturbed samples were tested in oedometers. The first oedometer test was performed in a sample at its natural moisture content and the second with water in the cell

saturating the sample. The collapse and the evaluation of the effect of saturation is then determined by the superimposition of the consolidation curves from both tests, assuming that no collapse may occur under equilibrium conditions with the overburden pressure in the field (Riani & Barbosa, 1989; Jennings & Knight, 1957).

Bonding between soil particles affects the collapse property of the soils and special attention was taken to their possible relation. They were separated carefully in the interpretation of the curves given by the double oedometer test.

The double oedometer test was carried out following the procedures recommended by Jennings and Knight (1975). Soil samples were subjected to eight loading conditions at 1, 6, 12, 25, 50, 100, 200 and 400 kPa and two unloadings from 400 to 200 and finally 50 kPa. The loading and unloading period was 24 hours.

### **3.2.4 – DETERMINATION OF SOIL EROSION SUSCEPTIBILITY**

#### **3.2.4.1 – Crumb Test**

The crumb test provides a very simple means of identifying dispersive soils and erodibility without requiring special equipment (Head, 1988). Few crumbs, each of about 6-10 mm diameter, were dropped in a beaker containing sodium hydroxide solution. Occurrence of reaction was observed after allowing standing for 5-10 min (Head, 1988). The results depend on the observations in accordance with the guide to interpretation based on the level of reactions occurred. The procedure followed in this test is described by Sherard *et al.* (1976b).

#### **3.2.4.2 – Pinhole Test**

The Pinhole test is widely considered to be one of the most reliable physical tests to determine erodibility because it simulates the action of water draining through a pipe in soil. The test procedure is based on extensive trials and observational experience. Distilled water is caused to flow through a 1 mm diameter hole formed in a specimen of recompacted soil under heads of 50, 180 and 380 mm (Sherard *et al.*, 1976a). The water emerging for the dispersive soil carries a suspension of colloidal particles, whereas water from an erosion-resistant soil is crystal clear. The test is based purely on visual assessment. The results of the test are evaluated from the appearance (turbidity) of the discharged water, the rates of flow, and the final size of the hole in the specimen. The test was performed according to the procedures developed by Sherard *et al.*, (1976a).



### 3.2.4.3 – Flume Test

The flume test was developed to model the soil erodibility and the “*impact of flowing water over the sidewalls of the gullies*” (Rienks *et al.*, 2000). Undisturbed block samples were placed in a pre-designed metallic mould (73 x 73 x 20 mm) made from galvanized steel (1 mm thick), air-dried and weighed. The mould was then placed in a portable straight flume (Ravens & Gschwend, 1999; Ravens & Jepsen, 2006), 114 cm long and 23 cm in height, in which a known bottom shear stress is applied on the sediment bed to observe the rate of erosion, and infer the erosion parameters (Arulanandan & Heinzen, 1977; Ravens & Gschwend, 1999; Ravens, 2007; Ravens & Sindelar, 2008) (Figure 3.3).

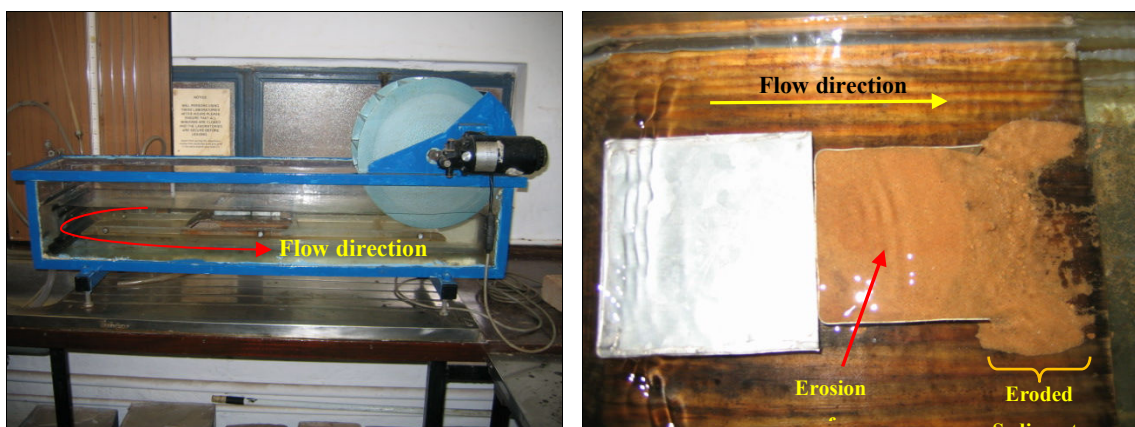


**Figure 3.3** – Straight flume apparatus with water circulated by a paddle-wheel (Left). Soil sample being tested in the flume apparatus with the top and downstream side of the mould left uncovered restricting the area exposed to water erosion. Photo taken from top (right).

Constant water depth was kept at 0.5 cm over every sample, the angular velocity of the wheel at 2.7 rad/s and the test was run during 10 minutes after which the eroded sediments were drained off with water from the flume tank as recommended by Rienks *et al.* (2002). The sediments were wet sieved without chemical dispersion, with mesh sizes of 2, 1, 0.5, 0.25, 0.125 and 0.063 mm to determine their particle size distribution.

### 3.2.4.4 – Exchangeable Sodium Percentage (ESP)

Soil erodibility is also related to the chemical composition of the clay fraction. A strong relationship between erodibility and the dispersion potential classification can be found, which is based on the ESP and Cation Exchange Capacity (CEC) (Bell & Walker, 2000). A threshold value of ESP of 10 % has been recommended, above which soils that have their free salts leached by seepage of relatively pure water are prone to erodibility. Soils with ESP above 15 % are highly dispersive. The ESP is determined from the exchangeable cations and the results were interpreted according to the proposal of Gerber & Harmse (1987).

#### **3.2.4.5 – Cation Exchange Capacity (CEC)**

The potential for dispersion is controlled by the CEC which is directly related to the properties of clay minerals. CEC is due to the type and nature of clay minerals present in the soil. Clay minerals that tend to be associated with dispersivity are smectites and other 2:1 phyllosilicates. The CEC of these minerals is in the range of 40 to 150 meq/100g clay. These minerals also influence the liquid and plastic limits of the soils because of their different reactivity. If these minerals are present in the clay fraction then the soils are likely to be erodible. However, the CEC alone cannot be used to identify erodibility as other factors, such as high organic content, may contribute to high CEC values (Bell & Walker, 2000). There are several methods for the determination of CEC. The method based on ammonium acetate was used in this research as most reliable although time and work consuming. The CEC was obtained from the exchangeable cations and the results were compared with the activity of clay content.

#### **3.2.4.6 – Sodium Adsorption Ratio (SAR)**

The Sodium adsorption ratio (SAR), the percentage sodium and the total dissolved solids (TDS) were obtained from the saturation extract cations. The SAR quantifies the role of sodium dispersion with respect to other free salts in the pore water. Harmse (1980) and Gerber & Harmse (1987) established reference values for evaluating the soil erodibility according to these chemical parameters.

## **CHAPTER 4**

### **SITE SPECIFIC INFORMATION**

#### **4.1 – LOCATION AND GENERAL GEOGRAPHICAL BACKGROUND**

Maputo City is the capital of Mozambique, a coastal city situated in the southern part of the country between the coordinates 25° 52' and 26° 10' S and 32° 30' and 32° 40' E. Maputo City is bounded by the Maputo Bay in the east, Matola Municipality in the west, Marracuene District in the north and Matutuíne District in the south (Figure 4.1). It has an area of 300 km<sup>2</sup> and a population of 1,099,102 according to the 2007 population census (INE, 2007). This population (which accounts for 5.4 % of the country's population) is distributed through seven Municipal Districts. The study area covers Municipal Districts one to five (Figure 4.1). Municipal Districts six (Catembe, South of Maputo Estuary) and seven (Inhaca Island, located 15 km from the main city) were not included in the study area because are outside the main city. The population density is 3,663.67 people/km<sup>2</sup>, with a greater population density in the outskirts of the main city. In last ten years population has risen 13.7 % with a consequent increase in land use pressure (Table 4.1).

The main activities in Maputo City are industry, services, artisanal and industrial fishing and urban agriculture, in the swamp areas and along Infulene River which constitutes the border with Matola Municipality.

#### **4.2 – CLIMATE**

The climate of Maputo City is tropical, moderately humid and dominated by seasonal movements of the Intertropical Convergence Zone. The city is partly influenced by the SE trade wind and occasionally by strong and cold Southerly winds or cyclones from the NE (Kalk, 1995; Hogueane, 1996; Canhanga & Dias, 2005). The climate has two seasons: the rainy season, which is warm and humid from November to March; and the dry season, which is cold and dry

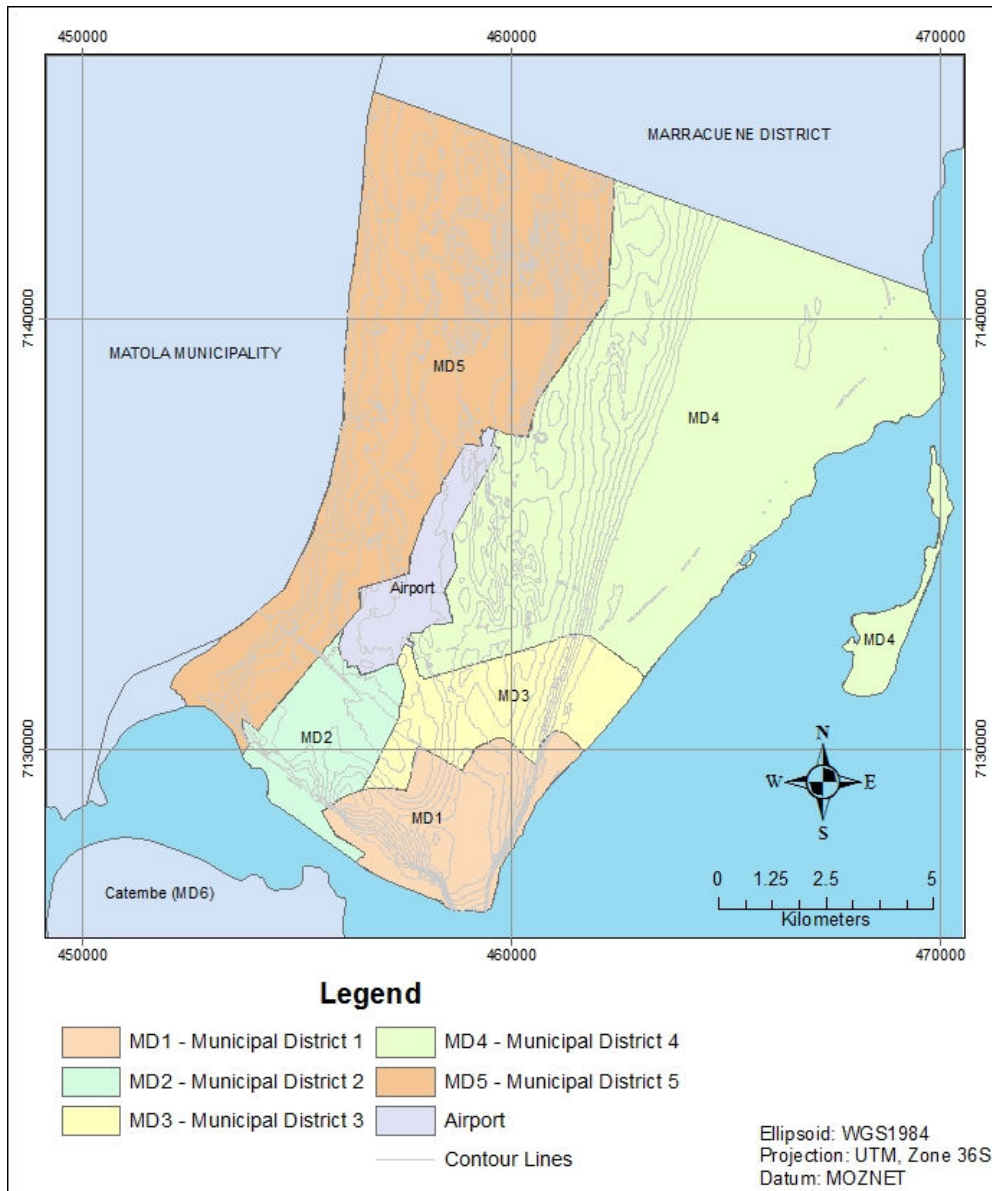


**Figure 4.1** – Geographic location of Maputo City with the boundaries of Municipal Districts. The Municipal District 7 the Inhaca Island and is not shown on the map

from May to September. April and October are the transition months between the two seasons (Faria & Gonçalves, 1968). The average diurnal temperature in the rainy season is 31°C and in the dry season is 24°C. The mean annual relative humidity is 87.3 % being high from January to March. The mean monthly precipitation during the rainy season is 132 mm while in the dry season is 28 mm (INAM, 2009). The mean annual precipitation is 927 mm, however, some consecutive events of heavy rainfall are registered such as in 1984 with 1261.3 mm and 2000 with 1600.6 mm when unusual heavy rainfall within a short span of time registered in February 2000 resulted in 502.1 mm in only four days. This last event is responsible for most of the gullying and landslides hazards in Maputo City. The distribution of rainfall throughout the last 30 years is given in the Figure 4.2. The extreme rainfalls events were registered in 1975, 1981,

1984, 1999 and 2000 (INAM, 2009).

**Table 4.1** – Variation of population by Municipal District in Maputo City in the last 10 years

| Municipal District | Area (Km <sup>2</sup> ) | Population     |                  |               |                                   |
|--------------------|-------------------------|----------------|------------------|---------------|-----------------------------------|
|                    |                         | 1997           | 2007             | Variation (%) | Density (people/km <sup>2</sup> ) |
| District nº 1      | 13.5                    | 154,284        | 106,259          | -20.6         | 7,870                             |
| District nº 2      | 8.8                     | 162,750        | 155,462          | -4.5          | 17,616                            |
| District nº 3      | 12.2                    | 210,551        | 223,688          | 6.2           | 18,335                            |
| District nº 4      | 76.9                    | 228,244        | 293,768          | 28.7          | 3,820                             |
| District nº 5      | 59.8                    | 211,008        | 293,998          | 39.3          | 4,916                             |
| District nº 6      | 89.3                    | 15,853         | 20,629           | 30.13         | 0.23                              |
| District nº 7      | 42.5                    | 4,672          | 5,211            | 11.54         | 0.12                              |
| <b>Total</b>       | <b>303</b>              | <b>966.837</b> | <b>1,099,112</b> | <b>13,7</b>   | <b>3,663.67</b>                   |

During the rainy season the Mozambican coast is affected by tropical depressions and cyclones but not all cause severe damage in Maputo City. Under normal conditions, some depressions develop into a cyclone, which normally means worsening of weather over a smaller area. In 2000 a particular tropical depression did not develop into a cyclone but became trapped by other meteorological factors and so remained, more or less stationary. It then fed moist maritime air into the region, which resulted in continuous rain that raised water tables. Then, the fully developed cyclone Eline followed almost immediately with disastrous flooding consequences in the Southern Mozambique.

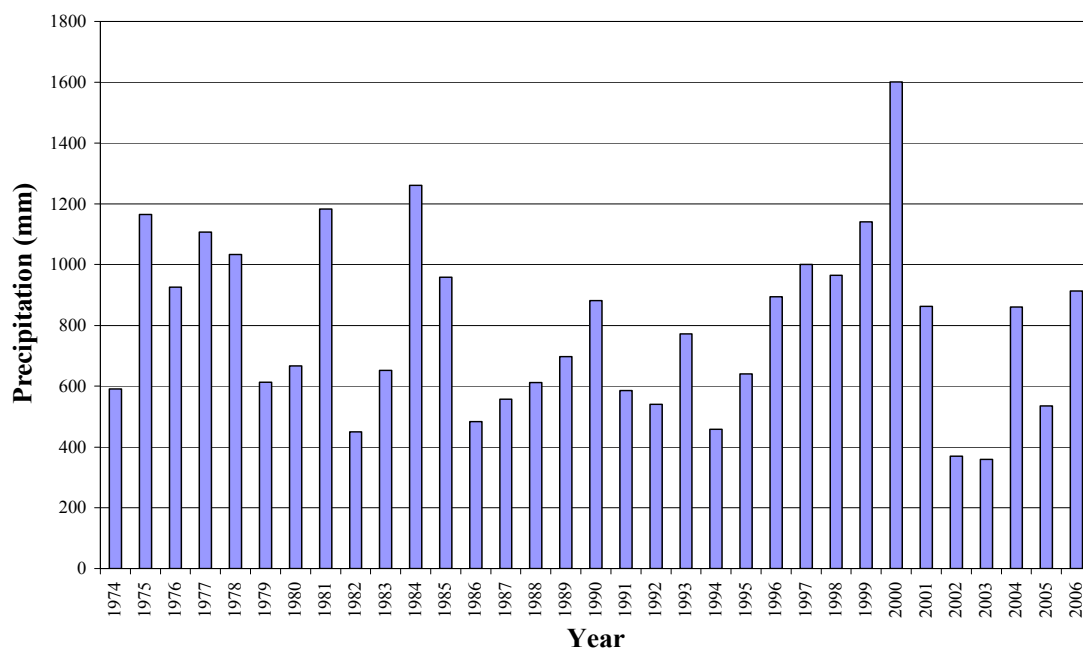


**Figure 4.2** – Distribution of rainfall in the last 30 years in Maputo City (INAM, 2009)

### 4.3 – GEOLOGY OF MAPUTO CITY

Maputo City is built in a coastal area underlain by Tertiary and Quaternary dunes. The development of these dune fields along the Mozambican coast has been associated with regression and transgression events. The sea level regression periods occurred in combination with cold and dry climatic conditions while the transgressions were associated to hot and wet climate and to the presence of sandy and gravely deposits, as well as to periods of intense weathering (Momade *et al.*, 1996). Between the transgression and regression events the geological formations that occur in Maputo City were formed being eolic, fluvial or a combination of both. The processes of soil formation include incorporation of humus, physical and chemical weathering, downward movement of fine particles and disturbance by root penetration and desiccation. These processes lead to the present soil characteristics of Maputo City.

According to the 1:50 000 geological sheet 2532D3 of Maputo produced by Momade *et al.* (1996) and published by the National Directorate of Geology, twelve stratigraphic units/formations are recognised in Maputo City characterized according to lithology, colour, consolidation level and grain size (Table 4.2). The geological formations outcropping in Maputo City and where most development occurs (Figure 4.3) are described in this document.

**Table 4.2** – Summary of the geological formations of Maputo City (After Momade *et al.*, (1996)

| Era        | Period      | Unity/Formation          | Symbol | Description/Composition   |
|------------|-------------|--------------------------|--------|---|
| Quaternary | Holocene    | Beach and tidal deposits | Qm     | White sand, and slime and mud in part temporarily submerged (beach and tidal deposits)                    |
|            |             | Alluvial deposits        | Qa     | Fluvial dark clays with intercalations of carbonaceous levels of marine influence                         |
|            |             | Intradune deposits       | Qi     | White sands   |
|            |             | Xefina Formation         | QXf    | Coastal dune sands and ilmenitic fossil sands   |
|            |             | Costa do Sol             | QCs    | Calcareous gritstone  |
|            | Pleistocene | Congolote Formation      | QCo    | White/yellow/orange coarse to fine sands  |
|            |             | Malhazine Formation      | QMa    | Reddish coarse to fine sands  |
|            |             | Machava Formation        | QMc    | Sandy clay intercalations   |
|            |             | Matola Formation         | QMt    | Sandy clay intercalations   |
|            |             | Ponta Vermelha Formation | TPv    | Red silty sand grading into yellow sandstone, locally with ferruginous crust                              |
| Tertiary   | Pliocene    |                          |        |   |
|            | Miocene     | Santiago Formation       | TSa    | Argillaceous gritstone, calcareous gritstone with <i>Ostrea Cullata</i> in the upper part                 |
|            | Oligocene   | Inharime Formation       | TIn    | Fine gritstone, silty and clay impregnated by organic material and intercalations of calcareous gritstone |



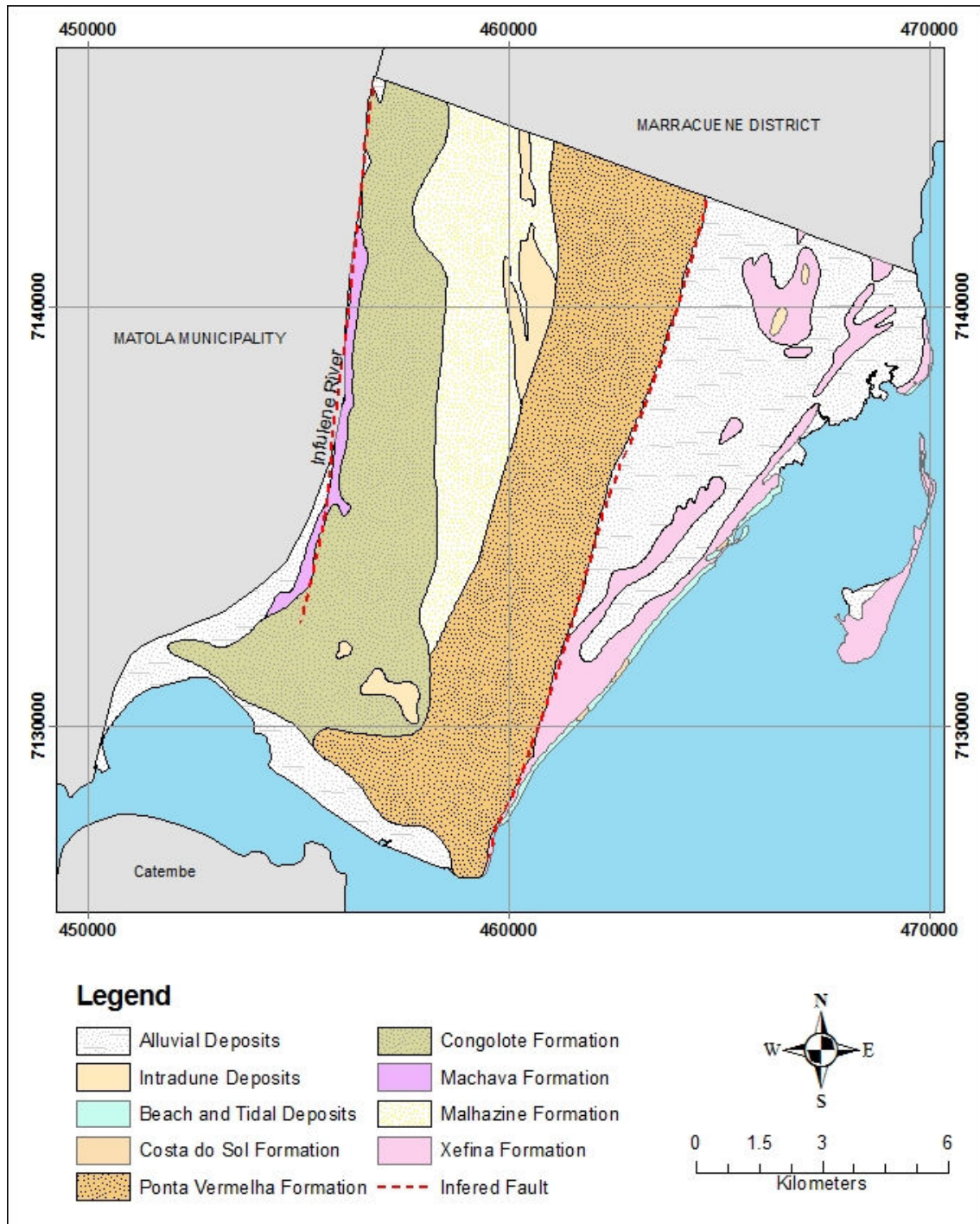


**Figure 4.3** – Geological Map of Maputo City (Momade *et al.*, (1996)

The Ponta Vermelha Formation (TPv), reported to be Pliocene in age, is constituted in the upper part by ferruginous sandstones and red silty sand grading down into yellow to white sand. Locally they are conglomerated with iron oxides giving rise to horizons of red ferruginous crust (ferricrete) of a depth of 3 and 5 m (Macedo, 1971), possibly of lateritic origin, which grades downwards into horizontally stratified carbonated and white sand. Siltstones and marls of the

Ponta Vermelha Formation are soft semi-consolidated rocks, showing bedding and characteristic ‘bad land’-type erosion (GTK Consortium, 2006). This formation is remarkably uniform in its composition, with no visible variation in lithology or structure (Momade *et al.*, 1996). The depth of this formation is variable, attaining values between 30-50 m on the higher part of the city (Macedo, 1971). It has a long coastal slope on the eastern side and extends to the District of Marracuene, 30 km North of Maputo City, in a 3-4 km wide strip oriented NE-SW. At the bottom of this geological formation has been described the presence of carbonated sands, sometimes with concretions and shell fragments of oyster (Beernaert, 1987; Barradas, 1965). Probably these fossils belong to the Santiago Formation located below Ponta Vermelha Formation.

The textural analysis of samples taken from drill cores shows well calibrated material. The shape of the asymmetric negative and leptokurtic curve, indicates that the sediments were deposited in a fluvial or aeolian environment. The roundness of grains is predominantly subangular and subrounded, occasionally rounded with low sphericity (Macedo, 1971). The chemical composition of Ponta Vermelha Formation, given by Momade *et al.* (1996) revealed high levels of silicon oxides ( $\text{SiO}_2$ ), followed by aluminum oxide and iron oxide ( $\text{Fe}_2\text{O}_3$ ) (Table 4.3). The mineralogy is dominated by quartz (90 to 95% on average) and comprises other minerals like feldspar, ilmenite, magnetite, zircon and hornblend, all in lower percentages (Macedo, 1971). With the currently available data it is difficult to define the genesis of the sandstones of the Ponta Vermelha Formation. Only the textures and granularity seem to suggest an aeolian origin, or a mixture of Aeolian and fluvial. The fact that the unit settles directly on a marine substrate (Santiago Formation), suggests that this is possibly an aeolian mantle on a platform of marine abrasion.

The Malhazine Formation (QMa) is part of the interior dune cordon and consists of coarse- to fine-grained sands, poorly consolidated with whitish to reddish colours. The dunes have visible expression and are longitudinal in type, reaching up to 30 m in height, with ridges systematically NNW oriented. The intradune depressions (intradune unit) are filled by very fine white sands and are also oriented NNW attaining several km in extension. The fact that the crests of the dunes are parallel to those occurring at the surface of Ponta Vermelha Formation suggests that both were affected by a similar wind regime, and that the reddish intercalations in the Malhazine Formation could result from the remobilization of Ponta Vermelha Formation. In terms of texture, the well-calibrated fine sandy fraction (92 to 98 %) is the most dominant. Mineralogically, quartz is the dominant mineral (98 %) appearing also are small concentrations



**Table 4.3** – Chemical composition, in percentage, of samples from the main geological formations outcropping in Maputo City and where most development occurs (After Momade *et al.*, (1996))

|                                | Ponta Vermelha Formation |              |              |              |              |              | Malhazine Formation |               |               |               |              |              | Congolote Formation |              |              | Xefina Formation |               |               |
|--------------------------------|--------------------------|--------------|--------------|--------------|--------------|--------------|---------------------|---------------|---------------|---------------|--------------|--------------|---------------------|--------------|--------------|------------------|---------------|---------------|
| Sample Number                  | 2440                     | 2441         | 2442         | 2443         | 2444         | 2445         | 2194                | 2195          | 2196          | 2197          | 2198         | 2199         | 2210                | 2211         | 2212         | 2187             | 2191          | 2192          |
| SiO <sub>2</sub>               | 88.43                    | 88.30        | 89.23        | 91.27        | 88.65        | 80.43        | 89.18               | 93.57         | 96.29         | 84.71         | 87.33        | 80.10        | 91.50               | 83.30        | 79.50        | 93.78            | 96.97         | 93.01         |
| TiO <sub>2</sub>               | <0.50                    | <0.50        | <0.50        | <0.50        | <0.50        | 0.53         | 0.39                | 0.21          | 0.17          | 0.10          | 0.52         | 0.19         | 0.33                | 1.62         | 0.17         | 0.15             | 0.15          | 5.70          |
| Al <sub>2</sub> O <sub>3</sub> | 3.23                     | 4.01         | 3.58         | 2.82         | 6.08         | 6.08         | 3.19                | 2.04          | 1.66          | 4.21          | 2.68         | 1.53         | 1.40                | 1.78         | 2.65         | 0.76             | 0.68          | 1.27          |
| Fe <sub>2</sub> O <sub>3</sub> | 1.31                     | 1.60         | 1.40         | 1.26         | 2.34         | 2.34         | 2.49                | 0.89          | 0.74          | 10.03         | 4.23         | 1.23         | 1.29                | 0.98         | 1.09         | 1.99             | 1.23          | 0.54          |
| MnO                            | 0.00                     | 0.01         | 0.03         | 0.02         | 0.05         | 0.05         | -                   | -             | -             | -             | -            | -            | -                   | -            | -            | -                | -             | -             |
| MgO                            | <0.05                    | 0.06         | <0.05        | <0.05        | 0.54         | 0.54         | 0.25                | 0.13          | 0.19          | 0.25          | 0.13         | 0.07         | 0.18                | 0.19         | 0.19         | 0.12             | 0.07          | <0.01         |
| CaO                            | 0.10                     | 0.08         | 0.04         | 0.26         | 0.78         | 0.78         | 0.26                | 0.26          | 0.26          | 0.70          | 0.26         | 0.26         | 0.30                | 0.26         | 0.26         | 0.52             | 0.26          | 0.18          |
| Na <sub>2</sub> O              | 0.29                     | 0.29         | 0.25         | 0.27         | 1.46         | 1.46         | 0.17                | 0.16          | 0.22          | 0.29          | 0.16         | 0.14         | 0.17                | 0.13         | 0.16         | 0.21             | 0.22          | 0.22          |
| K <sub>2</sub> O               | 0.64                     | 0.87         | 0.71         | 0.76         | 1.23         | 1.23         | 0.24                | 0.42          | 1.17          | 0.11          | 0.11         | 0.31         | 0.51                | 0.41         | 0.25         | 0.53             | 0.51          | 0.74          |
| P <sub>2</sub> O <sub>5</sub>  | 0.02                     | 0.02         | 0.01         | 0.01         | 0.02         | 0.02         | -                   | -             | -             | -             | -            | -            | -                   | -            | -            | -                | -             | -             |
| H <sub>2</sub> O               | 1.59                     | 1.40         | 1.23         | 1.07         | 2.90         | 2.90         | -                   | -             | -             | -             | -            | -            | -                   | -            | -            | -                | -             | -             |
| SO <sub>3</sub>                | -                        | -            | -            | -            | -            | -            | 0.89                | 0.70          | 0.89          | 0.56          | 0.51         | 0.40         | 0.41                | 0.51         | 0.36         | 0.67             | 0.52          | 0.39          |
| LOI/PR                         | 1.81                     | 4.71         | 1.38         | 1.31         | 1.80         | 1.80         | 3.65                | 2.48          | 0.96          | 6.34          | 3.46         | 0.75         | 1.11                | 0.23         | 0.88         | 0.38             | 1.12          | 0.65          |
| <b>Total</b>                   | <b>97.97</b>             | <b>98.85</b> | <b>98.46</b> | <b>99.60</b> | <b>98.16</b> | <b>98.16</b> | <b>100.71</b>       | <b>100.86</b> | <b>102.55</b> | <b>107.32</b> | <b>99.39</b> | <b>84.98</b> | <b>97.20</b>        | <b>89.41</b> | <b>85.51</b> | <b>99.11</b>     | <b>101.73</b> | <b>102.71</b> |

of ilmenite, leucoxene, monazite, silimanite, zircon and rutile (Momade *et al.*, 1996). Chemical analyses present high concentrations of silicium, iron and aluminium oxides (Tables 4.3). According to Barradas (1962) and Beernaert (1987), the deposition of this dune field is linked to regressive phenomena, associated to maximum glacial of Higher Wurm, i.e, the Higher Pleistocene.

The Congolote Formation (QCo) is mainly formed of internal dunes comprised by poorly consolidated aeolian silica sands with brownish, yellow, orange and whitish tones fine- to medium-grained. The dunes are located inland, generally not far from the present shoreline, but are not part of the present active dune system. Congolote Formation is considered to be the lateral equivalent of the Malhazine Formation in terms of age, as they show same morphological pattern, comprising alternating longitudinal dunes and elongated depressions, being probably from the same dune cordon. The elongated hills are not derived from dune migration, but rather from consecutive dune formation along a migrating shoreline. Migration of the shoreline denotes a regressive movement.

Texturally the fine to medium sandy fraction is dominant (with only 5 % of silt-clayey fraction) and well sorted (Momade *et al.*, 1996). The shape and symmetry of the granulometric curve suggests an aeolian deposition.

The chemical analyses reveal higher silica content, reaching values as high as 91% (Table 4.3). The carbonate content is very low ranging from 1.1 to 1.8%. The mineralogical analysis of the sandy fraction shows not only quartz but also ilmenite and monazite in its composition.

The intra-dune depressions are regarded as abandoned sea channels. They are composed of reddish fine- to medium-grained silica sands. As usual in aeolian deposits, the sand grains are rounded and relatively equigranular (GTK Consortium, 2006). The age of the internal dunes is intra-Pleistocene. Migration of the shoreline denotes a regressive movement.

The coastal dune cordon forms the Xefina Formation (QXf) and comprises quicksand white in colour (Momade *et al.*, 1996). Most conditions identified as “Quicksand” occur in sandy condition when upward seepage produces a vertical effective stress close to zero. However, Coduto (1999) defends that most conditions identified as quicksand are actually just very loose saturated sand and this probably applies to the Xefina Formation in Maputo City. The crests of these dunes are differently oriented contrasting with the dunes of older units. Texturally the unit is predominantly composed of fine- to medium-grained quartz sands, very uniform in size. Ilmenite, epidote, tourmaline and amphiboles also occur but only in small quantities. In various

locations of the Mozambican coast Heavy minerals occur very often in the coastal beach and dunes sands in concentrations that revealed very important from the economic point of view and large mining activities are recently taking place. Chemical analysis show higher contents of SiO<sub>2</sub> (Table 4.3) and lower carbonate content from 1.1 to 1.5%.

According to several authors, the dunes of Xefina Formation are from holocene. They may correspond to a dune field developed during regressive propulsion immediately before the current transgressive phase. The hypothesis that these dunes correspond to the old sand banks, reworked later by wind in regressive regime is not excluded (Momade et al., 1996). Tidal and Beach Deposits (Qm) are from recent Holocene and comprises mud and uniformly sized white sands. These deposits are in part temporarily submerged depending on the tides. The beach sands generally unconsolidated originate from the combined action of fluvial supply and erosional factors such as wind, sea waves, tidal and along-shore currents. Unlike the red and brown colours of the Pleistocene Internal Dunes, the recent dunes have white to light grey to yellowish colours (GTK Consortium, 2006). Chemical analysis of the Beach and Tidal Deposits revealed a high silica content. Quartz is the predominant mineral but ilmenite, epidote, tourmaline and amphibole also occur.

#### **4.4 – THE MAPUTO BAY AND ITS CHARACTERISTICS**

Maputo Bay is an inlet of the Indian Ocean in the Mozambican coast, a large embayment 90 km long, north to south, and 30 km wide. It covers an area of 1875 km<sup>2</sup> located between the latitudes 25° 55' and 26° 10' S and the longitudes 32° 40' and 32° 55' E (Barata *et al.*, 2001, Canhanga & Dias, 2005) (Figure 4.4).

The Maputo Bay is part of the sequence of lagoons located along the coast of Indian Ocean from Saint Lucia Bay in South Africa to the south of Mozambique. The opening of the bay is toward the NE to the north of the Inhaca Island from where it connects to the Indian Ocean. The bay is a shallow system with tidal flats and narrow channels. The water depths are generally less than 10 m but depths greater than 15 m can be found in the zones close to the Indian Ocean (Canhanga & Dias, 2005). In spite of dynamic sand banks at the opening of the bay and shallow areas within endangering navigation into the bay, the Maputo harbour located in the bay is accessible to large ships throughout the year.

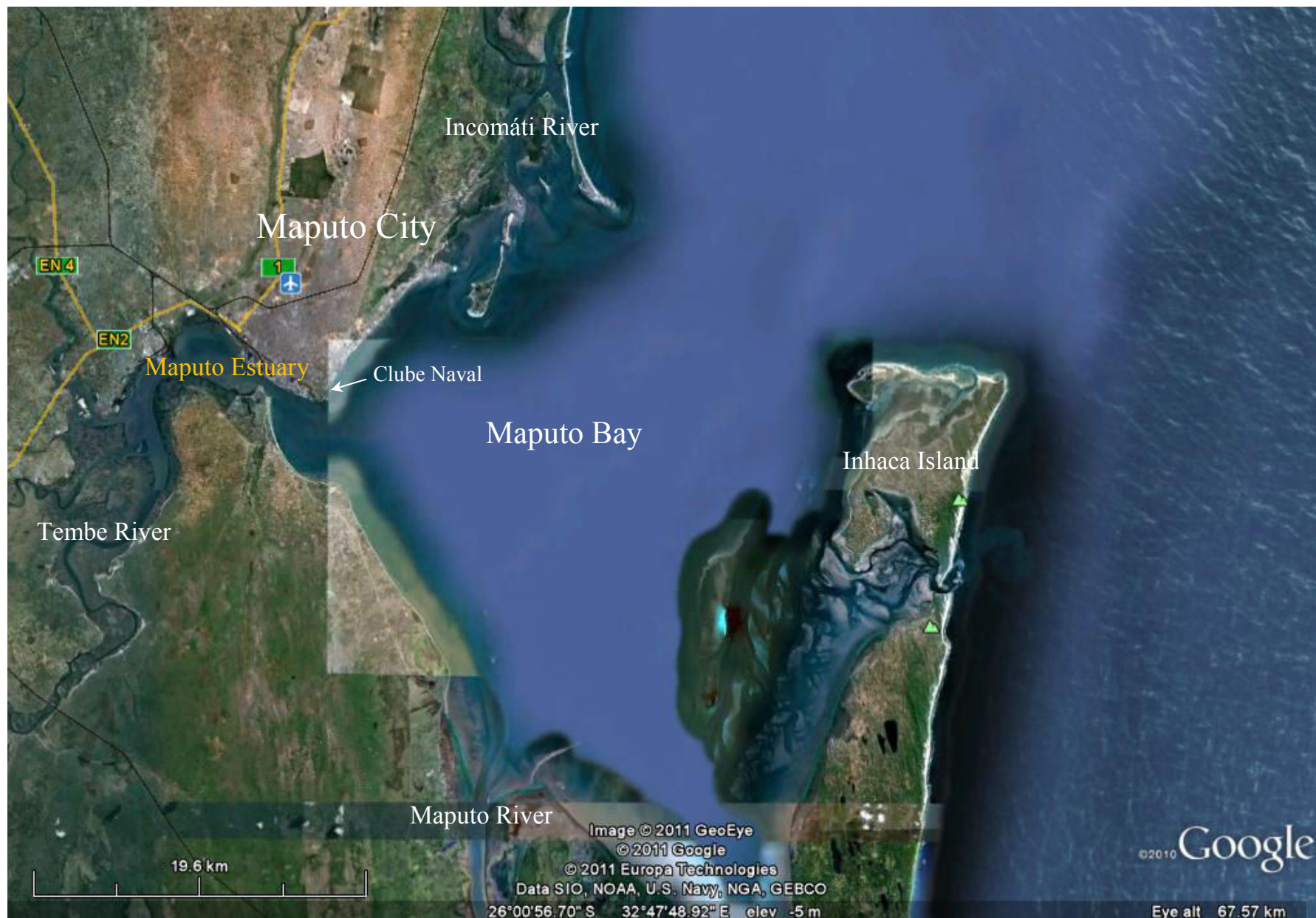


**Figure 4.4** – Google Earth image showing the geographic positioning of the Maputo Bay, the Inhaca Island and some rivers entering the bay

The Incomáti River is the main river entering the bay at its northern; several smaller rivers and streams, the Umbelúzi, the Matola, and the Tembe, with headwaters in the Lebombo Mountains, meet towards the middle of the bay in the Maputo Estuary; the Maputo River enters in the south of the bay. The total fluvial discharge is approximately 190 m<sup>3</sup>/s (Achimo *et al.*, 2004; Canhanga & Dias, 2005).

The Maputo Bay is protected from the sea by the Inhaca Island in the East and its coastline is a low-lying terrain primarily characterised by strips of sandy beaches of recent coastal dunes, marshes and small strips of beach rocks in the area of Clube Naval. The coastal type dominated by sandy beaches is very vulnerable to shoreline change and Maputo Bay is one of the areas experiencing severe coastal erosion in Mozambique (Lundin and Linden, 1996). This coastline is mainly composed of fine-to coarse-grained quartz sand with variable quantity of heavy minerals. Chemical analysis of the Beach and Tidal Deposits revealed high silica content. Quartz is the predominant mineral but also ilmenite, epidote, tourmaline and amphibole occur.

#### **4.5 – HYDROGEOLOGY**

Maputo City is characterized by two aquifers separated by one semi-permeable layer with one impermeable layer as base of the system (IWACO, 1986; Chutumiá, 1987). The phreatic or dunes aquifer is made up by sand of the interior dunes and lays down over a semi-permeable layer formed by sandy clays and silts. The average thickness of the saturated phreatic aquifer is of approximately 30 to 40 m. The permeability is moderate 2 to 10 m/day (IWACO, 1986).

The gritstone aquifer basically comprises argillaceous gritstone, calcareous gritstone and limestone of the Santiago Formation, Miopliocene in age and lays on an impermeable layer of greenish grey marga from the Oligocene (Inharrime Formation). This aquifer is semi-confined as covered by a semi permeable layer in large part of its extension in which only vertical flow is observed (IWACO, 1986). The grading analysis of the aquifer's sediments shows a mesocurtic curve whose shape suggests deposition of these sediments in marine environments (Momade *et al.*, 1996). The porosity and fractures give good permeability of 2 to 40 m/day in the gritstone. Many of the boreholes in Maputo City abstracts groundwater from this aquifer, being considered the main aquifer in the region, whose thickness varies from 20 to 45 m. In the coastal zone, water from this aquifer is in contact with seawater in the form of wedge, which penetrates 3 to 4 km from the limit between the sea and the continent to reach the base of the aquifer. This contact with seawater influences the groundwater quality of Maputo City.

A study by Amurane & Vicente (2008) indicates that two predominant groundwater flow

directions are observed in Maputo City. In the central and western part of the city the groundwater flows predominantly to the west towards the Infulene River and on the eastern part of the city the groundwater flows to the east towards the Maputo Bay. A third flow direction occurring occasionally in the central part is also observed. These flow patterns are closely related to the occurrence of these two large water bodies (Infulene River and Maputo Bay) as the main water divide is found to the east following a N-S bearing.

Groundwater recharge is generally by rainfall infiltration, but there are other recharge means as river water infiltration and groundwater flow. Infiltration rates are of about 150 to 250 mm/year (IWACO, 1986).

#### **4.6 – GEOMORPHOLOGY OF MAPUTO CITY AND SLOPE DEVELOPMENT**

The topography of Maputo city is characterised by a coastal plain to the east (with dunes and recent alluviums), which changes abruptly to a longitudinal escarpment running NNE–SSW. On top of this escarpment on the Ponta Vermelha Formation a flat highland is formed at approximately 65 m altitude (zone with old and fixed interior dunes). To the west of the city the Infulene river valley creates condition for a gradual descend where various depressions are found but without natural outlet. Some of these depressions are responsible for the flooding areas occurring in Maputo City together with the soil characteristics. Morphologically the following structures are recognised, according to Momade *et al.* (1996): (a) littoral accumulation zone, corresponding to beach and tidal deposits; (b) coastal zone, inclined to the sea, with a maximum height of 8 m, made up by dunes and alluvium; (c) platform of 40 to 50 meters, gently inclined to the West predominantly with degraded interior fixed dunes and sand sheets; (d) Maputo hill, 50 to 65 m in height, which constitutes a residual relief resistant to erosion, probably related with neotectonism phenomena. Actually, the tectonics in Maputo City is related to the probable occurrence of the Polana and Infulene faults (Figure 4.3). The Polana fault is responsible for slope development in the eastern and south side of Maputo City, and the Infulene fault is responsible for the Infulene River valley which forms the western border of Maputo City. The Polana Fault trends NNE/SSW and runs parallel to the coast (at the foot of the coastal slope) marking the boundary between Ponta Vermelha Formation (TPv) to the west and the Xefina Formation (QXf) to the coast. The down throw is approximately 25 metres to the east. To the south of the city the coastal slope curves inland along the Maputo Estuary leaving 100 to 500 m wide strip of Alluvial Deposits (Qa) between its foot and the estuary Figure 4.5.



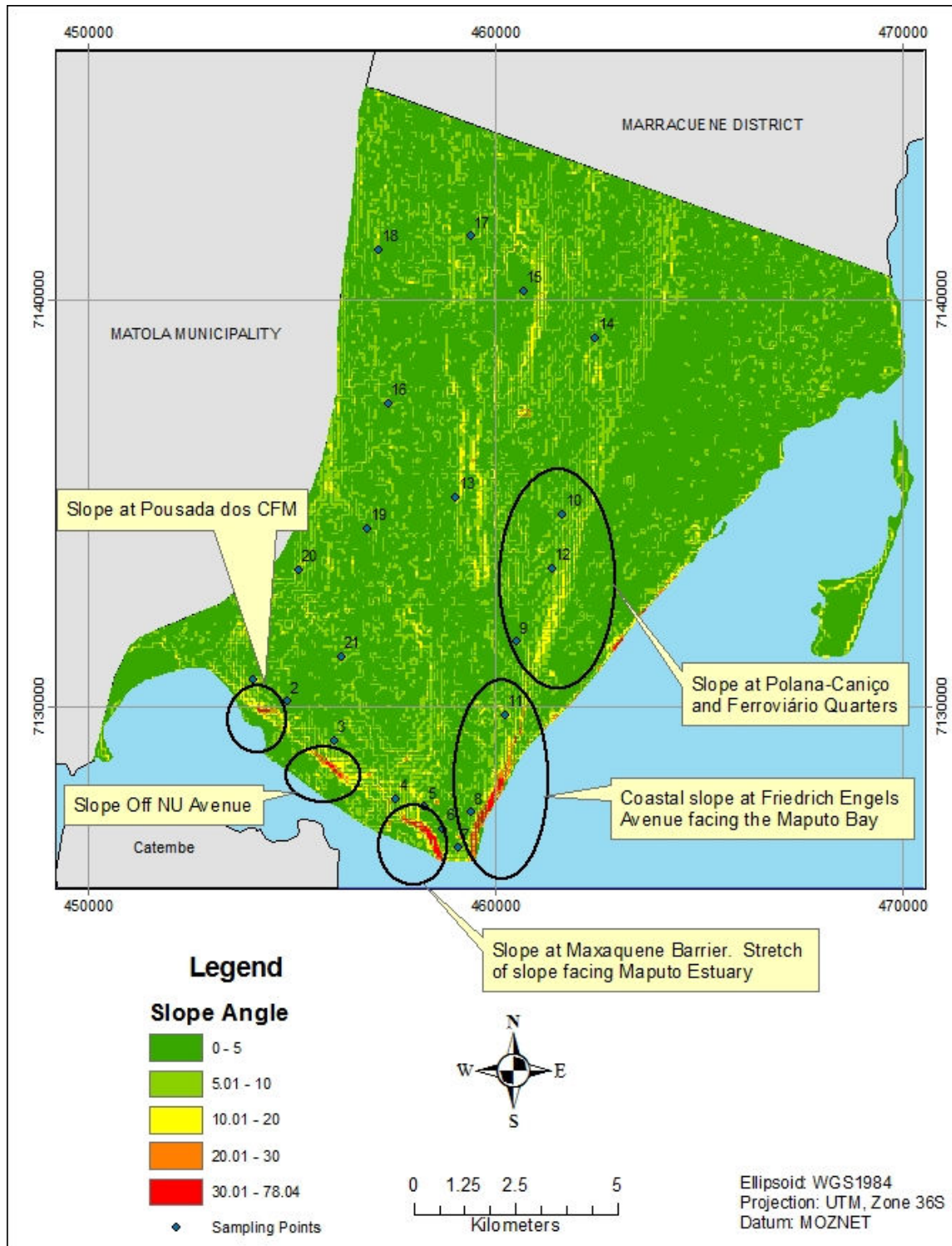


**Figure 4.5** – Location of the main slopes in Maputo City

The height of the natural slope in Ponta Vermelha Formation varies from 20 to 60 m and has three typical angles of significant facets (Forster, 2001). An angle of 5° appears common within Maputo City for quite long straight slopes. An angle of 20° appears to be typical of the long estuarine slope (Nações Unidas Avenue and Pousada dos CFM) and also of the north of the city

(Polana-Canico and Ferroviário Quarters) which is at distance of 2-6 km from the sea. An angle of 30-40° is typical of the coastal slope facing the Maputo Estuary (Maxaquene Barrier) while the slope at Friedrich Engels Avenue facing and close to the sea, where active erosion has only recently ceased, has more than 40° (locally a slope angle of 60° and higher is observed). It is possible that these slope angles are related to the geotechnical strength properties and erosion history of the geological formations.

#### **4.7 – URBAN LAND USE**

Land use is defined as the human modification of the natural environment into built environment such as fields, pastures, and settlements. In Mozambique land use has a number of regulations and legal framework inter-related which establish the conditions for access, use and transfer, as well as the regulation for preservation of natural resources (Cook & Doornkamp, 1990; FAO, 1997; FAO/UNEP, 1999).

The profile of Maputo City is well described in the works of Jenkins (1999) and Jenkins (2000). The distribution of land use is unproportional in the area of Maputo City with urban land use characteristics. Majority of the area is presently used for residential and urban agriculture while land use for economic activities, and social equipment and recreation is in low proportion (Jenkins, 1999). Considerable area in Malhazine Quarter is being used for military purposes where the storage of military equipment was located.

Twenty per cent of the residential land use has comparatively fully developed infrastructure, and a further 27% is in sites and services areas. The unplanned settlements count for the remaining 53% of residential land use (Jenkins, 2000). This author characterises the Maputo City in three different parts (Figure 4.6):

1. Urban Area (Cement City) – is the consolidated urban area developed mainly during the colonial time, although in recent years several housing and infrastructural development schemes have increased considerably the infrastructures in this area. The cement city is characterized by permanent buildings, including high rise and is relatively well provided with basic infrastructure such as roads, rainfall and sewage drainage system. It has high concentration of social equipment and work places, mainly administrative and commercial.
2. Suburban Area – are the unplanned residential settlements with high population density located immediately next to the Cement City. It is composed among others by the historical neighbourhoods of Mafalala, Chamanculo, Minkadjuine and Xipamanine (Figure 1.1) established during the colonial era and have a relatively high number of formal and



informal workplaces. They are characterized by non-permanent construction and with infrastructure and social equipment of lower quality. Recent efforts by the city council have resulted in provision of a drainage system in Mafalala and Minkadjuine Quarters (Figure 1.1) and requalification of parts of the Chamanculo Quarter.

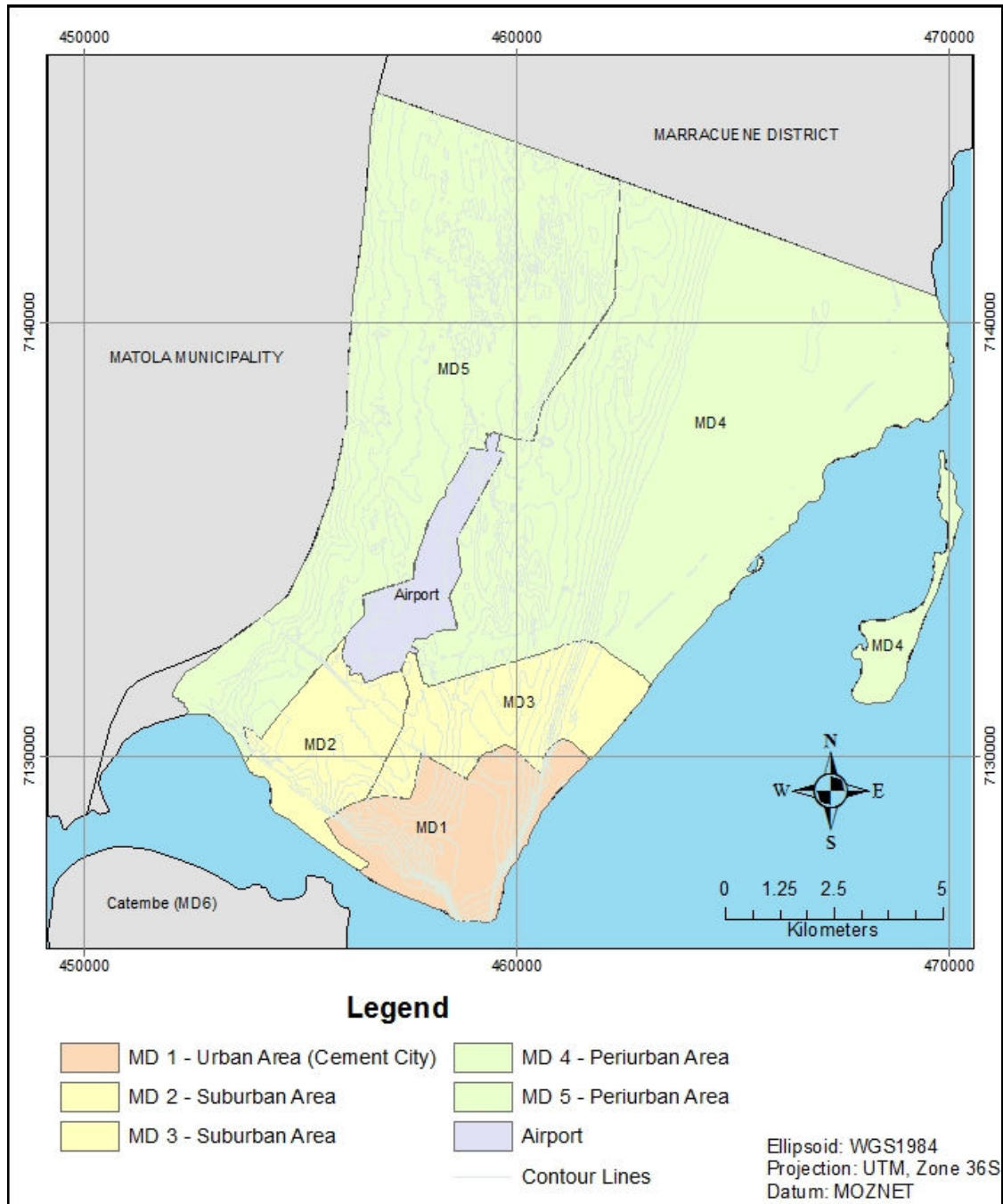


**Figure 4.6** – Distribution of urban form characteristics in Maputo City (Adapted from Jenkins (2000)).

3. Periurban Area – is characterized by a mixture of land use with significant areas of urban agriculture, some industrial development and both spontaneous and

planned residential areas. Like the Suburban area the provision of infrastructure and social equipment is very poor. Population density in the periurban area is the highest of Maputo City.

Housing problems in Maputo City have led to formal territorial expansion for residential purpose. Low-cost land development programme is being developed in the few available land spaces of the town consisting on dividing plots and providing space for roads. Some of these are unsuitable for urbanization as they are located in mangrove or on swampy areas or in low lying areas with groundwater table close to surface. In very past years the supply of land was to relocate people in response to natural disasters – for example gully erosion in Polana-Caniço and Ferroviário Quarters or flooding in Inhagóia Quarter (Figure 1.1) – or to allocate land in Luis Cabral Quarter for new development projects such N4 highway which is part of the Maputo Development Corridor (Jenkins, 1999).

A nucleus of well developed units characterizes the housing stock in the Cement City although many of them need serious rehabilitation. In suburban and periurban areas a mix of large stock units are found, but with predominance of low quality houses generally overcrowded (Jenkins, 2000). Owner occupiers are making house improvements in recent years and the municipality is also upgrading some public infrastructures.

The sewage and drainage system is mixed in Maputo City. The majority of the Cement City uses septic tanks, which have management problems as they are irregularly emptied. The drainage system covers part of the main city and drains directly to the bay part of the collected sewage. The remaining part is directed to a sewage treatment plant located in the Infulene River valley which has virtually low capacity to adequately manage the flow before draining into the Maputo Estuary. The population on the suburban and periurban areas rely on pit latrines as the unique alternative. *“The wide use of latrines has led to a build up of nitrates in the soil and contamination of shallow wells as well as subterranean aquifers”* (Jenkins, 1986). Assuming the low safe water supply coverage in these areas and the consequent use of groundwater, the spread of waterborne diseases are noticed. The poor natural drainage in the low lying areas presently occupied will increase the spread of diseases and risks to health (Jenkins, 2000).

The deficient land use and low enforcement of urban regulations has led to engineering geological problems of Maputo City mainly gully and coastal erosion, landslides and slope stability and flood prone areas.

## 4.8 – PROBLEMS PREVIOUSLY ENCOUNTERED IN MAPUTO CITY

The engineering geological problems of Maputo City are of various types and are spread out across the city. The main problems are erosion (gully and coastal), building damage, landslides and slope instability and flood prone areas. The main sites where these problems occur are herewith described.

### 4.8.1 – Gully and Coastal Erosion

Gully erosion in Maputo City occurs in the Ponta Vermelha Formation which divides the upper and down town. Changes in climatic conditions modified weather patterns and caused extreme rainfall which lead to gully formation in the upper town and sediment deposition in the beach (Figure 4.7). Thus, gullying problems started to be a cause of concern after the extreme rainfall events of 1999 and 2000, in this last case with a precipitation of 400 mm registered in four days. This precipitation is far beyond 132 mm, which is the mean monthly precipitation in the rainy season (November-March). The rain saturated the slopes and raised the water table resulting in flooding that caused movement. Combination with various other factors such as soil characteristics, poor urban planning and topography can have contributed to gullying failure and are discussed in full in Chapter 6.



**Figure 4.7** – Gullying failure in a built up area of Polana-Caniço Quarter in 2000 which caused destruction of a number of houses as it eroded. Gabion baskets of rhyolite were used to protect the floor of the gully (left) and depositional area of the eroded red sediments (right)

The main areas of gullying failure are described:

**a) Polana-Caniço Quarter.** The Polana-Caniço residential area has most of its area crossed by gullies. The gullies are extremely large, deeply cut, 1 to 15 m deep, very steep with side slopes generally up to 60° but locally steeper (Figure 4.7). They are W-E oriented but some follow the orientation of the roads, mainly the Julius Nyerere Avenue (Figure 4.8).

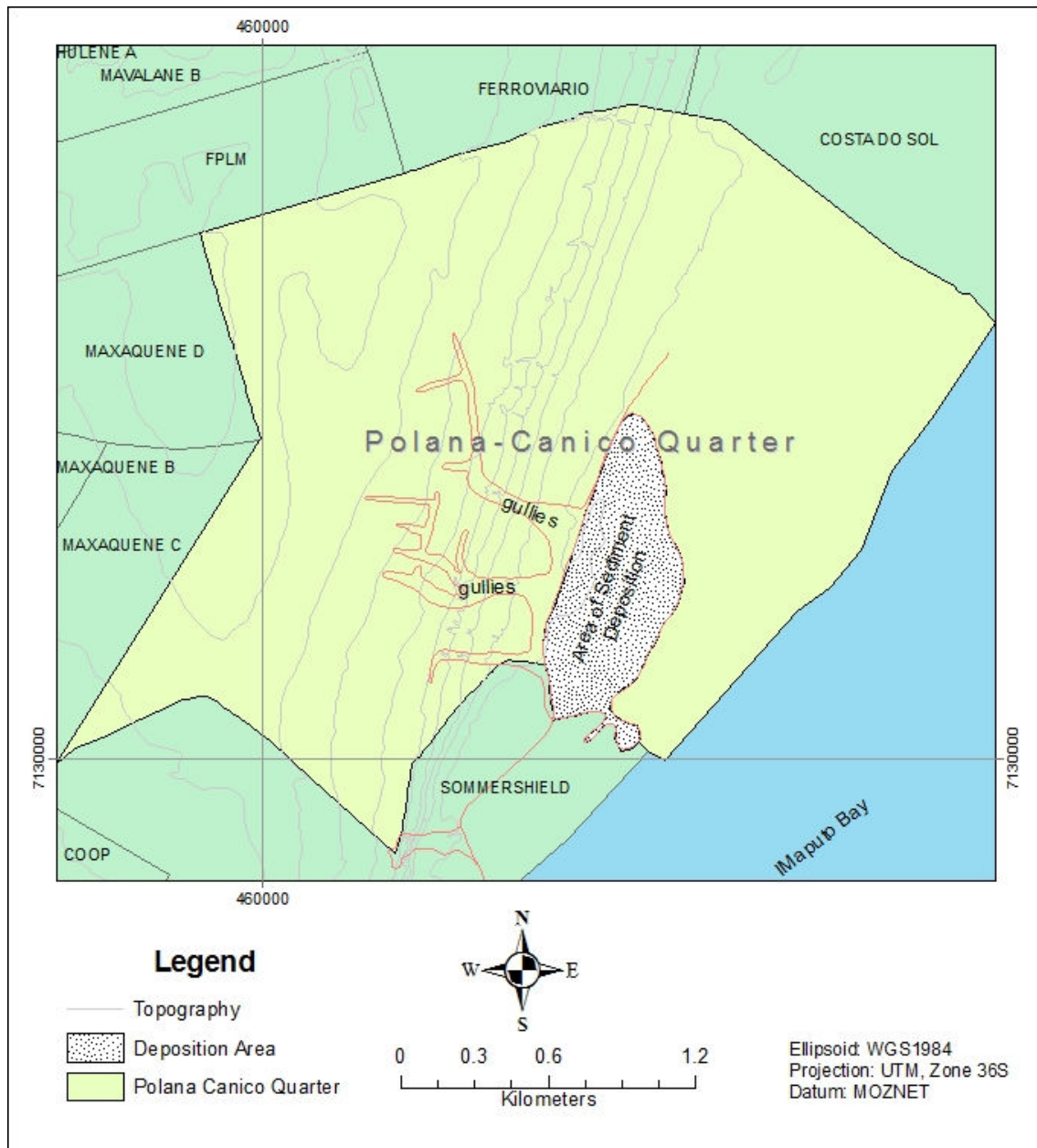


**Figure 4.8** – Location of gully failure in Polana-Canico Quarter in 2000

Gully failure has occurred in a built up area destroying a number of houses as it eroded. The housing development in the area is informal, unplanned and characterized by low quality houses. As any other informal settlement it is inhabited by the poor who have no access to tenured land or their own. The infrastructure and services are inadequate. Extensive remedial works have been completed soon after gully failure occurs. Gabion baskets of rhyolite had been used to protect the floor of the gullies, to support the base of the sides and to protect them from further erosion (Figure 4.7). The sides of the gullies are still uncovered due to their steepness and can be unstable in future events of heavy rainfall. Some gullies are being used as a solid waste dumping site without taking special attention to the minimum requirements for a landfill



site (e.g. leachate collection system, distance from residential area, impermeability of the place, etc). This can have implications in the future as waste can block the water flow and leachate contaminates the groundwater. People from the surrounding areas run into the site trying to get something of value (Figure 4.9).



**Figure 4.9** – Gully filled with solid waste with people searching for useful things

**b) Ferroviário Quarter.** Extremely large gullies developed in 2000 and were exacerbated by the 2003 rainfall event. Deep and steep sided, they descend rapidly to the flat ground below. Common to these gullies are their starting points in the drainage system of the railway going out of Maputo City. No remedial work has been done along the gullies, but only at the back slope (Figure 4.10).

**c) Nações Unidas (NU) Avenue.** The gully is in the slope in the north side of the Nações Unidas Avenue (Figure 4.11) and is generally straight and uniform facing south and the Maputo Estuary. Slope angle appeared to be about 20-25° which implies a gullying failure rather than a slump. Also the depth was greater than would be expected for a slump and the width of the failure is too narrow for the depth. The municipality has done extensive remedial work by supporting the slope with gabion baskets filled with rhyolite.





**Figure 4.10**– Extremely large gully in Ferroviário Quarter (left) and remedial work at the beginning of the gully in Ferroviário Quarter (right)



**Figure 4.11** – Gabion baskets filled with rhyolite used to support the slope at ONU Avenue

The gully was probably caused by failure of the drainage system that caused leakage in the top of the slope. Water seepage is also seen at the base of the slope. The remedial work undertaken to protect the gully appears to be effective for the problem.

The coastline around Maputo City is dynamic due to shifting of sand or its removal from a low-lying beach by longshore currents. It has moved tens of meters inland in the last two decades and shows clear signs of coastal erosion. The signs of coastal erosion are observed along the



Marginal Avenue, namely uncovered roots of trees, broken retaining walls and destruction of the Marginal Avenue (Figure 4.12).

Some measures have been undertaken to control coastal erosion such as groins and retaining walls at Miramar Beach and rip-raps in front of Costa do Sol Restaurant (Figure 4.13).



**Figure 4.12** – Signs of coastal erosion in Maputo City: (left) uncovered roots of trees along Marginal Avenue; (right) Destruction of the Marginal Ave.



**Figure 4.13** – Measures undertaken to control coastal erosion in Maputo City: (left) Groins at Miramar Beach; (right) Riprap in front of Costa do Sol Restaurant.

#### **4.8.2 – Building Settlement**

Building settlement is another problem occurring in Maputo City which results in their leaning due to differential settlement. The affected buildings are the ones with 8-10 floors (25-40 m high), tilting 150 to 400 mm sideward when measured at the top. These buildings are located along the Julius Nyerere Avenue at the stretch of road closest to the coastal slope located on its east side. Figure 4.14 shows the site location of the problematic buildings which are described below.

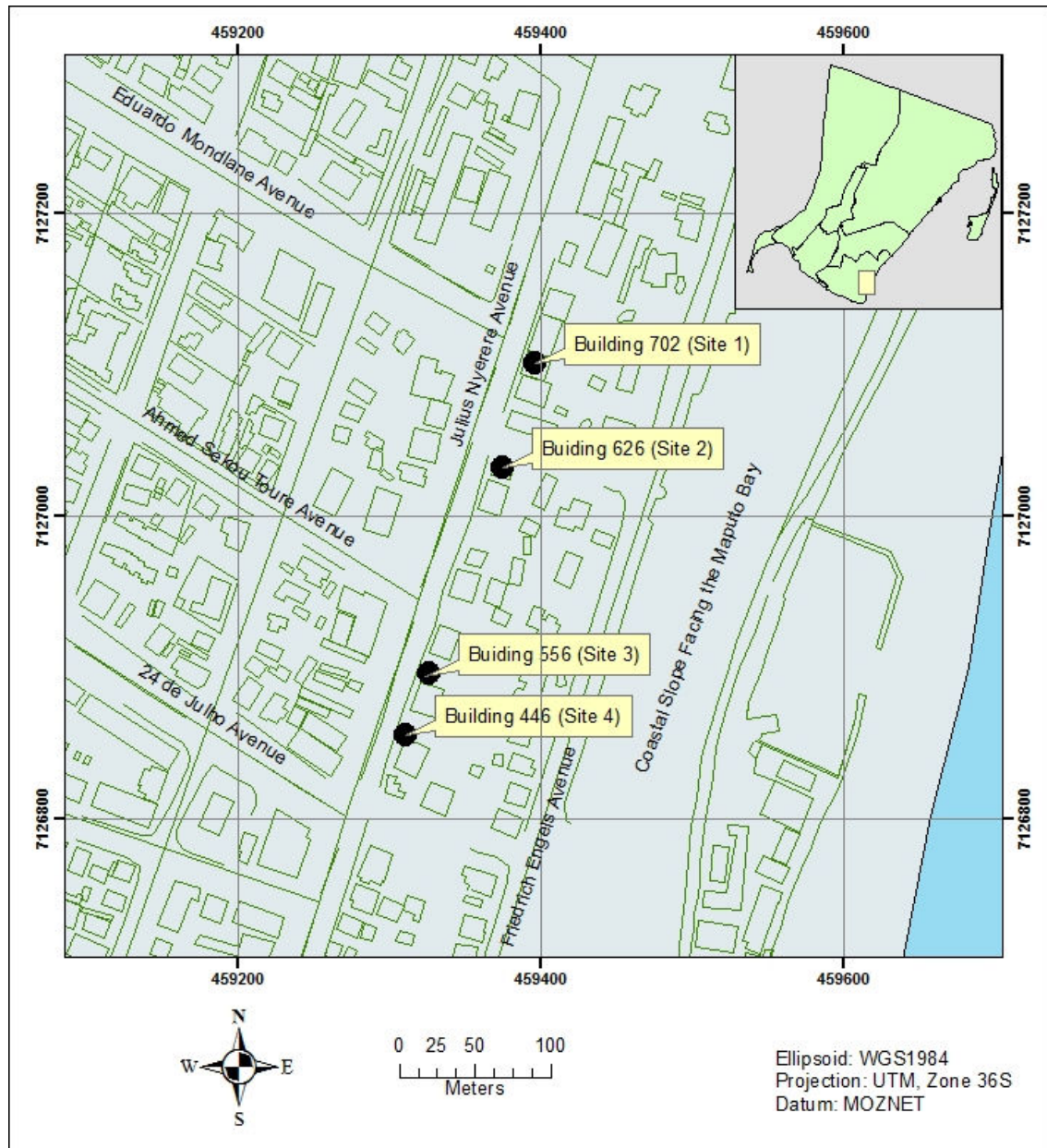


**Figure 4.14**– Site location of the problematic buildings covered in this study in Maputo City.

a) Site 1 – This building is located at 702, Julius Nyerere Avenue, by the side of the Embassy of Portugal and is the most severely tilted and causing most concern. It comprises 10 floors, is approximately 30 m high and 15 m wide, and has raft foundations. It was built in 1970 but tilting started at the end of 1990s (Ms Ana Nóvoa, personal communication, 29<sup>th</sup> November, 2003). The backward tilt, to the East, is 400 mm measured at the top of the building (Figure 4.15) and the side tilt is 200 mm to the South. At the back of the building there is a single story construction attached to the main building. The backward and sideways rotation of the building caused it to crush the attached engineering structures (Figure 4.16). The damage is in the form of cracks also reported at the boundary wall. The raft foundation of the building is



considered to be related to the absence of cracks in the building itself.



**Figure 4.15**– Frontal view of a problematic building at Site 1 (left). Backward (eastern) displacement observed from the top of the building (right).



**Figure 4.16**– Cracks on a single story construction on the North hand side of a building on Site 1 as a result of backward and sideways rotation of the building.

The problem of tilting started to be strongly noticed in 2001 (in the media as well). A study of the causes of the problem was recommended by the Ministry of Public Works and Habitation and undertaken by the Engineering Laboratory of Mozambique (Ms Ana Nóvoa, personal communication, 29<sup>th</sup> November, 2003). The study reported a leakage of 60 to 70 thousands of litres of water per day from damaged underground water reservoirs and recommended their

replacement with above ground reservoirs. A topographic study was also undertaken to measure the rate of tilting but its results were never disclosed.

b) Site 2 – The building is located at 626, Julius Nyerere Avenue, in front of Avenida Hotel comprising 8 floors and is approximately 25 m high and 13 m wide. It has tilted front (to west) relative to its neighbour by about 150 to 200 mm at its top and 100 mm to the side (north). This building has also settled 100 mm as seen from its front. Signs of possible water leaks into the ground from a service area were observed. Additional water leaks occur from the broken discharging pipe, not connecting to the sewerage system (Ms Julia Macamo, personal communication, 29<sup>th</sup> November, 2003). The north side of the building is therefore wet.

c) Site 3 – The building is located at 556, Julius Nyerere Avenue and comprises 8 floors and is about 25 m high and 14 m wide. The building appears to have tilted back (east) relative to its neighbour by about 150 to 200 mm at its top.

d) Site 4 – The building has 8 floors and is about 40 m high and 15 m wide and is located at 446, Julius Nyerere Avenue. It is tilting back (east) by about 300 to 400 mm and to the left (West) by about 0.1 m relative to its neighbour building.

#### **4.8.3 – Slope Instability**

Maputo City is divided in two distinct topographic areas: down town and upper town. The difference in height between the two areas varies from 20 to 60 m. The overall slope angle is between 20 and 40°, but it can locally reach 60° or more. Slope instability events occur on these slopes in the Ponta Vermelha Formation and are below described.

**Nações Unidas Avenue.** The slope is along this avenue located in the south of the city where the coastal slope curves inland along the Maputo Estuary leaving 100 to 500 m wide strip of Alluvial Deposits (Qa) between its foot and the estuary. The slope is at an angle of about 20-25° and is, in general, straight and uniform when viewed from south to the north. It is vegetated with grass and shrubs. This slope shows a typical case of a shallow landslide with a crack at the middle with a vertical displacement of 30-40 cm (Figure 4.17).

The slope appears unstable with evidence of active movement along the crack, because of it, remedial measures were undertaken by the municipality through the construction of gabions along the base of the slope. Evidence of water seepage is observed on the base of the slope. This water can be the trigger event of the landslide.



**Figure 4.17**– Shallow landslide along ONU Avenue with a vertical displacement of 30-40 cm

**Maxaquene Barrier.** This stretch of slope is also facing south and the Maputo Estuary, and starts some tens of meters east from the Vladimir Lenine Avenue up to the area behind the Mozambican Television (TVM) Building. This stretch of slope is separated from the estuary by a coastal plain of alluvium about 500 m wide. It is thickly vegetated with tall grass and not easily accessible. The overall slope angle is about 30 degrees but locally steeper and is, in general, not strait when viewed along the slope to the north. The slope is stable with no evidence of active movement or any evidence of water seepage on the slope.

**Friedrich Engels Avenue.** This area of active landslides is on the coastal slope about 40 metres high, angle of about 60° but locally steeper and face southeast and the Maputo Bay. It is thickly vegetated with shrubs and big trees and includes two active or recently active landslides. The most recent failure comprises a high angle slump that has moved from the top of the slope to rest above a slump earth flow at the bottom. This can be viewed by a gap of thick vegetation in an area of about 30 m wide (Figure 4.18). Additional evidences of movement are at the top of the slope. It has been cut back, with a masonry wall been constructed to form both a retaining wall (5 m height) and a short promenade. The retaining wall had been repaired after it had started to bulge (Figure 4.19). Other evidence includes distortions of the drainage system below the retaining wall and destruction of the protection wall in the north side of the promenade



(Figure 4.19). This evidence strongly suggests that this section of the slope is in an unstable state, and will continue to suffer minor failure unless stabilised.



**Figure 4.18**– Slump in coastal slope deposits marked by Gap of thick vegetation (30 m wide) in the slope along Friedrich Engels Avenue (photo taken from the Marginal Avenue)

The landslides problems in Friedrich Engels Avenue were first registered after the heavy rainfall that occurred in February 2000. A crack opened in the pavement allowed water to infiltrate the top of the slope. Most of this water was flowing in the Friedrich Engels Avenue which has few water drains. Thus, it is assumed that water flowing into the top of the slope was the process which triggered the landslide. The presence of water raised the water pressure and reduced the soil's shear strength. Additional factors can also be behind the failure, namely the existence of walls and paved surfaces with a weak drainage system, and head loading (construction of buildings at or near the top of a slope).



**Figure 4.19**– Evidence of movement at the top of the slope along Friedrich Engels Ave. (Left) retaining wall repaired after it had started to bulge. The dark part of the wall is the new; (Right) Protection wall in the North side of the promenade destroyed by the slope movement

#### 4.8.4 – Flooded Areas

Maputo City has areas prone to flooding in events of rainfall. The causes of flooding in these areas are mainly of geomorphological and geological nature. The most representative areas with these problems are the Inhagóia and Mafalala residential areas.

**Inhagóia Residential Area.** Extreme rainfall events in Maputo City result in inundation in the Inhagóia Quarter. The 2000 flood event was the main event but this problem has been registered several times. About 60.000 m<sup>2</sup> in a densely populated area were covered by water (Figure 4.20) leaving tens of houses submerged as well as roads, market and several public services. The affected area is a basin in shape and water from the neighbourhood flows to it. The area remains flooded for several months before the water evaporates.

Apart from the topographic shape of the affected area, many factors can be considered as the reasons for the problem. The surface sandy layers in Inhagóia Quarter are underlain by clayey layers which have low permeability. These clayey layers from the Machava Formation (QMc) underneath the sandy layers from the Congolote Formation make water infiltration nearly impossible.

**Mafalala and Minkadjuine Quarter.** This area is also residential, but built in a swamp. The place is therefore wet, being normally flooded during the rainy season every year. Some remedial works were done by the municipality in 1980's with the introduction of a full drainage system. Maintenance of the system is not regular, reducing its impact.





**Figure 4.20**– Flooded area in Inhagóia Quarter after the 2000 floods

## **CHAPTER 5**

### **ENGINEERING GEOLOGICAL CHARACTERISTICS AND GEOTECHNICAL PROPERTIES OF SOILS**

#### **5.1 INTRODUCTION**

Engineering geology and geotechnical engineering make a joint effort to form geotechnics. The degree of variability of the geotechnical characteristics found throughout Maputo City and within each geological unit was determined in order to understand the urban geological problems occurring in the city.

This chapter presents the description of geological formations which are mainly unconsolidated materials with soil like properties. The main laboratory results are given with interpretations in terms of engineering geological characteristics of Maputo City. The distribution patterns and spatial trends of the physical properties and their relations to the geology are discussed and related to engineering and construction. The shear strength and consolidation tests gave the standard geotechnical properties of the soils, and correlations are made between them and the engineering geological characteristics.

Figure 5.1 shows the sampling point distribution in the study area and Table 5.1 presents details of each sampling point. Whilst it was intended to cover all geological formations of Maputo City, efforts were concentrated on sampling the geological formations with development infrastructures on them. The Alluvial Deposits which occupy a large area in the North-Eastern part of the study area is a swampy area with no development observed at all. It was decided to apply no efforts in an area without any development perspective. The engineering geological characteristics and the geotechnical properties of each sample are summarised in Appendix A.

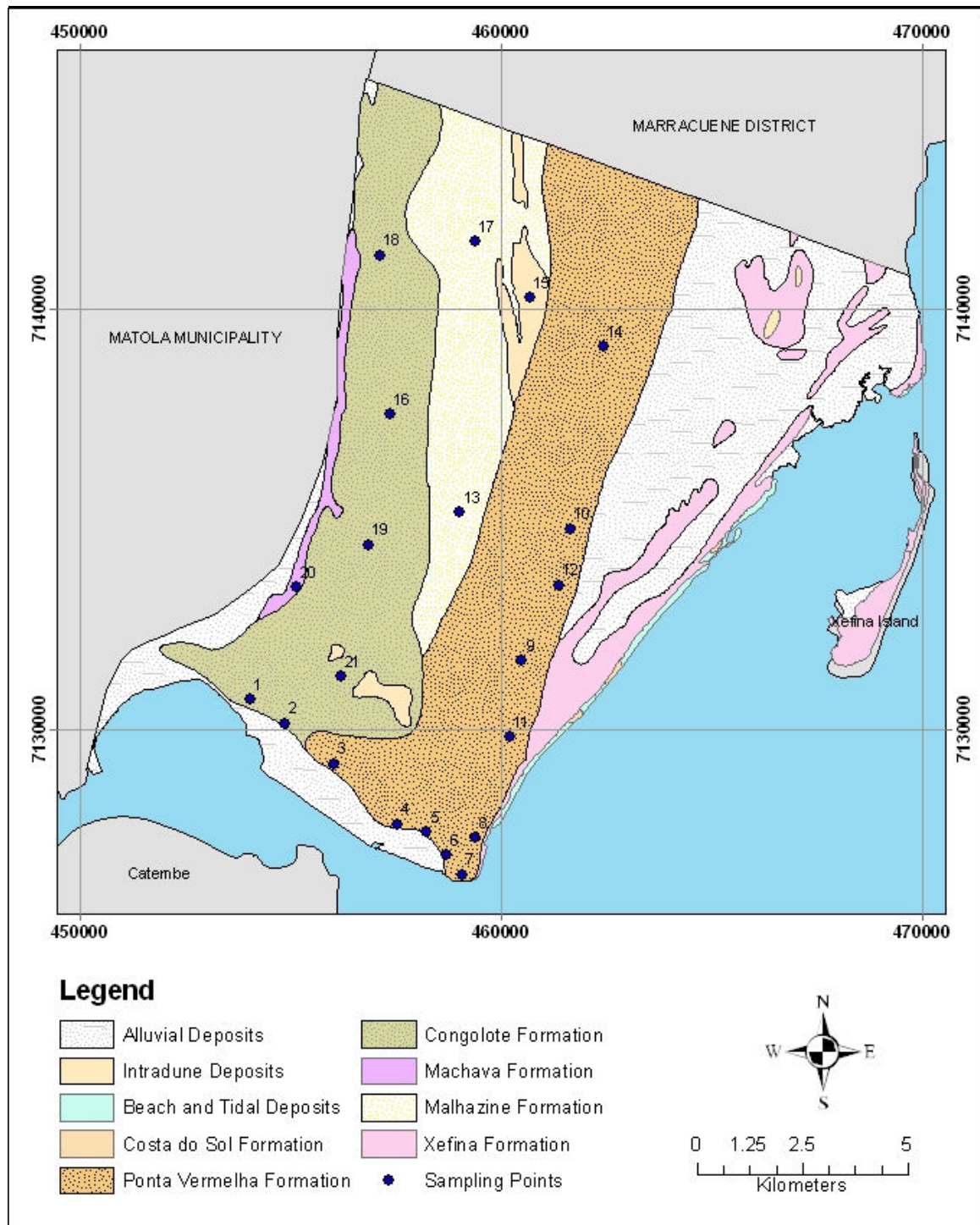


**Figure 5.1** – Geological formations and Sampling sites in Maputo City



## 5.2 DESCRIPTION OF SOIL TYPES

An accurate description of the soil profile is a basic requirement in site investigation for engineering purposes. In order to properly describe the profile, the soil was examined in its natural state. Six aspects were taken into account in the *in situ* soil description namely moisture content, colour, consistency, soil structure, soil texture and soil origin (MCCSSO) as recommended by the guidelines for soil and rock logging in South Africa (Brink & Bruin, 2002). Particulars of this description are also given by Jennings *et al.* (1973), Brink *et al.* (1984) and Fookes (1997).

**Table 5.1** – Details of the each sampling site

| Sample N°. | Location  | Sample Depth (m) | Elevation (m) | Geological Unit |
|------------|---|------------------|---------------|-----------------|
| 3          | Off Nações Unidas Av.                             | 1.6              | 43            | TPv             |
| 4          | Off Vladimir Lenine Av.                           | 2.4              | 31            | TPv             |
| 5          | Maxaquene Barrier/By the Side of Girassol Hotel   | 2.0              | 62            | TPv             |
| 6          | Maxaquene Barrier/In front of Escola Nautica      | 1.4              | 58            | TPv             |
| 7          | Maxaquene Barrier/Off Marginal Av.                | 1.4              | 48            | TPv             |
| 8          | Off Friedrich Engels Av./Jardim dos Namorados     | 1.4              | 56            | TPv             |
| 9          | Polana-Caniço Quarter/ Gully Area                 | 1.0              | 43            | TPv             |
| 10         | Ferrovial Quarter/Gully Area                      | 0.9              | 34            | TPv             |
| 11         | Off Julius Nyerere Av/Entrance of UEM Main Campus | 1.2              | 38            | TPv             |
| 12         | Ferrovial Quarter/ Gully Area                     | 1.0              | 34            | TPv             |
| 14         | Mahotas Quarter                                   | 2.1              | 33            | TPv             |
| 1          | Luis Cabral Quarter                               | 2.0              | 31            | QCo             |
| 2          | Pousada dos CFM/Top of Slope                      | 1.1              | 28            | QCo             |
| 16         | Benfica Quarter/Missao Roque                      | 1.8              | 31            | QCo             |
| 18         | Zimpeto Quarter/Off N1 (400 m West)               | 2.35             | 29            | QCo             |
| 19         | 25 de Junho Quarter/Close to the Airport          | 1.85             | 28            | QCo             |
| 21         | Inhagóia Quarter                                  | 1.5              | 26            | QCo             |
| 13         | Hulene Quarter                                    | 2.3              | 37            | Qma             |
| 17         | Zimpeto Quarter/Matendene                         | 1.9              | 47            | Qma             |
| 15         | Magoanine Quarter                                 | 1.7              | 32            | Qi              |
| 20         | Inhagóia Quarter                                  | 0.9              | 18            | Qmc             |

QCo: Congolote Formation; TPv: Ponta Vermelha Formation; QMa: Malhazine Formation; Qi: Intradune Deposits; QMc: Machava Formation.

The *in-situ* moisture condition of the soil types in Maputo City varies from slightly moist to wet being controlled by topography and the soil texture. Sampling occurred at the end of rainy season (March) therefore it is assumed that the moisture conditions were influenced by the climatic conditions. Wet soil samples were identified in depressions where the groundwater table is located

near the surface. This is the case of Samples 15 and 20, the first located in the intradune depression and the second in the area previously flooded in Inhagóia Quarter. Meanwhile, the very moist samples were found in the Ponta Vermelha Formation which in general has higher fine particles compared with other geological formations covered in this study. Moisture retention capacity is high in soils with high content of fine particles.

Colour is a very important factor in the identification of tropical soils and is linked to the chemical composition of the soil particles or to mineralogical changes, oxidising/reducing conditions and leaching (Fookes, 1997). Colour may also be due to groundwater conditions and have relation to drainage. For this reason the valid colour of the soil formation is the one observed at natural moisture content (Brink *et al.*, 1984). The Ponta Vermelha Formation is generally red in colour but shows different tonalities ranging from dark to brownish and whitish. The colour difference is a consequence of red ferruginous crust, observed locally and possibly of lateritic origin, which grades downwards into carbonated and white sand, horizontally stratified (Momade *et al.*, 1996). Colour distribution in Maputo City is particularly related to the distribution of soil types. Thus, soils from the Congolote Formation show lighter colours, whitish and light grey and brown. Soils from Malhazine Formation are brown to yellowish brown; the Intradune deposits are whitish brown while the Machava Formation is dark brown. Most of the soil colour distribution in Maputo City is related to the mineralogical composition of the soils types excepting Ponta Vermelha Formation where iron enrichment occurred to form ferricrete.

Consistency of a soil mass is the characterization of the hardness or denseness of a soil structure as a result mainly of the stress history. The proposed classification of Jennings *et al.* (1973) was used in this description (Table 5.2).

**Table 5.2** – Consistencies of non-cohesive soils (After Jennings *et al.*, 1973)

| Consistency  | Description  | Typical dry density ( $\text{kNm}^{-3}$ ) |
|--------------|--|---|
| Very loose   | Crumbles very easily when scraped with geological pick   | Less than 14.50                           |
| Loose        | Small resistance to penetration by sharp end of geological pick  | 14.50 to 16.0                             |
| Medium dense | Considerable resistance to penetration by sharp end of geological pick   | 16.0 to 17.50                             |
| Dense        | Very high resistance to penetration of sharp end of geological pick – requires many blows of pick for excavation | 17.50 to 19.25                            |
| Very dense   | High resistance to repeated blows of geological pick – requires power tools for excavation                       | More than 19.25                           |

Soil consistency distribution in Maputo City is consistent with the geological formations being Ponta Vermelha the one with high consistency soils. In this formation a large range of soil consistency classes can be found, from very loose to dense. Soils derived from other geological formations are only very loose to loose. The relatively high fines content (silt and clay) in the Ponta Vermelha Formation may be responsible for the higher soil strength compared to other geological formations. This is consistent with the strength parameters of the tested samples as discussed in Section 5.4.2.

Soil structure is described by the arrangement and assemblage of the individual solid particles of the soil (gravel, sand, silt, and clay) which may result in the presence or absence of fissures or other planes of weakness in the soil mass (Brink *et al.*, 1984; Brink & Bruin, 2002). The Ponta Vermelha Formation is intact and homogeneous and shows no cracks in the soil structure. The deposit consists essentially of a well distributed material and the humic topsoil horizon which supports vegetation is thin 15-20 cm thick. In the Congolote and Malhazine Formations this top horizon is thicker, reaching 80 cm and present lenses of different colours but the same grain size.

Soil texture is a characteristic which relates the grain size and shape of particles of a soil horizon. It is described using the established standard descriptions with respect to grain size and shape. For grain size the basic textural classes are gravel, sand, silt and clay (Brink *et al.*, 1984) while for shape they are under three characteristics: angularity, form and surface texture (Fookes, 1997). Two distinct situations are observed *in-situ* through field descriptions; the Ponta Vermelha Formation is likely to be well graded presenting a wide range of grain sizes and larger combinations of two or more grain size classes, e. g., sand mixed with relatively high silt and clay or gravel content. Descriptions like silty fine to medium sand, clayey and silty fine to medium sand or gravely medium to coarse sand are common in the field descriptions. This is not the case with other soils types where one interval of grain size classes was found (e. g. coarse to medium sand). The field characterization was then confirmed by the particle size distribution obtained with sieving test in the laboratory (Section 5.3.1).

Ferricrete (an iron-rich duricrust consisting of sand and gravel cemented into a hard mass by iron oxides) found in the area of samples 6 and 7 is composed dominantly of quartz and feldspars. Fookes (1997) states that as quartz is very resistant to weathering it has an important role in influencing the texture of the secondary products by remaining as quartz particles while silica in solution can lead to the formation of silcrete duricrusts. Feldspars either slowly weather to clay

minerals or release hydrated oxides of aluminium and small amounts of iron. The presence of gravelly particles on this area mainly from unweathered ferricrete can be related to the environmental conditions which complement the geological information on the weathering process.

### **5.3 – PHYSICAL PROPERTIES AND SOIL CLASSIFICATION**

#### **5.3.1 – Particle Size Distribution**

A soil consists of a mixture of individual particles of various sizes (solid phase), water and air. Particle size analysis aims at grouping the solid particles into separate size ranges and determine the relative proportions of each size range. Particle size analysis “expresses quantitatively the proportions by mass of the various sizes of particles present in the soil” (Head, 1984). This is a basic index test for soils, especially coarse-grained soils, as it determines the main soil component (gravel, sand, silt or clay sizes) and which of these size ranges is expected to control the engineering properties (Head, 1984). It is important to stress that the engineering behaviour also depends on factors other than size of particles, such as mineral type, structure, shape, grain packing and shape, geological history, which cannot be assessed from particle size.

Table 5.3 presents the grain size analysis of the tested soil samples and the textural characteristics. This Table 5.3 shows that clay content in the tested soils of Maputo City is very low ranging from 0.08 to 1.52 %; the silt content ranges from 1.80 to 27.09% and the sand content from 71.36 to 96.45%.

Soils almost always contain a variety of particle sizes as they rarely fall completely within only one of the soil categories of particle size classification; Therefore, the effective way to represent the distribution of particle sizes in a particular soil is the grain-size distribution curve, a plot of grain diameter against the percentage of the solids by weight smaller than the diameter (Coduto, 1999). Soils in Maputo City are in the range of coarse- to very fine-grained sand with low clay percentage, as shown by the grain-size distribution Curve A in Figure 5.2 (the classification by the unified soil classification system is given in Section 5.3.6). This steep grain-size distribution curve is the typical grain-size distribution of the soils of Maputo City. On the other hand, Curve B (with a wider range of particle sizes) represents the two samples that show a noticeable percentage of gravel, 11.99% and 12.87% for samples 6 and 7 respectively. These well-graded soils are located close to the section of Ponta Vermelha Formation with ferricrete (sites of samples 6 and 7).

**Table 5.3** – Grain size analysis and the textural characteristics of the tested soil in Maputo City

| Geological Unit | Sample N°. | Gravel (%) | Sand (%) | Silt (%) | Clay (%) | Coefficient of Uniformity ( $C_u$ ) | Coefficient of Curvature ( $C_c$ ) | Sorting Coefficient |
|-----------------|------------|------------|----------|----------|----------|-------------------------------------|------------------------------------|---------------------|
| TPv             | 3          | 0.00       | 84.6     | 14.1     | 1.4      | 2.9                                 | 2.0                                | 1.2                 |
|                 | 4          | 0.00       | 90.5     | 9.0      | 0.5      | 3.3                                 | 2.5                                | 1.2                 |
|                 | 5          | 0.3        | 93.7     | 5.7      | 0.3      | 1.6                                 | 1.1                                | 1.2                 |
|                 | 6          | 12.0       | 86.1     | 1.8      | 0.1      | 1.4                                 | 1.0                                | 1.1                 |
|                 | 7          | 12.9       | 79.1     | 7.6      | 0.3      | 3.0                                 | 1.2                                | 1.6                 |
|                 | 8          | 0.0        | 84.2     | 15.1     | 0.7      | 6.8                                 | 3.7                                | 1.6                 |
|                 | 9          | 0.00       | 83.9     | 15.2     | 0.7      | 7.4                                 | 4.5                                | 1.3                 |
|                 | 10         | 0.00       | 86.5     | 12.8     | 0.7      | 5.4                                 | 3.7                                | 1.4                 |
|                 | 11         | 0.00       | 93.3     | 6.4      | 0.3      | 1.8                                 | 1.3                                | 1.2                 |
|                 | 12         | 0.00       | 90.4     | 9.1      | 0.5      | 3.0                                 | 1.9                                | 1.3                 |
|                 | 14         | 0.1        | 90.7     | 8.7      | 0.5      | 2.0                                 | 1.1                                | 1.2                 |
| QCo             | 1          | 0.0        | 71.4     | 27.1     | 1.5      | 12.2                                | 1.6                                | 2.2                 |
|                 | 2          | 0.00       | 92.7     | 6.9      | 0.4      | 2.3                                 | 1.2                                | 1.3                 |
|                 | 16         | 0.00       | 93.7     | 6.1      | 0.2      | 1.6                                 | 1.4                                | 1.2                 |
|                 | 18         | 0.0        | 93.4     | 6.2      | 0.4      | 1.6                                 | 1.1                                | 1.2                 |
|                 | 19         | 0.00       | 93.9     | 5.9      | 0.4      | 1.5                                 | 1.0                                | 1.2                 |
|                 | 21         | 0.0        | 88.3     | 11.2     | 0.5      | 4.8                                 | 3.3                                | 1.2                 |
| QMa             | 13         | 0.00       | 94.6     | 5.1      | 0.3      | 1.7                                 | 1.2                                | 1.2                 |
|                 | 17         | 0.00       | 93.1     | 6.7      | 0.3      | 1.6                                 | 1.2                                | 1.2                 |
| Qi              | 15         | 0.00       | 96.5     | 3.3      | 0.2      | 1.5                                 | 1.0                                | 1.2                 |
| QMc             | 20         | 0.0        | 94.3     | 5.4      | 0.3      | 1.6                                 | 1.1                                | 1.2                 |

QCo: Congolote Formation; TPv: Ponta Vermelha Formation; QMa: Malhazine Formation; Qi: Intradune Deposits; QMc: Machava Formation.

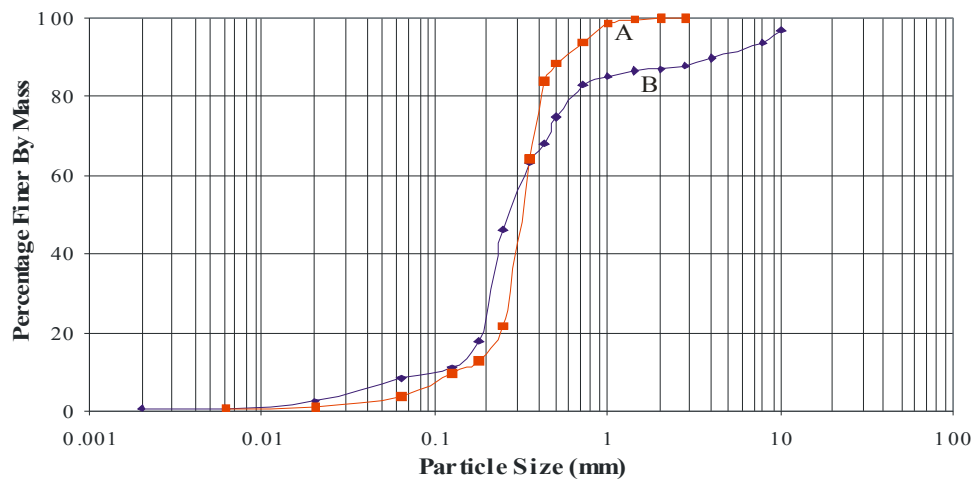


**Figure 5.2** – Typical grain-size distribution curves of the soils of Maputo City. Curve A, steep curve but with relatively well graded soil (Sample 2); Curve B, flatter curve with a wide range of particle sizes (Sample 7).

Steepness and smoothness of the grain-size distribution curve is supported respectively by the *Coefficient of Uniformity*,  $C_u$ , and the *Coefficient of Curvature*,  $C_c$  obtained from the curves. These coefficients were calculated for the soils of Maputo City based on the D-sizes, the particle diameters that correspond to certain percent-passing values for a given soil.

$$C_u = \frac{D_{60}}{D_{10}} \quad (\text{Eq. 5.1})$$

$$C_c = \frac{(D_{30})^2}{D_{10}D_{60}} \quad (\text{Eq. 5.2})$$

These indexes indicate soil gradation which is important aspect in determination of engineering properties. Geotechnical Properties that can be indicated from soil gradation (obtained from the  $C_u$ ) are the soil compressibility, shear strength and hydraulic conductivity (Holtz & Kovacs, 1981; Coduto, 1999).

Soils are considered to be poorly graded (steep curves) if  $C_u$  is less than 2, while well-graded (flat curves) have high values (Braja, 2006). Poorly graded soil is also used to name soils deficient in certain sizes (gap-graded material) while uniformly graded is used for the ones in which the majority of the grains are very nearly the same grain size (Lee, 1983). The  $C_u$  for this case is not much more than 1.0. Soils with smooth curves have  $C_c$  values between about 1 and 3, while irregular curves have higher or lower values (Lee, 1983; Coduto, 1999). Soils of most of the investigated sites have smooth grain-size distribution curves.

The investigated sites 5, 6, 11, 13, 14, 15, 16, 17, 18, 19 and 20 show a misleading  $C_u$  value therefore the conclusions taken from it may not be straightforward. These sites show very steep grain-size distribution curves in the area of medium to fine sands, what would likely give  $C_u$  less than 2, but this is not the case due to the lower clay content in every soil sample. Consequently they are steep curves but relatively well graded soils from sand to clay.

There is no evident difference in terms of grain size distribution in the sampled geological formations therefore it is not possible to explain how the particle size data relates to the nature of the various formations. However, few particularities are observed in some geological units but these are not correlated to the particle size distribution.

The Ponta Vermelha Formation is relatively well-graded, presenting a wide range of grain sizes

from gravel to clay. This is particularly true for samples 5, 6 and 7 located in the area where ferricrete is found in the surface. The gravel content reaches values as high as 11.99 and 12.87% for samples 6 and 7 respectively. From east to west of the geological formation a gradual sand content reduction is observed as can be seen sequentially from samples 5, 4 to 3 with 93.7, 90.5 and 84.6 % respectively (Figure 5.3). There is no clear evidence of the cause of this apparent finer westward trend of the Ponta Vermelha Formation however, the presence of red ferruginous crust (ferricrete) at a depth of 3 and 5 m (Macedo, 1971) caused by the local presence of conglomerates with iron oxides justifies the trend. This is not true for silt and clay content where enrichment occurs. In the south- to north direction there is a general trend for enrichment with sand while the silt and clay contents remain with very low variations.

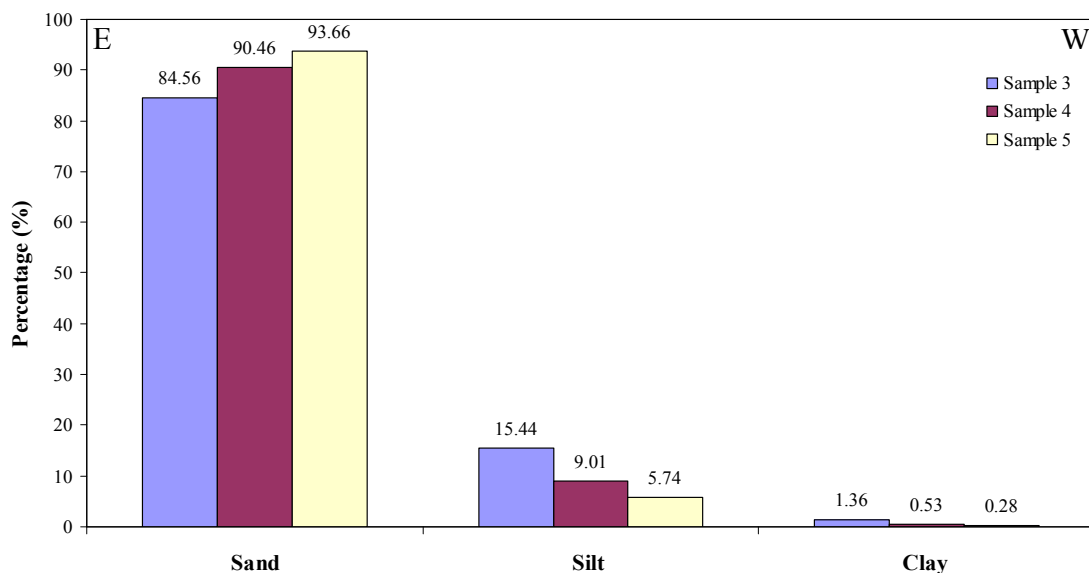


**Figure 5.3** – Geographical trend on the distribution of grain size particles in the Ponta Vermelha Formation (TPv). E – East; W – West.

In the Congolote Formation the grain size characteristics remain almost constant through all the tested soils. The sand content ranges from 88.34 to 93.68%, silt from 5.93 to 11.16% and clay content ranges from 0.24 to 0.49%. Sample 21 has the lowest sand content 88.34% which is compensated by the highest silt content 11.16% as clay do not show considerable difference to the other samples.

For the Malhazine Formation the two tested soils (samples 13 and 17) have sand contents

from 93.67 to 94.59%, silt from 5.14 to 6.65% and clay content from 0.26 to 0.29%. The sand content is very high only compared to the Intradunes Deposits which presents the highest sand content of the tested soils with 96.45%.

### 5.3.2 – Consistency Limits and Moisture Content

Naturally occurring soils nearly always contain water as part of their structure. The moisture content is the amount of water within the pore space between the soil particles which is removable by oven drying at 105–110°C, expressed as a percentage of the mass of dry soil (Head, 1984). It is dependent upon when the sample is taken: dry/wet season, immediately after rain or prolonged dry period, for example. Measurement of moisture content provides a useful method of identifying and classifying soils and gives an indication of likely soil behaviour and their *in-situ* conditions.

Moisture content in the tested soils of Maputo City varies from 2.27% to 20.72 % (Table 5.4).

**Table 5.4** – Consistency limits and moisture content of the tested soils in Maputo City

| Geological Unit | Sample N°. | Moisture content (%) | Liquid Limit (%) | Linear Shrinkage (LS) (%) | Plasticity Index (2.13xLS) |
|-----------------|------------|----------------------|------------------|---------------------------|----------------------------|
| TPv             | 3          | 4.82                 | 22               | 0.81                      | 1.72                       |
|                 | 4          | 2.27                 | 24               | 1.21                      | 2.57                       |
|                 | 5          | 5.34                 | 25               | 0.13                      | 0.29                       |
|                 | 6          | ND                   | ND               | 0.00                      | 0.00                       |
|                 | 7          | ND                   | 25               | 0.13                      | 0.29                       |
|                 | 8          | 3.13                 | 20               | 0.54                      | 1.14                       |
|                 | 9          | 6.76                 | 28               | 1.21                      | 2.57                       |
|                 | 10         | 4.48                 | 27               | 0.67                      | 1.43                       |
|                 | 11         | 13.88                | ND               | 0.54                      | 1.14                       |
|                 | 12         | 8.20                 | 26               | 1.07                      | 2.29                       |
|                 | 14         | ND                   | 14               | 0.00                      | 0.00                       |
| QCo             | 1          | 7.83                 | 21               | 0.07                      | 0.14                       |
|                 | 2          | 8.58                 | 23               | 0.07                      | 0.14                       |
|                 | 16         | 3.33                 | 19               | 0.00                      | 0.00                       |
|                 | 18         | 4.30                 | 19               | 0.00                      | 0.00                       |
|                 | 19         | 17.25                | 19               | 0.00                      | 0.00                       |
|                 | 21         | 5.00                 | 13               | 0.26                      | 0.55                       |
| Qma             | 13         | 4.11                 | 21               | 0.13                      | 0.28                       |
|                 | 17         | 3.21                 | 16               | 0.13                      | 0.28                       |
| Qi              | 15         | 20.72                | 9                | 0.00                      | 0.00                       |
| Qmc             | 20         | 20.64                | 17               | 0.07                      | 0.14                       |

QCo: Congolote Formation; TPv: Ponta Vermelha Formation; QMa: Malhazine Formation; Qi: Intradune Deposits; QMc: Machava Formation. ND: Not determined.

The highest moisture content is observed in samples 15 and 20 located in depressions where the



groundwater table is near the surface. Sample 15 is located in the intradune depression and sample 20 in the area previously flooded in the Inhagóia Quarter (Chapter 9).

The Atterberg limits are useful characteristics of assemblages of soil particles and are based on the concept that a soil can exist in any of four states depending on its water content (Lambe & Whitman, 1979). Thus, the soil is solid when dry, and upon the addition of water proceeds through the semisolid, plastic and finally liquid states. The water contents at the boundaries between adjacent states are respectively termed shrinkage limit, plastic limit and liquid limit (Lambe & Whitman, 1979).

Standard test methods were used for the determination of the Atterberg limits (Chapter 3). The tests were carried out on air dried remoulded soil, the fraction passing the 425  $\mu\text{m}$  sieve being used. The Atterberg limits show that all tested soils in the study area are sands of very low plasticity to non plastic. The liquid limit varies between 9 and 28% with the higher values (20 to 28%) observed in the Ponta Vermelha Formation. In two cases (samples 6 and 11) it was not possible to perform the liquid limit test due to the lower clay content of the soils and non plastic characteristics. This reason also applies for the plastic limit test which was not also performed in all tested samples. Linear Shrinkage (LS) was then used as an auxiliary method to find an approximate estimate of the plasticity index (PI) for these soils. This approximate relationship given by Head (1984) was used and therefore the results must be taken as an indication only. The plasticity index obtained with this equation varies from 0 to 3.

$$\text{PI} = 2.13 \times \text{LS} \qquad \text{Eq. 5.3}$$

The results of the Atterberg limits are consistent with previous laboratory test results (also using BS 1377) made on soil samples of the same geological formation by Vaz (1990) and Abel (1996), except for the plasticity index that is slightly higher ( $\sim 4$ ).

### **5.3.3 –Density, Unit Weight and Specific Gravity**

Particle density refers to the mass of particles per unit volume and is independent from the soil compaction. For that reason it is relatively well-defined property, dissimilar to the bulk density which can have different values depending on the measuring conditions, whether freely settled or compacted state and the moisture content. The particle density is required for determining the soil porosity or voids ratio, which can be related to fabric structure. The bulk density in Maputo City varies from 1.38 to 1.97  $\text{Mg/m}^3$  while the dry density ranges from 1.32 to 1.82  $\text{Mg/m}^3$  (Table 5.5).

**Table 5.5** – Bulk density, specific gravity and organic matter content of the tested soils in Maputo City

| Geological Unit | Sample N <sup>o</sup> . | Bulk Density (Mg/m <sup>3</sup> ) | Dry Density (Mg/m <sup>3</sup> ) | Specific Gravity (Mg/cm <sup>3</sup> ) | Unit Weight (kN/m <sup>3</sup> ) | Organic Matter (%) |
|-----------------|-------------------------|-----------------------------------|----------------------------------|--|----------------------------------|--------------------|
| TPv             | 3                       | 1.38                              | 1.32                             | 2.78                                   | 13.54                            | 1.90               |
|                 | 4                       | 1.66                              | 1.63                             | 2.96                                   | 16.28                            | 0.40               |
|                 | 5                       | 1.6                               | 1.52                             | 2.69                                   | 15.70                            | 0.85               |
|                 | 6                       | ND                                | ND                               | 2.89                                   | ND                               | 4.10               |
|                 | 7                       | ND                                | ND                               | 2.75                                   | ND                               | 1.95               |
|                 | 8                       | 1.45                              | 1.41                             | 2.89                                   | 14.22                            | 1.45               |
|                 | 9                       | 1.75                              | 1.64                             | 2.91                                   | 17.17                            | 1.75               |
|                 | 10                      | 1.58                              | 1.51                             | 2.95                                   | 15.50                            | 1.35               |
|                 | 11                      | 1.55                              | 1.36                             | 2.92                                   | 15.21                            | 0.78               |
|                 | 12                      | 1.63                              | 1.51                             | 2.86                                   | 15.99                            | 1.50               |
|                 | 14                      | ND                                | ND                               | 2.77                                   | ND                               | 0.92               |
| QCo             | 1                       | 1.52                              | 1.41                             | 2.94                                   | 14.91                            | 0.58               |
|                 | 2                       | 1.97                              | 1.82                             | 2.68                                   | 19.33                            | 1.99               |
|                 | 16                      | 1.64                              | 1.59                             | 2.49                                   | 16.09                            | 0.65               |
|                 | 18                      | 1.5                               | 1.43                             | 2.72                                   | 14.72                            | 0.21               |
|                 | 19                      | 1.55                              | 1.29                             | 2.72                                   | 15.21                            | 0.12               |
|                 | 21                      | 1.69                              | 1.61                             | 2.53                                   | 16.58                            | 1.46               |
| Qma             | 13                      | 1.86                              | 1.79                             | 2.81                                   | 18.25                            | 0.63               |
|                 | 17                      | 1.59                              | 1.55                             | 2.67                                   | 15.60                            | 0.75               |
| Qi              | 15                      | 1.6                               | 1.33                             | 2.60                                   | 15.70                            | 0.11               |
| Qmc             | 20                      | 1.76                              | 1.5                              | 2.55                                   | 17.27                            | 0.49               |

QCo: Congolote Formation; TPv: Ponta Vermelha Formation; QMa: Malhazine Formation; Qi: Intradune Deposits; QMc: Machava Formation. ND: Not determined.

In geotechnics it is often necessary to know the natural unit weight, as it is used to compute stress due to the weight of soil. Unit weight is defined by Head (1984) as the weight per unit volume of a material, equal to mass per unit volume (bulk density of the material) multiplied by local acceleration due to gravity. It can be obtained by direct measurement of the weight and total volume. In Maputo City the unit weight ranges from 13.54 to 19.33 kN/m<sup>3</sup> (Table 5.5).

A soil consists of an accumulation of particles which may be of a single mineral type or more usually a mixture of a number of mineral types, each with a different specific gravity. The mean specific gravity of soil particles is defined by the ratio between the material density and the water density at a specified temperature (Coduto, 1999). The specific gravity of the soil particles is also required in calculations of voids ratio, but it may also indicate the presence of unusual minerals. The measured specific gravity of the soils of Maputo City varies from 2.49 to 2.96 (Table 5.5) with the highest values found in Ponta Vermelha Formation due to predominance of iron oxides in the soil formation.

#### **5.3.4 – Organic Matter**

Soil is a multiphase system composed by gases, liquids and solids. *“The solid phase consists of inorganic and organic material containing most of the carbon of the soil and usually consists of both dead and living matter”* (Aysen, 2002). Organic matter influences the engineering properties of soils. The presence of organic matter in a soil composition increases soil compressibility and reduces the stability of the fine-grained components (Aysen, 2002). Soils with high organic matter can develop voids as a result chemical alteration or decay of organic matter, which changes the properties of the soil (Lambe & Whitman, 1979). This makes organic soils undesirable in construction engineering.

Organic matter content in the tested soils of Maputo City range from 0.40 to 4.10 % (Table 5.5). Sample 6 is an outlier with the highest organic matter probably due to root material that could have been incorporated in the soil sample. No clear trend is observed in the distribution of organic matter in the city which should comprise less than 1.5% of the total mass of the soil in order to reduce consolidation settlement after construction. This is not the case for almost 29% (Samples 2, 3, 6, 7, 9 and 12) of the soil samples in the study area.

#### **5.3.5 – Soil Permeability**

Permeability of a soil is the soil property that determines the ability of a pore system to allow the flow of fluid. The permeability level is determined by the pore sizes and their connectivity. Thus, high water flow will occur in soils with large pores with good connectivity between them while low permeability is characteristic for soils with poor pores connectivity. Soils with high porosity can have zero permeability if the pores are not connected or if the pores are very small, for instance in clay soils.

Permeability becomes important when the water flow through the soil mass has an influence on the stability of the soil material causing concern. This is the case of *“seepage through or under a dam, drainage from subgrades or backfills, knowing the rate at which a well can recharge, and dewatering for construction projects under or near the water table”* (Scott, 2008).

Permeability of a soil is influenced by several factors namely the size and shape of the soil particles water viscosity, voids ratio, degree of saturation, mineralogical composition and type of flow (Head, 1988).

The permeability of a soil is expressed as coefficient of permeability or hydraulic conductivity,  $k$ . This is obtained from the Darcy's Law:

$$Q = kiA \quad (\text{Eq. 5.4})$$

where:

$Q$  = flow rate

$k$  = hydraulic conductivity (also known as coefficient of permeability)

$i$  = hydraulic gradient

$A$  = area perpendicular to the flow direction

The Darcy's Law equation is the basic equation for permeability calculations. It is based on the presupposition that the flow of water is laminar, or streamline and not turbulent (Head, 1988). Although it was developed empirically, it has been found to be valid for various soil types, from clays through coarse sands (Lambe & Whitman, 1979; Head, 1988; Coduto, 1999), but may not be so for clean gravel, where its accuracy is diminished because of turbulent flow, and possibly in clays with low hydraulic gradients, because the flow rate is so small (Coduto, 1999).

Several formulae have been published relating the permeability of soils, especially sands, to their particle size and other classification data (Head, 1988, Odong, 2008). The empirical relationship given by Hazen (1892) is simple and indicates only the order of magnitude of permeability based on the particle size data. As given by Terzaghi & Peck (1948) is:

$$k \text{ (cm/s)} = 100 \times (D_{10})^2 \quad (\text{Eq. 5.5})$$

where  $D_{10}$  is the effective particle size expressed in millimetres. The 100 in this formula corresponds to the Hazen empirical coefficient ( $C_H$ ) which has received several values from various geotechnical textbooks ranging from 1 to 1,000. Carrier (2003) argues that these published values of the Hazen coefficient  $C_H$  have differences of three orders of magnitude which should alone be enough to disqualify the use of the Hazen formula.

Davison & Springman (2000) give also an alternative to obtain the coefficient of permeability through a simple formula based also in the particle size.

$$k \text{ (m/s)} = C_k \times (D_{10})^2 \quad (\text{Eq. 5.6})$$

where  $C_k$  is the coefficient of gradation (or Coefficient of Curvature) obtained by the following relationship:

$$C_k = \frac{(D_{30})^2}{D_{60} \times D_{10}} \quad (\text{Eq. 5.7})$$

The hydraulic conductivity in this study is an approximate indication obtained through empirical relationships based on that given by Kozeny (1927) and then modified by Carman (1938, 1956) to become the Kozeny-Carman formula. This is widely explained by Carrier (2003), Odong (2008) and Head (1988). The Kozeny-Carman formula is based on the characteristics of the soil medium and derived from the shape of the particles, the entire particle size distribution, the soil porosity and the void ratio, specific surface and viscosity of water (Carrier, 2003; Odong, 2008; and Head, 1988).

Head (1988) states that the Kozeny's formula modified by Carman (1939) agrees better than most other formulae which measure permeability as it takes into account the shape of the particles and the soil porosity, as well as the particle size distribution, specific surface and viscosity of water. The final Kozeny-Carman formula is:

$$k \text{ (m/s)} = \frac{2}{fS^2} \left( \frac{e^3}{1+e} \right) \quad (\text{Eq. 5.8})$$

Where:

$k$  = coefficient of permeability (m/s)

$f$  = angularity factor

$S$  = specific surface of grains ( $\text{mm}^{-1}$ )

$e$  = voids ration of soil

The Kozeny-Carman equation is presently the most widely accepted and is recommended by Carrier (2003) to be adopted to predict the permeability of porous media.

Coefficient of permeability results are presented in Table 5.6. From the results can be observed that the addition of several parameters such as shape of particles and soil porosity, as well as particle size distribution, specific surface and viscosity of water as provided by the Kozeny-Carman method, results in lower coefficients of permeability. This formula is more representative of the soil reality therefore its results will be assumed in this research as the  $k$  of the soils of Maputo City. These results are also in line with the  $k$  obtained in other studies undertaken in the area by Abel (1996), McKnight (2001) and Vaz (1990). The Coefficient of Permeability does not show a clear distribution pattern in Maputo City therefore no correlation with the geological formations can be

made. Table 5.7 presents the typical values of hydraulic conductivity of different soil types.

**Table 5.6** – Coefficient of permeability results obtained by three different empirical methods.

| Geological Unit | Sample No. | Coefficient of Permeability ( $k$ ) (m/s) |              |                            |
|-----------------|------------|---|--------------|----------------------------|
|                 |            | Kozeny-Carman Method                      | Hazen Method | Davison & Springman (2000) |
| TPv             | 3          | 2.99E-06                                  | 6.40E-05     | 1.25E-02                   |
|                 | 4          | 4.24E-06                                  | 4.90E-05     | 1.22E-02                   |
|                 | 5          | 6.43E-06                                  | 2.25E-04     | 2.50E-02                   |
|                 | 6          | 5.99E-05                                  | 2.56E-04     | 2.64E-02                   |
|                 | 7          | 1.13E-05                                  | 1.21E-04     | 1.46E-02                   |
|                 | 8          | 6.56E-06                                  | 1.16E-05     | 4.28E-03                   |
|                 | 9          | 1.86E-06                                  | 1.09E-05     | 4.87E-03                   |
|                 | 10         | 4.77E-06                                  | 1.68E-05     | 6.17E-03                   |
|                 | 11         | 1.17E-05                                  | 1.56E-04     | 2.05E-02                   |
|                 | 12         | 5.15E-06                                  | 6.40E-05     | 1.20E-02                   |
|                 | 14         | 1.31E-05                                  | 1.44E-04     | 1.63E-02                   |
| QCo             | 1          | 2.92E-06                                  | 3.24E-06     | 5.25E-04                   |
|                 | 2          | 1.34E-06                                  | 8.10E-05     | 9.64E-03                   |
|                 | 16         | 4.00E-06                                  | 1.82E-04     | 2.46E-02                   |
|                 | 18         | 7.04E-06                                  | 2.25E-04     | 2.50E-02                   |
|                 | 19         | 1.53E-05                                  | 2.89E-04     | 2.89E-02                   |
|                 | 21         | 1.89E-06                                  | 2.50E-05     | 8.33E-03                   |
| Qma             | 13         | 3.66E-06                                  | 2.25E-04     | 2.66E-02                   |
|                 | 17         | 6.46E-06                                  | 2.25E-04     | 2.63E-02                   |
| Qi              | 15         | 1.68E-05                                  | 3.06E-04     | 3.19E-02                   |
| Qmc             | 20         | 5.36E-06                                  | 2.25E-04     | 2.50E-02                   |

QCo: Congolote Formation; TPv: Ponta Vermelha Formation; QMa: Malhazine Formation; Qi: Intradune Deposits; QMc: Machava Formation.

**Table 5.7** – Typical Values of Hydraulic Conductivity,  $k$ , for saturated soils (modified from Coduto, 1999)

| Soil Description     | Hydraulic Conductivity (m/s) | Relative Permeability |
|----------------------|------------------------------|-----------------------|
| Clean Gravel         | $10^{-2}$ to 1               | Very High             |
| Sand-gravel mixtures | $10^{-3}$ to $10^{-1}$       | High                  |
| Clean coarse sand    | $10^{-3}$ to $10^{-2}$       | High                  |
| Fine sand            | $10^{-4}$ to $10^{-2}$       | Medium                |
| Silty sand           | $10^{-4}$ to $10^{-3}$       | Medium                |
| Clayey sand          | $10^{-5}$ to $10^{-3}$       | Low                   |
| Silt                 | $10^{-9}$ to $10^{-4}$       | Very Low              |
| Clay                 | $10^{-11}$ to $10^{-7}$      | Impervious            |

The values of  $k$  obtained in Maputo City ( $10^{-6}$  to  $10^{-5}$ ) are lower comparing to the typical  $k$  values proposed by Coduto (1999) for silty sand ( $10^{-4}$  to  $10^{-3}$ ) (Table 5.7), but are in line with the values measured by other authors in the study area.

### 5.3.6 – Soil Classification

The soils of Maputo City have been categorized in several ways, such as by their geologic origin, mineralogy, grain size, plasticity index, permeability and so on. Each of these methods is useful in a specific context, but a more comprehensive system is needed to better classify soils for engineering purposes. For this research the Unified Soil Classification System (USCS) was used as suggested by Lambe & Whitman (1979), Lee, *et al.*, (1983), Coduto, (1999) and others. This system takes into account the grain size, the coefficients of uniformity and curvature and the Atterberg limits (plasticity chart). All soils plot as ML (predominantly silt of low plasticity) in the Plasticity Chart (graph not shown), therefore do not require the Coefficient of Curvature conformity to define the group classification. Table 5.8 shows the conformity criteria to the Unified Soil Classification System (1985) and the group name for all soil samples in the study area.

**Table 5.8** – Soil classification of Maputo City according to the Unified Soil Classification System (1985).

| Sample No. | Geological Unit | % pass of Fines (Silt + Clay) | Coefficient Uniformity ( $C_u$ ) | Plasticity Chart | Group Symbol | % of Sand or Gravel | Group Name                   |
|------------|-----------------|-------------------------------|----------------------------------|------------------|--------------|---------------------|------------------------------|
| 3          | TPv             | 15.44 (>12%)                  | -                                | ML               | SM           | 0.00 (<15%)         | Silty sand                   |
| 4          |                 | 9.54 (5-12%)                  | 3.29 (< 6)                       | ML               | SP-SM        | 0.00 (<15%)         | Poorly-graded sand with silt |
| 5          |                 | 6.02 (5-12%)                  | 1.60 (< 6)                       | ML               | SP-SM        | 0.31 (<15%)         | Poorly-graded sand with silt |
| 6          |                 | 1.88 (< 5%)                   | 1.38 (< 6)                       | -                | SP           | 11.99 (<15%)        | Poorly-graded sand           |
| 7          |                 | 8.03 (5-12%)                  | 3.00 (< 6)                       | ML               | SP-SM        | 12.87 (<15%)        | Poorly-graded sand with silt |
| 8          |                 | 15.82 (>12%)                  | -                                | ML               | SM           | 0.01 (<15%)         | Silty sand                   |
| 9          |                 | 16.08 (>12%)                  | -                                | ML               | SM           | 0.00 (<15%)         | Silty sand                   |
| 10         |                 | 13.54 (>12%)                  | -                                | ML               | SM           | 0.00 (<15%)         | Silty sand                   |
| 11         |                 | 6.72 (5-12%)                  | 1.76 (< 6)                       | ML               | SP-SM        | 0.00 (<15%)         | Poorly-graded sand with silt |
| 12         |                 | 9.57 (5-12%)                  | 3.00 (< 6)                       | ML               | SP-SM        | 0.00 (<15%)         | Poorly-graded sand with silt |
| 14         |                 | 9.18 (5-12%)                  | 2.00 (< 6)                       | ML               | SP-SM        | 0.08 (<15%)         | Poorly-graded sand with silt |
| 1          | QCo             | 28.61 (>12%)                  | -                                | ML               | SM           | 0.03 (<15%)         | Silty sand                   |
| 2          |                 | 7.32 (5-12%)                  | 2.33 (< 6)                       | ML               | SP-SM        | 0.00 (<15%)         | Poorly-graded sand with silt |
| 16         |                 | 6.33 (5-12%)                  | 1.63 (< 6)                       | ML               | SP-SM        | 0.00 (<15%)         | Poorly-graded sand with silt |
| 18         |                 | 6.59 (5-12%)                  | 1.60 (< 6)                       | ML               | SP-SM        | 0.01 (<15%)         | Poorly-graded sand with silt |
| 19         |                 | 6.32 (5-12%)                  | 1.53 (< 6)                       | ML               | SP-SM        | 0.00 (<15%)         | Poorly-graded sand with silt |
| 21         |                 | 11.65 (5-12%)                 | 4.80 (< 6)                       | ML               | SP-SM        | 0.01 (<15%)         | Poorly-graded sand with silt |
| 13         | Qma             | 5.41 (5-12%)                  | 1.67 (< 6)                       | ML               | SP-SM        | 0.00 (<15%)         | Poorly-graded sand with silt |
| 17         |                 | 6.93 (5-12%)                  | 1.60 (< 6)                       | ML               | SP-SM        | 0.00 (<15%)         | Poorly-graded sand with silt |
| 15         | Qi              | 3.55 (< 5%)                   | 1.51 (< 6)                       | -                | SP           | 0.00 (<15%)         | Poorly-graded sand           |
| 20         | Qmc             | 5.66 (5-12%)                  | 1.60 (< 6)                       | ML               | SP-SM        | 0.03 (<15%)         | Poorly-graded sand with silt |

Based on this classification the soils of Maputo City are generally SP-SM (Poorly-graded sand with silt) as they are found in more than 2/3 of the investigated soil samples. Particularities of some sample locations can give rise to small variations on the soil classifications namely SM (Silty sand) and SP (Poorly-graded sand).

## 5.4 – SHEAR STRENGTH OF SOILS

### 5.4.1 – Introduction

Stresses in a soil mass are caused by the weight of overlying soil, and by the internal forces acting in a unit area, both as normal or shear stress. Stress assessment in the ground is very complex and in order to simplify this process certain assumptions were discussed by Lambe & Whitman (1979) and Coduto (1999): “(1) soil is a *continuous material* with uniform stresses, without cracks or joints which would reduce the stress transmission; (2) it is *homogeneous*, which means the relevant engineering properties are the same at all locations; (3) it is *isotropic*, which means the engineering properties are the same in all directions; (4) it has *linear elastic stress-strain properties*, which means each increment of stress is associated with corresponding increment of strain”.

In saturated soils, the normal stress ( $\sigma$ ) within the soil mass is carried by both the soil grains and the water within the pores. This is the concept of effective stress introduced by Karl Terzaghi in 1943 and considered as the most important contribution to soil mechanics. The *principle of effective stress* points the need to separate the stress carried by the soil skeleton from that carried by the water phase when a stress is applied to a saturated soil. The principle says also that strength and deformation are controlled by *effective stress* ( $\sigma'$ ) which acts on the soil grains. The remaining stress, of the normal component, acts in the pore water, and is denoted *pore water pressure* ( $u$ ). Therefore, the total stress within the soil mass is obtained by the following expression:

$$\sigma' = \sigma - u \quad (\text{Eq. 5.9})$$

For dry soils, because no pore water pressure is present, the total stress equals the effective stress. The principle of effective stress is important as civil engineering projects (buildings or structures) which are founded in or on the earth often introduce external loads in the soil which supports the foundations, producing induced stresses.

The performance of a soil in engineering is controlled by the soil strength. The soil strength is defined as the greatest shear stress it can sustain. If the stress exceeds the strength, failure occurs.



Shear failure in soils occurs when the stresses between particles are such that they slide or roll past each other. Failure is defined in several ways and different criteria have been adopted to identify the point where failure occurs in a stress-strain curve, for example, the yield point in some material. Holtz & Kovacs (1981) indicate that failure in soils occurs at 15 to 20% strain but not implying failure of the system.

The Mohr-Coulomb failure criterion is the most commonly used empirical failure criterion in soil mechanics. The shear strength primarily depends on interactions between the particles (frictional strength), not on their internal strength (cohesive strength). The most common situation in natural soils is to have both frictional and cohesive strength, and there is a need to combine these two sources into a single all-purpose strength formula. This is given by the Mohr-Coulomb failure criterion by the equation:

$$\tau = c' + \sigma' \tan \phi' \quad (\text{Eq. 5.10})$$

Where:

$\tau$  = Shear strength at failure;

$c'$  = Effective cohesion;

$\sigma'$  = effective stress acting on the shear surface;

$\phi'$  = effective friction angle on the sliding plane.

Shear strength in soils is the resistance of the particle to movement, due to “*particle interlocking, physical bonds formed across the contact areas (resulting from surface atoms sharing electrons at interparticle contacts), and chemical bonds (i.e. cementation-particles connected through a solid substance)*” (Terzaghi *et al.*, 1996). The soils’ stress-strain relationship, and consequently the shear strength is very complex, and is affected by the composition of the basic soil material, initial state of the soil material, Past stress history of the soil, loading conditions, and the soil Structure (Lambe & Whitman, 1979; Poulos, 1989).

The stress-strain relationship is preferably measured in the laboratory using stresses that will occur in the actual soil mass rather than use extremely complicated expressions based on the concepts from the theory of elasticity, namely *Young’s modulus* and *Poisson’s ratio*. This is the case of this study where the direct shear box was the main test used for the determination of shear strength characteristics. For practical purposes, the results obtained by direct shear, cohesion ( $c'$ ) and friction angle ( $\phi'$ ), are comparable to the ones from conventional drained triaxial compression tests

as extensively studied and stated by Maccarini (1993).

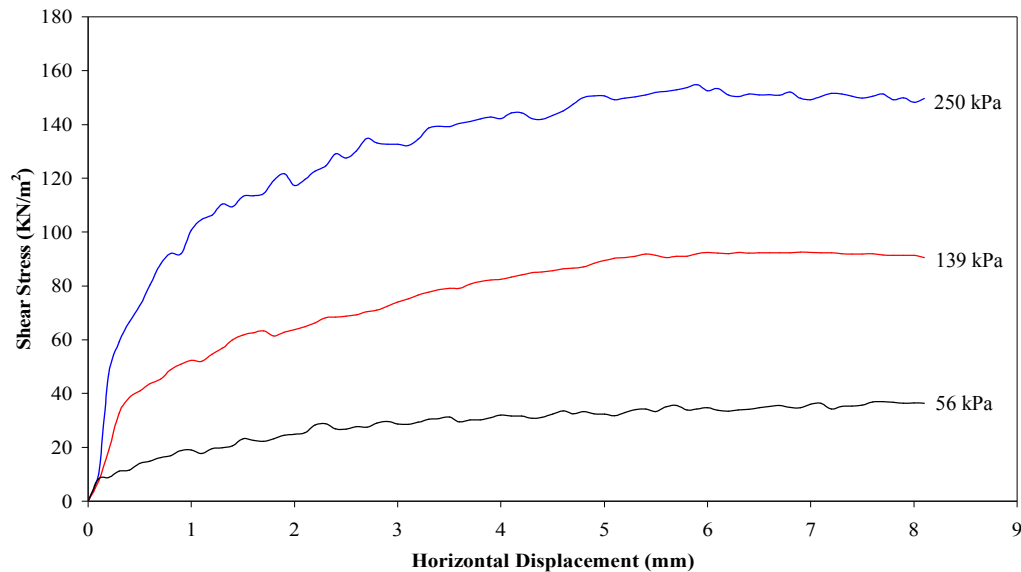
#### 5.4.2 – Shear Strength Characteristics

Table 5.9 presents some shear strength characteristics of the soils of Maputo City tested in direct shear under saturated drained conditions. The drained condition is made possible through allowing a slow shearing rate so that extra pore water pressure is generated inside the sample and dissipated by drainage through the porous discs. Shear strength results obtained on saturated sand are very similar to those for dry sand, provided that the sand remains saturated during shear and that drainage takes place freely during shear (Head, 1988). The shear box tests were carried out under normal consolidation pressures of 56, 139 and 250 kN/m<sup>2</sup> from which the strength envelope of the Mohr-Coulomb failure criterion was obtained, and the cohesion and friction angle calculated (Appendix A).

**Table 5.9** – Shear strength characteristics (peak cohesion and friction angle) and plasticity index of the tested soils of Maputo City

| Geological Unit | Sample | Soil Classification | Friction Angle (°) | Cohesion (kN/m <sup>2</sup> ) |
|-----------------|--------|---------------------|--------------------|-------------------------------|
| TPv             | 3      | SM                  | 28.5               | 11.14                         |
|                 | 4      | SP-SM               | 31                 | 5.93                          |
|                 | 5      | SP-SM               | 31.5               | 9.42                          |
|                 | 6      | SP                  | ND                 | ND                            |
|                 | 7      | SP-SM               | ND                 | ND                            |
|                 | 8      | SM                  | 32                 | 5.33                          |
|                 | 9      | SM                  | 31.5               | 2.14                          |
|                 | 10     | SM                  | 33.5               | 3.47                          |
|                 | 11     | SP-SM               | 31                 | 5.71                          |
|                 | 12     | SP-SM               | 31.5               | 8.57                          |
|                 | 14     | SP-SM               | ND                 | ND                            |
| QCo             | 1      | SM                  | 32.5               | 1.38                          |
|                 | 2      | SP-SM               | 32                 | 9.86                          |
|                 | 16     | SP-SM               | 28                 | 9.29                          |
|                 | 18     | SP-SM               | 28                 | 9.29                          |
|                 | 19     | SP-SM               | 30                 | 5.71                          |
|                 | 21     | SP-SM               | 29                 | 6.43                          |
| Qma             | 13     | SP-SM               | 30                 | 5.71                          |
|                 | 17     | SP-SM               | 28.4               | 0.83                          |
| Qi              | 15     | SP                  | 30                 | 3.43                          |
| Qmc             | 20     | SP-SM               | 30.6               | 6.43                          |

QCo: Congolote Formation; TPv: Ponta Vermelha Formation; QMa: Malhazine Formation; Qi: Intradune Deposits; QMc: Machava Formation; ND: Not Determined.



**Figure 5.4** – Shear stress-horizontal displacement curve of direct shear tests of Sample 8. This curve is typical for the loose and normally consolidated soil specimens of Maputo City

Figure 5.4 illustrates the typical shear stress versus horizontal displacement curves derived from the shear box test in the samples collected in Maputo City. The shear stress–shear strain plots in Figure 5.4 show that the deformation modulus and shear strength increase with normal pressure and that shear strength does not create a peak before reaching a residual level even at high shear strain.

The asymptotic shaped curves in Figure 5.4 are representative for 66.7% of the analysed samples. These curves have high level of residual strength and do not show peak. This kind of plastic failure indicates that these soils are loose and normally consolidated.

The remaining 33% of tested soils present shear stress-shear strain plots illustrated as in Figure 5.5. It is clear from Figure 5.5 that shear stress curve at 250 kN/m<sup>2</sup> rises quite sharply to a peak and then falls off to a somewhat lower value. The excess of peak over the residual value, denoted by *E*, represents the extra work which has to be put in to produce the vertical movement due to dilatancy (Head, 1988). The behaviour observed in Figure 5.5 denotes dense sand or bonded soils and to some extent the cohesion of the soil. This *E* value shows also the effect of bonding on soil strength (Maccarini, 1993). The difference in values between the peak of the shear stress and the residual strength (*E* value) observed amongst samples corresponds to the differences in soil consistency as described in section 5.2.

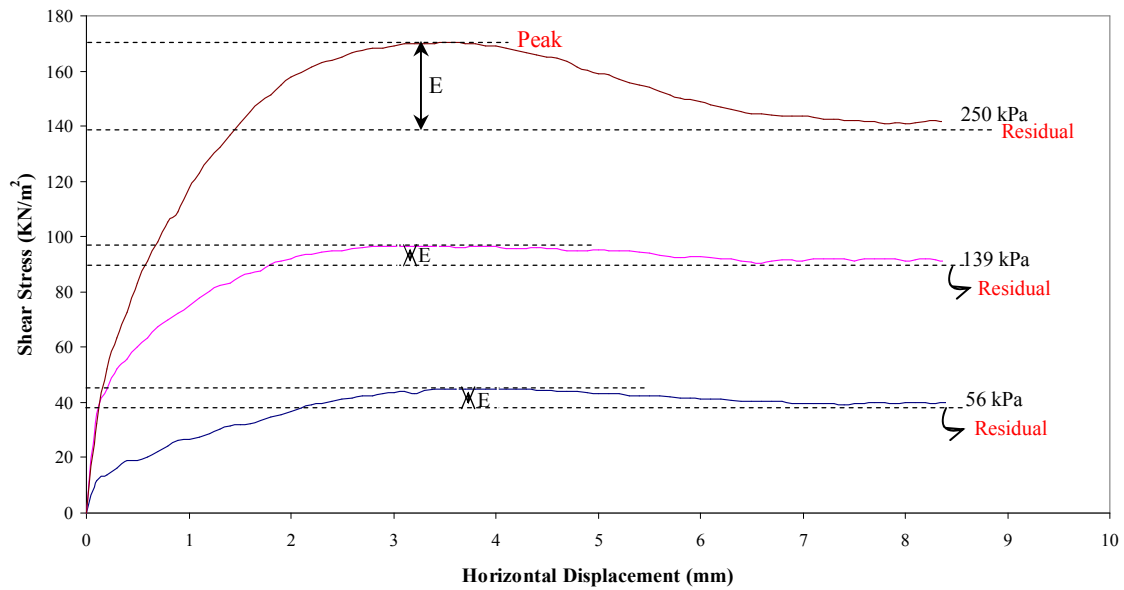


**Figure 5.5** – Stress–strain diagram of direct shear tests of the dense sand or bonded soils of Maputo City

The corresponding vertical vs. horizontal displacement curves from the shear box test are presented in Figure 5.6. Volume decrease (contraction) is observed in the tested soils with the three selected normal pressures. The general characteristics of shear deformation and volume change reflect structure sensitive nature of the soils as correlations can be made with the general parameters of soil characterization.

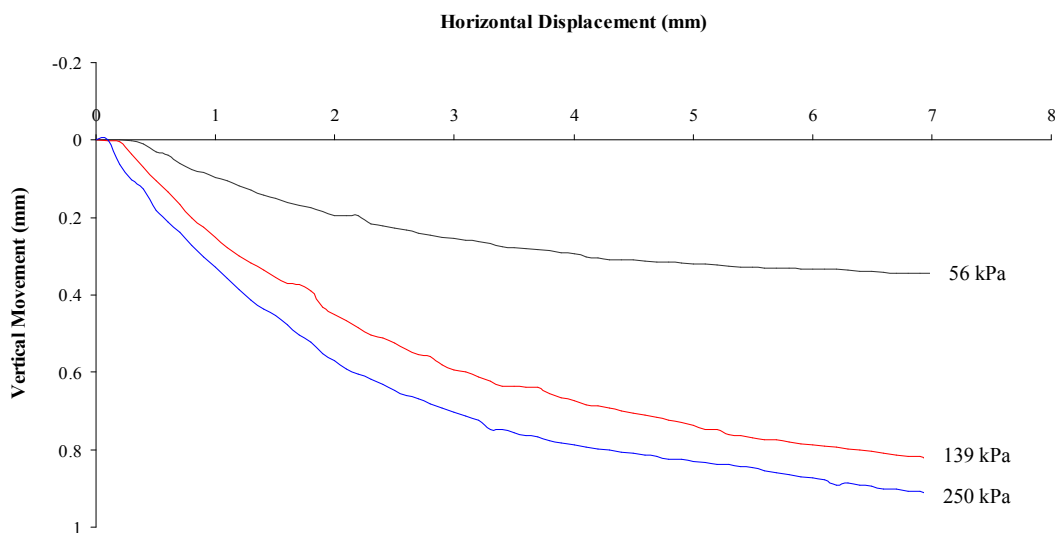


**Figure 5.6** – Vertical versus horizontal displacement curves for the tested soil of Maputo City

The stress-strain curves obtained in this study are the ones expected for the type of soils occurring in Maputo City showing characteristics of contraction for loose and normally consolidated soils as predicted by Maccarini (1993).

The maximum shear stress obtained in the shear stress-displacement curve of each of the three tests carried out on specimens of soil under different normal loads were plotted against the corresponding value of normal stress to obtain the shear strength parameters (Figure 5.7). Cohesion and angle of internal friction (angle of shear resistance), are the ones determined based on direct shear box test. The angle of internal friction of the soils of Maputo City varies from 28 to 33.5°. Only five samples had friction angles less than 30° (samples 3, 16, 17, 18 and 21). The highest friction angles are observed in the Ponta Vermelha Formation, 31–33.5°, and the lowest are in the Congolote and Malhazine Formations, 28–30°. Cohesion ranges from 0.83 to 11.14 kN/m<sup>2</sup>, with the highest values in the Ponta Vermelha Formation.

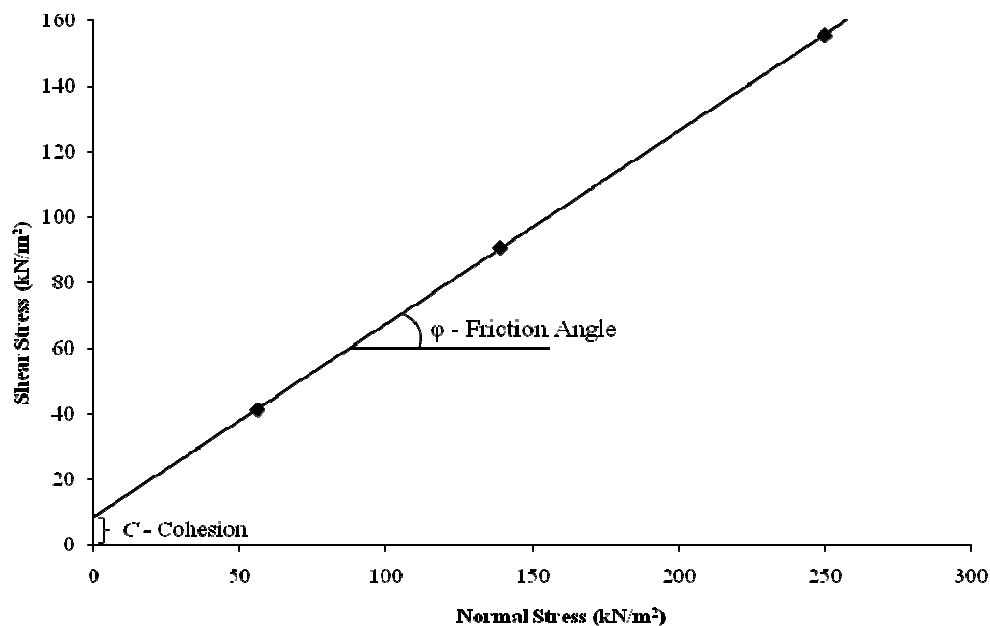


**Figure 5.7** – Shear stress vs. Normal stress for Sample 16 with the indication of the procedure to obtain the friction angle and cohesion

As guided by the predominant shape of the shear stress-horizontal displacement curves in the study area (Figure 5.4), the measured cohesion in the majority of the tested samples is an apparent cohesion found in the very loose normally consolidated sands. True cohesion from overburden pressures, as obtained from the failure envelope, can be assumed to act on the soil presenting

cementing or bonding between grains and from low effective stress acting on the shear surface. High iron oxide content in the geological formations of Maputo City, mainly in the Ponta Vermelha Formation with red ferruginous sands, it is assumed that acts as a bonding agent. The presence of a bonding agent is confirmed by the consolidation tests as explained in Section 5.5.

The various shear strength parameters can be correlated between them, and correlated with the general parameters of soil characterization. Friction angle should decrease with an increase in the cohesion of soil particles. However, no correlation is presented ( $r^2 = 0.09$ ). The very low clay content makes the correlation meaningless.

It is known that grain size and textural characteristics affect the shear strength characteristics of sandy soils (Charles, 1992), therefore, the relationship between these parameters was investigated in the analysed samples. The mean grain diameter ( $D_{50}$ ) showed a very weak correlation with cohesion but an increase in grain size with minor decrease in the angle of internal friction ( $R^2 = 0.08$ ). This trend is in line with the conclusion made by Lambe & Whitman (1979) that the angle of internal friction of the quartz sands, like the ones of the study area, decreases with increasing particle diameter as a consequence of an increase in rolling and sliding between particles during shearing.

Lambe & Whitman (1979) also stress the influence of soil characteristics on the shear strength parameters. They showed that soil plasticity affects the shear strength parameters, however, the very low plasticity index (PI) together with the low plastic clay content observed in the soils of the study area explain the no clear correlation of these parameters with the shear strength parameters. It was expected that the friction angle would decrease with an increase in PI as predicted by Mitchell (1993). Although his study was undertaken on clay soils it could be assumed that the clay content in sandy soils would have the same influence as investigated by Mitchell (1993). The chemical analysis of the sandy soils of Maputo City show very high silica content (80-97%) with soil mineralogy indicating quartz and feldspar as the main minerals present in the sandy fraction (Momade *et al.*, 1996). The low clay fraction (0.08 to 1.52 %) gives non plastic properties to these soils. From the explanation above, the friction angle cannot be assumed as directly related to the clay content and in turn to the plasticity index, but to the mineral composition of the soils as predicted by Mitchell (1993). Soils with high content of quartz and feldspar are predicted by Mitchell (1993) to potentially have high friction angle because their quartz component has a friction angle between 21 and 31° when saturated.

## **5.5 – CONSOLIDATION CHARACTERISTICS OF SOILS**

### **5.5.1 – Introduction**

Consolidation in a soil is a decrease in volume as a result of the rearrangement of the soil particles in response to an increase in effective stress over a period of time. Consolidation results in particles packed more closely together, and accompanied by drainage of water from the soil when consolidation occurs under saturated conditions. The resulting settlement is known as consolidation settlement and is the most important source of settlement in soils. The compressibility characteristics of soils are very important parameters required in structural design and are part of any soil investigation (Sridharan & Gurtug, 2005). Analysis, prediction and the rate of settlement of foundations due to the applied structural loads is one of the most important components of geotechnics (Coduto, 1999).

The magnitude and rate of consolidation can be foreseen by several methods. In this research soils were tested in an oedometer to determine their compressibility characteristics. The compressibility characteristics of soils are given by the coefficient of volume compressibility ( $m_v$ ), the coefficient of compressibility, ( $a_v$ ), the compression index ( $C_c$ ) and recompression index ( $C_r$ ) (Sridharan & Gurtug, 2005; Coduto, 1999; Lambe & Whitman, 1979; Lee *et al.*, 1983). The coefficient of compressibility ( $a_v$ ) and the coefficient of volume compressibility ( $m_v$ ) are strongly dependent on pressure level (Sridharan & Gurtug, 2005). The purpose of performing consolidation tests is to define the stress-strain properties of the soil and thus allow predicting consolidation settlement in the field. The laboratory results are projected back to the field conditions.

Discussions of consolidation settlement predictions in this research consider only the case of one-dimensional consolidation which assumes only vertical strains occurring in the soil.

### **5.5.2 – Magnitude and Rate of Consolidation of the Soil of Maputo City**

Consolidation results of the tested samples are presented as a graph of voids ratio,  $e$  vs. log vertical effective stress, which emphasizes the reduction in void size that occurs during consolidation. Figure 5.8 shows the typical consolidation curve of the tested soils in Maputo City at natural moisture content as well as under saturated conditions. In this last case, besides the curve illustrated in Figure 5.8, few samples gave straight lines for collapse settlement. This matter will be discussed

in full later in this chapter.

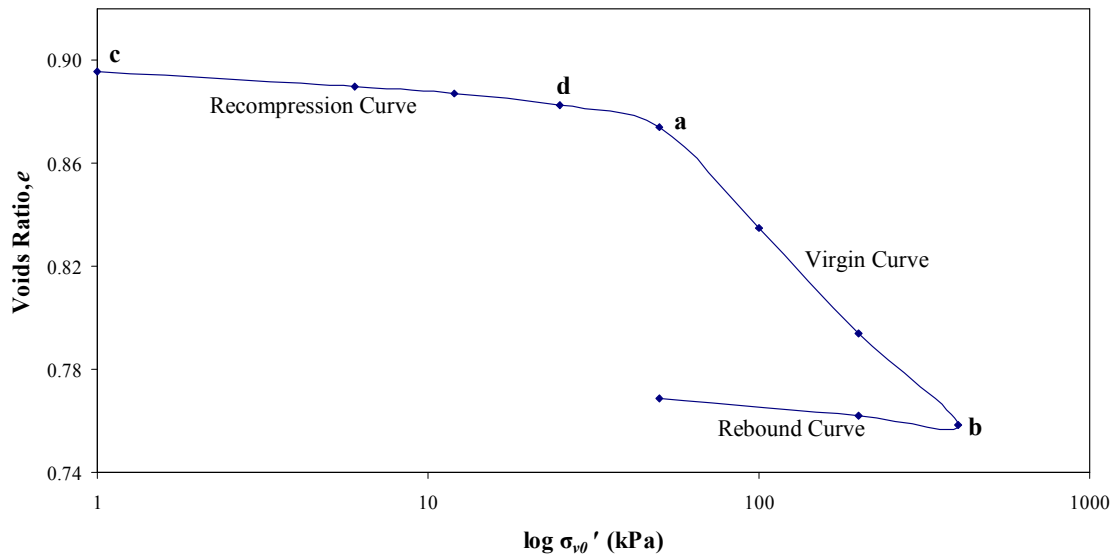


**Figure 5.8** – Typical consolidation voids ratio vs. vertical stress curve of the tested soils in Maputo City (Sample 18 tested fully saturated). Schematic representation of the curves is from Coduto (1999).

From the consolidation curves the very pronounced preconsolidation stress was determined. This point where the slope of the consolidation curve changes (transition between the recompression and virgin curves) is very important in the consolidation process (Coduto, 1999). The preconsolidation stress is the greatest vertical effective stress the soil has ever experienced in its stress history and represents the stress conditions at the sampling point (Coduto, 1999). The Casagrande's procedure was adopted to determine the preconsolidation stress (Figure 5.9) which varies from 6.5 to 54 kN/m<sup>2</sup> in the analysed soils (Table 5.10). This table gives also the basic parameters obtained from the consolidation curves of the tested samples in the research area.

The compressibility parameters of the tested soils are obtained from the consolidation graph where the slopes of the curves play important role. The *highly compressible* soils are given by the steep slopes of the consolidation plot, meaning larger strain or a large change in voids ratio with a given increase in  $\sigma'_v$ ; the *slightly compressible* soils are given by the shallow slopes (Coduto, 1999). The compression index is an important property of soil, extensively used in geotechnical engineering practice, because it is used to predict settlement that will occur from the load of an engineering structure. Clay-rich soils and soils with high organic content have the highest compressibility.



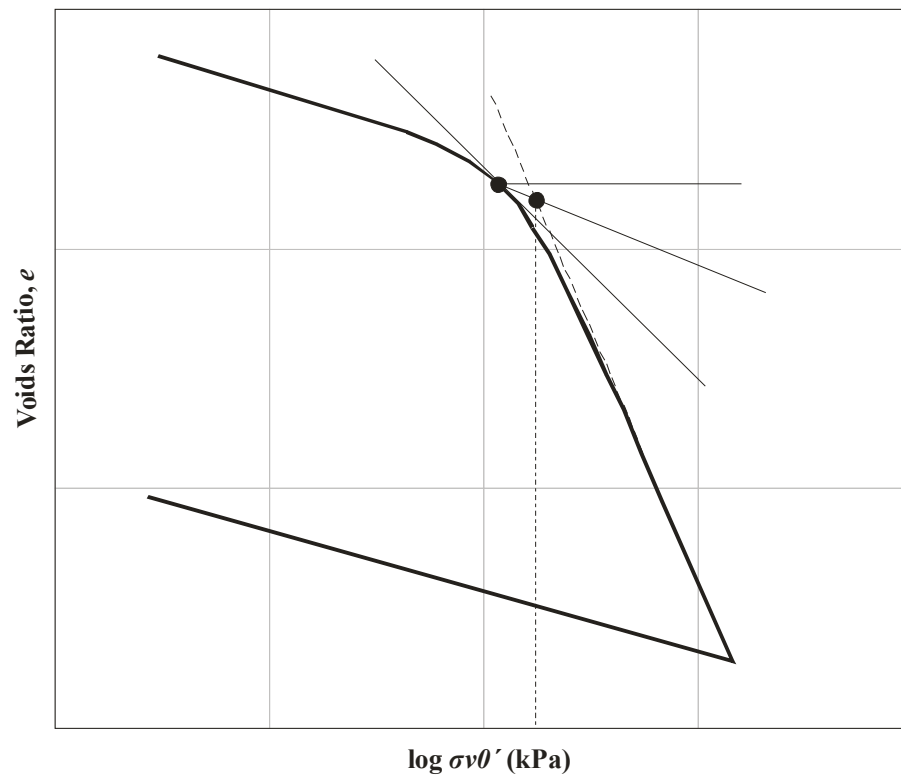


**Figure 5.9** – Casagrande's method of finding the preconsolidation stress (From Coduto, 1999)

**Table 5.10** – Basic parameters obtained from the consolidation curves of the tested samples in Maputo City

| Geological Unit | Sample No. | Unit Weight ( $\gamma$ ) (kN/m <sup>3</sup> ) | Voids Ratio (e) | Preconsolidation Stress ( $\sigma_c'$ ) (kN/m <sup>2</sup> ) | Depth of Sample Collection (m) | Initial Vertical Effective Stress ( $\sigma_{v0}'$ ) | Compression Index ( $C_c$ ) | Recompression Index ( $C_r$ ) | Compressibility            | $\sigma_{v0}'$ vs. $\sigma_c'$ | Consolidation Status |
|-----------------|------------|---|-----------------|--|--------------------------------|--|-----------------------------|-------------------------------|----------------------------|--------------------------------|----------------------|
| TPv             | 3          | 13.5  | 1.11            | 17   | 1.6                            | 21.7   | 0.069                       | 0.076                         | Slightly Compressible      | $\approx$                      | NC                   |
|                 | 4          | 16.3  | 0.82            | 26   | 1.8                            | 29.3   | 0.059                       | 0.032                         | Slightly Compressible      | $\approx$                      | NC                   |
|                 | 5          | 15.7  | 0.77            | 42   | 2.5                            | 39.2   | 0.058                       | 0.025                         | Slightly Compressible      | $\approx$                      | NC                   |
|                 | 6          | ND  | ND              | ND   | ND                             | ND   | ND                          | ND                            | ND                         | ND                             | -                    |
|                 | 7          | ND  | ND              | ND   | ND                             | ND   | ND                          | ND                            | ND                         | ND                             | -                    |
|                 | 8          | 14.2  | 1.05            | 12   | 1.4                            | 19.9   | 0.145                       | 0.014                         | Moderately Compressible    | $>$                            | UC                   |
|                 | 9          | 17.2  | 0.77            | 34   | 1.9                            | 32.6   | 0.150                       | 0.034                         | Moderately Compressible    | $\approx$                      | NC                   |
|                 | 10         | 15.5  | 1.01            | 6.5  | 0.9                            | 13.9   | 0.082                       | 0.075                         | Slightly Compressible      | $>$                            | UC                   |
|                 | 11         | 15.2  | 1.14            | 22   | 1.4                            | 21.3   | 0.114                       | 0.038                         | Moderately Compressible    | $\approx$                      | NC                   |
|                 | 12         | 16.0  | 0.90            | 26   | 1.6                            | 25.6   | 0.109                       | 0.116                         | Moderately Compressible    | $\approx$                      | NC                   |
|                 | 14         | ND  | ND              | ND   | ND                             | ND   | ND                          | ND                            | ND                         | ND                             | -                    |
| QCo             | 1          | 14.9  | 1.08            | 45   | 2.4                            | 35.8   | 0.060                       | 0.062                         | Slightly Compressible      | $<$                            | OC                   |
|                 | 2          | 19.3  | 0.47            | 23   | 1.1                            | 21.3   | 0.045                       | 0.034                         | Very slightly compressible | $\approx$                      | NC                   |
|                 | 16         | 16.1  | 0.57            | 9.2  | 1.8                            | 29.0   | 0.038                       | 0.031                         | Very slightly compressible | $>$                            | UC                   |
|                 | 18         | 14.7  | 0.90            | 46   | 2.35                           | 34.6   | 0.132                       | 0.009                         | Moderately Compressible    | $<$                            | OC                   |
|                 | 19         | 15.2  | 1.11            | 25   | 1.5                            | 22.8   | 0.114                       | 0.008                         | Moderately Compressible    | $\approx$                      | NC                   |
|                 | 21         | 16.6  | 0.57            | 16   | 1.5                            | 24.9   | 0.076                       | 0.010                         | Slightly Compressible      | $>$                            | UC                   |
| Qma             | 13         | 18.2  | 0.57            | 42   | 2.4                            | 43.8   | 0.023                       | 0.007                         | Very slightly compressible | $\approx$                      | NC                   |
|                 | 17         | 15.6  | 0.73            | 54   | 2.50                           | 39.0   | 0.092                       | 0.020                         | Slightly Compressible      | $<$                            | OC                   |
| Qi              | 15         | 15.7  | 0.96            | 33   | 1.9                            | 29.8   | 0.043                       | 0.015                         | Very slightly compressible | $\approx$                      | NC                   |
| Qmc             | 20         | 17.3  | 0.70            | 27   | 0.9                            | 15.5   | 0.035                       | 0.001                         | Very slightly compressible | $<$                            | OC                   |

ND: Not Determined; NC: Normally consolidated condition; OC: Overconsolidated or preconsolidated condition; UC: Underconsolidated condition

The Compression Index ( $C_c$ ) is the change in voids ratio,  $e$ , per logarithmic cycle of effective pressure  $p$  ( $\log p$ ). It is given by the slope of the virgin curve while the Recompression Index ( $C_r$ ) by the decompression curve. Based on Figure 5.8 the following mathematical equations are used (Coduto, 1999):

$$C_c = \frac{e_a - e_b}{(\log \sigma_{v0}')_b - (\log \sigma_{v0}')_a} \quad (\text{Eq. 5.11})$$

$$C_r = \frac{e_c - e_d}{(\log \sigma_{v0}')_d - (\log \sigma_{v0}')_c} \quad (\text{Eq. 5.12})$$

Compression index,  $C_c$ , is assumed as practically constant and independent of the pressure level as the  $e$ - $\log p$  is considered linear at higher pressure range (Sridharan & Gurtug, 2005). These authors argue that assuming  $C_c$  to be constant may not be a correct assumption in many situations as it is proven that  $e$  vs.  $\log p$  can have several shapes (curved, concave upwards or concave downwards) and non correct results in the estimate of settlements may arise from this. The shape of the curves depends on the soil plasticity characteristics and initial water content.

Compressibility of sands is smaller than that of silts and clays and Coduto (1999) suggests that it is often sufficient to use estimated values of  $C_c$  and  $C_r$  based on the data gathered by Burmister (1962) and presented in Table 5.11. For the purpose of this research,  $C_c$  and  $C_r$  values were calculated and are shown in Table 5.10. The soils of Maputo City are distributed through three classes from very slightly compressible to moderately compressible as given by Table 5.12 which classifies the soil compressibility. The majority of the soils of Maputo City fall in the slightly compressible class with no clear trend amongst the geological formations.

**Table 5.11** – Typical compression index at various relative densities ( $Dr$ ) for the three types of normally consolidated sandy soils occurring in Maputo City (From Burmister, 1962 and adapted from Coduto, 1999)

| Soil Type  | Compression Index |             |             |             |             |              |
|--|-------------------|-------------|-------------|-------------|-------------|--------------|
|  | $Dr = 0\%$        | $Dr = 20\%$ | $Dr = 40\%$ | $Dr = 60\%$ | $Dr = 80\%$ | $Dr = 100\%$ |
| Fine to medium sand (SP)                         | 0.013             | 0.010       | 0.008       | 0.006       | 0.005       | 0.003        |
| Fine sand (SP)                                   | 0.015             | 0.013       | 0.010       | 0.008       | 0.005       | 0.003        |
| Fine sand with trace fine to coarse silt (SP-SM) | -                 | -           | 0.011       | -           | -           | -            |
| Fine sand with little fine to coarse silt (SM)   | 0.017             | 0.014       | 0.012       | 0.009       | 0.006       | 0.003        |
| Fine sand with some fine to coarse silt (SM)     | -                 | -           | 0.014       | -           | -           | -            |

**Table 5.12** – Classification of Soil Compressibility (From Coduto, 1999)

| $C_c$ or $C_r$ | Classification             |
|----------------|----------------------------|
| 0-0.05         | Very slightly compressible |
| 0.05-0.10      | slightly compressible      |
| 0.1-0.20       | Moderately compressible    |
| 0.20-0.35      | Highly compressible        |
| >0.35          | Very highly compressible   |

The preconsolidation stress  $\sigma_c'$  was compared with the initial effective stress,  $\sigma_{v0}'$  in order to classify the soils in terms of consolidation status in the field. The initial effective stress was determined by the equation 5.13, from Coduto (1999) and Lambe & Whitman (1979), for the original field conditions at the same depth of the sample subjected to consolidation test.

$$\sigma_{v0}' = \sum \gamma H - u \quad (\text{Eq. 5.13})$$

Where,  $\sigma_{v0}'$  = initial effective stress

$\gamma$  = unit weight

H = thickness to the soil sample

$u$  = pore water pressure

Soil in the field can be under three possible consolidation conditions as discussed by Lee *et al.* (1983):

- (i) Normally consolidated condition – when the  $\sigma_{v0}' \approx \sigma_c'$  – the vertical effective stress in the field has never been higher than the current magnitude;
- (ii) Overconsolidated or preconsolidated condition – when  $\sigma_{v0}' < \sigma_c'$  – the vertical effective stress in the field was once higher than its current magnitude;
- (iii) Underconsolidated condition – when  $\sigma_{v0}' > \sigma_c'$  – the soil is still in the process of consolidating under a previously applied load.

The tested soils of Maputo City are, in majority, in a normally consolidated condition as proven by the comparison between initial effective stress ( $\sigma_{v0}'$ ) and preconsolidation stress ( $\sigma_c'$ ) (Table 5.10). This distribution of the consolidation status in the field is concomitant with the one already given by the shape of the shear stress–horizontal displacement curves obtained from the direct shear tests

(Figure 5.4). The few tested soils showing overconsolidation characteristics have overconsolidation margin ( $\sigma_m'$ ) between 3.2 and 15 kN/m<sup>2</sup>. This indicates that these soils are just slightly overconsolidated. Overconsolidation margin ( $\sigma_m'$ ) is obtained by the difference between preconsolidation stress ( $\sigma_c'$ ) and initial vertical effective stress ( $\sigma_{v0}'$ ) and should be independent of depth as no differences are expected in same stratum (Coduto, 1999).

The Coefficient of Compressibility ( $a_v$ ) is the amount by which a stratum of given thickness will compress under increasing load pressure. It is measured as the decrease in voids ratio per unit increase in pressure.

$$a_v = \frac{\Delta e}{\Delta \sigma_v'} \quad (\text{Eq. 5.14})$$

This coefficient was calculated for the different loading stages and the values obtained from the tested samples of Maputo City vary from 2.00E-04 to 9.20E-03 m<sup>2</sup>/kN for the lower loads (up to 25 kN/m<sup>2</sup>) and from 4.50E-05 to 1.87E-03 m<sup>2</sup>/kN for the higher loads (from 25 to 400 kN/m<sup>2</sup>) (Table 5.13). As expected the values of the Coefficient of Compressibility ( $a_v$ ), decrease as the stress increases in a single sample. The highest compressibility values are observed in the Ponta Vermelha Formation where are also found the highest fine material content.

The Coefficient of Volume Decrease ( $m_v$ ) quantifies the volume change that occurs when a soil mass is subjected to loading. It represents the decrease of volume with increase of pressure (Fredlund & Rahardjo, 1993) and is given by the equation:

$$m_v = \frac{a_v}{1 + e_0} \quad (\text{Eq. 5.15})$$

The coefficient of volume decrease was also calculated for every load increase on the tested soils of Maputo City. At lower loadings (up to 25 kN/m<sup>2</sup>) the coefficient of volume decrease varies from 1.27E-01 to 4.63 m<sup>2</sup>/MN while for the higher loads (from 25 to 400 kN/m<sup>2</sup>) it ranges from 3.01E-02 to 1.07 m<sup>2</sup>/MN (Table 5.13). There is no clear trend in the distribution of this coefficient in the study area.

**Table 5.13** – Coefficient of Compressibility and Coefficient of Volume Decrease of the tested soils in Maputo City at different loading stages.

| Geological Unit | Sample No. | Coefficient of Compressibility ( $a_v$ ) (m <sup>2</sup> /kN) |                             |                              |                              |                               |                                |                                | Coefficient of Volume Decrease ( $m_v$ ) (m <sup>2</sup> /MN) |                             |                              |                              |                               |                                |                                |
|-----------------|------------|---|-----------------------------|------------------------------|------------------------------|-------------------------------|--------------------------------|--------------------------------|---|-----------------------------|------------------------------|------------------------------|-------------------------------|--------------------------------|--------------------------------|
|                 |            | 1 - 25*   |                             |                              |                              |                               |                                |                                | 1 - 25*   |                             |                              |                              |                               |                                |                                |
|                 |            | 1 – 6<br>kN/m <sup>2</sup>                                    | 6 – 12<br>kN/m <sup>2</sup> | 12 – 25<br>kN/m <sup>2</sup> | 25 – 50<br>kN/m <sup>2</sup> | 50 – 100<br>kN/m <sup>2</sup> | 100 – 200<br>kN/m <sup>2</sup> | 200 – 400<br>kN/m <sup>2</sup> | 1 – 6<br>kN/m <sup>2</sup>                                    | 6 – 12<br>kN/m <sup>2</sup> | 12 – 25<br>kN/m <sup>2</sup> | 25 – 50<br>kN/m <sup>2</sup> | 50 – 100<br>kN/m <sup>2</sup> | 100 – 200<br>kN/m <sup>2</sup> | 200 – 400<br>kN/m <sup>2</sup> |
| TPv             | 3          | 4.41E-03  |                             |                              | 9.39E-04                     | 3.97E-04                      | 2.05E-04                       | 1.11E-04                       | 2.50E+00  |                             |                              | 5.67E-01                     | 2.43E-01                      | 1.27E-01                       | 6.95E-02                       |
|                 | 4          | 1.96E-03  |                             |                              | 8.80E-04                     | 4.80E-04                      | 2.10E-04                       | 1.10E-04                       | 1.05E+00  |                             |                              | 4.84E-01                     | 2.67E-01                      | 1.19E-01                       | 6.28E-02                       |
|                 | 5          | 1.46E-03  |                             |                              | 4.44E-04                     | 2.40E-04                      | 1.69E-04                       | 8.89E-05                       | 8.27E-01  |                             |                              | 2.56E-01                     | 1.40E-01                      | 9.89E-02                       | 5.26E-02                       |
|                 | 6          | ND  | ND                          | ND                           | ND                           | ND                            | ND                             | ND                             | ND  | ND                          | ND                           | ND                           | ND                            | ND                             | ND                             |
|                 | 7          | ND  | ND                          | ND                           | ND                           | ND                            | ND                             | ND                             | ND  | ND                          | ND                           | ND                           | ND                            | ND                             | ND                             |
|                 | 8          | 2.16E-03  | 3.47E-03                    | 2.79E-03                     | 1.87E-03                     | 8.59E-04                      | 4.32E-04                       | 2.10E-04                       | 1.18E+00  | 1.9E+00                     | 1.55E+00                     | 1.06E+0                      | 5.00E-01                      | 2.58E-01                       | 1.28E-01                       |
|                 | 9          | ND  | ND                          | ND                           | ND                           | ND                            | ND                             | ND                             | ND  | ND                          | ND                           | ND                           | ND                            | ND                             | ND                             |
|                 | 10         | 9.20E-03  | 3.50E-03                    | 1.77E-03                     | 1.00E-03                     | 4.80E-04                      | 2.50E-04                       | 1.55E-04                       | 4.65E+00  | 1.81E+0                     | 9.25E-01                     | 5.29E-01                     | 2.57E-01                      | 1.36E-01                       | 8.54E-02                       |
|                 | 11         | 2.21E-03  |                             |                              | 1.48E-03                     | 7.20E-04                      | 3.50E-04                       | 1.60E-04                       | 1.13E+00  |                             |                              | 7.81E-01                     | 3.87E-01                      | 1.92E-01                       | 8.95E-02                       |
|                 | 12         | 6.75E-03  |                             |                              | 1.36E-03                     | 6.72E-04                      | 2.99E-04                       | 1.73E-04                       | 3.42E+00  |                             |                              | 7.51E-01                     | 3.78E-01                      | 1.72E-01                       | 1.01E-01                       |
|                 | 14         | ND  | ND                          | ND                           | ND                           | ND                            | ND                             | ND                             | ND  | ND                          | ND                           | ND                           | ND                            | ND                             | ND                             |
| QCo             | 1          | 3.58E-03  |                             |                              | 6.80E-04                     | 3.20E-04                      | 1.60E-04                       | 1.10E-04                       | 1.91E+00  |                             |                              | 3.80E-01                     | 1.81E-01                      | 9.12E-02                       | 6.33E-02                       |
|                 | 2          | 1.97E-03  |                             |                              | 4.98E-04                     | 2.08E-04                      | 1.19E-04                       | 7.55E-05                       | 1.34E+00  |                             |                              | 3.49E-01                     | 1.47E-01                      | 8.49E-02                       | 5.43E-02                       |
|                 | 16         | 4.20E-03  | 1.67E-03                    | 1.00E-03                     | 3.60E-04                     | 2.00E-04                      | 1.30E-04                       | 8.50E-05                       | 2.85E+00  | 1.15E+00                    | 6.94E-01                     | 2.52E-01                     | 1.41E-01                      | 9.23E-02                       | 6.09E-02                       |
|                 | 18         | 1.53E-03  | 1.83E-03                    | 5.47E-04                     | 4.08E-04                     | 2.29E-04                      | 1.74E-04                       | 9.48E-05                       | 7.85E-01  | 9.44E-01                    | 2.84E-01                     | 2.13E-01                     | 1.20E-01                      | 9.20E-02                       | 5.05E-02                       |
|                 | 19         | 2.80E-03  | 2.00E-03                    | 8.46E-04                     | 4.80E-04                     | 3.40E-04                      | 2.10E-04                       | 1.15E-04                       | 1.30E+00  | 9.32E-01                    | 3.97E-01                     | 2.26E-01                     | 1.61E-01                      | 1.00E-01                       | 5.55E-02                       |
|                 | 21         | 2.00E-04  | 1.33E-03                    | 1.08E-03                     | 1.28E-03                     | 3.60E-04                      | 2.30E-04                       | 2.25E-04                       | 1.27E-01  | 8.49E-01                    | 6.89E-01                     | 8.27E-01                     | 2.37E-01                      | 1.54E-01                       | 1.53E-01                       |
| Qma             | 13         | 4.17E-04  |                             |                              | 2.40E-04                     | 1.00E-04                      | 7.00E-05                       | 4.50E-05                       | 2.66E-01  |                             |                              | 1.54E-01                     | 6.44E-02                      | 4.52E-02                       | 2.92E-02                       |
|                 | 17         | 3.20E-03  | 1.33E-                      | 9.23E-04                     | 5.20E-04                     | 2.60E-04                      | 1.50E-04                       | 2.05E-04                       | 2.01E+00  | 8.47E-01                    | 5.89E-01                     | 3.35E-01                     | 1.69E-01                      | 9.82E-02                       | 1.35E-01                       |
| Qi              | 15         | 3.33E-04  |                             |                              | 3.20E-04                     | 2.60E-04                      | 1.30E-04                       | 5.50E-05                       | 1.69E-01  |                             |                              | 1.63E-01                     | 1.33E-01                      | 6.67E-02                       | 2.84E-02                       |
| Qmc             | 20         | 6.00E-04  | 8.33E-                      | 3.85E-04                     | 2.40E-04                     | 1.60E-04                      | 1.00E-04                       | 6.50E-05                       | 3.25E-01  | 4.52E-01                    | 2.09E-01                     | 1.31E-01                     | 8.76E-02                      | 5.50E-02                       | 3.60E-02                       |

\* Loading stage 1-25 kN/m<sup>2</sup> for the samples not analysed for lower stage intervals.

ND: Not Determined

The consolidation test aims at defining the stress-strain properties of the soil in order to anticipate the soil total settlement under loading. Soils subjected to loading reveal their settlement in three phases namely immediate settlement, primary consolidation and secondary consolidation (Lambe & Whitman, 1979; Lee *et al.*, 1983; Coduto, 1999). These components of settlement are time-dependent as the volume decrease is related to the pore water flow out from the soil material, introducing the component of rate of consolidation. The time for consolidation to occur can be predicted using the oedometer test and in sandy soils it occurs very quickly. Their hydraulic conductivity is high what allows water to drain freely out of the soil taking therefore an exceptionally short time (Lambe & Whitman, 1979; Coduto, 1999). The rate of flow is controlled by the pore pressure, the permeability and the compressibility of the soil. While drainage is occurring, “the pore water pressure is greater than normal because it is carrying part of the applied stress (as opposed to the soil particles). As the pore pressure dissipates the rate of flow decreases and eventually the process will be essentially completed, leading to a condition of constant effective stress” (Lee *et al.*, 1983).

From the consolidation test it was observed that the primary settlement of the tested sandy soils of Maputo is almost quick and immediate in all samples. The higher porosity and hydraulic conductivity of the sandy soils allow water to drain quickly favouring dissipation of the excess pore water pressures. Coduto (1999) states that “it is not necessary to conduct rate of consolidation analyses in sandy and gravelly soils, simply computing the ultimate consolidation settlement,  $(\delta_c)_{ult}$ , and assume it occurs as quickly as the load is applied”. For the purpose of this research, the rate of consolidation is calculated in order to evaluate its magnitude. The coefficient of consolidation was calculated through the following equation given by Shroff & Shah (2003):

$$C_v = \frac{k}{m_v \gamma_w} \quad (\text{Eq. 5.16})$$

The coefficient of consolidation has the dimensions  $\text{m}^2/\text{year}$ . Being proportional to the ratio between the coefficients of permeability and compressibility, both of which decrease with an increase in pressure, the coefficient of consolidation shows much less variation with pressure (Shroff & Shah, 2003).

The results of the coefficient of consolidation are in accordance with the expected in these circumstances with the highest values on the slightly overconsolidated soils (Table 5.14) comparing

with the normally consolidated. It ranges from  $3.83\text{E-}02$  to  $5.56 \text{ m}^2/\text{year}$  for the normal consolidated samples and from  $3.73\text{E-}02$  to  $2.2\text{E}01 \text{ m}^2/\text{year}$  for the slightly overconsolidated soil samples. This type of soil has  $C_v$  values five to ten times greater than the same soils in a normally consolidated condition. The distribution of this consolidation parameter does not follow a specific pattern over the soil types of Maputo City.

**Table 5.14** – Coefficient of consolidation of the tested soils of Maputo City at different loading stages

| Geological Unit | Sample No. | Coefficient of Consolidation ( $C_v$ ) ( $\text{m}^2/\text{year}$ ) |                        |                         |                         |                          |                           |                           |
|-----------------|------------|---|------------------------|-------------------------|-------------------------|--------------------------|---------------------------|---------------------------|
|                 |            | 1 - 25 $\text{kN/m}^2$ *  |                        |                         |                         |                          |                           |                           |
|                 |            | 1 – 6 $\text{kN/m}^2$   | 6 - 12 $\text{kN/m}^2$ | 12 - 25 $\text{kN/m}^2$ | 25 – 50 $\text{kN/m}^2$ | 50 - 100 $\text{kN/m}^2$ | 100 - 200 $\text{kN/m}^2$ | 200 - 400 $\text{kN/m}^2$ |
| TPv             | 3          |   |                        | 4.45E-02                | 1.96E-01                | 4.58E-01                 | 8.76E-01                  | 1.60E+00                  |
|                 | 4          |   |                        | 1.50E-01                | 3.26E-01                | 5.91E-01                 | 1.33E+00                  | 2.52E+00                  |
|                 | 5          |   |                        | 2.90E-01                | 9.34E-01                | 1.72E+00                 | 2.42E+00                  | 4.56E+00                  |
|                 | 6          | ND  | ND                     | ND                      | ND                      | ND                       | ND                        | ND                        |
|                 | 7          | ND  | ND                     | ND                      | ND                      | ND                       | ND                        | ND                        |
|                 | 8          | 2.08E-01  | 1.28E-01               | 1.58E-01                | 2.31E-01                | 4.89E-01                 | 9.49E-01                  | 1.91E+00                  |
|                 | 9          | ND  | ND                     | ND                      | ND                      | ND                       | ND                        | ND                        |
|                 | 10         | 3.83E-02  | 9.82E-02               | 1.92E-01                | 3.36E-01                | 6.91E-01                 | 1.31E+00                  | 2.08E+00                  |
|                 | 11         |   |                        | 3.85E-01                | 5.59E-01                | 1.13E+00                 | 2.27E+00                  | 4.87E+00                  |
|                 | 12         |   |                        | 5.61E-02                | 2.56E-01                | 5.08E-01                 | 1.12E+00                  | 1.91E+00                  |
|                 | 14         | ND  | ND                     | ND                      | ND                      | ND                       | ND                        | ND                        |
| QCo             | 1          |   |                        | 5.70E-02                | 2.87E-01                | 6.03E-01                 | 1.20E+00                  | 1.72E+00                  |
|                 | 2          |   |                        | 3.73E-02                | 1.43E-01                | 3.39E-01                 | 5.88E-01                  | 9.19E-01                  |
|                 | 16         | 5.22E-02  | 1.30E-01               | 2.15E-01                | 5.91E-01                | 1.06E+00                 | 1.61E+00                  | 2.45E+00                  |
|                 | 18         | 3.34E-01  | 2.78E-01               | 9.23E-01                | 1.23E+00                | 2.19E+00                 | 2.85E+00                  | 5.20E+00                  |
|                 | 19         | 4.40E-01  | 6.12E-01               | 1.44E+00                | 2.52E+00                | 3.54E+00                 | 5.68E+00                  | 1.03E+01                  |
|                 | 21         | 5.53E-01  | 8.29E-02               | 1.02E-01                | 8.52E-02                | 2.97E-01                 | 4.59E-01                  | 4.62E-01                  |
| Qma             | 13         |   |                        | 5.14E-01                | 8.86E-01                | 2.12E+00                 | 3.02E+00                  | 4.67E+00                  |
|                 | 17         | 1.20E-01  | 2.84E-01               | 4.09E-01                | 7.20E-01                | 1.43E+00                 | 2.45E+00                  | 1.78E+00                  |
| Qi              | 15         |   |                        | 3.71E+00                | 3.85E+00                | 4.72E+00                 | 9.38E+00                  | 2.20E+01                  |
| Qmc             | 20         | 6.14E-01  | 4.42E-01               | 9.54E-01                | 1.52E+00                | 2.28E+00                 | 3.63E+00                  | 5.56E+00                  |

\* Loading stage 1-25  $\text{kN/m}^2$  for the samples not analysed for lower stage intervals; ND – Not Determined

### 5.5.3 – Collapsible Soils Identification by Physical Properties

Collapsible soils are defined as “any unsaturated soil that goes through a radical rearrangement of particles” (Clemence & Finbarr, 1981) and great volumetric reduction upon wetting either subjected or not to additional loading (Signer *et al.*, 1989). The conditions required for appreciable collapse to occur are:

- (1) an open, potentially unstable and partly saturated structure (Barden *et al.*, 1973). The soil



structure should be porous enough to enable the collapse to take place as it is manifested by volume reduction (Feda, 1988); Silty to sandy soils (Schwartz, 1985; Brink *et al.*, 1982) and content of clay particles (Clemence & Finbarr, 1981) with open texture are likely to have collapsible fabric;

- (2) an increase on percentage of moisture content as it causes strength loss (Schwartz, 1985; Signer *et al.*, 1989; Houston *et al.*, 2001; Feda, 1988). This is considered to be the triggering action for collapse to occur;
- (3) low initial density and water content at saturation (Houston *et al.*, 2001);
- (4) high value of an applied or existing stress component to develop a metastable condition (Barden *et al.*, 1973; Schwartz, 1985);
- (5) “a strong soil bonding or cementing agent to stabilise intergranular contacts, with a reduction of which, upon wetting, collapse will occur” (Barden *et al.*, 1973, Vaughan *et al.* 1988);
- (6) leaching, mainly due to the high evaporation rates in arid and semi-arid regions where this soils likely occur (Signer *et al.*, 1989);

Foreseeing these conditions in the study area, a soil collapse potential assessment was developed following two approaches: (a) an approach based on physical properties suggested by El-Ruwaih & Touma (1986), and (b) an approach based on oedometer tests proposed by Jennings & Knight (1957) (Chapter 2).

The approach based on physical properties uses qualitative methods to evaluate the soil collapse potential. Soil properties such as the Atterberg limits and plasticity index, grain size characteristics, voids ratio, natural moisture content and the degree of saturation are used in this approach. The disadvantage of this approach is that it does not take into account the influence of loading, types of minerals present in the soil or the nature of the soil structure and bonding between particles (El-Ruwaih & Touma, 1986). Table 5.15 shows the criteria for identification of collapsible soils using physical properties developed by several authors.

Calculations to determine the collapsible behaviour of the tested soils using the indicated criteria in Table 5.15 are presented in Table 5.16. Tested soils were then classified according to the collapse behaviour as indicated in Table 5.17.

**Table 5.15** – Criteria for identification of collapsible soils based on the physical properties (After Futai, 1999)

| Author                   | Criteria                            | Conditions to Identify Collapse                | Soil Condition  |
|--------------------------|-------------------------------------|--|---|
| Feda (1966)              | $KL = \frac{(w_o/S) - Wp}{Wl - Wp}$ | $S > 80\%$<br>$KL > 0,85$                      | Collapsible   |
| Prikloński (1952)        | $Kd = \frac{Wl - w_o}{Wl - Wp}$     | $Kd < 0$<br>$1 > Kd > 0$<br>$Kd > 1$           | Highly Collapsible<br>Collapsible<br>Expansive                                    |
| Kassif e Henkin (1967)   | $K = \gamma_d * w$                  | $K < 15$                                       | Collapsible   |
| Jennings e Knight (1975) | Fine Sand                           | $S < 50 \%$<br>$S > 60 \%$                     | Collapsible<br>Non Collapsible  |
| Handy (1973)             | Fines Content (<0,002 mm)           | $< 16\%$<br>$16 \text{ a } 32 \%$<br>$> 32 \%$ | High Probability of Collapse<br>Probably Collapsible<br>Generally non Collapsible |

KL – Collapsibility Coefficient; Kd – Coefficient of deformation ;  $Wp$  – Plastic Limit;  $Wl$  – Liquid Limit; K – Subsidence Coefficient;  $\gamma_d$  – dry unit weight;  $w_o$  – Initial moisture Content;  $w$  – Natural Moisture Content; S – Degree of Saturation

**Table 5.16** – Results of collapse identification based on the physical parameters

| Geological Unit | Sample N° | Parameter       |                 |                |                    |                         |
|-----------------|-----------|-----------------|-----------------|----------------|--------------------|-------------------------|
|                 |           | KL <sup>1</sup> | Kd <sup>2</sup> | K <sup>3</sup> | S (%) <sup>4</sup> | % of fines <sup>5</sup> |
| TPv             | 3         | -11.56          | 9.99            | 6.36           | 12.12              | 1.36                    |
|                 | 4         | -8.23           | 8.46            | 3.70           | 8.19               | 0.55                    |
|                 | 5         | -84.22          | 67.79           | 8.12           | 18.75              | 0.30                    |
|                 | 6         | ND              | ND              | ND             | ND                 | 0.08                    |
|                 | 7         | ND              | 86.21           | ND             | ND                 | 0.41                    |
|                 | 8         | -16.22          | 14.80           | 4.41           | 8.6                | 0.68                    |
|                 | 9         | -9.79           | 8.26            | 11.09          | 25.46              | 0.88                    |
|                 | 10        | -17.65          | 15.75           | 6.76           | 13.46              | 0.72                    |
|                 | 11        | ND              | ND              | 18.88          | 35.45              | 0.37                    |
|                 | 12        | -10.22          | 7.77            | 12.38          | 26.18              | 0.50                    |
|                 | 14        | ND              | ND              | ND             | ND                 | 0.47                    |
| QCo             | 1         | -146.37         | 94.07           | 11.04          | 21.28              | 1.52                    |
|                 | 2         | -162.03         | 103.00          | 15.62          | 48.72              | 0.40                    |
|                 | 16        | ND              | ND              | 5.29           | 14.69              | 0.24                    |
|                 | 18        | ND              | ND              | 6.15           | 13.06              | 0.43                    |
|                 | 19        | ND              | ND              | 26.63          | 50.64              | 0.35                    |
|                 | 21        | -22.23          | 14.55           | 8.05           | 22.25              | 0.49                    |
| Qma             | 13        | -73.27          | 60.32           | 7.36           | 20.23              | 0.26                    |
|                 | 15        | ND              | ND              | 27.56          | 56.19              | 0.22                    |
| Qi              | 17        | -55.17          | 45.68           | 4.98           | 11.77              | 0.29                    |
| Qmc             | 20        | -118.47         | -1.79           | 25.88          | 62.8               | 0.29                    |

ND – Not Determined; <sup>1</sup>Feda (1966); <sup>2</sup>Prikloński (1952); <sup>3</sup>Kassif & Henkin (1967);

<sup>4</sup>Jennings & Knight (1975); <sup>5</sup>Handy (1973)

Looking at Table 5.17, it is evident that the soils of Maputo City comply with the criteria of collapse behaviour established by Kassif & Henkin (1967), Jennings & Knight (1975) and Handy

(1973) but they do not comply with the Feda (1966) and Priklopskij (1952) criteria. The high degree of saturation ( $S > 80\%$ ) established by the Feda (1966) criterion made the soils of Maputo not to qualify as collapsible.

**Table 5.17** – Soils of Maputo City characterized according to their collapse behaviour using the different classification based on the physical parameters

| Geological Unit | Sample N <sup>o</sup> | Parameters      |                    |                 |                     |                           |
|-----------------|-----------------------|-----------------|--------------------|-----------------|---------------------|---------------------------|
|                 |                       | KL <sup>1</sup> | Kd <sup>2</sup>    | K <sup>3</sup>  | Sr (%) <sup>4</sup> | % of fines <sup>5</sup>   |
| TPv             | 3                     | Non Collapsible | Expansive          | Collapsible     | Collapsible         | High Collapse Probability |
|                 | 4                     | Non Collapsible | Expansive          | Collapsible     | Collapsible         | High Collapse Probability |
|                 | 5                     | Non Collapsible | Expansive          | Collapsible     | Collapsible         | High Collapse Probability |
|                 | 6                     | ND              | ND                 | ND              | ND                  | High Collapse Probability |
|                 | 7                     | ND              | Expansive          | ND              | ND                  | High Collapse Probability |
|                 | 8                     | Non Collapsible | Expansive          | Collapsible     | Collapsible         | High Collapse Probability |
|                 | 9                     | ND              | Expansive          | Collapsible     | Collapsible         | High Collapse Probability |
|                 | 10                    | Non Collapsible | ND                 | Non Collapsible | Collapsible         | High Collapse Probability |
|                 | 11                    | ND              | Expansive          | Collapsible     | Collapsible         | High Collapse Probability |
|                 | 12                    | Non Collapsible | Expansive          | Collapsible     | Collapsible         | High Collapse Probability |
|                 | 14                    | ND              | ND                 | ND              | ND                  | High Collapse Probability |
| QCo             | 1                     | Non Collapsible | Expansive          | Collapsible     | Collapsible         | High Collapse Probability |
|                 | 2                     | Non Collapsible | Expansive          | Non Collapsible | Collapsible         | High Collapse Probability |
|                 | 16                    | ND              | ND                 | Collapsible     | Collapsible         | High Collapse Probability |
|                 | 18                    | ND              | ND                 | Collapsible     | Collapsible         | High Collapse Probability |
|                 | 19                    | ND              | ND                 | Non Collapsible | Collapsible         | High Collapse Probability |
|                 | 21                    | Non Collapsible | Highly Collapsible | Collapsible     | Collapsible         | High Collapse Probability |
| Qma             | 13                    | Non Collapsible | Expansive          | Collapsible     | Collapsible         | High Collapse Probability |
|                 | 17                    | Non Collapsible | Expansive          | Collapsible     | Collapsible         | High Collapse Probability |
| Qi              | 15                    | ND              | ND                 | Non Collapsible | Collapsible         | High Collapse Probability |
| Qmc             | 20                    | Non Collapsible | Expansive          | Non Collapsible | Non Collapsible     | High Collapse Probability |

ND – Non Determined; <sup>1</sup>Feda (1966); <sup>2</sup>Priklopskij (1952), cited by Feda (1966); <sup>3</sup>Kassif & Henkin (1967);

<sup>4</sup>Jennings & Knight (1975); <sup>5</sup>Handy (1973), cited by Lutenegeger & Saber (1988).

Clemence & Finbarr (1981) cited Gibbs & Bara (1962) as proposing also the use of the dry unit weight and liquid limit as criteria to predict soil collapse. The method is based in the argument that “a soil, which has sufficient void spaces to hold its liquid limit moisture at saturation, is susceptible to collapse upon wetting” (Clemence & Finbarr, 1981). A specific density line of 2.7 in the Figure 5.10 separates the areas for collapsible and for non collapsible soils in a dry unit weight vs. liquid limit plot. According to Clemence & Finbarr (1981) soils in loose condition have been observed to collapse because their moisture content becomes greater than the liquid limit when the soils are fully saturated. Using this criterion, only 6 samples (33% of the tested samples in Maputo City) fall in the area of non-collapsible soils (Samples 2, 4, 9, 10, 12 and 13).

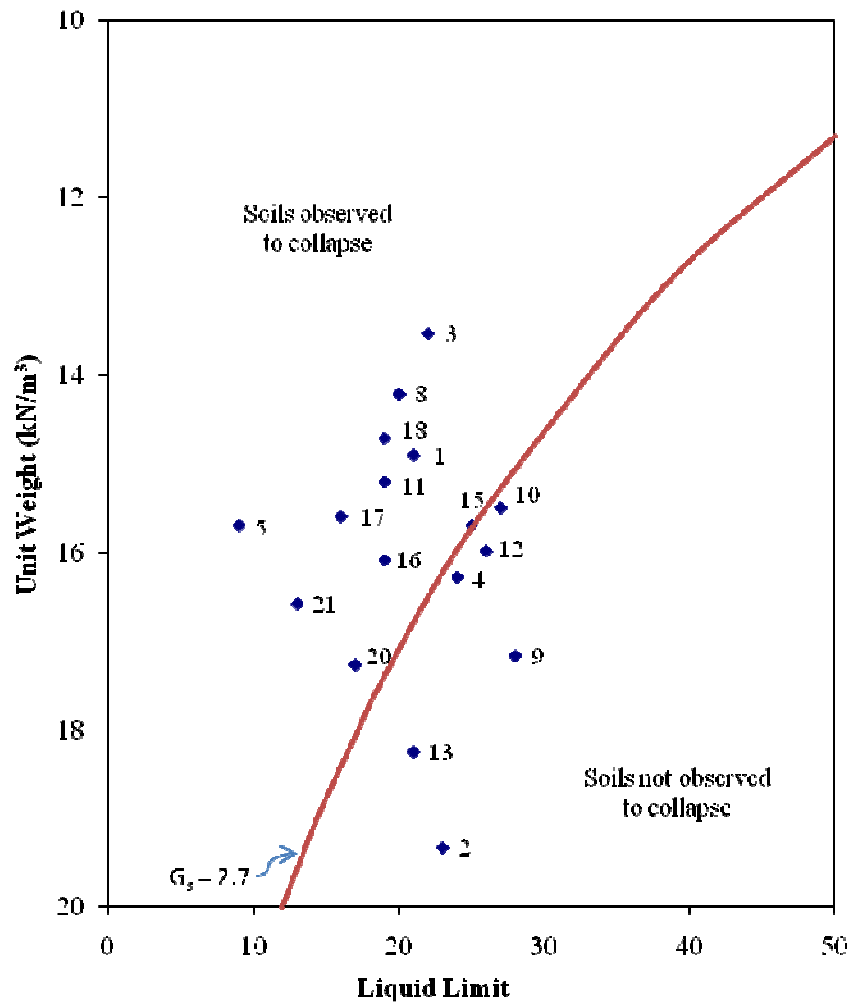


**Figure 5.10** – Collapsible and non collapsible soil using the Gibb (1962) criterion based on dry density and liquid limit. Most of the tested soils plot in the area of soils likely to collapse.

#### 5.5.4 – Collapsible Soils: Identification with Double Oedometer

The approach based on the oedometer test on natural soil samples provides the qualitative prediction of the possibilities of collapse, as well as the quantitative information to allow estimates of the magnitude and rate of soil collapse. The well established method developed on this basis and used in this research is from Jennings & Knight (1957). This method also called “double consolidation” technique evaluates the effect of both saturation and loading at various levels. Two oedometer tests are performed simultaneously on undisturbed identical soil samples. One oedometer test is conducted on a sample at natural moisture content (NMC) and the second is carried out as an ordinary consolidation test, then the cell is flooded with water. The collapse, and

the evaluation of the effect of saturation, is then determined by the superimposition of the consolidation curves from both tests, assuming that no collapse may occur under equilibrium conditions with the overburden pressure in the field (Jennings & Knight, 1957; Riani & Barbosa, 1989).

Figure 5.11 shows voids ratio vs. vertical effective stress ( $e/\log \sigma_{v0}'$ ), in log scale, curves from the double oedometer test (remaining curves in the Appendix A). This graph, characteristic for 33.3% of the tested soils in Maputo City (Samples 1, 2, 3, 10, 12, and 16), with no clear trend through the geological formations, shows that the curve  $e/\log \sigma_{v0}'$  of the test at natural moisture content (NMC) is always on top of the graph  $e/\log \sigma_{v0}'$  of the saturated test. From the plot it can also be observed that the initial voids ratio of the two samples after the first 24 hours of loading, and from then on, are not identical. This clearly indicates large reduction of voids ratio which occurs with load increase in the saturated test and is disclosed as straight line. This considerable reduction of the voids ratio in the saturated test corresponds to the additional vertical strain experienced by the soil which is linked to collapse of the soil structure in the presence of water. The test results show the soil compressibility and its significant sensitivity to collapse upon wetting. These soils can be considered as truly collapsible as showing full collapse of the soil structure.

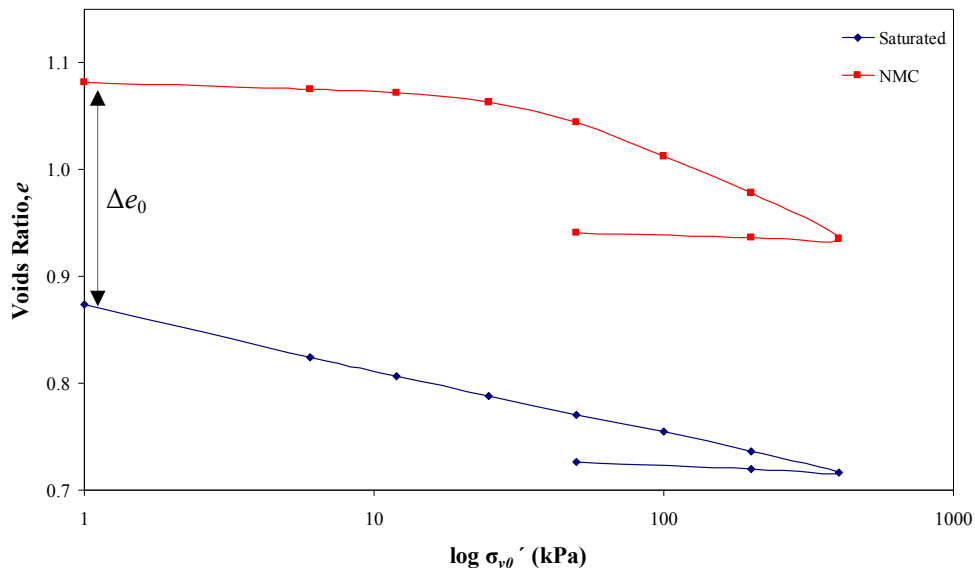


**Figure 5.11** – Double consolidation test of Sample 1 showing full collapse of the soil structure of the saturated soil. This graph is also characteristic for samples 2, 3, 10, 12 and 16.  $\Delta e_0$  denotes reduction of voids ratio with addition of water under 1kPa at the beginning of the test

The two curves do not originate from the same point proving the definition of collapsible soil at the beginning of soil testing of the saturated sample. After being placed in a consolidometer under a light 1 kPa load, inundation of the soil sample with water was accompanied by quick consolidation without additional loading. This is explained by the relatively higher porosity and hydraulic conductivity of the sandy soils of Maputo City, which allows water to drain quickly. The reduction of the sample thickness reflects the reduction on the voids ratio ( $\Delta e_0$ ) and the collapse of the soil structure without being a consequence of additional load to the soil structure (Figure 5.11).

Calculation of the soil collapse potential was based on the procedure proposed by Jennings & Knight (1957). According to this procedure, for the normal consolidated soils where compression is considered to take place on the virgin curve, the natural moisture content curve is moved down parallel to adjusted to the  $e_0, \sigma_{v0}'$  point. This  $e_0, \sigma_{v0}'$  point represents the voids ratio at the total effective stress acting at the depth of the sample (Figure 5.12). From the difference of  $e$  ( $\Delta e$ ) between the new curve, parallel to the NMC curve, and the saturated curve it is possible to determine the collapse potential of the soils at different loadings intervals.

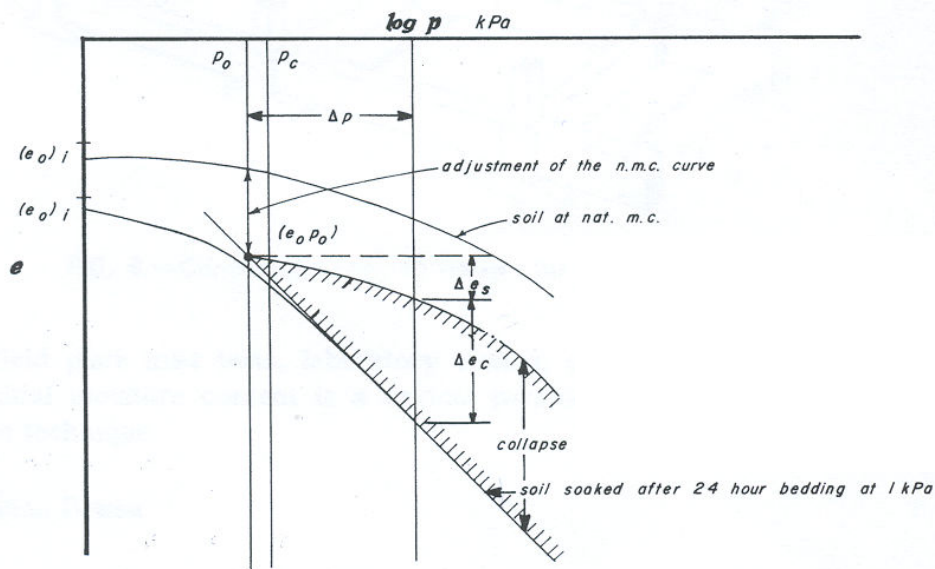


**Figure 5.12** – Double consolidation test and adjustments of curves for normally consolidated soils (Jennings & Knight, 1957; Clemence & Finbarr, 1981)

Riani & Barbosa (1989) suggest an analysis using the stress vs. collapse settlement curves in order to define and evaluate the collapse peak behaviour in relation to the applied loadings. Figure 5.13 presents the stress vs. collapse curve for the tested soils in Maputo City showing full collapse

settlement. The highest collapse behaviour is observed in Samples 12, 10 and 3 (Ponta Vermelha Formation) reaching values above 5% predicted to cause moderate trouble in foundation design according to the suggested values for collapse potential by Jennings & Knight (1975) (Table 5.18). Samples 1, 2, 12 and 16 showed peak collapse at early stages of applied loadings between, 25 and 50 kN/m<sup>2</sup>, which falls gradually (Samples 2 and 12) or abruptly (Samples 1 and 16) before it stabilises at higher loadings. Samples 3 and 10 do not show peak collapse in the range of loading used in this research as it continues to increase even at higher loadings. This behaviour is explained by the relatively high coefficient of compressibility and coefficient of volume decrease shown by these samples, particularly for Sample 3.

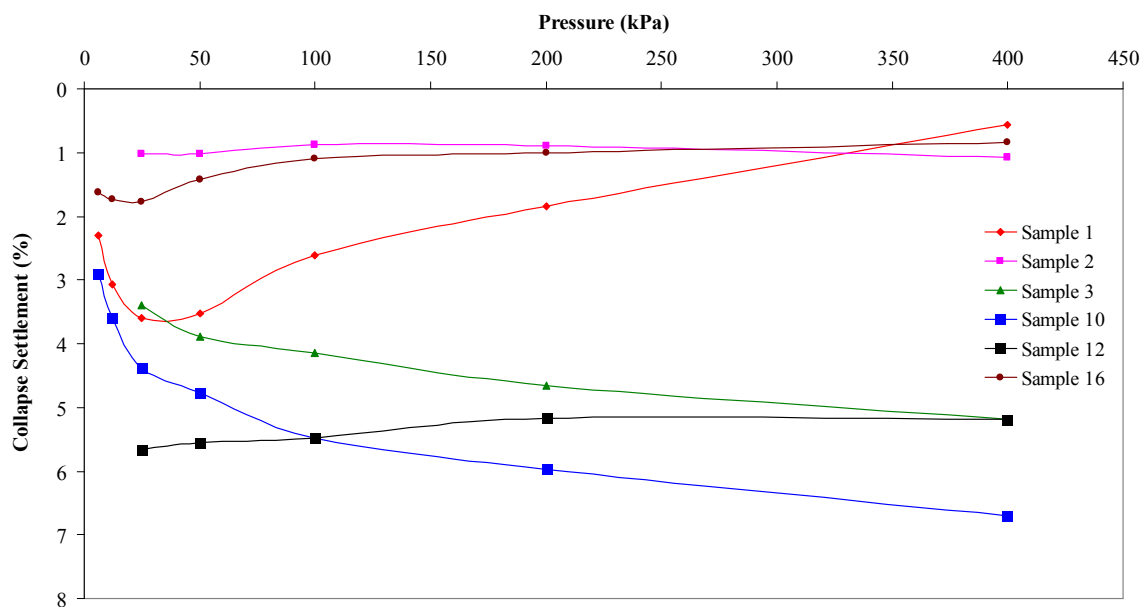


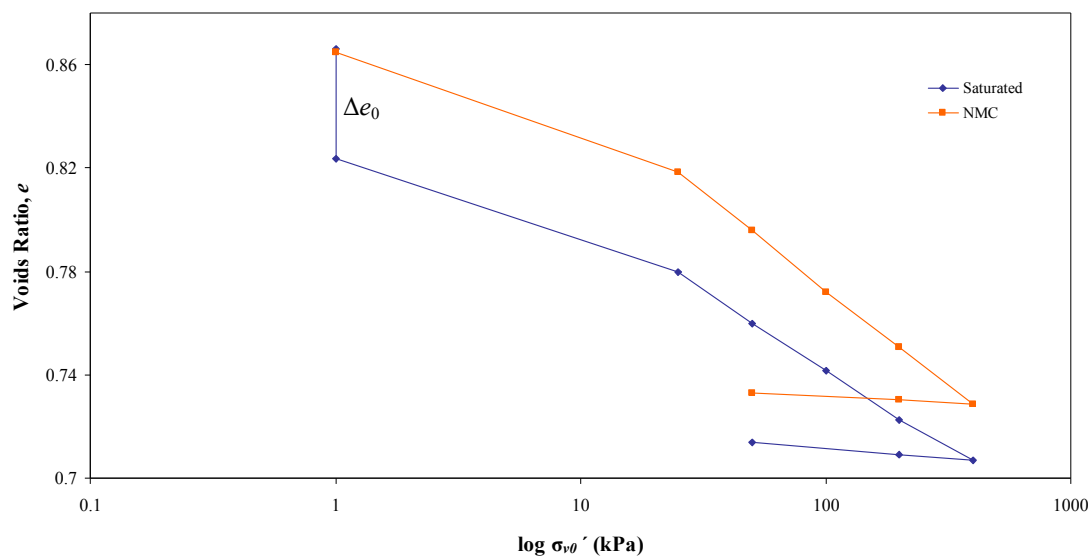
Figure 5.13 – Collapse ranges for the collapsible soils of Maputo City.

Table 5.18 – Collapse Potential Values indicating the severity of problem for foundation design (From Jennings & Knight, 1975; Clemence & Finbarr, 1981).

| Collapse Potential (%) | Severity of the Problem |
|------------------------|-------------------------|
| 0 – 1                  | No Problem              |
| 1 – 5                  | Moderate Trouble        |
| 5 – 10                 | Trouble                 |
| 10 – 20                | Severe Trouble          |
| > 20                   | Very Severe Trouble     |

### 5.5.5 – Partial Collapse: Presence and Influence of Bonding

The largest part (66.7%) of the soils submitted to double oedometer test in the study area (Samples 4, 5, 8, 9, 11, 13, 15, 17, 18, 19, 20 and 21) show the shape of curves represented in Figure 5.14. Similar to the other set of graphs the curve  $e/\log \sigma_{v0}'$  of the test at natural moisture content (NMC) is always on top of the graph  $e/\log \sigma_{v0}'$  of the saturated test. The two curves do not start from the same point due to the same reason pointed out earlier, but for this particular case the soil structure does not break completely to the point of full collapse as proved in the following loadings. Apart from the samples of Ponta Vermelha Formation (Samples 4, 5, 8, 9, 11 and 13), there is evidence of bonding in samples that do not have "high iron oxide content". This is shown by the shape of curves of double consolidation test (Figure 5.14) and by comparing the compressibility of two samples at the same voids ratio and water content, one being undisturbed and other being completely remoulded (Figure 5.15).



**Figure 5.14** – Typical  $e/\log \sigma_{v0}'$  curves from the double consolidation test performed on the soils of Maputo City showing the presence of the bonding material in the soil structure.

From Figure 5.14 it can be observed that the rate of reduction of voids ratio in both samples is identical and this is disclosed as parallel lines. Although the initial reduction in terms of voids ratio caused by addition of water, the consolidation rate of the saturated soil continues similar to the one of the soil at natural moisture content. This is explained by the presence of a strong bonding



material of soil particles which obstructs total destruction of the soil structure with moisture content increase.

On the other end, soils from Maputo City showed yield in the consolidation test giving rise to the observed apparent preconsolidation pressure in half of the tested soil samples (Samples 1, 2, 5, 9, 11, 12, 15, 17, 18, 19 and 20) with no clear trend through the geological formations. Most of the values of preconsolidation pressure are significantly higher than the corresponding overburden pressure. The reason for this is also attributed to the existence of strong bonding agent linking the soils particles together (Maccarini *et al.*, 1989). Vaughan *et al.* (1988) have also stressed that yield observed in the consolidation test comes from bond strength and initial voids ratio. Seventy three percent of the samples showing preconsolidation pressure higher than the overburden pressure proven later bonding characteristics (Samples 5, 9, 11, 15, 17, 18, 19, 20). Although bonding strength is difficult to determine experimentally its influence in the behaviour and characteristics of porous material has been predicted by various authors as Elliot & Brown (1985), Maccarini (1987), Maccarini *et al.* (1989), Vaughan *et al.* (1988) among others. The effect of bonding is observed in most of the *in situ* materials (weak soils as well as stronger porous rocks) investigated in soil mechanics (Vaughan *et al.*, 1988).

The presence and influence of bonding can also be detected by comparing the compressibility of two samples at the same voids ratio and water content, one being undisturbed and other being completely remoulded (Maccarini, 1987; Maccarini *et al.*, 1989). For the purpose of this research, bonding was investigated through running oedometer test on the soil material in its remoulded state with the greatest initial voids ratio as possible which was obtained by placing in a moist un-compacted state as recommended by Vaughan *et al.* (1988). Bonds have been removed through destruction of the soil structure by remoulding between the fingers. This was considered enough to destruct or remould the soil structure (Leroueil *et al.*, 1979 and Vaughan *et al.*, 1988).

Figure 5.15 shows the typical compression curve of an oedometer test of the remoulded soil of Maputo City compared with the curve of a bonded soil tested at NMC. The remoulded samples showed a significantly higher compression than that of the bonded soil. This difference occurs because part of the stress applied to the bonded soil is carried by the bonds themselves (denoted bond stress), as the bonded soil is stiffer than the same soil without bonds. Yield of the bonds makes the bonding contribution to the soil strength (the bond strength) decreases and with increasing strain the soil loses its bonding entirely and becomes de-structured (Vaughan *et al.*, 1988).

The curves of the remoulded samples are used to establish the limit between the stable and meta-stable states (Figure 5.15) of the soil and the compression curves of the bonded soils are located in the meta-stable space (Maccarini *et al.*, 1989). This boundary between the stable and meta-stable states combined with the *in situ* void ratio is used for soil engineering classification and indicates the capacity of the soil to remain in the stable zone when loaded with engineering infrastructures and the extent to which it will contract or dilate during shearing (Vaughan *et al.*, 1988). These behaviours depend on the strength characteristics and the stiffness of the bonding agent present in the soil.

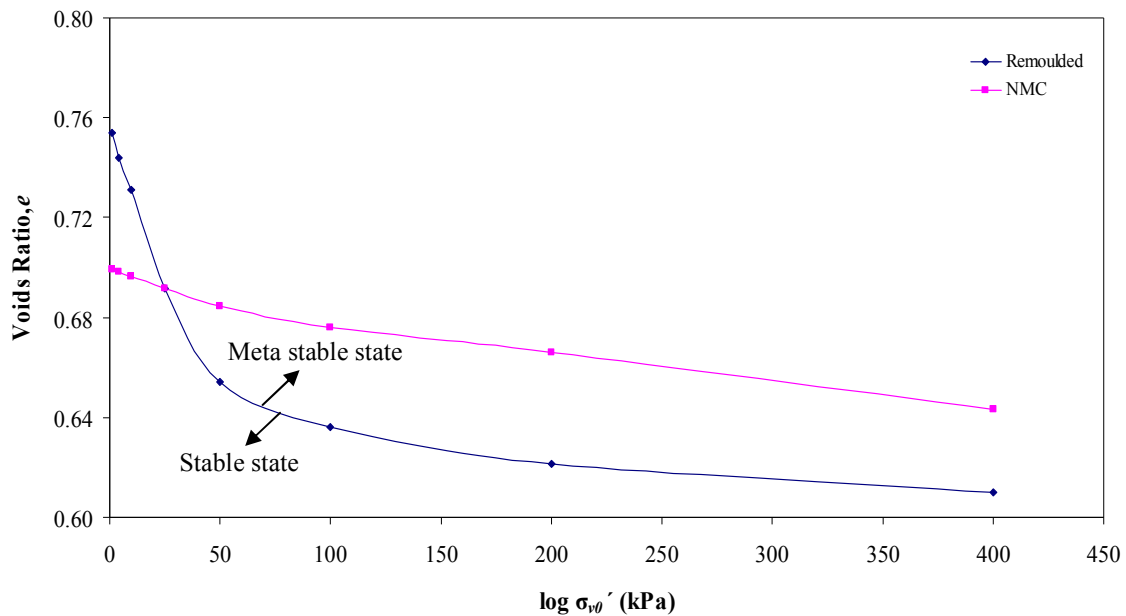


**Figure 5.15** – Typical compression curve in a normal scale of an oedometer test of the remoulded soil compared with the curve of a bonded soil occurring in Maputo City (Sample 20)

## 5.6 – COLLAPSE SETTLEMENT AND BUILDINGS DAMAGE

Discussions in the above Sections 5.5.4. and 5.5.5 proved the collapsible behaviour of the majority of the tested soils in Maputo. For example, the reported leakage of 60 to 70 thousands of litres of water per day from the underground damaged water reservoirs in the building in Site 1 (Figure 4.12), was responsible to trigger collapse settlement. Raising the water content in a soil reduces the effective stress at any given depth in the soil and thereby results in a lower bearing capacity and greater settlement. However, the detailed behaviour of a shallow foundation depends very much on the type of soil on which the foundation rests (Lambe & Whitman, 1979).

Position of the broken underground reservoirs and pipes in relation to the building, normally located at the rear side, the position of the building in relation to adjacent buildings and to the coastal slope to the eastern side of Julius Nyerere Avenue has controlled the tilting direction of the affected buildings (Chapter 4, Section 4.8.2). Flooding resulting from leakage of underground reservoirs will be high close to the leaking point than to the points located away. The moisture of the places is allowing soils collapsing to occur causing settlement in the wet area. This difference in moisture content was therefore reflected in terms of collapse in the different points below the affected buildings and differential settlement resulted on buildings tilting. The raft foundation of the buildings is considered to be related to the absence of cracks in the buildings.

The damage of these buildings can also be linked to the removal of fine material from below the foundation at the flooded areas of the buildings by internal erosion (water flow). The removal of fine material by internal erosion due to water flow in the buildings founded on silty sand can occur since the silt component may be removed through the intergranular pore spaces. If there is some degree of infiltration from the damaged underground water reservoirs it is feasible that groundwater will migrate laterally towards the free face of the coastal slope (to the east at Friedrich Engels Avenue). It is likely that the flow will be greatest in the upper few metres where sand is in a loose condition rather than downwards where sand is in dense condition. If this is a correct assumption, then internal erosion would be concentrated in the upper zone. Taller buildings would have founded on piles at greater depth and, for a greater proportion of their length, below the affected zone. Information from the foundation design would have been crucial to understand why the taller buildings are not affected by tilting. This information is not available in the municipal records.

The fact that the tilting buildings be located in the same side of Julius Nyerere Avenue (Figure 4.12) on top of the coastal slope behind Friedrich Engels Avenue exactly at the stretch of road where the coastal slope is at its closest can be more than coincidence (Forster, 2001). The proximity of the slope may suggest that it is involved in some way in the cause of movement that caused tilting probably due to the load imposed to the slope by the high rise buildings. Additional investigations would be required to reach further conclusions.

## **5.7 SUMMARY AND CONCLUSIONS**

The geological formations of Maputo City which are mainly unconsolidated materials with soil like properties were described in terms of engineering geological characteristics with relevance to their

distribution patterns and spatial trends and related to engineering and construction. Shear strength and consolidation tests gave the standard geotechnical properties of the soils and correlations were made between them and the engineering geological characteristics.

Field soil descriptions show that the *in-situ* moisture condition of the soils in Maputo City varies from slightly moist to wet being controlled by topography and the soil texture although the influence of the climatic conditions on the sample collection. The very moist samples were found in the Ponta Vermelha Formation which in general has higher fine particles. The soil colour distribution is related to the mineralogical composition of the soils. Soils from the Congolote Formation show lighter colours, whitish and light grey and brown; Soils from Malhazine Formation are brown to yellowish brown; the Intradune deposits are whitish brown while the Machava Formation is dark brown. The Ponta Vermelha Formation is the only case where colour is also related to iron enrichment that occurred to form ferricrete. The Ponta Vermelha Formation is generally red in colour but shows different tonalities ranging from dark to brownish and whitish (Momade *et al.*, 1996).

Soil consistency distribution in Maputo City is consistent with the geological formations, Ponta Vermelha being the one with high consistency soils. In this formation a large range of soil consistency classes can be found, from very loose to dense. Soils derived from other geological formations are only very loose to loose. The relatively high fines content (silt and clay) in the Ponta Vermelha Formation may be responsible for the higher soil strength compared to other geological formations. The Ponta Vermelha Formation has intact and homogeneous soil macro-fabric/structure and shows no cracks in the soil structure. The deposit consists essentially of a well distributed material and the humic topsoil horizon which supports vegetation is thin, 15-20 cm thick. This geological formation is likely to be well graded presenting a wide range of grain sizes and larger combinations of two or more grain size classes. In the Congolote and Malhazine Formations the top horizon is thicker, reaching 80 cm and present lenses of different colours but with same grain size.

In general, soils in Maputo City are in the range of coarse-to very fine-grained sand (71.36 to 96.45%) with low clay (0.08 to 1.52 %) and silt (1.80 to 27.09%) percentage, as shown by the grain-size distribution curves. The Ponta Vermelha Formation is relatively well-graded compared to other formations, presenting a wide range of grain sizes from gravel to clay. In the remaining geological formations the grain size characteristics remain almost constant through all the tested

soils. The high sand content in the study area gives the soil very low plasticity to non plasticity. The liquid limit varies between 9 and 28% with the higher values (20 to 28%) observed in the Ponta Vermelha Formation. Fourteen samples (2/3 of the total) were classified in the group SP-SM (Poorly-graded sand with silt) of the Unified Soil Classification System (USCS) of 1985. From the remaining, four are SM (Silty sand) and two are SP (Poorly-graded sand).

The soils of Maputo City are normally consolidated as illustrated by the asymptotic shape of the shear stress vs. horizontal displacement curves derived from the shear box test, with high level of residual strength and an absence of peak. Only 33% of the tested soils presented peak over the residual value in this type of graph denoting dense sand or bonded soils.

The angle of internal friction of the soils of Maputo City varies from 28 to 33.5°. Only five samples had friction angle less than 30° (samples 3, 16, 17, 18 and 21). The highest friction angles are observed in the Ponta Vermelha Formation, 31–33.5°, and the lowest are in the Congolote and Malhazine Formations, 28–30°. The friction angle is related to the mineral composition of the soils as predicted by Mitchell (1993). Soils with high content of quartz and feldspar are predicted by Mitchell (1993) to potentially have high friction angle because their quartz component has a friction angle between 21 and 31° when saturated. Cohesion ranges from 0.83 to 11.14 kN/m<sup>2</sup>, with the highest values also in the Ponta Vermelha Formation. As guided by the predominant shape of the shear stress-horizontal displacement curves in the study area, the measured cohesion in the majority of the tested samples is an apparent cohesion found in the very loose normally consolidated sands. True cohesion from overburden pressures, as obtained from the failure envelope, can be assumed as occurring on the soil presenting cementing or bonding between grains and from low effective stress acting on the shear surface. High iron oxide content in the geological formations of Maputo City, mainly in the Ponta Vermelha Formation (red ferruginous sands), acts as bonding agent. The presence of a bonding agent is confirmed by the consolidation tests as explained earlier.

The Coefficient of Compressibility ( $a_v$ ) was also calculated for every load increase in the tested soils of Maputo City. It varies from 2.00E-04 to 9.20E-03 m<sup>2</sup>/kN for the lower loads (up to 25 kN/m<sup>2</sup>) and from 4.50E-05 to 1.87E-03 m<sup>2</sup>/kN for the higher loads (from 25 to 400 kN/m<sup>2</sup>). The highest compressibility values are observed in the Ponta Vermelha Formation. By other side, at lower loadings the coefficient of volume decrease ( $m_v$ ) varies from 1.27E-01 to 4.63 m<sup>2</sup>/MN and for the higher loads it ranges from 3.01E-02 to 1.07 m<sup>2</sup>/MN. There is no clear trend in the distribution of this coefficient in the study area.

From the consolidation test it was observed that the primary settlement of the tested sandy soils of Maputo is almost quick and immediate in all samples. The higher porosity and hydraulic conductivity of the sandy soils allow water to drain quickly favouring dissipation of the excess pore water pressures. The coefficient of consolidation ( $C_v$ ) is higher in the slightly overconsolidated ( $3.73\text{E-}02$  to  $2.2\text{E}01$   $\text{m}^2/\text{year}$ ) soils comparing with the normally consolidated ( $3.83\text{E-}02$  to  $5.56$   $\text{m}^2/\text{year}$ ). The difference in  $C_v$  values is five times lower in a normally consolidated soil condition. The distribution of this consolidation parameter does not follow a specific pattern over the soil types of Maputo City.

The soil collapse potential as investigated through the physical properties approach showed that the soils of Maputo City comply with 3 of the 5 established criteria of collapse behaviour used in this research. The double consolidation test identified 33.3% of the tested soils in Maputo City (Samples 1, 2, 3, 10, 12, and 16) as collapsible and the collapse potential at different loadings intervals was calculated. These samples showed considerable reduction of the voids ratio in the saturated test corresponding to the additional vertical strain experienced by the soil which is linked to collapse of the soil structure in the presence of water. The soil compressibility and its significant sensibility to collapse upon wetting makes it to be considered as truly collapsible as showing full collapse of the soil structure. This can be above 5% predicted to cause moderate trouble in foundation design according to the suggested values for collapse potential by Jennings & Knight (1975).

Bonding of the soil samples is characteristic for 66.7% of the tested soils (Samples 4, 5, 8, 9, 11, 13, 15, 17, 18, 19, 20 and 21). The rate of voids ratio reduction in samples tested at NMC is identical to the samples tested saturated and this is disclosed as parallel lines of the  $e/\log \sigma_{v0}'$  curves. Although the initial reduction in terms of voids ratio caused by addition of water, the consolidation rate of the saturated soil continues similar to the one of the soil at natural moisture content. This is explained by the presence of a strong bonding material of soil particles which obstructs total destruction of the soil structure with moisture content increase. The presence of bonding material was also disclosed by the higher preconsolidation pressure compared with the corresponding overburden pressure as predicted by Maccarini *et al.* (1989) and Vaughan *et al.* (1988).

The presence and influence of bonding was also detected by comparing the compressibility of two samples at the same voids ratio and water content, one being undisturbed and other completely remoulded (Maccarini, 1987; Maccarini *et al.*, 1989). The remoulded samples showed a

significantly higher compression than that of the bonded soil. The difference came from the fact that part of the stress applied to the bonded soil was carried by the bonds themselves, as the bonded soil is stiffer than the same soil without bonds (Vaughan *et al.*, 1988). The curves of the remoulded samples were also used to establish the limit between the stable and meta-stable states of the soil and the compression curves of the bonded soils are located in the meta-stable space (Maccarini *et al.*, 1989). This boundary between the stable and meta-stable states combined with the *in situ* void ratio is used for soil engineering classification and indicates the capacity of the soil to remain in the stable zone when loaded with engineering infrastructures and the extent to which it will contract or dilate during shearing (Vaughan *et al.*, 1988). These behaviours depend on the strength characteristics and the stiffness of the bonding agent present in the soil.

## CHAPTER 6

### SOIL EROSION SUSCEPTIBILITY

#### 6.1 – INTRODUCTION

Soil erosion and the related problems are the primary and major cause of soil degradation in Mozambique, affecting the population of both urban and rural areas. In Maputo City it is the most prominent environmental and engineering geological problem due to the dimension of the affected area, the huge environmental and economic impacts on the population and the threat to the sustainability of the affected residential areas. This is not only the case of Maputo City as soil erosion has caused great societal and environmental concern in the world due to large degraded areas (Fu & Gulinck, 1994; Elsen *et al.*, 2003; Singha *et al.*, 2006; Wei *et al.*, 2007).

Soil erosion is the process of detachment and movement of solids, including soil, sediment, rock and other particles, in the environment by the action of flowing water, wind or ice and by mass movement of soil downslope under the influence of gravity (Coch, 1995; McGraw-Hill, 2003; Mayhew, 2004; Quartel *et al.*, 2007). Although soil erosion is a naturally occurring and a normal geologic process associated with the hydrologic cycle, in many places it has been accelerated by human activities and poor land use planning, becoming much faster than under natural conditions (French, 1997). Erosion in Maputo City appears as rills and gullies triggered or accelerated by extreme surface water flow along the slopes and are controlled by a broad range of aspect. In fact, rill and gully processes are three-dimensional in nature and are governed by a variety of factors and processes (Valentin *et al.*, 2005), for example topography, soil lithology, terrain geomorphological units, land use, infrastructures and construction sites, and extreme climatic events (Esteves *et al.*, 2005; Nyssen *et al.*, 2002; Bryan, 2004; Archibold *et al.*, 2003).

Bell & Maud (1994) regarded gullies as indicator of the existence of dispersive soil material, but, gully erosion has been described by various authors, including Beckedahl (1996) and



Walker (1997), in soil materials not exceeding the assigned reference indices to identify dispersive soils. Paige-Green (2008) argues that it is important that all manifestations of surface erosion in the engineering context are not simply attributed to a dispersive mechanism as it is often noted. He indicates that although the surface appearance of the eroded material is frequently similar the eroded soil material can be dispersive, erodible or slaking. Erodible soils are those in which the cohesion (or surface shear strength) when wet is insufficient to resist to tractive forces of rain or runoff water flowing over them (Bryan *et al.*, 1989; Paige-Green, 2008). Many of these soils do not show any erosion on short slopes, flat slopes or when the rate at which water flows across the slope is insufficient to develop sufficient tractive force. Dispersive soils, conversely, are those in which the fine clay component goes into suspension in non-flowing water (Elges, 1985). In this study, soil dispersivity is assumed as an index of the likelihood of initiation of erosion. Slaking soils are those that when dry or partially saturated have considerable soil suction which is totally lost on soaking, an extreme case of being erodible (Paige-Green, 2008). The erosion characteristics described above are likely to occur on the soils of Maputo City therefore the description and characterization of soil erosion susceptibility given in this chapter will be all inclusive.

Chapter 6 presents the results of the soil water erosion susceptibility study and determines the relationship with the topographic and geomorphological characteristics of the area, the land use practices (human interference), the soil types, soil properties and climatic events. The effect of soil properties on erosion have been examined in several studies in different environmental situations with good results (Bryan, 2000). These studies show that nearly every soil property may control the soil erosion response, but, unfortunately no single soil property can fully be successful in identifying soil erodibility in every instance (Lal, 1990; Bryan, 2000; Bell & Maud, 1994). Physical and chemical properties of soils were determined to assess the soil erodibility and find out which have influence on the weakness of the soils controlling rill and gully erosion in the study area.

## 6.2 – MECHANISM OF SOIL EROSION

Soil water erosion may occur both gradually and relatively unnoticed, as a result of many small rainfall events, and more noticeably at an alarming rate, as a result of large but relatively rare storms. Soil water erosion is the detachment of soil material as a consequence of the impact of raindrops on bare soil and removal by the power of running water on the soil surface (Assouline & Ben-Hur, 2006; Kinnell, 2005). The beginning and most important part of the erosion process is the impact caused by the raindrops on surface (Kinnell, 2005). The extent of erosion

caused by rainfall (erosivity) depends on the size and velocity of raindrops and the amount of precipitation (Duiker, 2009). Four types of water erosion can be found according to Plummer *et al.* (2007) and Duiker (2009): Interrill erosion, Rill erosion, Gully erosion and Streambank erosion.

Interrill erosion is the result primarily of the detachment of soil particles by raindrop impact (rain splash) on bare soil surface and transport of sediments by thin surface sheet flow (Watson & Laflen, 1986; Kinnell, 2005; Assouline & Ben-Hur, 2006; Bradford *et al.*, 1987). Soil detachment normally is the erosion rate-determining process (Bradford *et al.*, 1987) and both splash and sheet flow erosion depend on soil conditions and soil surface properties (Levy *et al.*, 1994). This type of erosion normally occurs without being seen and has slow impact therefore it was not included in the frames of this research in Maputo City.

Rill erosion is the taking away of soil particles by concentrated water flow in closely-spaced small rivulets, streamlets or headcuts, few centimeters deep or less (Øygarden, 2003). Rill erosion occurs when precipitation rates exceed soil infiltration rates and runoff begins to form small concentrated channels becoming faster-flowing channels (Øygarden, 2003; Watson & Evans, 1991). Detachment of particles in rill erosion occurs when the sediments in the flow are less than the load it can carry and if the flow is higher than the resistance of the soil to detachment (Chmelová & Šarapatka, 2002). It must be noted that not all flow concentration cause rill cut as the soil surface properties also play a very important role (Bryan, 2000). As rill erosion begins, erosion rates increase dramatically due to the resulting concentrated higher velocity flows and the rills become wider and deeper (Chmelová & Šarapatka, 2002) increasing detaching soil particles and scouring channels up to 30 cm deep (Assouline & Ben-Hur, 2006). Turbulence caused by surface runoff often causes more erosion than the impact of initial raindrop and rill erosion corresponds to the intermediate process between sheet and gully erosion. Figure 6.1 shows the rill erosion occurring in Maputo City. Rills occur mostly in the sub-urban and peri-urban areas and because these areas are heavily built they preferentially follow the roads and footpaths.

Gully erosion is the major evidence of soil erosion and occurs when the runoff concentration causes flow at a velocity enough to detach and transport soil particles scouring large sharp sided entrenched channels (deeper than 30 cm) (Carey, 2006). They are steep-sided watercourses carrying ephemeral flows in the events of heavy or extensive rainfall.

Gully development requires large amounts of energy (high runoff) both for detachment and transport of particles (Øygarden, 2003) and often involves complex regional geomorphic factors



**Figure 6.1** – Rill erosion in Ferroviário Quarter, Maputo City. The rills preferentially follow the roads and footpaths

(Bryan, 2000). They develop because of an increase in the erosional forces or decrease in the erosional resistance of the land surface. In the gully erosion the surface channels are well developed in such a way that cannot be smoothed over by normal tillage operations. It is a major water erosion source of sediments with 50–80% of the sediment production (Poesen *et al.*, 2002a). Polana-Caniço and Ferroviário Quarters are the most affected areas with gully erosion in Maputo City. Figure 4.8 (page 48) in Chapter 4 shows the location of gullies in Polana-Caniço Quarter. The gullies are extremely large, deeply cut, 1 to 15 m deep (Figure 6.2) with the biggest occurring in the Ferroviário Quarter. They are W-E oriented but some follow the orientation of the roads where they occur, mainly the Julius Nyerere Avenue.



**Figure 6.2** – V-shaped gullies occurring in Ferroviário Quarter (left); U-shaped gully crossing the Polana-Caniço Quarter in Maputo City (right)

The shape of the gully cross-sections depends on the properties and strength of the soil matrix (Øygarden, 2003). Although the two most affected areas are in the same geological formation composed by silty sand, the gullies show different cross-sectional shapes. Gullies in Ferroviário Quarter are mainly V-shaped while the ones in the Polana-Caniço are U-shaped (Figure 6.2).

The cohesion of the soil particles is higher in Site 10 (Ferroviário Quarter) than in Site 9 (Polana-Caniço). Øygarden (2003) found also that as the silt or silt and fine sand fraction increases, clay content decreases and erodibility increases. Comparing the two locations it is seen that the silt and fine sand fraction for Ferroviário Quarter is higher in more than 17 % supporting the occurrence of bigger gullies in this area comparing with Polana-Caniço.

The location of the gully erosion problems in the Ponta Vermelha Formation, which separates the upper and down town through a long slope on the East and South sides of the city, is an indication that the topography has also played an important role on the gully development. Further observations indicate that other factors have also contributed to gullying and are discussed later on this chapter.

The sidewalls of most of the gullies are still uncovered due to their steepness. They are unstable and suffer continuous erosion in every heavy rainfall event. Poesen *et al.* (2002b) and Vandekerckhove *et al.* (2003) estimate that sidewall erosion can be responsible for more than 50% of the total sediment produced in gullies. Study from Martínez-Casasnovas *et al.* (2004) indicates that the sidewall processes are multifaceted and result from a combination of factors. Their intensity is probably related to the duration and intensity of rainfall and to the potential energy variations linked to changes in soil moisture content (Poesen *et al.*, 2002b; Collison, 2001). These authors reveal also that gully sidewall failure is controlled by the gully-wall slope angle and height and that, *tension crack development is the main process promoting wall collapse in gully walls with high slope angles*. The sidewalls in every affected area in Maputo City are very steep with slope angles generally up to 60 degrees but locally steeper. This slope angle favours the development of tension cracks in gully sidewalls (Figure 6.3) which are the starting point of future gully widening (Collison, 2001; Martínez-Casasnovas *et al.*, 2004; Oostwoud Wijdenes *et al.*, 2000). This comes from the assumption that the tension cracks is likely to lower the stability of the gully sidewall by reducing cohesion and increasing pore water pressure as they easily allow water flow inside the soil and are filled with runoff water in a rainy event which will lower the shearing resistance of the soil (Martínez-Casasnovas *et al.*, 2004; Collison, 2001; Poesen *et al.*, 2002b).

Streambank erosion is a natural process, and occurs “particularly during peak storm flows and is part of an on-going cycle of sediment erosion and deposition within the stream system” (Ziebell, 1999; EB, 2009). Streambank erosion processes, although complex, are driven by two major components: stream bank characteristics (erodibility) and hydraulic/gravitational forces (Ziebell, 1999; Carey, 2006).



**Figure 6.3** – Tension crack development at a gully sidewall in Ferroviário Quarter, Maputo City. The load of people using the footpath on top of the crack will trigger the mass sliding downward (Left). Soil fall of 1.80 m occurred on a gully sidewall in Polana-Caniço Quarter (right).

Acceleration of this natural process leads to a disproportionate sediment supply, stream channel instability, land loss, habitat loss and other adverse effects. Streambank erosion occurs when increased runoff from catchments places significant erosive stress on streams and when vegetation is removed from the stream-side. This vegetation removal can lead to extensive erosion when soils do not have enough strength to resist water erosion. Streambank erosion does not occur in Maputo City as no stream crosses the city. The Infulene River which borders Maputo City with Matola Municipality is a small stream running at low lying area with negligible erosion capacity.

### 6.3 – PHYSICAL PROPERTIES AND EROSION SUSCEPTIBILITY

A qualitative evaluation of the erosion susceptibility has been investigated by tests such as the crumb test, pinhole test, Atterberg limits and the shear strength characteristics. On the contrary, a flume test was used to obtain the quantitative assessment of the soil erodibility. The flume test evaluates the “*resistance of the materials against abrasive action of waterflow, and the impact of flowing water over the sidewalls of the gullies*” (Rienks *et al.*, 2000). The rate of soil erosion can be calculated and a model of soil erodibility developed. Table 6.1 shows the results of the physical properties with qualitative direct influence on erosion susceptibility.

#### 6.3.1 – Crumb Test

The Crumb test is a very quick method to measure soil erodibility and is also used for the identification of a dispersive soil (Head, 1988; Elges, 1985; Walker, 1997; Bell & Walker, 2000). It is the simplest of the physical tests and indicates the tendency of the soil to deflocculate in the presence of sodium hydroxide solution (Head, 1988; Elges, 1985). The use

of sodium hydroxide solution is advisable laboratory procedure in place of distilled water with the only purpose to easily identify dispersion because many dispersive soils do not show reaction in distilled water but do react in the sodium hydroxide solution (Head, 1988; Sherard *et al.*, 1976b).

**Table 6.1** – Crumb test, Atterberg Limits and Shear Strength results of the tested soil of Maputo City

| Geological Unit | Sample N° | Crumb Test* | Plasticity Index | Friction Angle (°) | Cohesion (kN/m <sup>2</sup> ) |
|-----------------|-----------|-------------|------------------|--------------------|-------------------------------|
| TPv             | 3         | 4           | 1.72             | 28.5               | 11.14                         |
|                 | 4         | 3           | 2.57             | 31                 | 5.93                          |
|                 | 5         | 2           | 0.29             | 31.5               | 9.42                          |
|                 | 6         | 2           | 0.00             | ND                 | ND                            |
|                 | 7         | 1           | 0.29             | ND                 | ND                            |
|                 | 8         | 2           | 1.14             | 32                 | 5.33                          |
|                 | 9         | 2           | 2.57             | 31.5               | 2.14                          |
|                 | 10        | 3           | 1.43             | 33.5               | 3.47                          |
|                 | 11        | 4           | 1.14             | 31                 | 5.71                          |
|                 | 12        | 2           | 2.29             | 31.5               | 8.57                          |
|                 | 14        | 1           | 0.00             | ND                 | ND                            |
| QCo             | 1         | 4           | 0.14             | 32.5               | 1.38                          |
|                 | 2         | 4           | 0.14             | 32                 | 9.86                          |
|                 | 16        | 2           | 0.00             | 28                 | 9.29                          |
|                 | 18        | 3           | 0.00             | 28                 | 9.29                          |
|                 | 19        | 3           | 0.00             | 30                 | 5.71                          |
|                 | 21        | 3           | 0.55             | 29                 | 6.43                          |
| Qma             | 13        | 2           | 0.28             | 30                 | 5.71                          |
|                 | 17        | 3           | 0.28             | 28.4               | 0.83                          |
| Qi              | 15        | 2           | 0.00             | 30                 | 3.43                          |
| Qmc             | 20        | 1           | 0.14             | 30.6               | 6.43                          |

QCo: Congolote Formation; TPv: Ponta Vermelha Formation; QMa: Malhazine Formation; Qi: Intradune Deposits; QMc: Machava Formation; ND: Not Determined; (\*) Explanation of the grades of crumb test are presented in Table 6.2

Two to three soil crumbs, each about 6-10 mm diameter, were prepared from representative portions of the soil at the natural moisture content. The crumbs were carefully placed into a beaker containing 100 ml of a dilute 0.001N solution of sodium hydroxide and occurrence of reaction is observed after allowing to 5-10 min of immersion (Head, 1988; Sherard *et al.*, 1976b). As the soil crumb begins to hydrate the colloidal-sized particles tend to deflocculate and to go into suspension. Dispersive soils and soil erodibility are identified by observing reaction as the soil begins to hydrate.

The crumb test generally gives a good indication of the potential erodibility of soils, although a dispersive soil may sometimes give a non-dispersive reaction (Elges, 1985). Sherard *et al.* (1976b) indicate that about 40% of the dispersive soils have non-dispersive reactions in the



crumb test run in distilled water but that percentage drops significantly when using sodium hydroxide solution. Conversely, if the crumb test indicates dispersion, the soil is probably dispersive (Elges, 1985). Therefore, the results of the crumb test must be validated by other erodibility identification tests.

The results depend on the observations in accordance with the guide to interpretation based on the level of reactions occurred. Four grades of reaction can be identified according to the guide on Table 6.2 taken from Sherard *et al.* (1976a) and Walker (1997).

**Table 6.2** – Guide to interpretation based on the level of reactions during the crumb test (From Sherard *et al.*, 1976a and Walker, 1997)

| Grade   | Reaction          | Interpretation   |
|---------|-------------------|--|
| Grade 1 | No Reaction       | Crumbs may slake, but no sign of cloudiness caused by colloids in suspension                                   |
| Grade 2 | Slight Reaction   | Bare hint of cloud in water at the surface of crumb  |
| Grade 3 | Moderate Reaction | Easily recognisable cloud of colloids in suspension, usually spreading out in thin streaks on bottom of beaker |
| Grade 4 | Strong Reaction   | Colloidal cloud covers nearly the whole of bottom of the beaker, usually as thin skin                          |

Although the test is considered very highly subjective by Arulanandan & Heinzen (1977), the crumb test results are highly reproducible (Sherard *et al.* (1976a) and for the study area they gave a good indication of the soil erodibility. More than one crumb test was conducted in every sample to ensure that the test gives a true reflection of the erodibility of the soil. Although the classification of the reaction is left to the decision of the operator as no standards for the deflocculation assessment have been established, the repetitiveness was very good. From the results three sample shown no reaction (Samples 7, 14 and 20), seven samples were of grade 2 (samples 5, 6, 8, 9, 12, 13, 15 and 16), six of grade 3 (Samples 4, 10, 17, 18, 19 and 21) and four samples were highly reactive (grade 4) on the sodium hydroxide solution (Samples 1, 2, 3, 11). According to this classification criteria suggested by Sherard *et al.* (1976a) Grades 1 and 2 are indication of non-dispersive samples while Grades 3 and 4 are for dispersive samples. The crumb test results shown no correlation with the clay content, silt, ESP and SAR. These findings indicate that these parameters do not contribute in the susceptibility of the soils to break up and give an idea that the disintegration observed in the crumb test is not simply physico-chemical dispersion process or at least other factors have contributed negatively to the dispersion process to occur. The same conclusions were also found by Walker (1997) and Rienks *et al.*, (2000) who have reservations on the consistency of this technique in identifying dispersive soils.

### 6.3.2 – Pinhole Test

The pinhole erosion test is widely considered to be one of the most reliable physical tests to determine erodibility because it simulates the action of water draining through a pipe in soil (Ismail *et al.*, 2008; Head, 1988; Sherard *et al.*, 1976a; Walker, 1997). The test represents a direct qualitative measurement of the dispersivity and consequent colloidal erodibility of soils. The test procedure is based on extensive trials at different constant hydraulic heads of 50, 180 and 380 mm, from where the water is allowed to flow through a 1 mm diameter pierced hole of a specimen (Sherard *et al.*, 1976a; Head, 1988). The resistance to erosion of the specimen is evaluated from the appearance (turbidity) of the discharged water, the rates of flow, and the final size of the hole in the specimen. If the effluent remains clear and the pinhole unenlarged, then the soil is nondispersive. Conversely, the effluent is highly turbid and the pinhole is enlarged for a dispersive soil. Although the test was designed for clay soils it was used in this research to assess its workability in sandy soils that dominate the study area. Because the soil consistency of the majority of the soil samples of Maputo City vary from very loose to loose sandy soils except a few cases of medium dense soils, the pinhole test did not work well. The soil sample disaggregated completely with the water flowing through it making impossible to record the rates of flow and the final size of the hole in the specimen.

### 6.3.3 – Atterberg Limits and Shear Strength

The Atterberg limits are useful soil characteristics giving the relative activity of the soils. They define the soil behaviour with changes in soil moisture content. The liquid limit (LL), plastic limit (PL), and shrinkage limits (SL) define the relative stages of behaviour when the soil moves from the liquid to solid state. The plasticity index (PI) is the range given by the difference between the liquid and plastic limits. These routine soil mechanics testing cannot differentiate dispersive from non-dispersive soils (Bell, 2000) but influences many aspects of erosional response (Bryan, 2000). It has been proved that the higher PL and LL, the higher will be the resistance of the soil to dispersion (Bell & Maud, 1994; Rienks *et al.*, 2000).

As the liquid limit is the moisture content above which the soil behaves as a semi liquid, the measure of this property will indicate how much water, in this case rainfall, needs to enter the soil before it flows under its own weight. This is particularly relevant for high plasticity soils because they are rich in clay which reflects on the low infiltration rates giving the soil a certain degree of stability (Rienks *et al.*, 2000). This is not the case of Maputo City where the soils are highly sandy with low clay content (from 0.08 to 1.52%) and plasticity index ranging from 0 to



3.

The Atterberg limits will assist on the acquisition of basic soil index information to estimate strength characteristics. The liquid and plastic limits define boundaries between material consistency states, therefore correlate with strength. The resistance of soils to erosion is mostly controlled by the soil shear strength, but appears to be difficult to obtain shear strength characteristics of the soil portion directly affected by erosion (Bryan, 2000). Shear strength of the soils as given by the Coulomb equation ( $\tau = c' + \sigma' \tan \phi'$ ) (Eq. 5.10), measures the resistance to failure under applied load, where cohesion and bonding agents play important role. Bryan (2000) states also that it is difficult to establish precisely the relationship between soil shear strength, consistency and aggregation, although their linkage to the same bonding mechanisms. Results from this study indicate very weak correlation between friction angle and plasticity index and no clear trend is observed for the influence of plasticity index on cohesion. The low plasticity index together with the low plastic clay content observed in the soils of the study area can be the cause of the absence of a clear correlation. It was expected that the friction angle would decrease with an increase in plasticity index as predicted by Mitchell (1993).

#### 6.3.4 – Flume Test

Pinhole test and the crumb test are qualitative methods and are considered to be inconclusive in the evaluation of the erosion potential (Arulanandan & Perry, 1983). A quantitative evaluation of the erosion potential and the soil's erodibility characteristics can be obtained by a recirculation flume in which a known bottom shear stress is applied on the sediment bed to observe the rate of erosion, and infer the erosion parameters given some model of the erosion process (Arulanandan & Heinzen, 1977; Ravens & Gschwend, 1999; Ravens, 2007; Ravens & Sindelar, 2008).

The flume test was developed in this research to model the soil erodibility, *“the resistance of the materials against abrasive action of waterflow, and the impact of flowing water over the sidewalls of the gullies”* (Rienks *et al.*, 2000). The soil erosion mechanism involves the structure of the soil and the complex interaction between the eroding fluids and the soil pores at the surface. Erosion occurs when the shearing stresses caused by fluid flow on a soil surface is higher than the shear strength of the soil. In those cases the fluid flow has capacity to detach particles from the soil surface (Arulanandan & Heinzen, 1977).

Undisturbed block samples were positioned in a flume with horizontal water circulation by a paddle-wheel. Constant water depth was kept at 0.5 cm over every sample, the angular velocity

of the wheel at 2.7 rad/s and the test was run during 10 minutes (Chapter 3, Section 3.2.4.3). The eroded sediments were drained off with water from the flume tank as recommended by Rienks *et al.* (2002), and wet sieved without chemical dispersion, with mesh sizes of 2, 1, 0.5, 0.25, 0.125 and 0.063 mm to determine their particle size distribution. The amount of sediments eroded was then related to the surface area of the sample placed in the flume (Table 6.3).

**Table 6.3** – Results of the flume erodibility tested in samples collected in Maputo City

| Geological Unit | Sample Number | Initial Weight (g) | Final Weight (g) | Eroded Sediments (g) | Area of Sample (cm <sup>2</sup> ) | Total Eroded/Area/10 min test (kg/m <sup>2</sup> /10 min) | Percentage of sediments passing per sieve size |        |        |        |        |       |
|-----------------|---------------|--------------------|------------------|----------------------|-----------------------------------|---|--|--------|--------|--------|--------|-------|
|                 |               |                    |                  |                      |                                   |   | 2 mm   | 1 mm   | 500 µm | 300 µm | 125 µm | 63 µm |
| TPv             | 3             | 197.5              | 169.8            | 27.70                | 5074.68                           | 0.0546  | 100.00   | 99.68  | 97.87  | 88.12  | 15.20  | 9.78  |
|                 | 4             | 207                | 177.2            | 29.80                | 5074.68                           | 0.0587  | 100.00   | 99.93  | 97.25  | 81.48  | 16.04  | 12.01 |
|                 | 5             | 203.2              | 179.2            | 24.00                | 4909.31                           | 0.0489  | 100.00   | 99.17  | 97.50  | 84.58  | 9.62   | 3.79  |
|                 | 6             | ND                 | ND               | ND                   | ND                                | ND  | ND   | ND     | ND     | ND     | ND     | ND    |
|                 | 7             | ND                 | ND               | ND                   | ND                                | ND  | ND   | ND     | ND     | ND     | ND     | ND    |
|                 | 8             | 217                | 177.4            | 39.60                | 5309.55                           | 0.0746  | 100.00   | 97.98  | 84.09  | 68.18  | 24.95  | 17.37 |
|                 | 9             | 207.8              | 182.6            | 25.20                | 4909.31                           | 0.0513  | 100.00   | 99.21  | 94.44  | 80.99  | 25.83  | 17.10 |
|                 | 10            | 217.9              | 170.7            | 47.20                | 5309.55                           | 0.0889  | 100.00   | 99.79  | 98.09  | 90.25  | 19.47  | 12.25 |
|                 | 11            | 204.8              | 171.1            | 33.70                | 5199.52                           | 0.0648  | 99.70  | 99.11  | 94.96  | 84.57  | 27.00  | 17.21 |
|                 | 12            | 211                | 185.6            | 25.40                | 5199.52                           | 0.0489  | 100.00   | 99.65  | 93.78  | 77.24  | 19.41  | 13.11 |
|                 | 14            | ND                 | ND               | ND                   | ND                                | ND  | ND   | ND     | ND     | ND     | ND     | ND    |
| QCo             | 1             | 216.2              | 179.5            | 36.70                | 5671.94                           | 0.0647  | 100.00   | 99.73  | 97.00  | 68.94  | 11.39  | 7.30  |
|                 | 2             | 222.1              | 198.09           | 24.01                | 5671.94                           | 0.0423  | 100.00   | 99.58  | 98.29  | 89.55  | 23.70  | 16.62 |
|                 | 16            | 195.3              | 184.4            | 10.90                | 5074.68                           | 0.0215  | 100.00   | 99.08  | 96.33  | 82.57  | 11.01  | 4.59  |
|                 | 18            | 192.4              | 158.2            | 34.20                | 5074.68                           | 0.0674  | 100.00   | 99.88  | 97.25  | 82.92  | 16.84  | 9.82  |
|                 | 19            | 195.7              | 151.2            | 44.50                | 5309.55                           | 0.0838  | 100.00   | 99.78  | 98.20  | 81.12  | 9.66   | 5.17  |
|                 | 21            | 194.9              | 172.1            | 22.80                | 4909.31                           | 0.0464  | 100.00   | 99.65  | 97.46  | 78.60  | 16.32  | 11.49 |
| QMa             | 13            | 208.8              | 164.8            | 44.00                | 5309.55                           | 0.0829  | 100.00   | 99.77  | 97.73  | 82.73  | 5.68   | 2.73  |
|                 | 17            | 200.7              | 169.23           | 31.47                | 5671.94                           | 0.0555  | 100.00   | 100.00 | 98.73  | 84.75  | 10.45  | 6.64  |
| Qi              | 15            | 208.7              | 173.3            | 35.40                | 5199.52                           | 0.0681  | 100.00   | 99.89  | 97.34  | 80.96  | 6.38   | 3.84  |
| QMc             | 20            | 207.6              | 172.9            | 34.70                | 5671.94                           | 0.0612  | 100.00   | 99.80  | 98.36  | 82.51  | 9.60   | 4.70  |

ND: Not Determined.

The material eroded from the samples during flume test was generally coarser than that chemically dispersed obtained during particle size determination for soil classification (Chapter 5, Section 5.3.1). This means that coarser material is prone to detachment from the soil mass than finer material during surface erosion process. According to Rienks *et al.* (2000) this is not in agreement with what is expected for erosion active processes dominated by dispersion.

The amount of eroded sediments was related to the surface area of the sample placed in the flume and the erosion rate calculated based on the particle concentration. The erosion rate ranged from 0.022 to 0.089 kg/m<sup>2</sup> for the 10 minutes of testing. The relative low erosion rate observed is due to the small test section in the flume as compared to the reality. For the purpose of categorizing the erosion rates in the different tested soils, three classes of erosion were

defined: low erodibility for erosion rate less than  $0.05 \text{ kg/m}^2$ , intermediate erodibility for samples with between  $0.05\text{-}0.07 \text{ kg/m}^2$  and high erodibility for over  $0.07 \text{ kg/m}^2$  of erosion rate for the 10 minutes of testing. Five samples had low erodibility (Samples 2, 5, 12, 16, 21), nine samples had intermediate erodibility (Samples 1, 3, 4, 9, 11, 15, 17, 18, 20) while the remaining 4 samples were highly erodible (Samples 8, 10, 13, 19).

The distribution of the erosion rates obtained with the flume erodibility test has no clear relation with the geological formations and very weak with cohesion ( $r^2 = 0.17$ ) and friction angle ( $r^2 = 0.11$ ). Wan & Fell (2004) predict that the rate of erosion is dependent on the soil fines and that coarse-grained and non-cohesive soils, in general, erode more rapidly than fine-grained soils. However, a poor relationship was found between the eroded sediments in the flume test with the particle size distribution in the soil types. The very similarities in terms of particle size distribution amongst the tested samples suppressed the possibility to test this argument. Results of the flume erodibility test have little correlation with the chemical properties related to dispersion. The correlation is weak with EC ( $r^2 = 0.09$ ), SAR ( $r^2 = 0.13$ ), ESP ( $r^2 = 0.12$ ) and CEC ( $r^2 = 0.10$ ). These findings indicate that the erosion susceptibility and gullying in Maputo City are more related to the physical processes than to the dispersion related chemical properties of the soils. These physical processes were also accelerated by the land use and topographic setting (Section 6.6.1).

The flume test can be regarded as the best indicator of the erodibility processes occurring in Maputo City as it imposed shearing forces on the sample by the flowing water and produced turbulence in the water, leading to better mixing of the pore water with water of low EC. In contrast, the dispersion related tests are based on static conditions with low mixing between soil and water, for example in the crumb test where intrusion of water with a low salts concentration takes place only by diffusion and there is no mechanical mixing of pore water with water of low salts concentration (Rienks *et al.*, 2000).

The concentrated overflow created by the paddle wheel on the soil sample is expressed in terms of flow shear stress. This can be calculated by the following expression (Poesen *et al.*, 2003):

$$\tau_b = \rho g d s \quad \text{Eq. 6.1}$$

Where:  $\tau_b$  = flow shear stress;

$\rho$  = density of runoff water;

$g$  = acceleration due to gravity;

$d$  = depth of flow; and

$s$  = sine of the soil surface gradient.

The critical flow shear stress to initiate detachment of individual soil particles of fine to medium sand soils is of less than 1 Pa being also influenced by the soil properties, texture, soil water content, calcium content, iron, organic carbon and potassium (Poesen *et al.*, 2003). Transferring the lab conditions of the flume test to the real environment and using the surface gradient of Maputo City presented in Figure 6.4, the flow shear stress would range from 0.59 to 41.86 Pa. Only site 21 would have flow shear stress below 1 Pa. This critical flow shear stress may also be affected by the land use practice and for the specific case of the eroded areas in Maputo City, by the poor urban land use planning (Section 6.6) which interferes with the concentration of water flow, increasing the erosion capacity. In general, an inverse relation between concentrated flow width and critical flow shear stress to initiate gullyng is observed (Poesen *et al.*, 2003). Taking into account the poor urban land use of the affected areas which are unplanned informal settlements, water flow is concentrated along the footpaths initiating gullyng (Section 6.10). Even though the footpaths are very compacted, the intense rainfall that preceded all gullyng events in Maputo City reduced the effective stress creating conditions for particles detachment by the concentrated water flowing on the footpaths. Table 6.4 shows that prior to the February 2000 rainfall event that created most of the gullies in Maputo City the rainfall was also very above the normal during January 2000.

**Table 6.4** – Precipitation values during the 1999-2000 rainy season in Maputo City

| Months        | Rainfall (mm) |
|---------------|---------------|
| October/1999  | 161.5         |
| November/1999 | 162.6         |
| December/1999 | 124.2         |
| January/2000  | 234.8         |
| February/2000 | 502.1         |
| March/2000    | 364.8         |

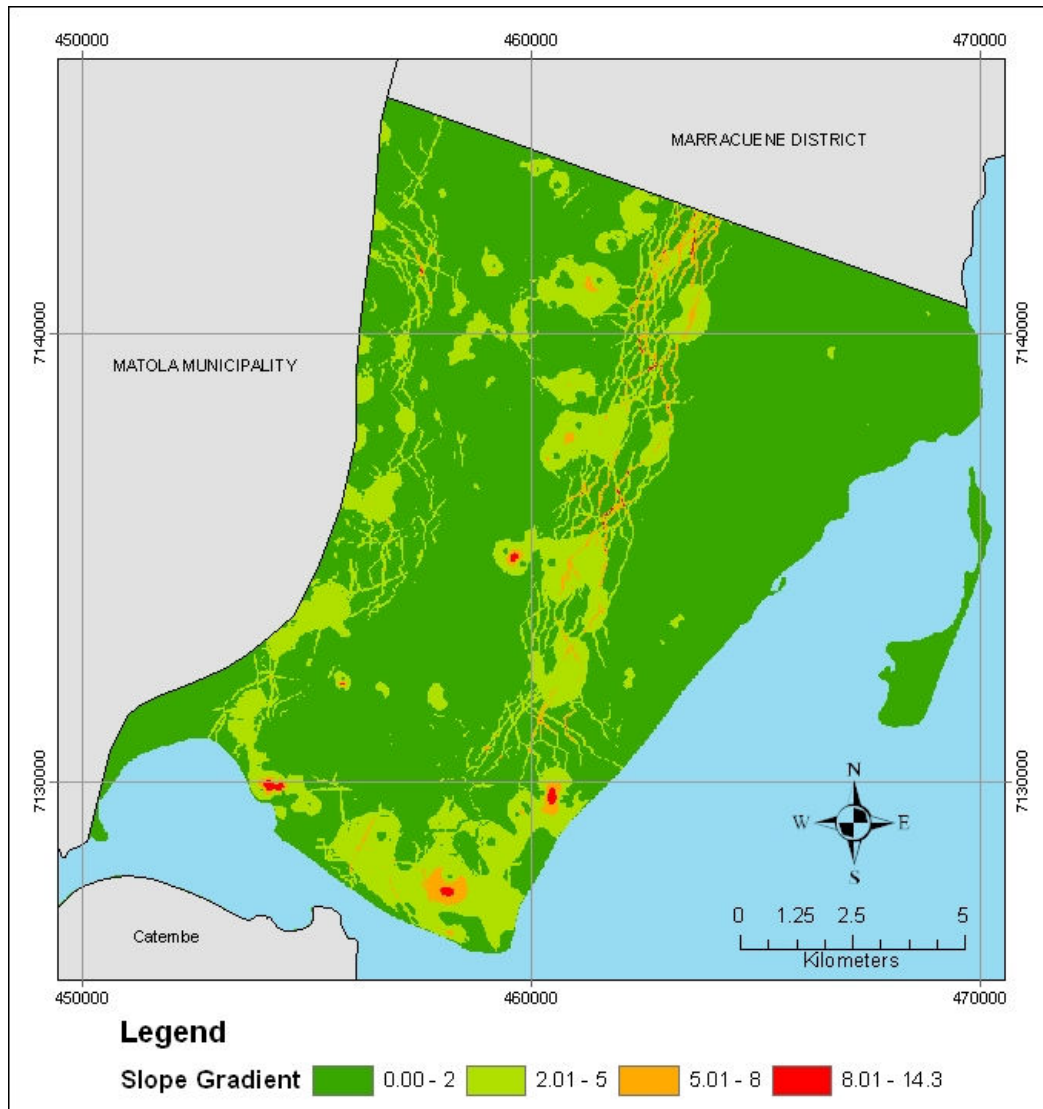


**Figure 6.4 – Surface gradient of Maputo City**

#### 6.4 – CHEMICAL DETERMINATION OF EROSION SUSCEPTIBILITY

Soil erosion by water depends primarily on soil detachment by the impact cause by raindrop and on the transport capacity of the water flow (Levy *et al.*, 1994). Water flow and splash erosion are influenced by the composition of the eroding fluid and by the soil surface structure and soil properties (Arulanandan & Heinzen, 1977; Levy *et al.*, 1994). Studies from Gerber & Harmse (1987), Elges (1985), Bell & Walker (2000), Walker (1997) has proven the possibility to quantitatively identify the soil dispersiveness, therefore, the role in the erodibility of the soils. This used to be a problem previously because the dispersion is a physical manifestation of chemical and physico-chemical properties of soils which were not been considered (Gerber & Harmse, 1987). Soil dispersivity tests in this study measure dispersivity as an index of the likelihood of initiation of erosion processes as recommended by Wan & Fell (2004).

At present it is confirmed that the physical properties of soils, including dispersion, are related to the concentration and composition and of salts in the soil solution and to the interactions between various soil properties (Gerber & Harmse, 1987). It is now also proved that the positive identification of dispersive and erodible soils can only be carried out by a combination of various techniques (Paige-Green, 2008; Bell & Walker, 2000). Bell & Maud (1994) state “that soils with less than 10% clay particles may not have enough colloids to support dispersive piping”. The tested soils of Maputo City have very low clay content (0.08 to 1.52 %) however the exchangeable sodium percentage, from the exchangeable cations, and the percent sodium, from the saturation extract, are in quantities high enough to be used to identify dispersive soils. Therefore, assessment of dispersivity using the chemical properties was undertaken in order to assess its workability in the context of the tested soils mainly in the gully erosion areas. Moreover, some of the characteristics of dispersive soils were observed in the tested soils. Table 6.5 presents the chemical parameters used to identify and predict the soil dispersivity and erodibility. The raw data are presented in the Appendix B.

**Table 6.5** – Chemical results of the soil samples collected in Maputo City

| Geological Unit | Sample Number | pH   | EC (mS/m) | CEC (meq/l) | CEC (meq/100g) | ESP   | SAR   | TDS (meq/l) | %Na   |
|-----------------|---------------|------|-----------|-------------|----------------|-------|-------|-------------|-------|
| TPv             | 3             | 7.81 | 89.00     | 3.90        | 2.87           | 12.21 | 3.70  | 7.00        | 61.43 |
|                 | 4             | 5.93 | 10.00     | 1.10        | 2.08           | 6.26  | 1.57  | 1.10        | 63.64 |
|                 | 5             | 7.96 | 32.00     | 2.70        | 9.64           | 1.24  | 1.36  | 2.40        | 45.83 |
|                 | 6             | 9.21 | 29.00     | 27.30       | 341.25         | 0.10  | 2.83  | 3.00        | 66.67 |
|                 | 7             | 8.71 | 30.00     | 19.70       | 61.56          | 0.26  | 0.84  | 2.60        | 30.77 |
|                 | 8             | 8.19 | 20.00     | 3.70        | 5.52           | 1.09  | 0.94  | 1.80        | 38.89 |
|                 | 9             | 5.81 | 11.00     | 1.20        | 1.82           | 4.95  | 0.91  | 1.10        | 45.45 |
|                 | 10            | 6.18 | 8.00      | 1.10        | 1.67           | 3.60  | 1.03  | 0.70        | 57.14 |
|                 | 11            | 5.39 | 15.00     | 1.00        | 3.03           | 2.64  | 0.76  | 3.00        | 26.67 |
|                 | 12            | 5.18 | 8.00      | 0.80        | 1.74           | 4.60  | 1.00  | 1.00        | 50.00 |
| QCo             | 14            | 5.47 | 4.00      | 0.40        | 0.85           | 8.23  | 0.60  | 0.80        | 37.50 |
|                 | 1             | 7.73 | 101.00    | 2.47        | 1.63           | 36.92 | 14.00 | 7.50        | 93.33 |
|                 | 2             | 8.17 | 22.00     | 3.30        | 9.17           | 0.65  | 0.81  | 1.70        | 35.29 |
|                 | 16            | 4.74 | 53.00     | 0.60        | 2.50           | 2.80  | 1.33  | 3.20        | 40.63 |
|                 | 18            | 6.12 | 46.00     | 0.50        | 1.16           | 13.76 | 3.91  | 4.00        | 72.50 |
|                 | 19            | 7.08 | 19.00     | 0.60        | 1.71           | 6.42  | 1.86  | 1.80        | 61.11 |
| Qma             | 21            | 5.09 | 75.00     | 1.40        | 2.86           | 7.70  | 3.90  | 5.70        | 66.67 |
|                 | 13            | 5.52 | 8.00      | 0.30        | 1.15           | 3.47  | 0.80  | 0.90        | 44.44 |
| Qi              | 17            | 5.15 | 16.00     | 0.40        | 1.38           | 7.25  | 2.24  | 1.40        | 71.43 |
|                 | 15            | 6.26 | 7.00      | 0.40        | 1.82           | 4.40  | 0.85  | 1.20        | 41.67 |
| Qmc             | 20            | 7.23 | 0,0       | 0.00        | 0.00           | 0.00  | 0.00  | 0.00        | 0.00  |

EC: Electrical Conductivity; CEC: Cation Exchange Capacity; ESP: Exchangeable Sodium Percentage; SAR: Sodium Adsorption Ratio; TDS: Total Dissolved Solids; QCo: Congolote Formation; TPv: Ponta Vermelha Formation; QMa: Malhazine Formation; Qi: Intradune Deposits; QMc: Machava Formation

#### 6.4.1 – Exchangeable Sodium Percentage and Cation Exchange Capacity

The exchangeable Sodium Percentage (ESP) has been identified as the most contributor chemical factor and reliable method of identifying dispersive soils (Elges, 1985; Bell & Walker, 2000; Gerber & Harmse, 1987). ESP was determined from the exchangeable cations which are those attached to the clay surface, being determined using the ammonium acetate extract. Exchangeable cations were expressed in milliequivalents per 100 grams of soil (Appendix B).

The ESP was calculated from the following expression:

$$\text{ESP} = \frac{\text{Exchangeable Sodium}}{\text{Cation Exchange Capacity (CEC)}} \times 100 \quad \text{Eq. 6.1}$$

with the CEC units are expressed in terms of meq/100 g of dry soil.

Various authors established criteria for identification of dispersive soils using ESP. Harmse (1980) presented a classification indicating that the soil is dispersive if the ESP value is higher than 5%. This ESP reference value above which soils that have their free salts leached are prone to be dispersive was raised to 6% by Gerber & Harmse (1987) and to 10% by Elges (1985) and Bell & Walker (2000). For both classifications ESP value above 15% was assigned as a threshold for highly dispersive soils.

ESP values of the tested samples of Maputo City vary from 0 to 36.92%. Using this simple classification of Harmse (1980), only 8 samples showed dispersive results (samples 1, 3, 4, 14, 17, 18, 19 and 21), most of them in the top north and in the south of Maputo City, sample 1 presented the extremely high ESP value compared to other samples (Figure 6.5). Samples 9, 10, 11 and 12 are from the Polana-Caniço and Ferroviário Quarters, areas heavily affected by gully erosion. However, the ESP values of these points are lower than the reference value indicating dispersive soils. This can be an indication that the gully erosion occurring in those areas is not controlled by the ESP but by other factors. This is also proved by the weak correlation ( $r^2 = 0.12$ ) shown by the ESP and the amount of eroded sediments in the flume test. The distribution of the ESP values is strongly correlated ( $r^2 = 0.88$ ) to the distribution of sodium adsorption ratio (SAR) (Figure 6.6). The results obtained with this method correlates to the ones obtained with the classification based on SAR and TDS vs. %Na diagram as they identified almost the same samples as dispersive.

Soil dispersivity is also controlled by the mineralogical composition of the clay fraction present in the soil as suggested by Elges (1985) and Gerber & Harmse (1987). The type and nature of

clay present in the soil sample can be predicted by the cation exchange capacity (CEC) if it cannot be determined directly by X-ray diffraction analysis (Walker 1997). Gerber & Harmse (1987) noted that the cation exchange capacity must not be determined by the summation of extractable cations if soluble salts occur in soil solution or if the base saturation of the soil is less than 100%.

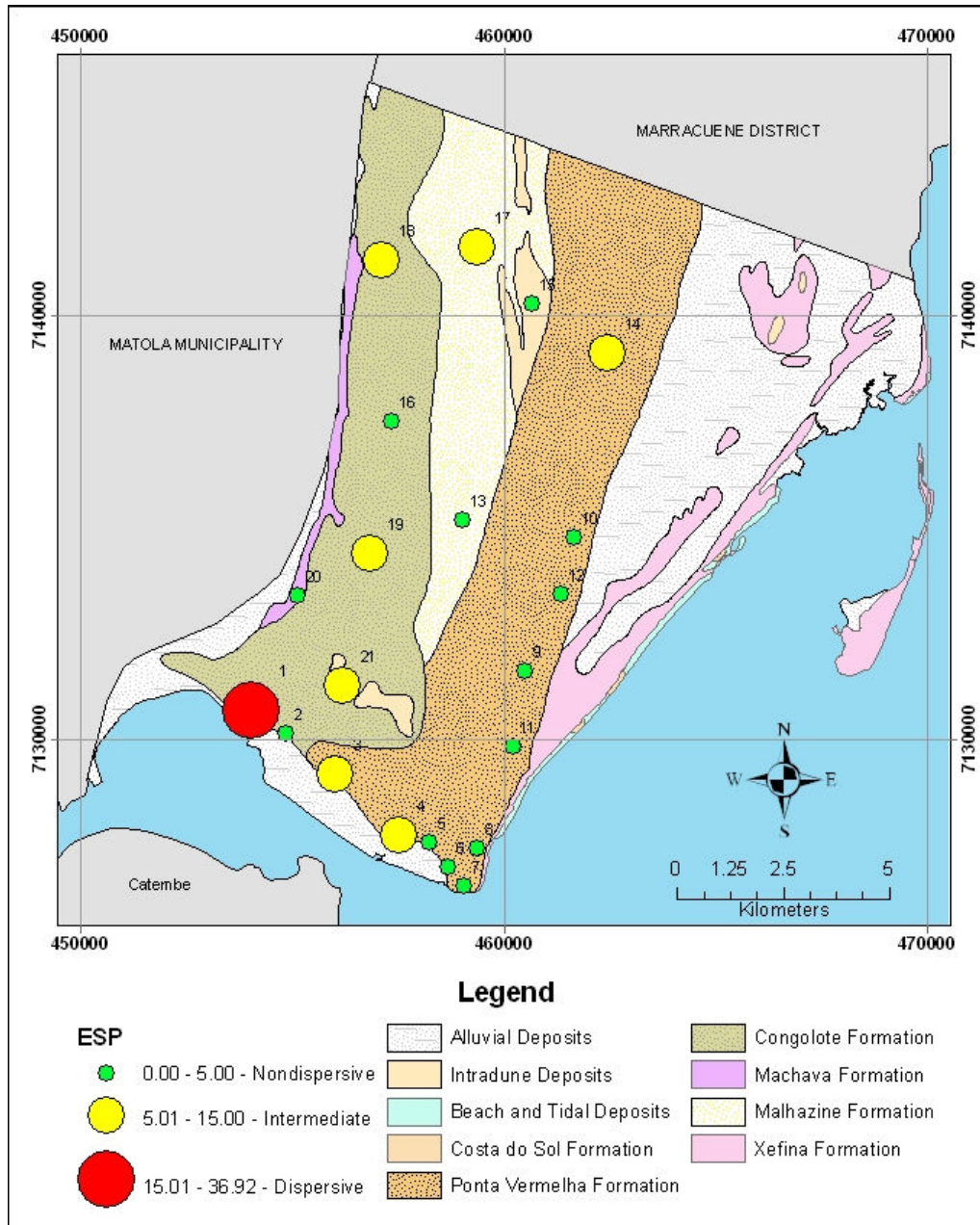


**Figure 6.5** – Exchangeable Sodium Percentage of the tested soils of Maputo City

Cation exchange capacity (CEC) is the ability of a soil to hold cations and is directly related to the properties of clay minerals. The primary factor determining CEC is the clay and organic matter content of the soil. Camberato (2001) states that in coarse native sands of coastal plains



and coastal regions the CEC arises almost entirely from organic matter, and higher quantities of clay and organic matter result in higher CEC.

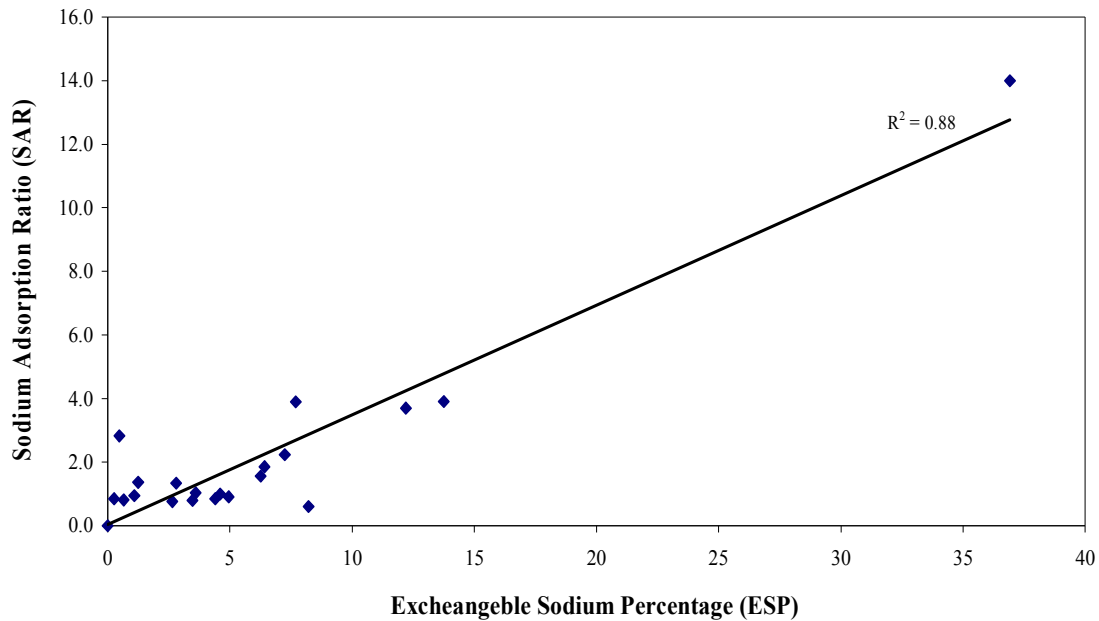


**Figure 6.6** – Correlation of ESP values and sodium adsorption ratio (SAR) of the tested soils of Maputo City

Cation exchange capacity values for 100g of clay were obtained by dividing the CEC of the whole soil by the percentage of clay present in the soil. These results were compared to the CEC of different clay minerals shown on Table 6.6. The presence of high levels of organic matter (humus) and/or 2:1 clay minerals such as illite, smectites and montmorillonite in the clay fraction is an indication of dispersive soils while kaolinitic soils seldom have a high ESP (Rienks, 2000; Bell & Maud, 1994). Therefore, soils with CEC less than 15 meq/100g clay may be considered nondispersive.

Soils with CEC values between 40-150 meq/100g clay, according to Gerber & Harmse (1987), are highly dispersive. Those with cation exchange values between 5-40 meq/100g of clay are less dispersive while those with CEC between 1-5 meq/100g of clay have been found to be completely non-dispersive.

**Table 6.6** – Cation exchange capacity of different clay minerals

| Clay mineral    | Cation Exchange Capacity (meq/100g Clay) |
|-----------------|--|
| Kaolinite       | 3 – 15                                   |
| Illite          | 15 – 40                                  |
| Montmorillonite | 80 – 100                                 |

This parameter indicates the largest portion of the study area with nondispersive soils (Figure 6.7), probably due to the low clay percentage in the soil as this is directly related to the CEC values.

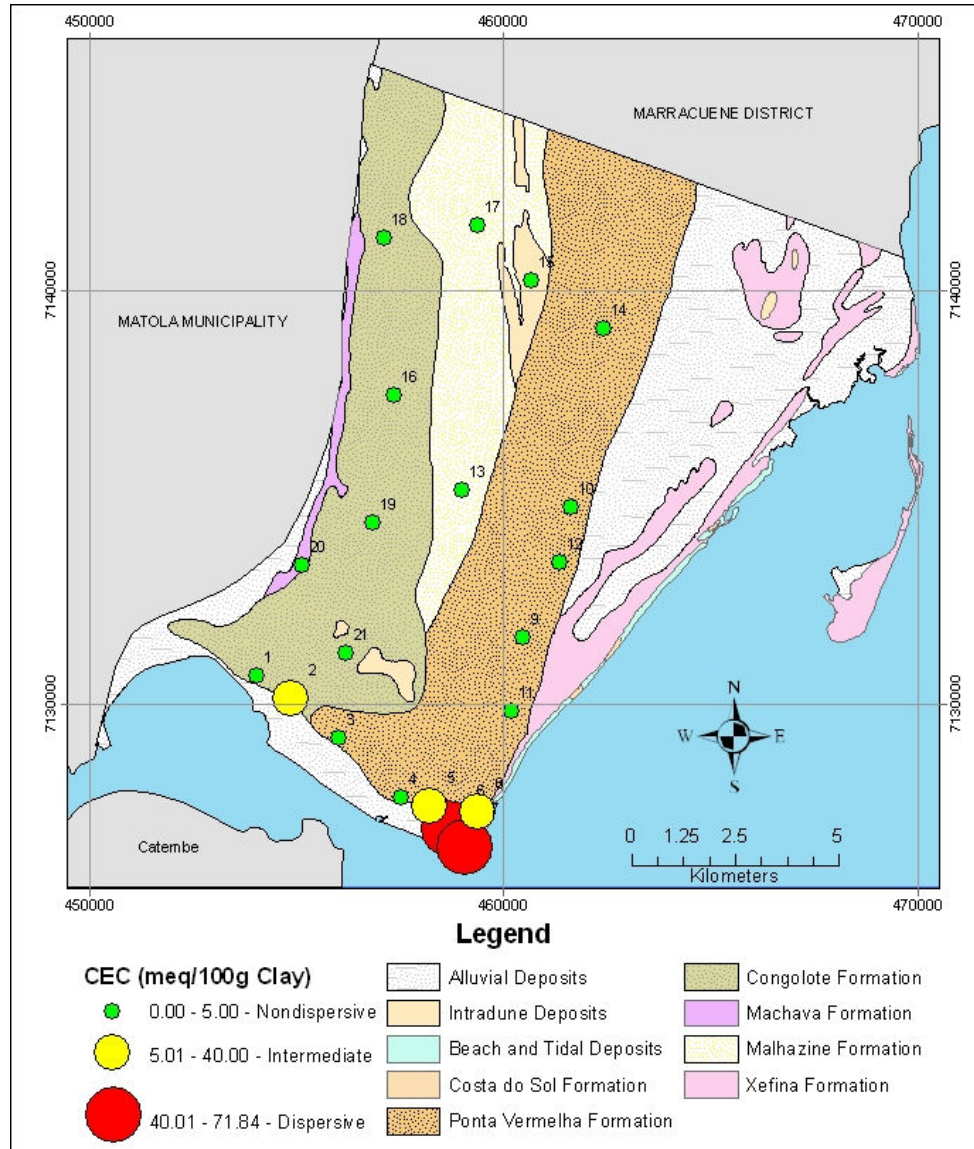


**Figure 6.7** – Cation exchange capacity of the tested soils of Maputo City.

Gerber (1983) prepared a chart division using the CEC of the clay fraction and the ESP of the soil to assess the soil dispersivity and Gerber & Harmse (1987) also highlighted the strong correlation between ESP and cation exchange capacity for the determination of soil erodibility. Gerber (1983) considered soils with an ESP value greater than 15 % as highly dispersive, whilst those with an ESP between 15 and 6 % are dispersive. ESP between 6 and 4% are marginal and values below 4% are for nondispersive soils.

Similarly, soils with low CEC values (15 meq/100g clay) at ESP values of 6 % or below are

regarded as completely nondispersive by Gerber & Harmse (1987) and Bell & Maud (1994). Combination of these two important factors of soil dispersivity and erodibility (CEC vs. ESP) has proven to be the most accurate of the chemical assessment (Bell & Walker, 2000).

The plot in Figure 6.9 shows that most of the samples (2, 4, 5, 8, 9, 10, 11, 12, 13, 15, 16, and 19) of Maputo City fall in the area of completely nondispersive soils while the remaining 8 samples (3, 6, 7, 14, 17, 18, 20 and 21) are nondispersive. Sample 1 has high CEC value not predicted in this Gerber & Harmse (1987) diagram. The nondispersive character of all samples given by the ESP vs. CEC method do not correlate with any other method, e. g. TDS vs %Na, which present the samples well distributed through the different dispersivity classes.

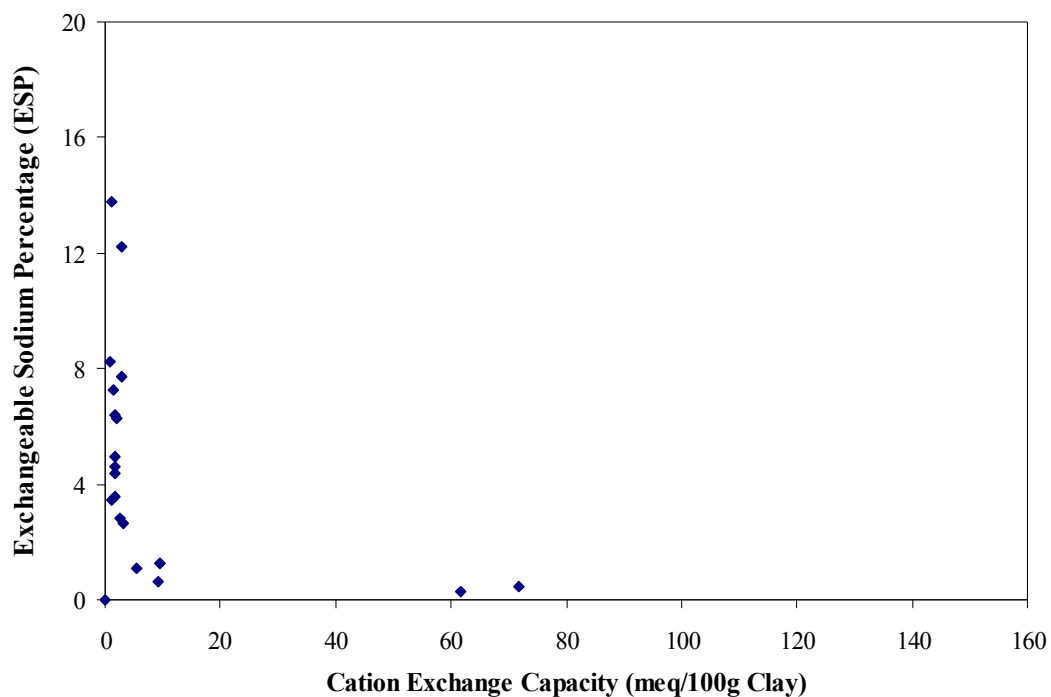


**Figure 6.8** – Plot of the Maputo City soil samples on the ESP vs. CEC of Gerber & Harmse (1987) showing the distribution on the different dispersivity classes.

#### 6.4.2 – Sodium Adsorption Ratio

The sodium adsorption ratio (SAR) is utilized to quantify the role of sodium in dispersion with the presence of other free salts in the pore water. It compares, in soil solutions, the concentrations of  $\text{Na}^+$ , in relation to the concentrations of  $\text{Ca}^{2+}$  and  $\text{Mg}^{2+}$ . It is assumed that soils disperse because they have higher content of dissolved sodium than ordinary soils (Elges, 1985; Bell & Walker, 2000). SAR is used because the soil in nature is in equilibrium with its environment where the electrolyte concentration of the soil water is closely related to the

exchangeable ions (Elges, 1985). SAR was calculated from the saturation extract cations and determined from the following expression with of all parameters in meq/l:

$$\text{SAR} = \frac{\text{Na}^+}{\sqrt{0.5(\text{Ca}^{2+} + \text{Mg}^{2+})}} \quad \text{Eq. 6.2}$$

Harmse (1980) and Gerber & Harmse (1987) suggested that SAR greater than 10 indicates dispersive soils, if between 6 and 10 indicates intermediate dispersion and below 6 is for nondispersive soils. However, subsequent studies by Walker (1997) and Bell & Walker (2000) indicate that the SAR greater than 2 should best assign the boundary for dispersive soils whilst that for nondispersive soil should be less than 1.5 (Table 6.7). Hence, the limit of 40 meq/l of free salts in the soil established to the use of SAR for the identification of dispersive soils should also be revised down. Actually, some authors like Beckedahl (1996) and Walker (1997) argue that the critical values assigned to predict the dispersion appear to be too high to the Southern Africa environment.

**Table 6.7** – New SAR grading for dispersivity suggested by Walker (1997) and Bell & Walker (2000)

| Grade     | Dispersive | Intermediate | Nondispersive |
|-----------|------------|--------------|---------------|
| SAR value | > 2        | 1.5 - 2      | < 1.5         |

Using this simple parameter the majority of the analysed soil samples (13 samples) of Maputo City showed nondispersive (Samples 2, 5, 7, 8, 9, 10, 11, 12, 13, 14, 15, 16 and 20), 6 samples are dispersive (Samples 1, 3, 6, 17, 18 and 21) while the remaining 2 samples have intermediate dispersion (samples 4 and 19) (Figure 6.9). Southwest of Maputo City is the area with more dispersivity characteristics together with the North top. These results are in full similar to the ones obtained with ESP and the TDS vs. %Na diagram.

#### 6.4.3 – Total Dissolved Salts and Percentage of Sodium

The total of the dissolved salts (TDS) in the pore water or saturation extract is another currently accepted method of evaluating the chemical influence on dispersive behaviour of soils (Sherard *et al.* 1976a; Dolen *et al.*, 1988; Bell, 2000). The soil is mixed with distilled water to a saturated paste, with a consistency near its liquid limit and the paste is tested to determine the amount of calcium, magnesium, sodium and potassium in milli-equivalents per litre. The analysis are done after allowing the mixture to stand for a number of hours until equilibrium between the salts in the pore water and the cation exchange complex is attained (Sherard *et al.*, 1976a; Bell, 2000).

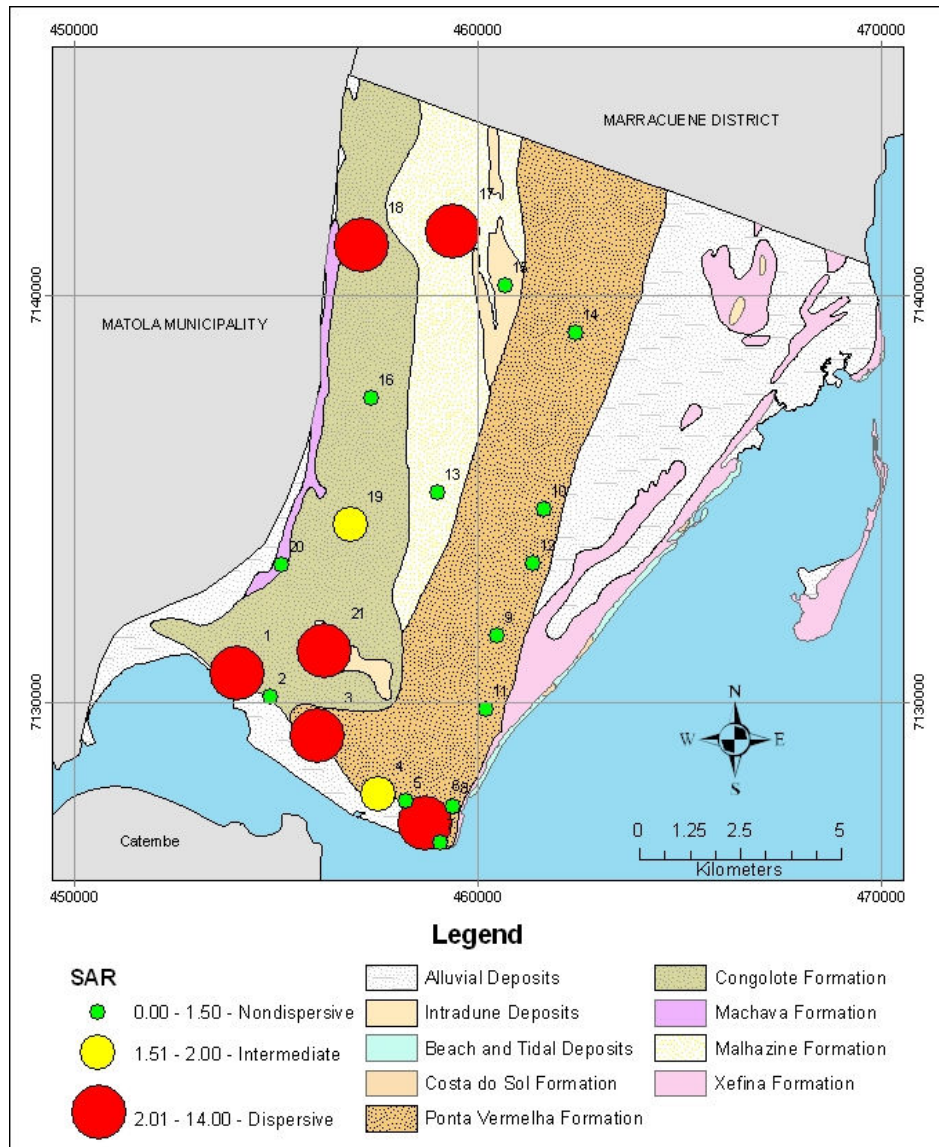


**Figure 6.9** – Distribution of SAR values in Maputo City

The TDS is the total of the four analyzed cations:

$$TDS = Na^{+} + Ca^{2+} + Mg^{2+} + K^{+} \quad \text{Eq. 6.3}$$

Sherard *et al.* (1976a) used the relationship between percentage sodium and TDS to propose another method to identify dispersive soils (Figure 6.10). The percentage sodium is obtained from the following relationship:

$$\%Na = \frac{Na^{+}}{TDS} \quad \text{Eq. 6.4}$$

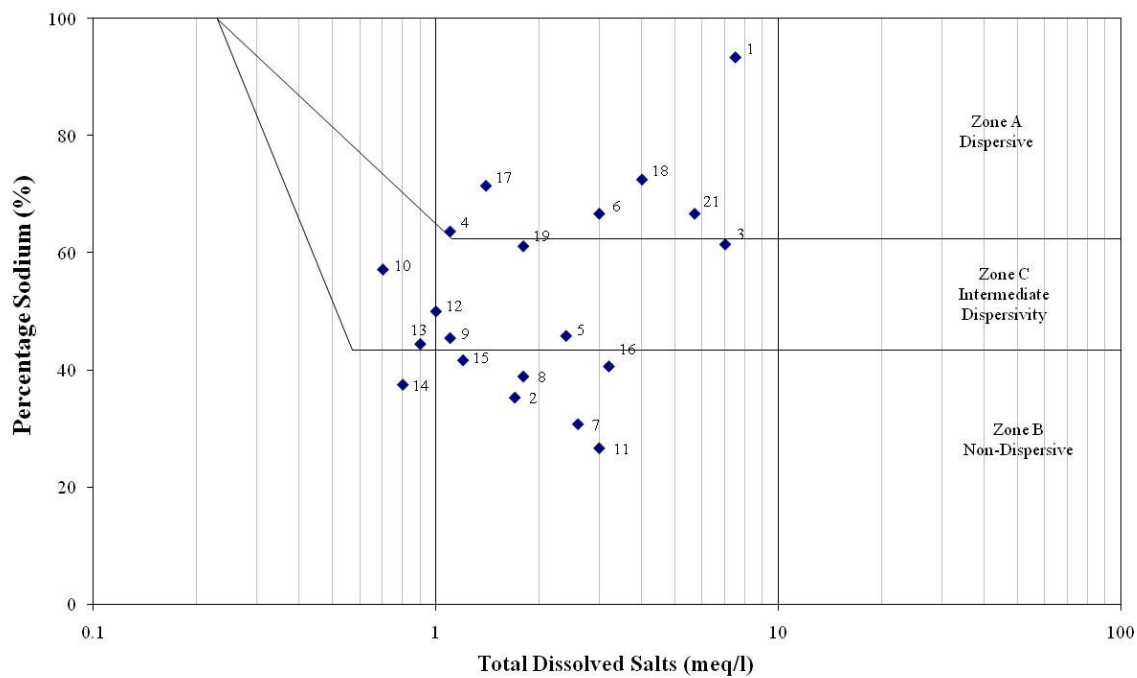


**Figure 6.10** – Percentage Sodium vs. TDS chart as proposed by Sherard *et al.* (1976a) for the identification of dispersive soils

The relationship shown on figure 6.10 is only valid for relatively pure eroding waters (e.g. TDS less than 0.5 meq/l or about 300 mg/l) (Sherard *et al.*, 1976a; Bell, 2000). Soils with high pore water TDS and more than 50% sodium are considered dispersive (Bell, 2000). This chart shows the three areas of dispersivity: Zone A for dispersive soil has %Na higher than 60% and TDS greater than 1 meq/l; Zone B for nondispersive soils is for the soils with %Na less than 40% and TDS more than 0.2 meq/l; and Zone C for intermediate soil has %Na between 40 and 60%. On this zone both dispersive and nondispersive soils plot.

Figure 6.10 shows that 7 sampling points (1, 3, 4, 6, 17, 18, and 21) fall in the area of dispersive soils while the other of 7 points (samples 2, 7, 8, 11, 14, 15 and 16) fall in the area of non dispersive soils. The remaining of the samples (5, 9, 10, 12, 13 and 19) is of intermediate dispersion. However, Craft & Acciardi (1984) and Dolen *et al.* (1988) show that percentage sodium plotted against total dissolved salts has a poor overall agreement with results of physical tests, therefore the identification of dispersive and non-dispersive soil cannot be adequately provided by the pore water cation data. The findings of these authors were partially confirmed in this study as there is discrepancy between the results obtained with this method with the ones from ESP vs. CEC diagram and flowchart of Harmse (1980) (Section 6.4.5) regarded as the best methods for identification of dispersive soils. Nevertheless, samples classified as dispersive with the TDS vs. Na diagram (Samples 1, 3, 4, 6, 17, 18 and 21) were also found dispersive or

with intermediate dispersion with the SAR and ESP methods.

#### **6.4.4 – pH and Electrical Conductivity**

Soil dispersivity is caused by the nature of the cations in the soil and these can be related to the soil pH. Bell & Maud (1994) indicate that soils with pH greater than 8 are often highly dispersive and the pH value of dispersive soils generally ranges between 6 and 8. pH less than 6 indicates non dispersive soil. From the tested soils eight samples can be regarded as dispersive (samples 1, 3, 5, 10, 15, 18, 19 and 20) and four have shown pH greater than 8 indicating high dispersivity (2, 6, 7 and 8). However, pH cannot be used individually to distinguish dispersive from non-dispersive soil. Not all samples that tested dispersive with the TDS vs. %Na, SAR and ESP were classified as dispersive using pH. This was true only for half of the samples (samples 1, 3, 18 and 19).

Electrical conductivity (EC) gives an indication of the soil salinity and indicates transmission of an electric current through water, or a soil water extract (Ehsani & Sullivan, 2002). Soil electrical conductivity correlates to soil texture, water content, cation exchange capacity, drainage conditions, organic matter level, temperature, salinity and subsoil characteristics (Doerge, 2001) and can reflect the amount of soluble salts in a soil extract (Ehsani & Sullivan, 2002; Doerge, 2001). Figure 6.11 shows the relation of EC and soluble salts of the tested soils of Maputo City. Because EC does not correlated to sodicity of the soil, it cannot be used as an indication of dispersivity (Walker, 1997). Conductivity is obtained from the saturation paste extract. The salts are allowed to dissolve in the standing distilled water for one hour, and the extracted paste is used to measure the electrical conductivity using electrodes (Doerge, 2001). EC is expressed in milliSiemens per meter (mS/m).

#### **6.4.5 – Combination of Chemical Properties**

Combination of different chemical properties in the identification of dispersive soils have been proposed by Harmse (1980) and also recommended by Elges (1985), Gerber & Harmse (1987), Bell & Maud (1994) and Walker (1997). This method is based on a flowchart (Figure 6.12) and is capable to determine the susceptibility of a soil to disperse even in soils containing free salts (Gerber & Harmse, 1987). This is not true for the physical tests like pinhole test, double hydrometer and crumb test where the results are not reliable if the soil solution contains soluble free salts even below the threshold concentration (Gerber & Harmse, 1987).

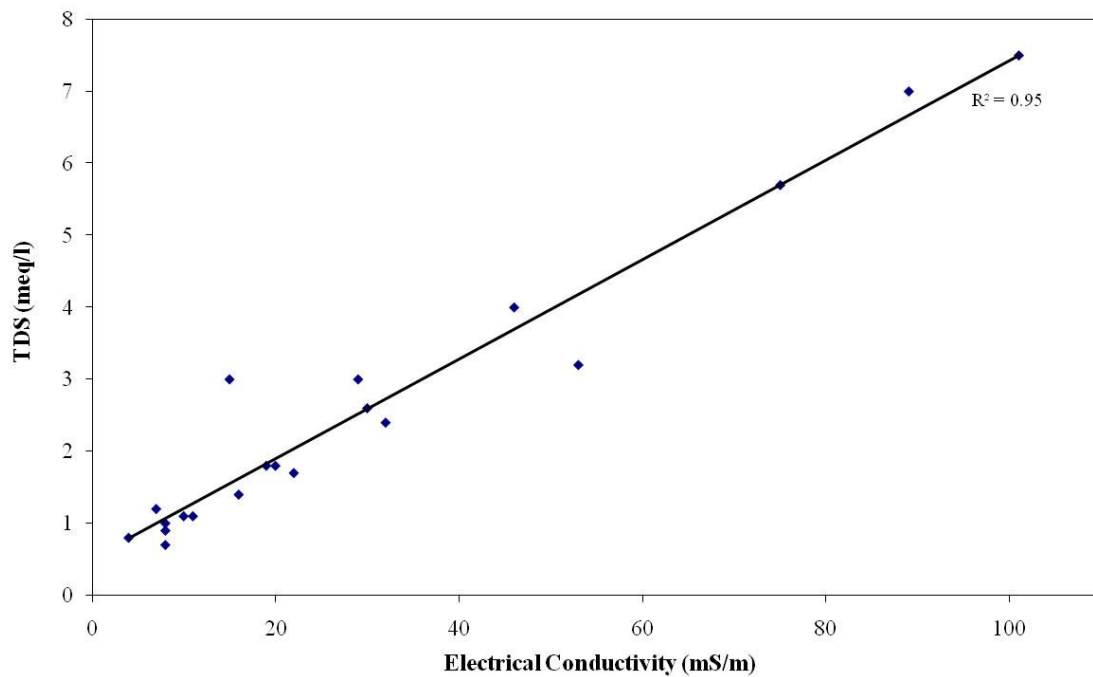


**Figure 6.11** – Strait line relationship between the total dissolved solids and the electrical conductivity of the tested soils of Maputo City.

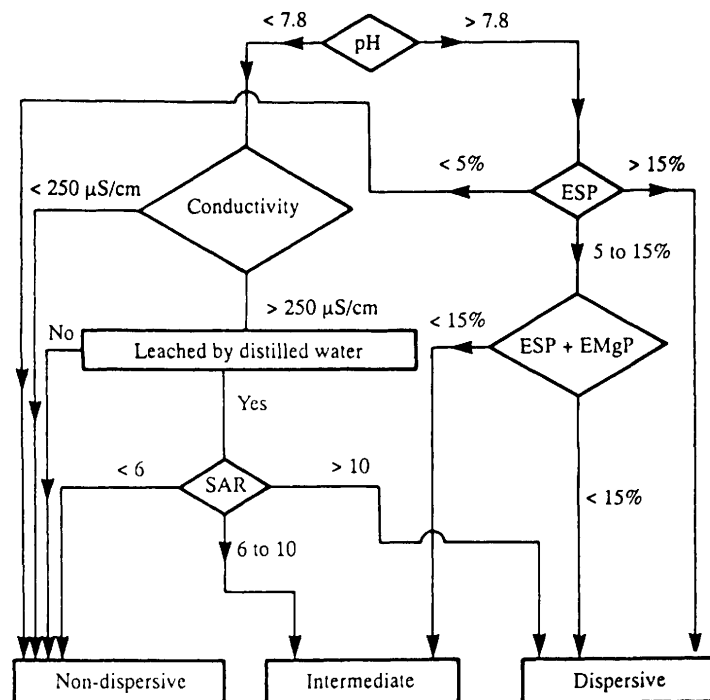


**Figure 6.12** – Chemical evaluation to identify the dispersive soils (Harmse, 1980).

The flowchart starts with the pH of the soil solution. If the pH value is higher than 7.8 and the ESP is below 5%, the soil is probably non dispersive; if the ESP is above 15% the soil is dispersive; if the ESP falls between 5% and 15% and the combined exchangeable sodium and



magnesium percentages is greater than 15%, then the soil is generally dispersive (Bell & Maud, 1994). If this combination is below 15 % the soil will probably be of intermediate dispersion. Conversely, if the pH value is lower than 7.8 the soil can be regarded as dispersive if its free salts are giving electrical conductivity higher than 2500  $\mu\text{S}/\text{cm}$  and the SAR is higher than 10. Intermediate dispersion will be found when SAR is between 6 and 10.

This method identified only samples 1 and 3 as dispersive while the remaining 19 samples of the study area are non dispersive; no intermediate dispersion was identified with this method. The pH criterion on the top of the flowchart makes the evaluation depend a lot from the pH value. Most of the samples in the study area have pH less than 7.8 and their free salts are also low explaining the non dispersive character given by this method even for samples identified as dispersive with SAR and ESP.

## 6.5 – RATING SYSTEM FOR SANDY SOILS

Dispersive soils are difficult to identify as the boundary between dispersive and non dispersive states varies significantly from one soil to another and its transition point is difficult to recognize (Bell, 2000). As no single test has been developed to reliably identify all dispersive soils with absolute certainty a tentative rating system was suggested by Bell & Maud (1994) using a number of tests results. This rating system was then modified by Bell *et al.* (1998) (Table 6.8) and adopted by Bell & Walker (2000). A rating system allows several parameters to be taken into account and their influence on dispersivity weighted according to their importance in the process. The inclusion of both physical and chemical factors in the rating assessment allows several aspects of dispersivity to be taken into account (Bell, 2000).

**Table 6.8** – Rating system modified by Bell *et al.* (1998) and adopted by Bell & Walker (2000)

|              |              |                        |                   |               |                    |
|--------------|--------------|------------------------|-------------------|---------------|--------------------|
| Pinhole test | Class Rating | Highly Dispersive<br>5 | Moderate<br>3     | Slightly<br>1 | Nondispersive<br>0 |
| CEC vs. ESP  | Class Rating | Highly Dispersive<br>4 | Dispersive<br>3   | Marginal<br>1 | Nondispersive<br>0 |
| Crumb Test   | Class Rating | Strong reaction<br>3   | Moderate<br>2     | Slightly<br>1 | No reaction<br>0   |
| SAR          | Class Rating | Over 2<br>2            | 1.5-2<br>1        |               | Less than<br>0     |
| TDS vs. %Na  | Class Rating | Dispersive<br>2        | Intermediate<br>1 |               | Nondispersive<br>0 |

The modified rating system of Bell & Walker (2000) proposes the use of the following tests: pinhole test, crumb test, the SAR value and the assessments according to the dispersivity charts TDS vs %Na of Sherard *et al.* (1976a) and CEC vs ESP of Gerber & Harmse (1987). This

rating system assigned high rating values to more reliable tests and lower values to the less reliable. Not all tests in the modified rating system of Bell & Walker (2000) were performed in this research, for example, the pinhole test did not work because of the sandy characteristics of the soils in the study area and for that reason an alternative rating is proposed.

As previously mentioned, dispersivity and erodibility occur when solid particles are detached and moved away from the soil under the influence of flowing water. The detachment is the result of this physical process, therefore, the dispersive soils are best investigated using physical tests. However, the chemical soil composition has also influence on the dispersive behaviour of the soil, and ESP and the amount of dissolved salts in the pore water have been identified by Walker (1997) as the most important. These combinations of physical and chemical factors are taken into consideration on the definition of the new rating system for sandy soils.

The tests that are found reliable to identify the soil susceptibility to disperse and erode in this study were the flume test, crumb test, TDS/%Na, SAR and ESP. Although regarded by Gerber & Harmse (1987) as the most effective in the identification of dispersive soils, the CEC vs. ESP relation did not help on differentiate the soil samples of Maputo City as all were observed to be non dispersive. This was the criteria used to select the tests to the new rating system. The flume test which simulates the water flowing over the soil and quantifies the eroded material is the most reliable test to identify the erodibility rate. The crumb test indicates the predisposition of the soil to deflocculate in the presence of sodium hydroxide solution (Head, 1988; Elges, 1985). The TDS vs %Na chart and the SAR value represent the influence of saturation extract cations which determines if the soil exists in a flocculated or dispersed state. ESP represents in the rating system the exchangeable cations which are those attached to the clay surface. Although pH represents aspects not related directly to dispersion its results were fairly correlated to ESP and SAR.

The erosion rate of a given soil will definitely be related to the geomorphologic setting where the topography plays a very important role (Section 6.6.1). The topography and slope gradient were taken into account in the rating system and three classes of influence on erodibility were identified.

The remaining parameters were not included in the rating system because they were not able to differentiate the soils occurring in Maputo City. This is the case of EC, CEC, CEC vs ESP chart and the flow chart method of Harmse (1980).

It is proved that each physical and chemical parameter has different influence on the soil

dispersion therefore, this rating system assigned high rating values to more reliable tests and lower values to the less reliable (Table 6.9).

**Table 6.9** – New rating system for the susceptibility of the sandy soils to erosion

|                |              | <b>High Susceptibility</b>                             | <b>Moderate or Intermediate Susceptibility</b>  | <b>Low Susceptibility</b>                                   |
|----------------|--------------|--|---|---|
| Flume Test     | Class Rating | Highly Erodible<br>(Over 0.07 kg/m <sup>2</sup> )<br>5 | Moderate<br>(0.05-0.07 kg/m <sup>2</sup> )<br>3 | Low Erodibility<br>(less than 0.05 kg/m <sup>2</sup> )<br>1 |
| Slope Gradient | Class Rating | Over 5.<br>4   | 5 - 2<br>2                                      | Less than 2<br>1  |
| Crumb Test     | Class Rating | Strong reaction<br>3                                   | Moderate or Slight<br>2                         | No Reaction<br>1  |
| TDS vs. %Na    | Class Rating | Dispersive<br>3  | Intermediate<br>2                               | Nondispersive<br>1  |
| SAR            | Class Rating | Dispersive (Over > 2)<br>2                             | Intermediate (1.5–2)<br>1                       | Less than 1.5<br>0  |
| ESP            | Class Rating | Dispersive<br>2  | Intermediate<br>1                               | Nondispersive<br>0  |
| pH             | Class Rating | Over 8<br>2  | 6 - 8<br>1                                      | Less than 6<br>0  |

The highest rating of 5 was given to the high erodibility in the flume test as it gives the best indication. To the highest class of slope gradient was assigned the rating of 4 while the strong reaction of the crumb test received a rating of 3 as well as the dispersive results from the TDS vs %Na. To SAR and ESP were assigned a maximum rating of 2 for dispersive results. Although pH represents aspects not related directly to dispersion it was included in the rating system because of its positive correlation to ESP and SAR results. A maximum rating of 2 was assigned to the highly dispersive soil result with pH.

With this rating system a maximum range of 21 is expected and a minimum of 4. If the total rating is equal or greater than 16 the soil is considered as with high susceptibility to erosion. If the rating is between 8 and 16 the susceptibility to erosion is moderate or intermediate and lastly if less than 8 is regarded as with low susceptibility to erosion.

The proposed rating system was applied to the tested soils of Maputo City (Table 6.10). Fifteen samples were classified with intermediate susceptibility to erosion (samples 1, 3, 4, 5, 8, 9, 10, 11, 13, 15, 17, 18, 19, 20 and 21) while 3 samples were assigned as of low susceptibility to erosion (samples 2, 12 and 16). The highest scores, between 11 and 15, were obtained by the same samples that shown dispersive behaviour with SAR, ESP and TDS/%Na (Samples 1, 3, 4, 17, 18, 19 and 21). This group, except Sample 21, were of intermediate erodibility in the flume test.

**Table 6.10** – Rating system for the susceptibility of the sandy soils to erosion applied to the soils of Maputo City

| Sample N° | Geological Unit | Flume Test | Rating | Slope Gradient | Rating | Crumb Test | Rating | TDS/%Na | Rating | SAR   | Rating | ESP   | Rating | pH   | Rating | Total rating |
|-----------|-----------------|------------|--------|----------------|--------|------------|--------|---------|--------|-------|--------|-------|--------|------|--------|--------------|
| 1         | QCo             | 0.0647     | 3      | 1.43           | 1      | 4          | 4      | D       | 3      | 14.00 | 2      | 36.92 | 2      | 7.73 | 1      | 15           |
| 2         | QCo             | 0.0423     | 1      | 2.16           | 2      | 4          | 4      | ND      | 1      | 0.81  | 0      | 0.65  | 0      | 8.17 | 2      | 8            |
| 3         | TPv             | 0.0546     | 3      | 1.51           | 1      | 4          | 4      | D       | 3      | 3.70  | 2      | 12.21 | 2      | 7.81 | 1      | 15           |
| 4         | TPv             | 0.0587     | 3      | 4.97           | 2      | 3          | 2      | D       | 3      | 1.57  | 1      | 6.26  | 2      | 5.93 | 0      | 13           |
| 5         | TPv             | 0.0489     | 1      | 8.55           | 4      | 2          | 2      | ID      | 2      | 1.36  | 0      | 1.24  | 0      | 7.96 | 1      | 9            |
| 6         | TPv             | ND         | NC     | 2.11           | 2      | 2          | 2      | D       | 3      | 2.83  | 2      | 0.47  | 0      | 9.21 | 2      | NC           |
| 7         | TPv             | ND         | NC     | 2.25           | 2      | 1          | 1      | ND      | 1      | 0.84  | 0      | 0.26  | 0      | 8.71 | 2      | NC           |
| 8         | TPv             | 0.0746     | 5      | 2.7            | 2      | 2          | 2      | ND      | 1      | 0.94  | 0      | 1.09  | 0      | 8.19 | 2      | 10           |
| 9         | TPv             | 0.0513     | 3      | 1.99           | 1      | 2          | 2      | ID      | 2      | 0.91  | 0      | 4.95  | 1      | 5.81 | 0      | 9            |
| 10        | TPv             | 0.0889     | 5      | 5.73           | 4      | 3          | 2      | ID      | 2      | 1.03  | 0      | 3.60  | 0      | 6.18 | 1      | 13           |
| 11        | TPv             | 0.0648     | 3      | 3.11           | 2      | 4          | 4      | ND      | 1      | 0.76  | 0      | 2.64  | 0      | 5.39 | 0      | 10           |
| 12        | TPv             | 0.0489     | 1      | 4.61           | 2      | 2          | 2      | ID      | 2      | 1.00  | 0      | 4.60  | 1      | 5.18 | 0      | 8            |
| 13        | Qma             | 0.0829     | 5      | 1.44           | 1      | 2          | 2      | ID      | 2      | 0.80  | 0      | 3.47  | 0      | 5.52 | 0      | 10           |
| 14        | TPv             | ND         | NC     | 5.66           | 4      | 1          | 1      | ND      | 1      | 0.60  | 0      | 8.23  | 2      | 5.47 | 0      | NC           |
| 15        | Qi              | 0.0681     | 3      | 0.64           | 1      | 2          | 2      | ID      | 2      | 0.85  | 0      | 4.40  | 1      | 6.26 | 1      | 9            |
| 16        | QCo             | 0.0215     | 1      | 1.38           | 1      | 2          | 2      | ID      | 2      | 1.33  | 0      | 2.80  | 0      | 4.74 | 0      | 6            |
| 17        | Qma             | 0.0555     | 3      | 1.36           | 1      | 3          | 2      | D       | 3      | 2.24  | 2      | 7.25  | 2      | 5.15 | 0      | 13           |
| 18        | QCo             | 0.0674     | 3      | 1.06           | 1      | 3          | 2      | D       | 3      | 3.91  | 2      | 13.76 | 2      | 6.12 | 1      | 13           |
| 19        | QCo             | 0.0838     | 5      | 0.63           | 1      | 3          | 2      | D       | 3      | 1.86  | 1      | 6.42  | 2      | 7.08 | 1      | 14           |
| 20        | Qmc             | 0.0612     | 3      | 2.47           | 2      | 1          | 2      | ND      | 3      | 0.00  | 0      | 0.00  | 0      | 7.23 | 1      | 10           |
| 21        | QCo             | 0.0464     | 1      | 0.12           | 1      | 3          | 2      | D       | 3      | 3.90  | 2      | 7.70  | 2      | 5.09 | 0      | 11           |

ND: Not Determined; NC: Not Classified



Nondispersive



Intermediate Dispersion



Dispersive

## 6.6 – SITE SPECIFIC CHARACTERISTICS AND EROSION PROBLEMS

### 6.6.1 – Topography and Slope Steepness

Topography is one of the main factors controlling mass movement. A lot of studies have discussed the relationship of rill and gully development as a function of slope lengths and slope gradients although the recognition that their development are also linked to relatively large quantities of water to supply energy for both detaching and transporting soil (Øygarden, 2003).

In fact, sufficient runoff to concentrate and initiate gullying is related to the size of critical drainage area and its runoff characteristics which depend on the slope gradient (Valentin *et al.*, 2005; Øygarden, 2003). The topographic threshold lines for gully initiation were developed as to define the place in the terrain where gully erosion is likely to occur using as reference the minimum physical characteristics for gullies initiation (Poesen *et al.*, 2003). Critical slope gradients of 2° for rills (< 0.3 m deep), 5° for shallow gullies (0.3–2 m deep) and 8° for deep gullies (> 2 m deep) were reported in a research developed in China by Guanglu *et al.* (2004). However, different critical values apply for different gully initiating processes and different environmental conditions (Poesen *et al.*, 2003).

In Maputo City the topography plays an important role in gully erosion as there is a topographic difference of up to 49 m between the beach/estuary areas with the upland composed by the Ponta Vermelha Formation. Slope angles in the most affected areas vary between 20 to 60° and the height difference, according to the geologic sheet of Maputo, constitutes an inferred tectonic fault. Steep slopes favour high runoff velocity and large quantity soil loss and thus rill and gully initiation. “Soil erosion by water also increases as the slope length increases due to the greater accumulation of runoff” (Wall *et al.*, 2003).

Figure 6.13 shows the slope gradient of Maputo City, from which it is possible to observe that the areas heavily affected by gully erosion (Polana-Caniço and Ferroviário Quarters) are not those with the highest slope gradient. Other factors such as soil characteristics, urban land use practice and hydrogeological characteristics have contributed more to gully erosion.

Valentin *et al.* (2005) argue that crusting rate on slopes influences the runoff volumes. Thus, the higher crusting rate expected in the lower slopes where the impact caused by the kinetic energy is also lower comparing to the steep slopes, is reflected in the higher runoff volumes. This is not the case of Maputo City where the higher crusting rate occurs on the slopes with highest gradient. The origin of the slope, assumed to be tectonically controlled removes this argument

of lower crusting rate on steep slopes. This area of the slope is also well vegetated reducing the runoff erosivity. Vegetation cover explains better the differences in topographic thresholds comparing to the role of climatic conditions (Vandekerckhove *et al.*, 2003; Poesen *et al.*, 2003).

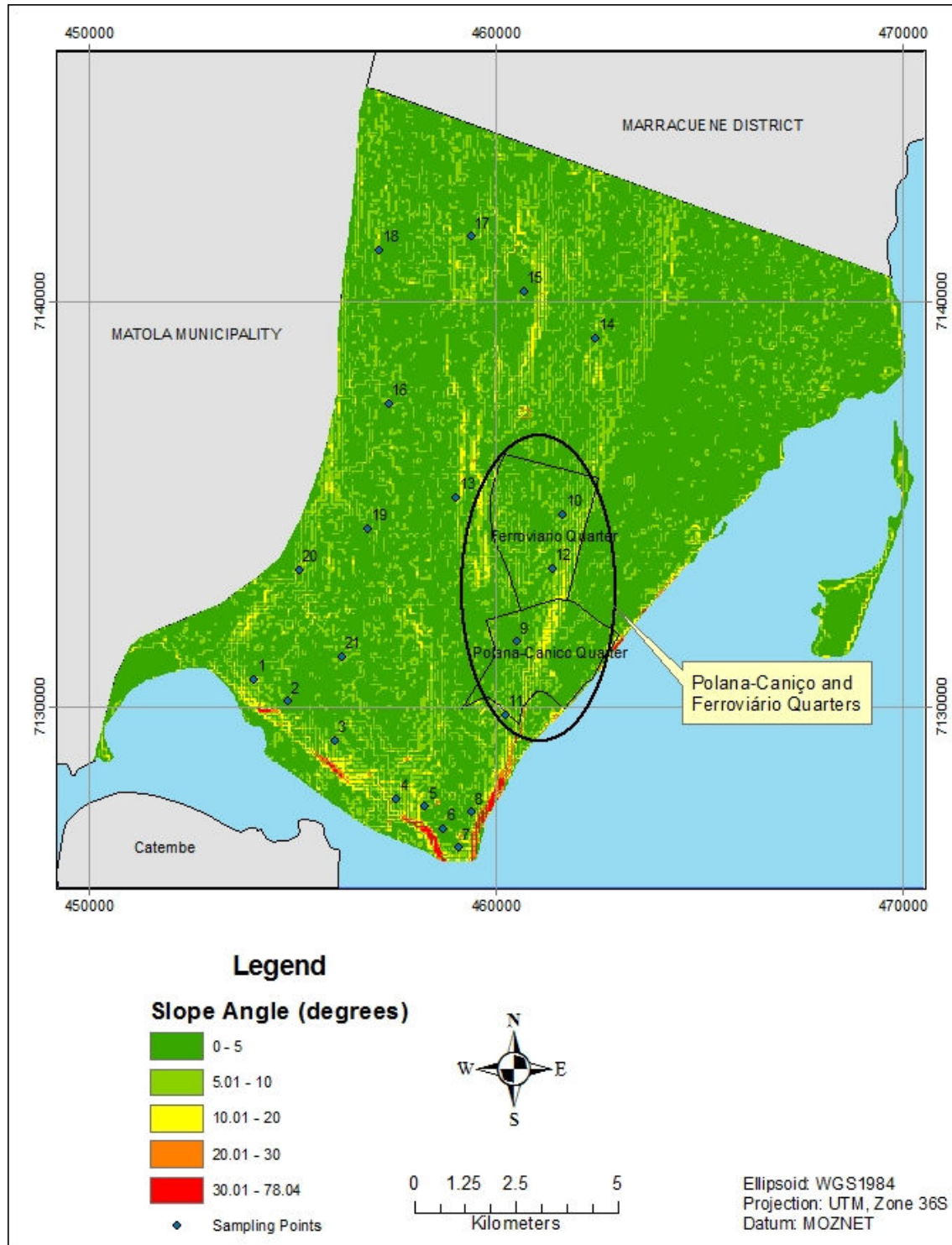


Figure 6.13 – Slope angle of Maputo City

### 6.6.2 – Soil Type and Lithologic Controls

Soil type and in particular soil profile properties have a lot with the rill and gully erosion development. The erosion resistance of the various soil horizons controls the characteristics of the gullies, namely the size, depth and cross-sectional morphology. The shape of the gully cross-sections depends on the properties and strength of the soil matrix (Øygarden, 2003). Discussion on Section 6.2 indicates that although the two most gully affected areas of Maputo City are in the same geological formation composed of silty sand, the gullies show different shape of the cross-sections. Gullies in Ferroviário Quarter are mainly V-Shaped while the ones in the Polana-Caniço are U-Shaped. These differences are linked to the difference on the cohesion of the soil particles together with the percentage of silt and fine sand fraction which is 17% higher in the Site 10 (Ferroviário Quarter) than in the Site 9 (Polana-Caniço).

The resistance of the Bt-horizon plays an important role in controlling gully depth (Poesen *et al.*, 2003; Bryan, 2004; Valentin *et al.*, 2005). The soil shear strength was not calculated for different soil horizons in this research but the occurrence of landscape heavily dissected by gullies, 1-15 m deep, is an indication of the low resistance of the soil horizons.

The presence of red silty sand soils, loose to very loose in consistency, in the geological formation most affected by gullies, makes the lithologic condition a factor controlling gully erosion as sandy soils, themselves, are highly susceptible to gully erosion. However, although the fact that the gully erosion occurring in two areas located in the Ponta Vermelha Formation, the soil characteristics of this formation must not be taken as the trigger factor of gully erosion in Maputo City. Other factors like the topographic setting and the land use pattern in the affected areas can have contributed most for gully erosion.

### 6.6.3 – Rainfall-Runoff Erosivity and Soil Water Conditions

The rainfall intensity and runoff erosivity factor relate the climate factor in the erosion process and are important in the assessment of water erosion. The impact of raindrop, flow traction and rain splash are responsible for the disaggregation, detachment and dispersion of the primary soil particles (Wall *et al.*, 2003). Flowing water or saltation are responsible for moving particles down slope or directly into rills and gullies and promoting turbulence in runoff that increases transport capacity. Raindrop splash and low energy runoff water are enough to remove the aggregate materials with low density such as organic matter, clay, silt, and very fine sand (Wall *et al.*, 2003; Dahal, 2006). The overland flow production is influenced by the moisture content existing before the rainfall and is much higher when

the soil is saturated, or nearly to so, at the time when the rain starts to fall (Cooke & Doornkamp, 1990).

Runoff is the most important agent of water erosion. Its influence in soil erosion intensity is well recognised, therefore its analysis has to be taken into account in any study of the processes influencing runoff. “*Runoff occur whenever there is excess water on a slope that cannot be absorbed into the soil or trapped on the surface*” (Yang *et al.*, 2008; Abegunde *et al.*, 2006). Soil compaction and crusting can increase the amount of runoff if they are responsible of the reduction of infiltration rates.

Rainfall-runoff erosivity factor (R) is the average annual summation of the erosion-index values in a normal year's rain and reflects the amount of rainfall and peak intensity. These two parameters determine the erosivity of a storm (Renard *et al.*, 1997). The transferability of the RUSLE/USLE (Revised/Universal Soil Loss Equation) of respectively Renard *et al.* (1997) and Wischmeier & Smith (1978), to tropical environments is questionable because the environmental factors (climate, topography and soil factors) are different from the ones used to derive the equations (Scholten, 1997). For this reason the rainfall-runoff erosivity factor (R) for the study area was not computed as no attempt have been made yet to develop and validate soil erodibility/erosivity indexes for Mozambique.

However, the rainfall-runoff erosivity factor (R) is predicted to be lower in tropical areas comparing to arid and semi-arid areas where the rainfall is intense and has a short period of duration. This scenario changes when the rainfall is caused by a particularly extreme climatic event as the one occurred in 2000 in Maputo City. Unusual, intense and prolonged rainstorm occurred in February 2000 where a precipitation of 400 mm was registered in only four days, far beyond 132 mm, which is the mean monthly precipitation in the rainy season occurring from November to March (Manuel & Vicente, 2002) and saturated the soils. Poesen *et al.* (2003) introduced the concept of rainfall threshold which are the critical rainfall characteristics above which gullies are likely to be developed. Precipitation between 14.5 and 22 mm was assumed as the threshold rain needed to initiate ephemeral gullies in cropland. Obviously, these values are dependent on other factors like land use, antecedent rains and difference on the state of the soil surface like roughness, topography and land use cover.

Water infiltration, percolation and retention into the soil determine the magnitude of soil erosion and are largely controlled by the soil structure and texture (size, volume, distribution and continuity of pore space) defined by the arrangement of particles and aggregates (Bryan, 2000). Water flow through the soil mass creates a soil-water balance which will be responsible for



maintaining the critical hydraulic properties and soil structure. Changes of this balance will control the erosional susceptibility of the soil. Increase in the pore water pressure reduces the effective stress of the soil mass making easy the erosional process. Water promotes movement as it increases the loading (weight) of soil by filling previously empty pores and also decreases the strength of the soil (Coch, 1995).

During rainstorms the erosional response of the soil is probably controlled by the soil water and rainfall variations (Bryan, 2000). Previous soil water content at the start of rainstorms event is particularly important for erosional response as it affects the resistance to runoff. High rainfall occurred during the end of January 2000 (total month precipitation of 234.8 mm) could have raised the moisture content creating conditions for massive erosion and gullies formation with the early February 2000 rainfall in Maputo City (total month precipitation of 502 mm). Instability and gully erosion may have been triggered by these changes in the groundwater conditions. Rainfall raised the water table, saturated the soils and the steep slopes causing deeply and steeply gullying failures. Groundwater seepage is observed in the gully affected area (Figure 6.14) creating a capillary zone of negative soil suction of approximately 1m above the water table (McKnight, 2001). Projection of the water table to the slope surface shows that the original gullies are indeed connected to phreatic surface which varies between 10 to 15 m in the affected areas and controlled by grain size distribution and Topography in this aquifer.



**Figure 6.14** – Groundwater seepage in the Polana-Caniço Quarter gully (photograph taken in the dry season)

McKnight (2001) supports the hypothesis that gullies propagation was caused by sudden rise in water table during rainfall periods causing daylight of the phreatic surface in gullies heads forming high hydraulic gradients. The rapid drop of the effective stress may have created conditions for complete loss of apparent cohesion (negative pore pressure) and flowslide of the lower fine sandy layer if hydraulic gradient of approximately 1.0 is realised (McKnight, 2001).

#### **6.6.4 – Land Use Pattern**

Like other African cities, Maputo has informal settlements located in the outskirts. As discussed in Chapter 4 (Section 4.7), only 20% of the residential land use has comparatively fully developed infrastructure, and a further 27% is in sites and services areas. The unplanned settlements count for the remaining 53% of residential land use (Jenkins, 2000) comprising the Suburban and Periurban areas. These areas, including the most affected by erosion problems in Maputo City (Polana-Caniço and Ferroviário Quarters) are characterized by relatively high density both unplanned and planned residential settlements, much in non-permanent construction. Population densities in these areas are growing rapidly as there is informal sector activity round markets (Jenkins, 2000). Common to the two areas is a very poor provision of infrastructure and social equipment lacking sewage and drainage system, clean water supplies, electricity and roads.

The unplanned land development is behind most of the engineering and environmental geological problems in Maputo City with construction along sensitive areas such as steep slopes and drainage lines without observing the appropriate techniques. During urbanization vegetative cover is eliminated, surfaces are paved reducing the infiltration and percolation area and preventing water from sinking into the ground (Coch, 1995). Consequently, water is accumulated and greater volume of water runs off faster over the surface before discharging into the low lying area flowing to the Maputo Bay. These changes caused by urbanization increased the peak discharge, the risk of flooding and the water erosive capacity. As these unplanned residential areas lack of drainage system to collect the storm water, it runs off over unprotected surfaces, mainly compacted footpaths, eroding and transporting the unconsolidated sandy soils downward to the bay. The initiation of several rills and gullies in Maputo City was caused by uncontrolled, concentrated water flow.

Improper design and construction of waterways during the rehabilitation of the railway route out of Maputo City has influenced on the erosion rates. Common to almost all gullies in the

Ferroviário Quarter are their starting points in the drainage system of this railway. Drainage System and other measures should have been designed for high runoff events and located in those parts where concentrated water flow occurs. The uncontrolled and concentrated water flow from the railway drainage system which found unprotected areas was responsible for the initiation of some gullies in the Ferroviário Quarter (Fig. 6.16). Erosion due to similar conditions was documented by Watson & Evans (1991) and Vandekerckhove *et al.* (1998). In these situations more efforts must be directed towards avoiding and controlling the concentrated runoff, since the effect is so significant if runoff is out of control (Vandekerckhove *et al.*, 1998; Øygarden (2003). Combination of factors as soil characteristics and urbanization made landslide and gully hazard to occur.



**Figure 6.15** – Gully initiating in the discharging point of concentrated water flow from the railway drainage system in Ferroviário Quarter, Maputo City.

## 6.7 – SUMMARY AND CONCLUSIONS

Soil erosion in Maputo is the most prominent engineering geological and environmental problem causing concern due to the large areal extent of the affected area, the huge environmental and economic impacts on the population and the threat to the sustainability of the affected residential areas. It occurs mainly as rills and gullies affecting Polana-Caniço and

Ferroviário Quarters. The gullies are extremely large, deeply cut, 1 to 15 m deep. Gullies in Ferroviário Quarter are mainly V-Shaped while the ones in the Polana-Caniço are U-Shaped.

Gullies were in the past regarded as indicator of the existence of dispersive soil material but, they have been reported in soil materials not exceeding the assigned reference indices to identify dispersive soils such as SAR, ESP and dispersion ratio (Rienks, 2000). In this context, a qualitative evaluation of the erosion susceptibility was investigated by physical tests such as the crumb test, Atterberg Limits and Shear Strength while a quantitative evaluation of the erodibility characteristics was obtained using a flume test. Presently it is confirmed that the physical properties of soils, including dispersion, are related to the composition and concentration of salts in the soil solution and to the interactions between various soil properties (Gerber & Harmse, 1987). It is now also proved that the positive identification of dispersive and erodible soils can only be done by combination of various techniques (Paige-Green, 2008; Bell & Walker, 2000). For this reason, assessment of dispersivity using the chemical properties was undertaken in order to assess its workability in the context of the tested soils mainly in the areas most affected by gully erosion.

Crumb test results shown weak correlation with the clay content, and no correlation with silt content, ESP and SAR. Results from this study also indicate very weak correlation between friction angle and plasticity index and no clear trend was observed for the influence of plasticity index on cohesion. The low plasticity index together with the low plastic clay content observed in the soils of the study area can be the cause of the absence of clear correlation. It was expected that the friction angle would decrease with increase in plasticity index. These findings indicate that these parameters have no clear influence on the soils erosion susceptibility and give an idea that the disintegration observed, for example, in the crumb test is not simply physico-chemical dispersion process or at least other factors have contributed negatively to the dispersion process to occur. Same conclusions were also found by Walker (1997) and Rienks *et al.* (2000) who have reservation on the consistence of this technique in identifying dispersive soils.

Results of the flume erodibility test revealed no correlation with the chemical properties related to dispersion. The obtained correlation data are: EC ( $r^2 = 0.09$ ), SAR ( $r^2 = 0.13$ ), ESP ( $r^2 = 0.12$ ) and CEC ( $r^2 = 0.10$ ). These findings show that the erosion susceptibility and gullying in Maputo City have more relation to the physical processes than to the dispersion related chemical properties of the soils. The physical processes were also accelerated by the land use and topographic setting. The flume test results have weak correlations with the shear strength parameters (cohesion and friction angle). However, the trend indicates that higher the cohesion,

the lower is the amount of eroded sediments in the flume ( $r^2 = 0.17$ ) and higher the friction angle, the higher is the amount of eroded sediments in the flume ( $r^2 = 0.11$ ).

Combination of different chemical properties in the identification of dispersive soils has been proposed by Harmse (1980) with which only Samples 1 and 3 were identified as dispersive. The pH criterion on the top of the flowchart makes the evaluation depending a lot from the pH value.

Some correlations were found between the results of various methods. Almost all samples that were found dispersive with ESP were also dispersive with TDS vs. %Na and SAR.

Dispersive soils are difficult to identify as the boundary between dispersive and non dispersive states varies significantly from one soil to another and no single test has been developed to reliably identify all dispersive soils with absolute certainty. Therefore, a rating system was suggested by Bell & Maud (1994) using a number of tests results, modified later by Bell *et al.* (1998) and by Bell & Walker (2000). A rating system allows several parameters to be taken into account and their influence on dispersivity weighted according to their importance in the process. A new rating for the sandy soils combining the physical and chemical factors of dispersion is proposed in this research. The tests that were found reliable to identify the soil susceptibility to disperse and erode in this study were the flume test, crumb test, TDS/%Na, SAR, ESP. The inclusion of both physical and chemical factors in the rating assessment allows several aspects of dispersivity to be taken into account (Bell, 2000). Although regarded by Gerber & Harmse (1987) as the most effective in the identification of dispersive soils, the CEC vs. ESP relation did not help on differentiate the soil samples of Maputo City as all were observed to be non dispersive. It is proved that each physical and chemical parameter has different influence on the soil dispersion therefore, this rating system assigned high rating values to more reliable tests and lower values to the less reliable.

The proposed rating system was applied to the tested soils of Maputo City. Fifteen samples were classified with intermediate susceptibility to erosion (samples 1, 3, 4, 5, 8, 9, 10, 11, 13, 15, 17, 18, 19, 20 and 21) while 3 samples were assigned as of low susceptibility to erosion (samples 2, 12 and 16). The highest scores, between 11 and 15, were obtained by the same samples that shown dispersive behaviour with SAR, ESP and TDS/%Na (Samples 1, 3, 4, 17, 18, 19 and 21). This group of samples, excepting Sample 21, were of intermediate erodibility in the flume test.

Site specific characteristics have largely contributed to the gully erosion in Maputo City. Topography, slope Steepness, Soil Type, lithology, Rainfall-Runoff Erosivity, Soil Water Conditions and Land Use Pattern were discussed and were found to have influence to gully erosion.

# **CHAPTER 7**

## **SLOPE STABILITY ANALYSIS**

### **7.1 – INTRODUCTION**

Slope instability is a significant problem in Maputo City, and is associated with factors such as geology (sandy characteristics of the Ponta Vermelha Formation where the problem is concentrated), topography, climatic conditions and inappropriate land use. Slope instability problems in Maputo City were first noticed in the late 1990's after prolonged tropical storms and heavy rainfall events. The incidence and severity of the slope instability problems raised in recently as land demand forced rapid urban development in hilly terrain (inherently unstable areas). Signs of slope movement are presented in Chapter 4. The area of landslide activity on the slope located on the Friedrich Engels Avenue appears to be currently the most active slope. There is the possibility of a catastrophic failure if extreme rainfall events continue.

The objective of this chapter is to analyse the slope instability problems occurring in Maputo City, including calculation of their factors of safety, the probabilistic and sensitivity analysis and modelling the stability using various geotechnical parameters and factors affecting slope stability. The causes of the problems and the conditions under which slope failures occurred will also be discussed as well as the remedial measures that might be undertaken to rehabilitate the affected areas and to improve the stability of the slopes.

### **7.2 – MECHANISM OF SLOPE FAILURE**

Slope failure can occur in different ways depending on the characteristics of earth material involved. Varnes (1978) defined a system to classify the different types and mechanisms of slope failures which is widely accepted and was used in this research. This system identifies 5 types of slope failure, namely flows, spreads, slides, topples and falls. The features that aid the recognition of the common types of slope movement and characteristics of slope instability are



well described in Lee *et al.* (1983) and Varnes (1984) referencing the work of Rib & Liang (1978).

The common type of slope instability occurring in Maputo City has been termed composite slide by Coduto (1999) who describes the mode of instability with mixed characteristics, in this case, of slides and flows. A slide is an instability mode where one or more blocks of soil or rock move downslope predominantly along a well-defined weakness surface or thin shear zone (Cruden & Varnes, 1996; Coduto, 1999) while flows occur with a mass movement of soil material behaving as a liquid (Lee *et al.*, 1983). The difference from the former is the absence of well-defined block movement along a weak shear surface. On this type of soil failure the water content is above the liquid limit and develops from smaller initial slides (Waltham, 1994).

The type of instability mechanism observed in Maputo City is slump or rotational failure with a mass of soil sliding along a curved surface of rupture followed by sand flow at the base as failure occurs in the presence of excess water. This type of curved surface failure is typical for slopes with homogeneous materials such as those observed in the affected area. Six borehole logs completed by McKnight (2001) in the gully affected area in Polana-Caniço (underlain by the Ponta Vermelha Formation) indicate that the area has 20-30m thickness of a duplex-type soil. The upper part consists of red, slightly clayey-silty oxidized and cemented to form a ferruginous capping that has in average 16 m in thickness (McKnight, 2001). This layer, as referred in Chapter 5, is potentially collapsible if saturated. Within the deeper portions of the gullies (> 15m depth), the red cemented sands grade into orange and pale yellowish orange, silty fine to medium sand. Near the base of the gullies this material becomes very moist with the capillary zone of negative soil suction approximately 1 m above the water table (McKnight, 2001). The majority of sites for slope stability analyses covered in this research occur in the Ponta Vermelha Formation.

Both shallow and deep-seated landslides can be found in Maputo City. A shallow landslide is observed in the slope in the Nações Unidas Avenue. A mid-slope contour concave crack, with a vertical displacement of 30-40 cm, is observed (Figure 7.1). The slope appears unstable with evidence of active movement along the crack. Shallow landslides, as the name implies, are characterized by a sliding surface at depths up to 2-3 metres (Abramson *et al.*, 2002). The shallow surface failure with translational character in this slope occurs in soils with high permeability and is probably controlled by its sandy composition. The shallow failures likely occur in slopes comprising sandy and gravelly soils, in contrast to those composed of clays and silts (Lee *et al.*, 1983). The soil grain size has been used to evaluate surficial stability which has



normally a bias in relation to cohesion. With rainfall and water infiltration, the groundwater table rises and a decrease in the matric suction of the slope soils is observed. The topsoil becomes saturated creating conditions for high pore water pressure and reduction of the soil shear strength (Abramson *et al.*, 2002). The high soil weight and the low shear strength trigger failure and rainfall-induced landslide (Li *et al.*, 2005).



**Figure 7.1** – Shallow landslide along Nações Unidas Av with a vertical displacement of 30-40 cm. The crack is located only some meters above the ground surface

Deep-seated landslides are found in the Polana-Caniço and Ferroviário Quarters where large gullies have formed as a consequence of slope failure. Deep-seated landslides are those with a failure surface located at depths greater than 10m (Abramson *et al.*, 2002) and normally involve a slope failure of large volume. In the Friedrich Engels Av, the most recent failure comprises a high angle rotational failure and soil flow at the bottom (Figure 4.16). The rotational failure is characterised by numerous tension cracks in the crown area which are predominantly concave in shape and the main scarp is steep angle and commonly high up to 60 m.

The soil masses formed as part of the slide at the toe end of the rotational slide were subjected to flow soon after failure because of soil liquefaction, as these instability events occurred under extreme rainfall conditions. A flow is a progressive movement of earth material presenting very low shear strength and behaving as a viscous liquid (Lee *et al.*, 1983). It can occur in loose cohesionless soils and silts. In this event, the sudden rise in water table and soil saturation during rainfall periods caused daylight of the phreatic surface in the slope head area forming high hydraulic gradients. The rapid drop of the effective stress may have created conditions for complete loss of apparent cohesion (negative pore pressure) and flowslide of the lower fine sandy layer if the hydraulic gradient of approximately 1.0 is realised (McKnight, 2001).

### 7.3 – CAUSES OF SLOPE FAILURE IN MAPUTO CITY

The slope instability problems in Maputo City are caused by a combination of various factors that can be classified into four groups, namely:

- Geomorphological causes;
- Physical and meteorological causes;
- Geological and Geotechnical properties of soils;
- Anthropogenic causes.

Each of these groups have several aspects which will be discussed in detail in the following sections.

#### 7.3.1 – Geomorphological Causes

Topography is one of the main factors controlling slope stability in Maputo City. It is known that the steeper the slope, the greater is the tendency of materials to move downward. The topography also determines the water velocity in the slope, which in turn determines the size and quantity of material transported downward. The topographic difference between the upper and down town (49 m) and the respective slope angle have contributed to slope instability hazards in Maputo City. The slope angle in the most affected areas varies between 20 and 60° which is considerably high. The local 1:50 000 scale geological map of the Maputo area (Momade *et al.* (1996) indicates that the prominent scarp to the north of the city is formed due to recent extensional faulting. The influence of the slope height and the slope angle on the factor of safety will be discussed later in this chapter.

Figure 7.2 shows the distribution of slope angle in Maputo City and the highlighted areas with the prominent slope instability problems in the city. It is possible to observe that the areas heavily affected by slope instability are the ones with the highest slope angle. However, other factors such as the soil characteristics, land use practice and hydrogeological characteristics may have also contributed significantly towards slope instability.

A study by Canda (2007) and Amurane & Vicente (2008) using a GIS approach based on a Digital Elevation Model (DEM) of the ground surface indicates that in the eastern part of Maputo city the groundwater flows to the east towards the Indian Ocean (Figure 7.3). This means that water infiltrated into the ground flows laterally towards the free face of the coastal slope. It is likely that the flow will be greatest in the upper few metres where the sand is in a loose condition rather than downwards where the sand is in a medium dense or dense condition

(Forster, 2001). If this is a correct assumption, then internal erosion can be occurring and concentrated in the upper zone (0 to 10m). Removal of material by internal erosion due to water flow is a possibility for the soils in the study area. The sands have a relatively high porosity and permeability and the silt component may be removed from the intergranular pore spaces.

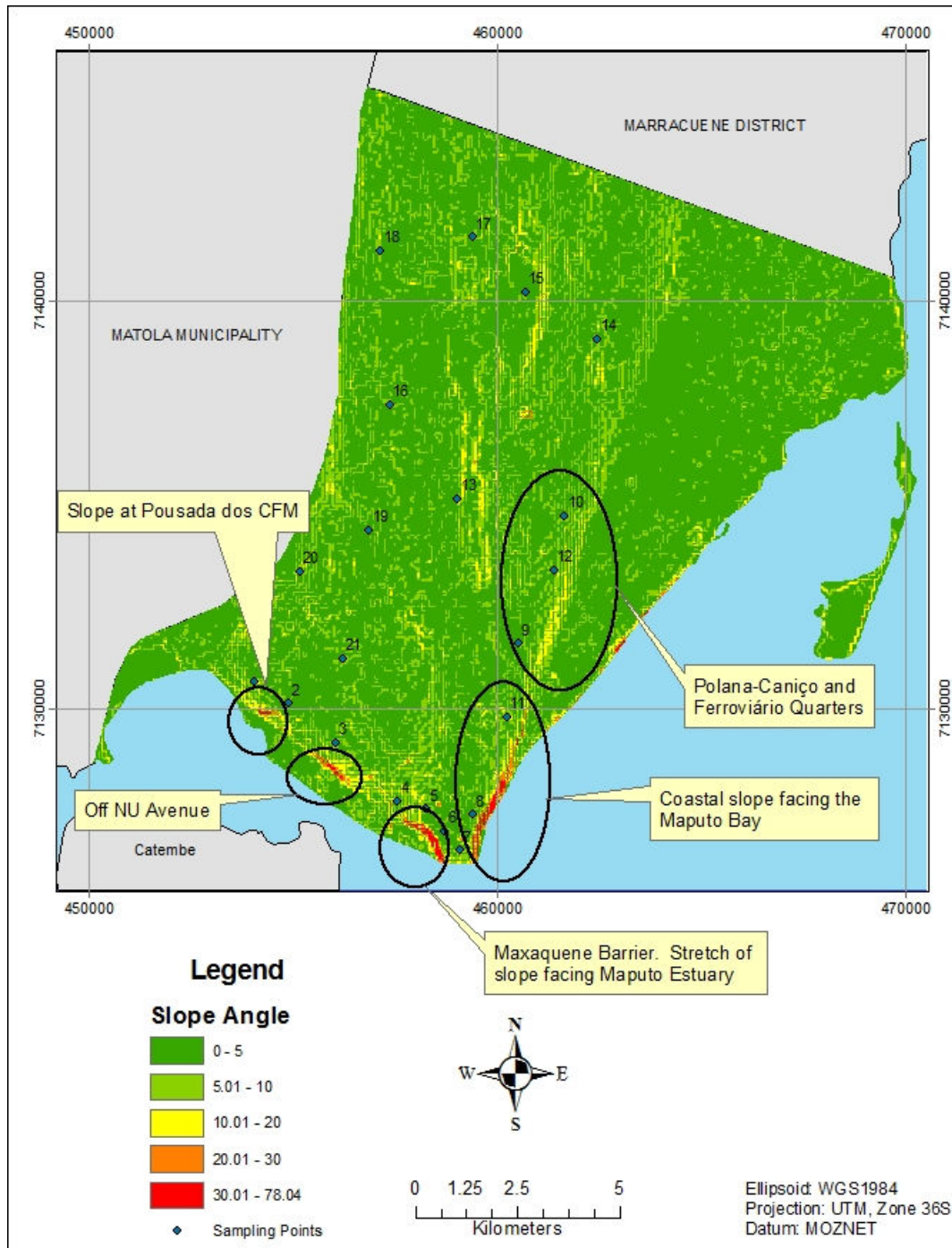


**Figure 7.2** – Distribution of slope angle in Maputo City and the areas with prominent slope instability problems

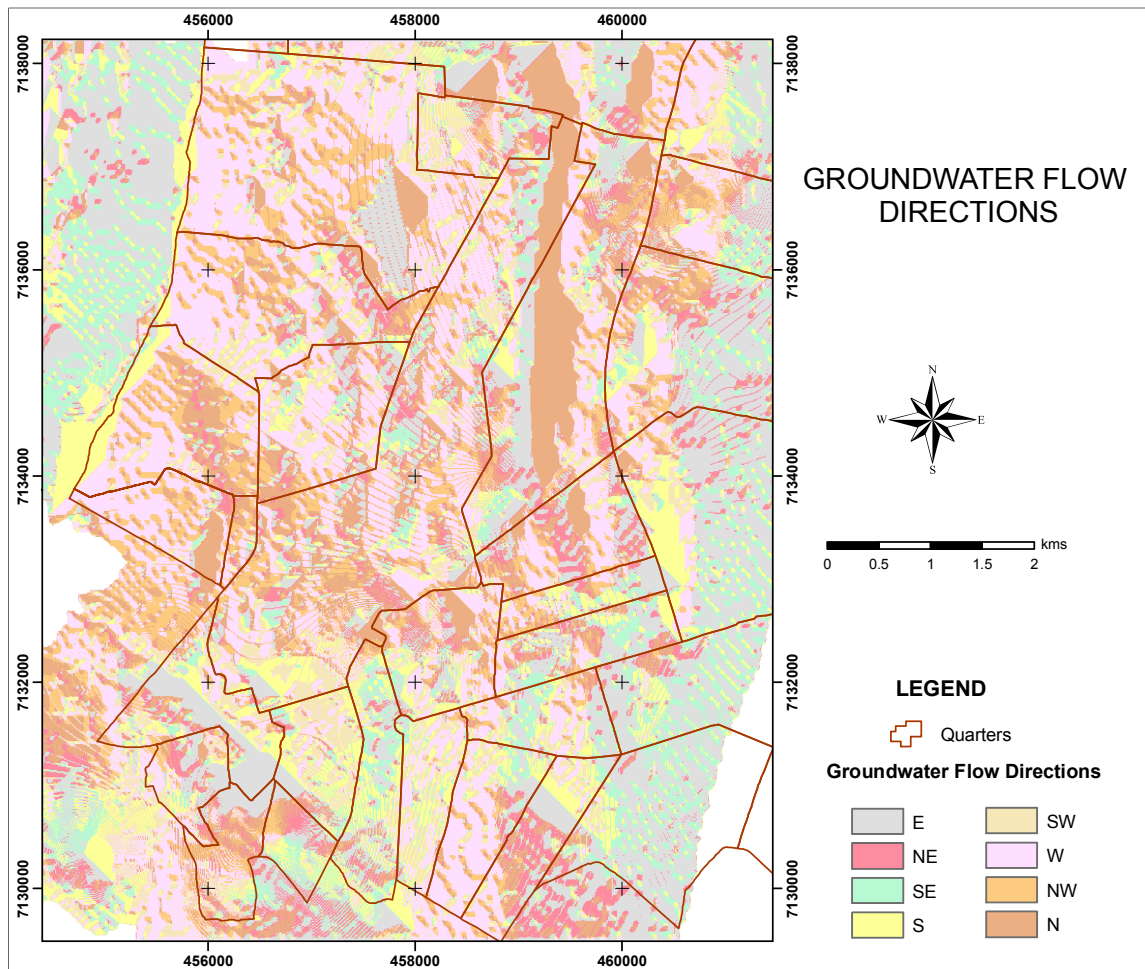


**Figure 7.3** – Groundwater flow directions in Maputo City (From Amurane & Vicente, 2008)

The study from McKnight (2001) indicates that groundwater table elevation varies from 7 to 17m above the median sea level in the area heavily affected by gullies in Polana-Canião. Extrapolating these results to other areas of the Ponta Vermelha Formation, and taking into account the elevation of this geological formation, it is observed that the depth to water table can be as close as 15 m to the surface in some areas. This depth corresponds, in the Polana-Canhão area, to the toe of the slopes where springs are observed which are associated with the gully erosion in this area. The groundwater data will be used to calculate the Factor of Safety.

### 7.3.2 – Physical and Meteorological Causes

The landslide and slope instability hazards in Maputo City are also related to unusual, intense and prolonged rainstorm events such as that which occurred in February 2000 where 400 mm of rainfall was registered in four days. This value constitutes 30% of the mean annual precipitation and is far beyond 132 mm, which is the mean monthly precipitation in the rainy season from



November to March (Manuel & Vicente, 2002). In fact, rainfall is regarded as the cause of the “majority of slope failures and landslides that happened in regions experiencing high seasonal rainfalls” (Huat *et al.*, 2005; Li *et al.*, 2005) because most of them are registered following long-lasting or antecedent heavy rainfall.

Apart from infiltration into the ground, the excess water has resulted in surface runoff in the top section and face of the slopes. Water infiltration, percolation and retention in the soil are of vital importance in slope stability and are largely controlled by the skeletal framework or geometric arrangement of textural particles and aggregates (Bryan, 2000). Infiltration in such extreme rainfall events recharges the aquifer and changes the soil-water balance and consequently the groundwater conditions.

### 7.3.3 – Geological and Geotechnical Properties of Soils

As discussed in Chapter 5, the consistency of the soils in the areas prone to slope instability is very low. The soil like materials of this geological formation (Ponta Vermelha) mainly comprise sand (more than 80%) with a clay content of less than 2%. This sand is normally medium dense-to-loose and granular but locally very loose. The soils are non-plastic which is reflected on low shear strength parameters, mainly cohesion. According to the geology of the area and to the geotechnical characteristics, the soils should allow easy water infiltration to lower layers. However, due to the low cohesion and collapse characteristics, during heavy rainfall water saturates the soils, decreasing soil strength and causing landslides.

A rapid rise in the groundwater table in the slopes may be the triggering factor for landslides to occur due to the weakening of a slope and a decrease in shear strength and effective stress along the potential slip surface on saturation (Simon, 2000; Abramson *et al.*, 2002). Water promotes failure in two ways: as an active agent, it increases the loading (increases bulk unit weight) of soil by filling previously empty pores, and as a passive agent, it decreases the strength of the soil (Coch, 1995). Further causes in loss of stability and shallow slides can be attributed to (a) seepage forces which induced collapse of the partially saturated soil slopes, porous soil mass, and (b) saturation of the soil material from the infiltration of rain water (Wolle, 1985; Lumb, 1975; Rouse, 1990; Mshana *et al.*, 1993; Rao, 1996; Abramson *et al.*, 2002). Common to these factors is water infiltration into the ground which is associated with matric suction. Indeed, the failure mechanism in a rainfall-induced landslide has been described by Li *et al.* (2005) as controlled by the matric suction of the slope.

Matric suction is a pore-water pressure developed by the soil material that induces water to flow

in an unsaturated soil. This pore-water pressure is negative and is a consequence of the shared effect of adsorption and capillarity caused by the soil matrix. The higher matric suction is observed in a dry soil while the lower matric suction occurs on a wet soil. This negative pore-water pressure is fundamental in the safety of unsaturated soil slopes (Fredlund & Rahardjo 1993; Au, 1998). Matric suction at shallow depths drops with rainfall infiltration into the slopes resulting in partial or complete disappearance of shear strength (Li *et al.*, 2005) consequently, a rainfall-induced landslide may occur (Abramson *et al.*, 2002; Li *et al.*, 2005). The failure mechanism is associated to the loss of soil matric suction in the presence of rainwater and possibly from destruction of the bonding agents. For cemented soil slopes the practical difficulty is to avoid the destruction of cementation as the loose structure makes the mass very susceptible to flow (Lee *et al.*, 1983). The effect of water infiltration on soil suction is likely to be influenced by the soil porosity and permeability, the surface cover, the soil type and angle of the soil slopes (Huat *et al.*, 2005). Head loading (construction of buildings at or near the top of a slope) can also contribute to failure.

Although it has been recognized that negative pore-water pressure plays a crucial role in the instability of unsaturated soil slopes, its effect is often ignored in slope stability studies. The negative pore-water pressure is assumed to dissipate with rainfall infiltration, therefore it has been taken out in design considerations (Zhang *et al.*, 2004). However, soil suction can be maintained under certain conditions. A study by Zhang *et al.* (2000) “based on the theory of infiltration and seepage through a saturated–unsaturated soil system”, showed that under stable conditions, the maintenance of matric suction is mostly influenced by the extent of rainfall flux through the coefficient of permeability of soil (expressed as a percentage). The high soil permeability in the slopes in Maputo City allows quick dissipation of matric suction and these conditions are not likely to occur.

#### **7.3.4 – Anthropogenic Causes**

The main identified anthropogenic causes of landslides and slope instability in Maputo City is urbanization. Maputo City registered rapid population growth in the last two decades. The last ten years have registered an overall population rise of 13.7% (INE, 2007) with the consequent increase of land use pressure to which the response capacity was absent or very weak. Housing problems led to informal territorial expansion for residential purposes and consequently environmental problems increased as the informal settlements grew in the suburban and periurban areas of the city. Deficiency of land use planning led to construction in sensitive areas such as steep soil slopes without observing the appropriate building or founding

techniques. The lack of adequate land use and strategic planning is behind most of the engineering geological problems of Maputo City mainly gully and coastal erosion, landslides and slope instability and urban flooding.

During urbanization in the dune sand areas of Maputo city, vegetation is removed and surfaces are paved reducing the infiltration and percolation area. Paving prevents water from sinking into the ground, so a greater volume of water runs off faster over the surface (Coch, 1995) into the sea as the rapid urbanization was not supported with an appropriate drainage system to collect the storm water. These land use changes caused by urbanization increase peak discharge, thus increasing the risk of flash floods and landslides as the water flows through the face of slopes.

The incidence and severity of landslides and slope instability problems was raised particularly in recent years as an increased lack of land has forced rapid urban development in hilly terrain (inherently unstable areas) above the neutral line of slides (construction of buildings at or near the top of a slope). Much of the development in the last decade (new residential areas) was along the slopes, mainly in Polana-Cimento, Sommerchild and Polana-Caniço Quarters, as these are sea facing areas. Loading of slopes has been reported as a cause of landslides. The fact that the tilting buildings be located in the same side of Julius Nyerere Avenue on top of the coastal slope behind Friedrich Engels Avenue exactly at the stretch of road where the coastal slope is at its closest is more than coincidence (Forster, 2001). This may suggest that the proximity of the slope is involved in the cause of movement in some way probably due to the load imposed to the slope by the high rise buildings.

Cultivation of the slopes and removal of vegetation is also a common activity on the outskirts of Maputo City (Figure 7.4). Slope face exposure is a starting point for surface runoff and destabilizes the already fragile slopes.

#### **7.4 – SLOPE STABILITY ANALYSIS AND FACTOR OF SAFETY**

Research has been conducted on deposits comprising dune sands under partially saturated conditions presenting high shear strength when dry, as they appear cemented and stable, and low when wet. Under partially saturated conditions a wide range of soil properties depend on the amount of water retained in the pore space, for example, increased tensile strength of partially saturated granular materials, such as sand, compared to their saturated state (Lechman *et al.*, 2006). This study analyses slope stability and calculates the factor of safety (FS) for the main slopes around Maputo City. The slope stability analyses are carried out to identify risk areas, assess their equilibrium conditions, determination of potential failure mechanisms and the

slope sensitivity to different triggering mechanisms, and the safe, reliable and economic design of both natural and man-made slopes (Abramson *et al.*, 2002; Eberhardt, 2003).



**Figure 7.4** – Slope face exposure as a result of cultivation

The methods used to determine the stability of slopes are based on *limit equilibrium* or *limit state* analyses (Lee *et al.*, 1983; Coduto, 1999). On these methods the slope is evaluated as if it was about to fail and the resulting shear stress along the failure surface is determined. Although the variation on the detailed procedures for the determination of the FS value resulting from different approximations and assumptions used in each method, the calculated FS present only small variations (Lee *et al.*, 1983).

FS is defined as the factor by which the shear strength of the soil slope has to be reduced in order to bring the slope to the state of failure. It is calculated using the ratio between the forces resisting movement by the available forces driving movement. These stresses are compared to determine the FS value:

$$FS = \frac{s}{\tau} \quad \text{Eq. 7.1}$$

Where:

FS = Factor of Safety



$S$  = Shear strength

$\tau$  = Shear stress

The description of slope stability analysis based on FS is also known as *deterministic analysis*. The other approach for stability analysis is the *probabilistic analysis* also based on the statistical analysis but measuring the probability of slope failure (Lee *et al.* 1983, Coduto, 1999) and will be dealt later in this section. As many uncertainties are linked to the determination of FS, a larger value is assumed as a reference to assure safety in the design of infrastructures although any slope with  $FS > 1$  would supposedly be stable. The uncertainties in the stability analysis are linked to the shear strength parameters, soil profile and groundwater conditions in the main. Commonly an FS value of 1.5 is assumed in most design criterion.

The rotational failures observed in the study area allows for a quantitative analysis of the potential for failure. This potential can be expressed as a FS. The slope failure mechanism was investigated using the conventional limit-equilibrium method of analysis through the slope stability software Slide 5.0.

Slide 5.0 by Rocscience, Inc (2003) is slope stability software providing 2D analysis for assessing the stability of circular or non-circular rupture surfaces in soil or rock slopes. Slide 5.0 uses vertical slice limit equilibrium methods to analyze the stability of slip surfaces. Individual slip surfaces can be analysed, and search methods can be applied to locate the likely slip surface in a given slope.

The main features of the software include methods to search the critical surface for circular or non-circular slip both for simple and layered multiple materials slopes based on the anisotropic, non-linear Mohr-Coulomb materials, and other strength models. The features given by Slide 5.0 that will also be important in this study are the probabilistic and sensitivity slope stability analysis. The probabilistic slope stability analysis is a complementary approach to traditional deterministic (safety factor) analyses and gives a valuable insight on the slope stability analysis.

The Slide 5.0 software is composed by three separate programs namely:

- *MODEL (M)* – which is a pre-processing program used to insert and edit the limits of the slope model, the weight, define material and sliding surface and save the inserted data;
- *COMPUTE (C)* – is the compute engine of the of the limit equilibrium
- *INTERPRET (I)* – is the post-processing component used to visualise the analysis

results.

These three programs, *MODEL*, *COMPUTE* and *INTERPRET*, run separately but are completely integrated as illustrated in the Figure 7.5. The *Compute* and *Interpret* can be started from the Model and before the analysis interpretation the file has to be run by *Compute*.

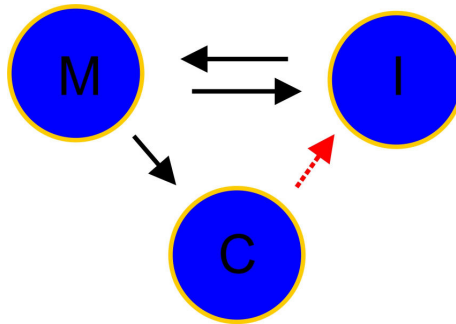


**Figure 7.5** – Interaction of the components of Slide 5.0

Computation and interpretation methods incorporated in SLIDE 5.0 include Bishop, Bishop simplified, Janbu simplified/corrected, Spencer, Corps of Engineers, General Limit Equilibrium (GLE)/Morgenstern-Price, Ordinary/Fellenius and Lowe-Karafiath. The concept behind the procedures for stability analysis is broadly similar for most of these methods. For this study the General Limit Equilibrium (GLE)/Morgenstern-Price analysis method was selected as it uses both the *theory of limit equilibrium of forces and moments to compute the FS*.

For the calculation of FS based on the limit equilibrium methods the following assumptions are assumed:

- The shear strength parameters are characterised by cohesion and friction angle;
- The material of the slopes is homogeneous;
- The failure mechanism is circular;
- The shear strength was estimated based on the Mohr-Coulomb equation.

A number of steps were followed using Slide 5.0:

- the geometry of the slope was drawn using the slope height and slope angle data collected in the field (Table 7.1).
- the material properties (cohesion, angle of internal friction and unit weight) were assigned. Friction angle and cohesion were determined from the residual shear stress.
- the method of analysis, failure surface and failure criteria assumed in the analyses were chosen. Limit-equilibrium analysis was performed using the General Limit Equilibrium (GLE)/Morgenstern-Price method and Mohr-Coulomb failure criteria and

circular failure surfaces were assumed.

- the computer program was allowed to compute and classify the Factor of Safety for a large number of failure surfaces and present the results with the lowest value chosen as the Factor of Safety of the slope.

For the samples 9, 10 and 12 located in Polana-Canico and Ferroviário Quarters heavily cut by gullies, two analyses were performed. As these samples were collected in areas between gullies, one Factor of Safety analysis was done looking at the general natural slope angle of the area and the second over the slope angle created by the adjacent gullies.


**Table 7.1** – Input data for the determination of Factor of Safety with Slide 5.0 and the Factor of Safety of analysed slopes in Maputo City

| Geological Unit | Sample N°. | Elevation sampling (m) | Slope Angle (°) | Slope Height (m) | Unit Weight (KN/m <sup>3</sup> ) | Friction Angle (°) | Cohesion (kN/m <sup>2</sup> ) | Factor of Safety |
|-----------------|------------|------------------------|-----------------|------------------|----------------------------------|--------------------|-------------------------------|------------------|
| QCo             | 1          | 31                     | 20.6            | 12               | 14.91                            | 32.5               | 1.38                          | 1.728            |
|                 | 2          | 28                     | 52.3            | 15               | 19.33                            | 32.00              | 9.86                          | 0.957            |
| TPv             | 3          | 43                     | 36.8            | 32.5             | 13.54                            | 28.50              | 11.14                         | 1.133            |
|                 | 4          | 31                     | 25              | 13.5             | 16.28                            | 31.00              | 5.93                          | 1.793            |
|                 | 5          | 62                     | 56.4            | 47               | 15.70                            | 31.50              | 9.42                          | 0.689            |
|                 | 6          | 58                     | 58.1            | 44               | ND                               | ND                 | ND                            | ND               |
|                 | 7          | 48                     | 59.5            | 39               | ND                               | ND                 | ND                            | ND               |
|                 | 8          | 56                     | 74.01           | 37               | 14.22                            | 32.00              | 5.33                          | 0.461            |
|                 | 9a         | 43                     | 18.1            | 33               | 17.17                            | 31.50              | 2.14                          | 1.565            |
|                 | 9b         | 43                     | 50              | 33               | 17.17                            | 31.50              | 2.14                          | 0.652            |
|                 | 10a        | 34                     | 12              | 31               | 15.50                            | 33.50              | 3.47                          | 2.556            |
|                 | 10b        | 34                     | 62              | 31               | 15.50                            | 33.50              | 3.47                          | 0.572            |
|                 | 11         | 38                     | 31.62           | 30.5             | 15.21                            | 31.00              | 5.71                          | 1.243            |
|                 | 12a        | 34                     | 14.01           | 30               | 15.99                            | 31.50              | 8.57                          | 2.136            |
|                 | 12b        | 34                     | 70              | 30               | 15.99                            | 31.50              | 8.57                          | 0.569            |


a: Data and Factor of Safety analysis looking at the general natural slope angle of the area

b: Data and Factor of Safety analysis looking at the slope angle created by the adjacent gullies

 FS > 1.5

 1.5 > FS > 1

 FS < 1

 FS calculated from adjacent gullies

The FS values obtained in the study area and presented in Table 7.1 vary from 0.461 to 2.556. Analysing these results it is seen that sites 2, 3, 5, 8 and 11 do not show stable slopes as assuming the reference value of 1.5 used in most design criterion. It is also observed that the FS is mainly controlled by the slope angle, i.e., there is a disproportionate relation between the slope angle and the FS, what is not possible to see in relation to friction angle, cohesion and unit weight because they are almost similar in all slopes. The influence of each parameter on the FS is determined through the sensitivity analysis discussed later in this chapter.

Sites 2, 5 and 8 are respectively in the Pousada dos CFM, Maxaquene Barrier and Friedrich Engels Avenue with very high slope angles and materials with similar characteristics. They are

thickly vegetated with tall grass, big trees and shrubs and are apparently stable (possibly due to the presence of Iron oxides which are present in the red ferruginous soils and act as bonding agent). Vertical slopes are quite stable even up to heights of 60 m provided the cementation is not broken down by water seepage (Lee *et al.*, 1983). While this is particularly true for the Pousada dos CFM and Maxaquene Barrier which are stable with no evidence of active movement or any evidence of water seepage on the slope, the slope at Friedrich Engels shows recently active landslides. High angle slump failure, distortions of the drainage system below the retaining wall and destruction of the protection wall in the north side of the promenade were described in Chapter 4 (Section 4.8.3) (Figures 4.16 and 4.17). As described earlier (Section 7.3), water infiltration through a crack opened in the pavement located on top of the slope during heavy rainfall that occurred in February 2000, could have triggered the landslide. The process that followed is described in Section 7.3.

Sites 9, 10, 11 and 12 have FS values indicating that the slopes are stable although located in the gully affected areas of Polana-Caniço and Ferroviário Quarters. As the FS for these areas is high and calculated using only the geological/geotechnical parameters, then failure in this areas must be due to anthropogenic factors related to inappropriate land use planning (Section 7.3). On the contrary, sands in the medium to dense states could form stable slopes provided the slope angle is less than the friction angle but all efforts would have been made to prevent surface erosion and particularly erosion at the toe of the slope where seepage may reduce the FS value (Lee *et al.*, 1983). This was the case in the Polana-Caniço and Ferroviário slope failures, with groundwater rising due to rainfall infiltration, seepage was observed at the toe of the slopes exactly where gullying started.

The FS calculated for Sites 9, 10 and 12 using the slope angles given by the adjacent gullies sidewall is very low (0.569 to 0.652) indicating instability. This proves that the sidewalls of most of the gullies are unstable and suffer continuous erosion in every heavy rainfall event (Figure 6.3). Gully-wall slope angle and height are the main factors controlling gully sidewall failure through tension crack development and wall collapse (Poesen *et al.*, 2002b; Collison, 2001). Figure 7.6 and 7.7 show respectively the geometry and Factor of Safety calculations of the slopes for Site 10 in relation to the general natural slope angle of the area and to the slope angle created by the adjacent gullies. Appendix C presents the geometry and FS calculations of the remaining slopes.

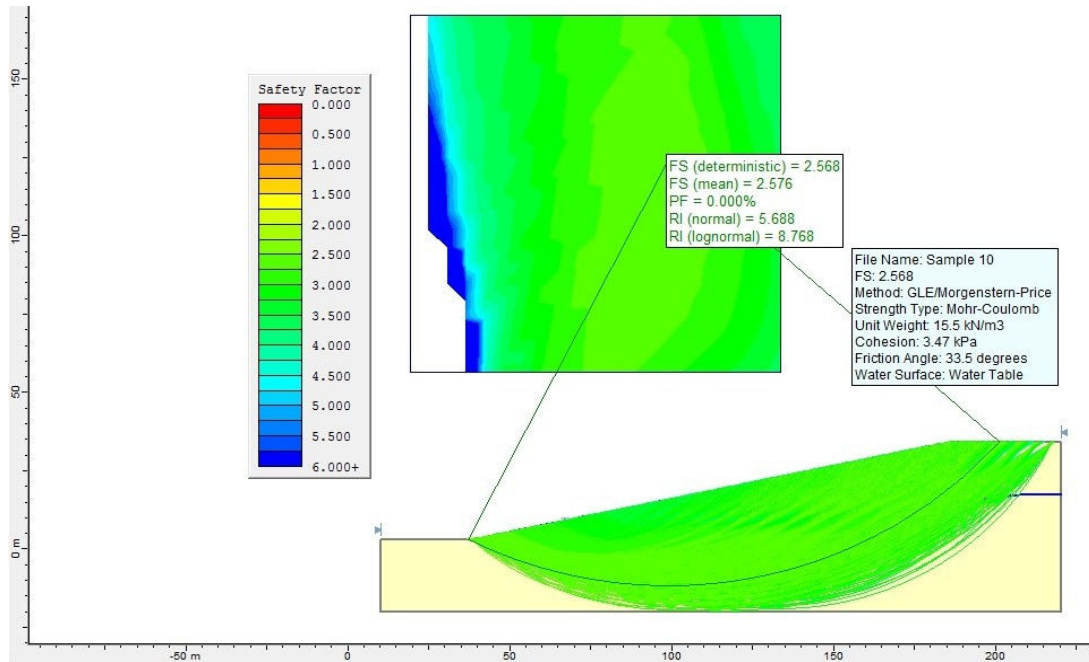


**Figure 7.6** – Geometry and Factor of Safety calculations of the slopes for Site 10 in relation to the general natural slope angle of the area

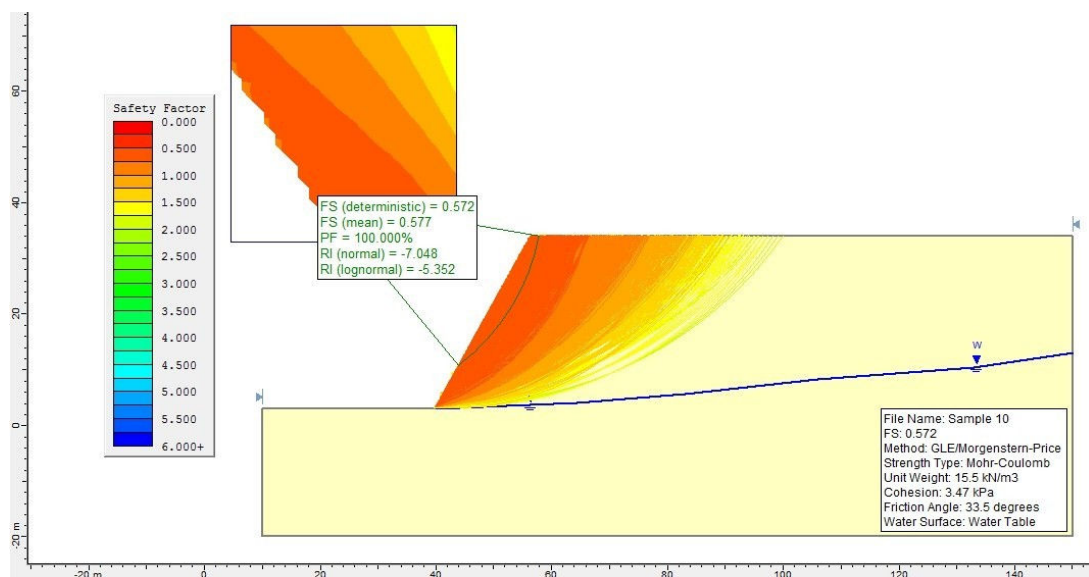


**Figure 7.7** - Geometry and Factor of Safety calculations of the slopes for Site 10 in relation to the slope angle created by the adjacent gullies

## 7.5 PROBABILISTIC ANALYSIS

Probabilistic analysis incorporated in Slide 5.0 determines the probability of failure and the reliability index of the calculations, which are used to better represent the level of safety and improve the slope stability analyses (Rocscience, 2003). The probabilistic analysis based on the *Monte Carlo* and *Latin Hypercube simulation* techniques and the procedure allows the definition of any input parameter as a random variable. To define a random variable the

statistical distribution for an input parameter is specified allowing for the degree of uncertainty in the value of the parameter.

Table 7.2 presents the probability of failure of the studied slopes and the reliability index of the calculated slope stability. The probability of failure is calculated using the ratio between the number of analyses with factor of safety less than 1 and the total number of samples as a percentage (Rocscience, 2003). The results of probability analyses were checked using the Convergence Plot which indicates whether or not the obtained probabilistic analysis is converging to a final answer by converging to a stable, final value. Figure 7.8 shows a convergence plot of the probability analysis for Site 2.

**Table 7.2** – Statistical data of the analysed slopes of Maputo City

| Sample N°. | Factor of Safety | Probability of Failure (%) |          | Reliability Index |                |
|------------|------------------|----------------------------|----------|-------------------|----------------|
|            |                  | FS > 1                     | FS > 1.5 | RI (Normal)       | RI (Lognormal) |
| 1          | 1.728            | 0                          | 10.1     | 3.900             | 5.055          |
| 2          | 0.957            | 69.8                       | 100      | -0.515            | -0.546         |
| 3          | 1.133            | 9.1                        | 100      | 1.323             | 1.368          |
| 4          | 1.793            | 0                          | 3.9      | 4.613             | 6.073          |
| 5          | 0.689            | 100                        | 100      | -4.977            | -4.173         |
| 6          | ND               | ND                         | ND       | ND                | ND             |
| 7          | ND               | ND                         | ND       | ND                | ND             |
| 8          | 0.461            | 100                        | 100      | -12.151           | -8.157         |
| 9a         | 1.565            | 0                          | 33.7     | 3.169             | 3.899          |
| 9b         | 0.652            | 100                        | 100      | -4.589            | -3.764         |
| 10a        | 2.556            | 0                          | 0        | 5.688             | 8.768          |
| 10b        | 0.572            | 100                        | 100      | -7.048            | -5.352         |
| 11         | 1.243            | 2.7                        | 97.9     | 2.001             | 2.187          |
| 12a        | 2.136            | 0                          | 0.1      | 5.119             | 7.281          |
| 12b        | 0.569            | 100                        | 100      | -8.763            | -6.603         |

a: Factor of Safety analysis looking at the general natural slope angle of the area

b: Factor of Safety analysis looking at the slope angle created by the adjacent gullies

FS > 1.5      1.5 > FS > 1      FS < 1      FS calculated from adjacent gullies

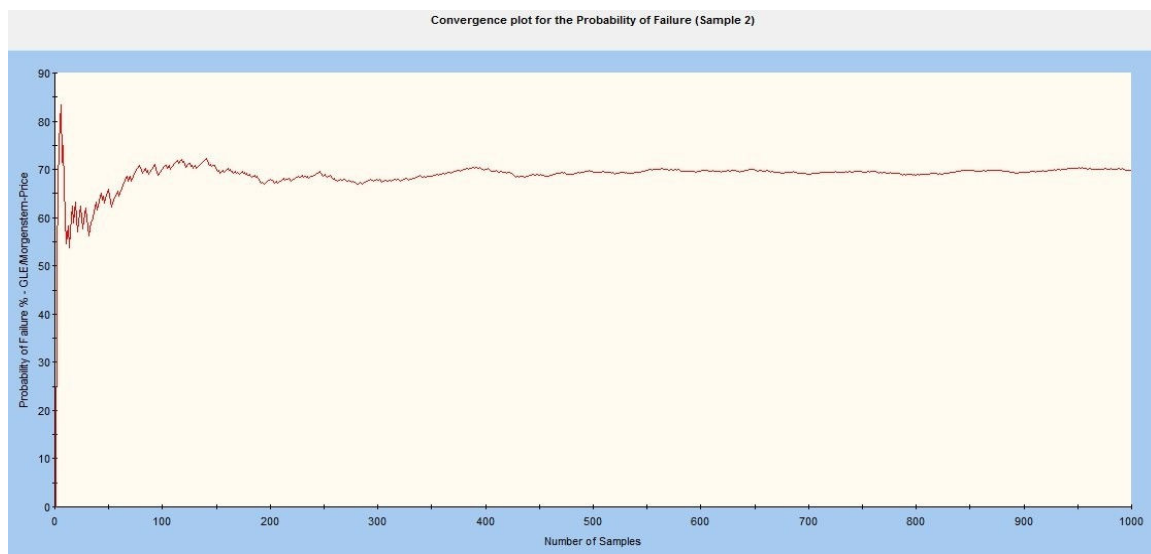


**Figure 7.8** - Convergence plot of the probability of failure analysis for Site 2

Sites 5 and 8 with the lowest Factor of Safety present 100% of probability of failure as well as the slopes given by the gullies sidewall which are also very steep and with low Factor of Safety. Site 2 has also high probability of failure (69.8%) while sites 3 and 11 with FS higher than 1 have low probability of failure.

The probability of failure for the FS = 1.5 was assessed using histograms. For this research the FS = 1.5 was assumed as it is the reference used in most design criterion. The histogram plots allow viewing the distribution of samples created from random variable(s) of the input data and the distribution of FS values calculated by the probabilistic analysis. The histograms show that only Sites 4, 10a and 12a would remain safe for design purpose. Figure 7.9 is a histogram illustrating the probability of failure for the Slope at Site 9a taking 1.5 as reference. The red bars illustrate the analyses with FS less than 1.5. The histograms of the remaining slopes are illustrated in the Appendix C.

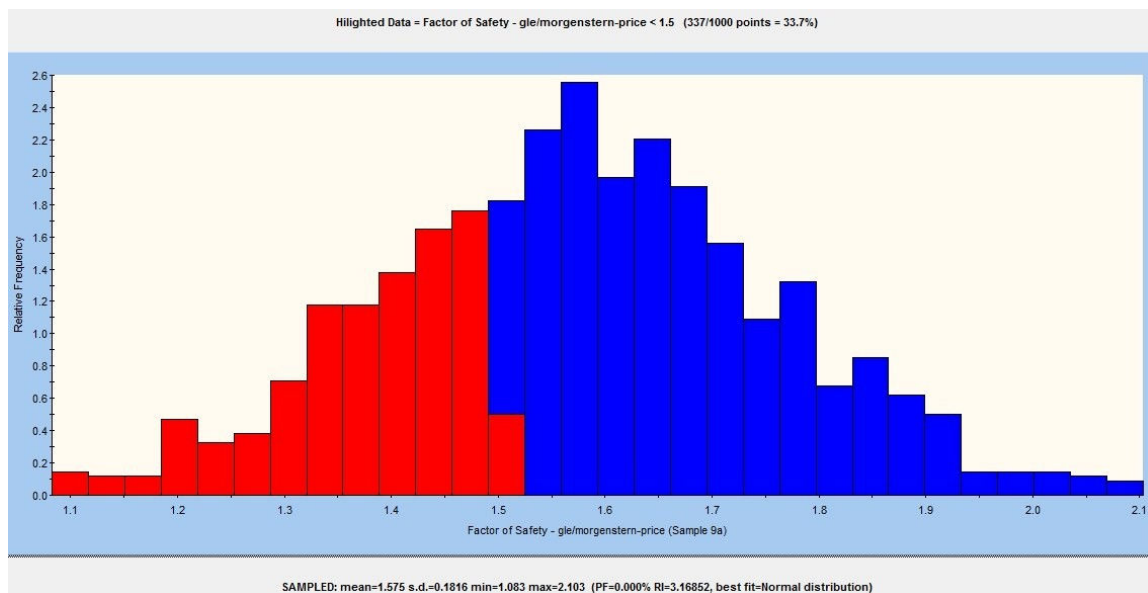


**Figure 7.9** – Histogram illustration the probability of failure for the slope on Site 9a

The Reliability Index (RI) is another parameter used to measure the slope stability. It indicates the *number of standard deviations which separate the mean safety factor from the critical safety factor (= 1)* (Rocscience, 2003). The Info Viewer from the output obtained after the safety factor calculation indicates that the normal distribution best fits the calculation of the RI for the input data.

In order to assure a safe slope design a RI of at least 3 is suggested. The RI values in the study area in concordance with the slope stability results. Only sites 1, 4, 9a, 10a and 12a have a satisfactory level of safety for the slope using the RI.

## 7.6 – SENSIBILITY ANALYSIS

The main purpose of the slope stability investigation is to provide required information to civil engineering practitioners in Maputo, so that they can use it to accommodate project design or apply the necessary corrective measures for slope stabilization to *in situ* ground conditions. Therefore, sensitivity analysis was carried out to widen the range of options to be used when solving slope stability related problems.

The slopes covered in this study occur on two geological formations, the Congolote (site 1 and 2) and Ponta Vermelha Formations (remaining sites). The geological characteristics of these formations are similar and the laboratory results confirm that there are no clear typical geotechnical characteristics differentiating them. Cohesion and friction angle of the tested samples from the slopes in Maputo City show very small differences giving an indication that differences in the FS are influenced by the morphological characteristics of the slopes. Therefore, a sensitivity analysis was performed in relation to cohesion, friction angle and unit weight, geotechnical parameters used in the calculation of the Factor of Safety.

Sensitivity analysis is an interactive process adopted to more realistically simulate slope instability and determine the influence of the different parameters in FS analysis. It indicates the critical and the less important parameters in the assessment of slope stability. Sensitivity analysis in relation to soil relevant shear strength parameters can be particularly important for the cases of instability in Maputo, namely, in places where the best corrective measures have to be the application of soil stabilization techniques. In Figure 7.10, the effect of individual shear strength parameters on the FS is determined by varying uniformly between minimum and maximum values. The graphs of sensitivity analysis of the remaining slopes are in Appendix C.

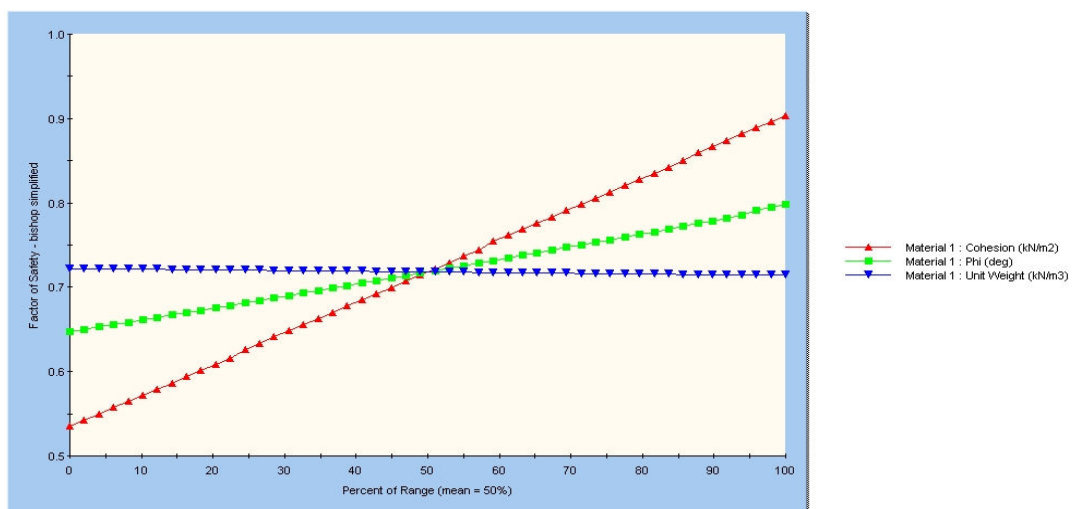


**Figure 7.10**– Typical graph of sensitivity analysis in relation to cohesion, friction angle and unit weight in the slopes of Maputo City



The results show that FS is sensitive to the value of cohesion in 70% of the sites and to the value of friction angle in the other 30% of sites (Vicente, 2006). The FS is not sensitive to the value of unit weight. In addition it can be concluded that the steep curve of cohesion on a sensitivity plot suggests a great effect on FS. Unit weight has a nearly flat curve, indicating that the FS is not sensitive to the value of unit weight, while the friction angle curve is an intermediate curve.

## 7.7 – MEASURES FOR IMPROVING THE STABILITY OF THE SLOPES

The soil slopes in Maputo City are generally in unstable conditions as given by the calculations of safety factor. Measures to improve the stability are required and have to be intrinsically dealt with case by case. These measures were classified into six groups by Abramson *et al.* (2002): unloading, buttressing, structural stabilization, drainage, reinforcement and vegetation.

Most of these measures have already been applied for the stabilisation of slopes in Maputo City, some in an effective manner and others that have been less effective. For the slopes at Sites 2 and 5 respectively in Pousada dos CFM and Maxaquene, no additional improvement measures can be recommended different to the ones already in place, despite the low FS values. They are well vegetated with tall grass, trees and shrubs (Figure 7.11) and are apparently stable with no evidence of active movement or any evidence of water seepage from the slope. At Site 2 vegetation is also combined with a retaining wall at the base of the slope that has shown to be effective in stabilization. The retaining walls are structural elements that maintain adjacent ground surfaces at two different elevations of the ground surface (Coduto, 1999).

The slope at Site 3 at the NU Avenue has a mid-slope contour concave crack with a vertical displacement of 30-40 cm (Figure 7.1). To control this shallow landslide gabion baskets filled with rhyolite have been constructed at the toe of the slope (Figure 7.12). This solution has been taken to control gully erosion at NU Avenue and at Polana-Caniço Quarter. The toe weight is an effective solution to control sliding but the main concern is related to the limited area of the toe that is covered by these gabion baskets. The construction of gabions across the toe of all sliding surfaces would assure a long term solution. The source of instability in this slope was water leakage that also caused the adjacent gully erosion, maintenance of the drainage system for the infrastructures at the crest of the slope (culverts, sewers and water pipes) and surface drainage construction would also assure definitive solution. Surface drainage has been used with relative success in the slope in the front of the Cardoso Hotel (Figure 7.13).

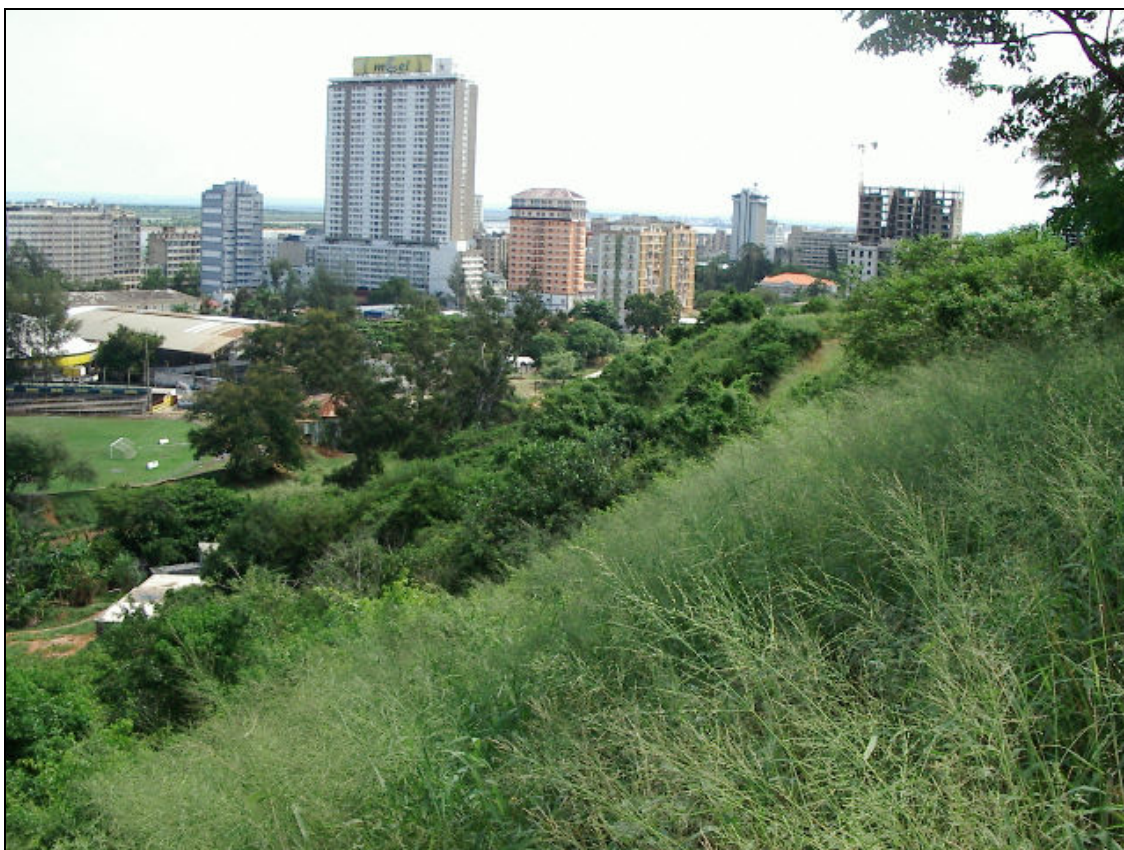


**Figure 7.11** – Lateral view of the Maxaquene Barrier heavily vegetated giving stability to the slope



**Figure 7.12** – Gabion baskets filled with rhyolite constructed at the toe of the slope located at NU Avenue



**Figure 7.13**– Surface slope drainage in front of Cardoso Hotel used with relative success as lack of maintenance limits its usefulness

The slope at Site 8, along Friedrich Engels Avenue, causes most concern due not only to the slope height and angle but also to the dimension of infrastructures at the crest, mainly high rise buildings along the Julius Nyerere Avenue (Figure 7.12). This slope indicates ongoing landslide activity. Apart from vegetation (composed of very thick vegetation with large trees creating cracks in ground into which water infiltrates), the improvement measures undertaken are already obsolete due to lack of maintenance. Several retaining walls were constructed at the slope face and along paths that cross the slope. Figure 7.14 shows the state of some remedial measures taken in the slope of Friedrich Engels.

Measures to improve the stability of the slope at Friedrich Engels Avenue must combine maintenance and reinforcement of the retaining walls, rehabilitation of the drainage system along the Friedrich Engels and Julius Nyerere Avenues because any water leakage in water pipes and underground reservoirs, culverts and sewers could cause an decrease in shear stress in the slopes. It is important to make sure that water flowing at the top of the slope is correctly controlled to avoid rainfall infiltration and excess pore water pressure in the slope. Modifications of the slope profile would not be appropriate for this site because it has permanent infrastructures.





**Figure 7.14**– Some remedial measures undertaken on the slope of Friedrich Engels (Site 8) showing deficiencies of maintenance

The Polana-Caniço and Ferroviário Quarters have the largest area affected by slope instability which is also linked to soil erosion and gullying. The slopes are facing the sea and are therefore very attractive to development. The Municipal Council has plans to rehabilitate these areas by filling up the gullies with sand in parallel with re-zoning of the area to ensure that building standards are adhered to.

The geological/geotechnical conditions should be optimized and modify the slope gradient in order to stabilise the slopes and construct drainage stabilization measures. With this in mind, the factor of safety was modelled in relation to slope angle in order to identify the optimum slope angle for the available geotechnical conditions.

Fortunately, the overall slope angle in the area is such that allows a high safety factor as proved by the analysis 9a, 10a and 12a. The slope angle at Site 11 should be lowered to less than 25°. The major effort to stabilise these slopes should be the construction of an adequate drainage system as seepage is observed at the toe of the slopes. Subsurface horizontal drains would divert the water to a safer place thus preventing rising of groundwater levels.

## **7.8 – SUMMARY AND CONCLUSIONS**

The instability mechanisms observed in Maputo City are predominantly rotational failures with a mass of soil sliding along a curved surface of rupture followed by sand flow as failure occurs in the presence of excess water. This type of curved surface failure is typical for slopes with homogeneous materials as observed in the affected area. The landslides are both shallow and deep-seated. Shallow landslide is observed in the slope in the NU Avenue while deep-seated are observed mainly in Polana-Caniço Quarters. The soil masses formed as part of the slide at the toe end of the rotational slide were subjected to flow soon after failure because of soil liquefaction, as these instability events occurred under extreme rainfall conditions.

Four groups of factors account for the slope instability problems in Maputo City: geomorphological causes, physical and meteorological causes, geological and geotechnical properties of soils, and anthropogenic causes. The interrelationship between these factors has caused landslides to occur. Topography has a significant influence as well as inappropriate land use and slides are triggered by excessive rainfall. The mechanism of failure is mostly due to the loss of matric suction of soils in the presence of rainwater and possibly from destruction of bonding agents. The Factor of Safety as calculated with Slide 5.0 which indicated that the slopes are generally unstable with the control being the slope angle.

Pousada dos CFM and Maxaquene Barrier slopes although presenting low FS are stable showing the efficiency of the stabilization measures in place. In contrast, the slopes in Polana-Caniço and Ferroviário Quarters show high FS values but are the area most affected by slope instability. This is evidence that slope failure in these areas was intrinsically caused by anthropogenic factors related to inappropriate land use planning. The gully sidewalls are unstable as the slope created is very steep. The slope at Friedrich Engels Avenue causes most concern due not only to the slope height and angle but also to the size and number of buildings constructed at the crest, mainly high rise buildings along the Julius Nyerere Avenue, the integrity of which could be threatened by a landslide event (this slope has recently been affected by active landslides).

The probability of failure for the slopes was also investigated and the results are in accordance with the deterministic analysis. The sensitivity analysis indicates that the FS is sensitive to the value of cohesion in 70% of the sites and to the value of friction angle in the other 30% of sites and is not sensitive to the value of unit weight.

Several stabilisation measures are already in place. Some are efficient while others were not

well designed and are thus less effective. In general, the most effective stabilization measure recommended for the unstable slopes of Maputo City is a well designed drainage system.

## CHAPTER 8

### CONCLUSIONS

The geological formations of Maputo City which are mainly unconsolidated materials with soil like properties were described in terms of engineering geological characteristics with relevance to their distribution patterns and spatial trends and related to engineering and construction. Shear strength and consolidation tests gave the standard geotechnical properties of the soils and correlations were made between them and the engineering geological characteristics.

Field soil descriptions showed that the *in-situ* moisture condition of the soils in Maputo City varies from slightly moist to wet being controlled by topography and the soil texture although the influence of the climatic conditions on the sample collection. The very moist samples were found in the Ponta Vermelha Formation which in general has higher fine particles. The soil colour distribution is related to the mineralogical composition of the soils. Soils from the Congolote Formation showed lighter colours, whitish and light grey and brown; Soils from Malhazine Formation are brown to yellowish brown; the Intradune deposits are whitish brown while the Machava Formation is dark brown. The Ponta Vermelha Formation is the only case where colour is also related to iron enrichment that occurred to form ferricrete. The Ponta Vermelha Formation is generally red in colour but shows different tonalities ranging from dark to brownish and whitish (Momade *et al.*, 1996).

In general, soils in Maputo City are in the range of coarse-to very fine-grained sand (71.36 to 96.45%) with low clay (0.08 to 1.52 %) and silt (1.80 to 27.09%) percentage, as shown by the grain-size distribution curves. The Ponta Vermelha Formation is relatively well-graded, compared to other formations, presenting a wide range of grain sizes from gravel to clay. In the remaining geological formations the grain size characteristics remain almost constant through all the tested soils. The high sand content in the study area gives the soil very low plasticity to non plasticity. The liquid limit varies between 9 and 28% with the higher values (20 to 28%) observed in the Ponta Vermelha Formation.

As from the Unified Soil Classification System (USCS) the soils of Maputo City are generally SP-SM (Poorly-graded sand with silt) as they are found in more than 2/3 of the investigated soil samples. Particularities of some sample locations can give rise to small variations on the soil classifications namely SM (Silty sand) and SP (Poorly-graded sand).

The soils of Maputo City are normally consolidated as illustrated by the asymptotic shape of the shear stress vs. horizontal displacement curves derived from the shear box test, with high level of residual strength and an absence of peak. Only 33% of the tested soils presented peak over the residual value in this type of graph denoting dense sand or bonded soils.

The angle of internal friction of the soils of Maputo City varies from 28 to 33.5°. The highest friction angles are observed in the Ponta Vermelha Formation, 31–33.5°, and the lowest are in the Congolote and Malhazine Formations, 28–30°. Soils with high quartz and feldspar content are predicted by Mitchell (1993) to potentially have high friction angle because their quartz component has a friction angle between 21 and 31° when saturated. Cohesion ranges from 0.83 to 11.14 kN/m<sup>2</sup>, with the highest values also in the Ponta Vermelha Formation. As guided by the predominant shape of the shear stress-horizontal displacement curves in the study area, the measured cohesion in the majority of the tested samples is an apparent cohesion found in the very loose normally consolidated sands. True cohesion from overburden pressures, as obtained from the failure envelope, can be assumed as occurring on the soil presenting cementing or bonding between grains and from low effective stress acting on the shear surface. High iron oxide content in the geological formations of Maputo City, mainly in the Ponta Vermelha Formation (red ferruginous sands), acts as bonding agent. The presence of a bonding agent is confirmed by the consolidation tests as explained earlier.

The Coefficient of Compressibility ( $a_v$ ) was calculated for every load increase in the tested soils of Maputo City. It varies from 2.00E-04 to 9.20E-03 m<sup>2</sup>/kN for the lower loads (up to 25 kN/m<sup>2</sup>) and from 4.50E-05 to 1.87E-03 m<sup>2</sup>/kN for the higher loads (from 25 to 400 kN/m<sup>2</sup>). The highest compressibility values are observed in the Ponta Vermelha Formation. The coefficient of volume decrease ( $m_v$ ) at lower loadings varies from 1.27E-01 to 4.63 m<sup>2</sup>/MN and for the higher loads it ranges from 3.01E-02 to 1.07 m<sup>2</sup>/MN. There is no clear trend in the distribution of this coefficient in the study area.

From the consolidation test it was observed that the primary settlement of the tested sandy soils of Maputo City is almost quick and immediate in all samples. The higher porosity and hydraulic conductivity of the sandy soils allow water to drain quickly favouring dissipation of the excess pore water pressures. The coefficient of consolidation ( $C_v$ ) is higher in the slightly



overconsolidated ( $3.73\text{E-}02$  to  $2.2\text{E}01 \text{ m}^2/\text{year}$ ) soils comparing with the normally consolidated ( $3.83\text{E-}02$  to  $5.56 \text{ m}^2/\text{year}$ ). The difference in  $C_v$  values is five times lower in a normally consolidated soil condition. The distribution of this consolidation parameter does not follow a specific pattern over the soil types of Maputo City.

The soil collapse potential as investigated through the physical properties approach showed that the soils of Maputo City comply with 3 of the 5 established criteria of collapse behaviour used in this research. The double consolidation test identified 33.3% of the tested soils in Maputo City as collapsible and the collapse potential at different loadings intervals was calculated. These samples showed considerable reduction of the voids ratio in the saturated test corresponding to the additional vertical strain experienced by the soil which is linked to collapse of the soil structure in the presence of water. The soil compressibility and its significant sensibility to collapse upon wetting makes it to be considered as truly collapsible because it shows full collapse of the soil structure. This can be above 5%, predicted to cause moderate trouble in foundation design.

Bonding of the soil samples is characteristic for 66.7% of the tested soils. The rate of voids ratio reduction in samples tested at NMC is identical to the samples tested saturated and this is disclosed as parallel lines of the  $e/\log \sigma_{v0}'$  curves. Although the initial reduction in terms of voids ratio caused by addition of water, the consolidation rate of the saturated soil continues similar to the one of the soil at natural moisture content. This is explained by the presence of a strong bonding material of soil particles which blocked total destruction of the soil structure with moisture content increase. The presence of bonding material was also disclosed by the higher preconsolidation pressure compared with the corresponding overburden pressure.

The presence and influence of bonding was also detected by comparing the compressibility of two samples at the same voids ratio and water content, one being undisturbed and other completely remoulded. The remoulded samples showed a significantly higher compression than that of the bonded soil. The difference came from the fact that part of the stress applied to the bonded soil was carried by the bonds themselves, as the bonded soil is stiffer than the same soil without bonds. The curves of the remoulded samples were also used to establish the limit between the stable and meta-stable states of the soil and the compression curves of the bonded soils are located in the meta-stable space. This boundary between the stable and meta-stable states combined with the *in situ* void ratio indicates the capacity of the soil to remain in the stable zone when loaded with engineering infrastructures and the extent to which it will contract or dilate during shearing (Vaughan *et al.*, 1988).

Soil erosion in Maputo is the most prominent engineering geological and environmental problem causing concern and occurs mainly as rills and gullies affecting Polana-Caniço and Ferroviário Quarters. The gullies are extremely large, deeply cut, 1 to 15 m deep. Gullies in Ferroviário Quarter are mainly V-Shaped while the ones in the Polana-Caniço are U-Shaped.

A qualitative and quantitative evaluation of the erosion susceptibility was investigated using physical and chemical properties of soils. The assessment of dispersivity using the chemical properties was undertaken in order to assess its workability in the context of the tested soils mainly in the areas most affected by gully erosion.

Crumb test results showed weak correlation with the clay content, and no correlation with silt content, ESP and SAR. Results from this study also indicate very weak correlation between friction angle and plasticity index and no clear trend was observed for the influence of plasticity index on cohesion. These findings indicate that these parameters have no clear influence on the soils erosion susceptibility and give an idea that the disintegration observed, for example, in the crumb test is not simply physico-chemical dispersion process or at least other factors have contributed negatively to the dispersion process to occur. Same conclusions were also found by Walker (1997) and Rienks *et al.* (2000) who have reservation on the consistence of this technique in identifying dispersive soils. Site specific characteristics have largely contributed to the gully erosion in Maputo City. Topography, slope steepness, soil type, lithology, rainfall-runoff erosivity, soil water conditions and land use pattern were discussed and were found to have influence to gully erosion.

Results of the flume erodibility test revealed very little correlation with the chemical properties related to dispersion. The correlation is weak with EC, SAR, ESP and CEC. These findings show that the erosion susceptibility and gully erosion in Maputo City have more relation to the physical processes than to the dispersion related chemical properties of the soils. The physical processes were also accelerated by the land use and topographic setting. The flume test results have weak correlations with the shear strength parameters (cohesion and friction angle). However, the trend indicates that higher the cohesion, the lower is the amount of eroded sediments in the flume and higher the friction angle, the higher is the amount of eroded sediments in the flume.

Dispersive soils are difficult to identify as the boundary between dispersive and non dispersive states varies significantly from one soil to another and no single test has been developed to reliably identify all dispersive soils with absolute certainty. Therefore, a rating system was suggested by Bell & Maud (1994) using a number of tests results, modified later by Bell *et al.*

(1998) and by Bell & Walker (2000). A rating system allows several parameters to be taken into account and their influence on dispersivity weighted according to their importance in the process. A new rating for sandy soils combining the physical and chemical factors of dispersion is proposed in this research. The tests that were found reliable to identify the soil susceptibility to disperse and erode in this study were the flume test, crumb test, TDS/%Na, SAR, ESP. These tests were selected because their results were well correlated. For example, almost all samples that were found dispersive with ESP were also dispersive with TDS vs. %Na chart and SAR. The inclusion of both physical and chemical factors in the rating assessment allows several aspects of dispersivity to be taken into account.

It is proved that each physical and chemical parameter has different influence on the soil dispersion therefore, this rating system assigned high rating values to more reliable tests and lower values to the less reliable. The proposed rating system was applied to the tested soils of Maputo City. Fifteen samples (83% of the rated samples) were classified with intermediate susceptibility to erosion while 3 samples (17%) were assigned as of low susceptibility to erosion. The highest rating cores were obtained by the same samples that shown dispersive behaviour with SAR, ESP and TDS/%Na. This group of samples was of intermediate erodibility in the flume test.

The instability mechanisms observed in Maputo City are predominantly rotational failures with a mass of soil sliding along a curved surface of rupture followed by sand flow as failure occurs in the presence of excess water. This type of curved surface failure is typical for slopes with homogeneous materials like observed in the affected area. The landslides are both shallow and deep-seated. Shallow landslide is observed in the slope in the Nações Unidas Avenue while deep-seated are observed mainly in Polana-Caniço and Ferroviário Quarters. The soil masses formed as part of the slide at the toe end of the rotational slide were subjected to flow soon after failure because of soil liquefaction, as these instability events occurred under extreme rainfall conditions.

Four groups of factors account for the slope instability problems in Maputo City: geomorphological causes, physical and meteorological causes, geological and geotechnical properties of soils, and anthropogenic causes. The interrelationship between these factors has caused landslides to occur. Topography has a significant influence as well as inappropriate land use and slides are triggered by excessive rainfall. The mechanism of failure is mostly due to the loss of matric suction of soils in the presence of rainwater and possibly from destruction of bonding agents. The FS calculated with Slide 5.0 indicated that the slopes are generally

unstable with the control being the slope angle.

Pousada dos CFM and Maxaquene Barrier slopes although presenting low FS are stable showing the efficiency of the stabilization measures in place. In contrast, the slopes in Polana-Canico and Ferroviário Quarters show high FS values but are the area most affected by slope instability. This is evidence that slope failure in these areas was intrinsically caused by anthropogenic factors related to inappropriate land use planning. The gully sidewalls are unstable as the slope created is very steep. The slope at Friedrich Engels Avenue causes most concern due not only to the slope height and angle but also to the size and number of buildings constructed at the crest, mainly high rise buildings along the Julius Nyerere Avenue, the integrity of which could be threatened by a landslide event (this slope has recently been affected by active landslides).

The probability of failure for the slopes was also investigated and the results are in accordance with the deterministic analysis. The sensitivity analysis indicates that the FS is sensitive to the value of cohesion in 70% of the sites and to the value of friction angle in the other 30% of sites and is not sensitive to the value of unit weight.

Several stabilisation measures are already in place. Some are efficient while others were not well designed and are thus less effective. In general, the most effective stabilization measure recommended for the unstable slopes of Maputo City is a well designed drainage system.

## REFERENCES

- Aarninkhof, S. G. J., Turner, I. L., Dronkers, T. D. T., Caljouw, M., Nipius, L. (2003). A Video-based Technique for Mapping Intertidal Beach Bathymetry. *Coastal Engineering*, Vol. 49, pp. 275-289.
- Abdel-Aal, F.M. (1999). Beach Evolution and Protection. In: Fabbri, P. (ed) *Coastlines of the Mediterranean. American Society of Civil Engineers, USA.*, 22-34.
- Abel, L. S. 1996. Geotechnical Reconnaissance Over the Site for the Expansion of the Building of Parliament. Engineering Laboratory of Mozambique. Report N° 20.948 (in Portuguese).
- Abegunde, A. A.; Adeyinka, S. A.; Olawuni, P. O. & Oluodo, O. A. (2006). An Assessment of the Socio Economic Impacts of Soil Erosion in South-Eastern Nigeria. Proceedings of the XXIII FIG Congress, Munich, 15 p.
- Abramson, L. W., Lee, T. S., Sharma, S. & Boyce, G. M. (2002). Slope Stability and Stabilization Methods. 2<sup>nd</sup> edition, 712 p. New York: John Wiley & Sons.
- Achimo, M., Mugabe, J. A., Cuamba, F. M. and Haldorsen, S. (2004). Late Weichselian to Holocene Evolution of the Maputo Bay, Mozambique. In: Mussa A., Haldorsen, S. & Momade F. J. (eds), *The impact of sea-level change: Past – Present – Future. Proceedings of the INQUA – Commission on the Holocene workshop in Inhaca, Mozambique November 4-8, 2002. Bulletin of the Geological Survey of Mozambique 43*, pp. 27-38.
- Afonso, R. S., Marques, J. M. & Ferrara, M.(1998). The Geological Evolution of Mozambique. Maputo: National Directorate of Geology.
- Amurane, D. P. & Vicente, E. M. (2008). GIS-Based Determination of Groundwater Flow Patterns and Groundwater Quality Analysis in Maputo City: A Key to Identify Waterborne Diseases Prone Areas. Proceedings of the International Disaster Reduction Conference. Davos.
- Anbalagan, R. & Singh, B. (1996). Landslide Hazard and Risk Assessment Mapping of Mountainous Terrains: A Case Study From Kumaun Himalaya, India. *Engineering Geology*. Vol. 43, pp. 237-246.
- Annandale, G. W. (1995). Erodibility. *Journal of Hydraulic Research*. Vol. 33, N 4, pp 471-494.
- Archibold, O.W., Levesque, L.M.J., de Boer, D.H., Aitken, A.E., Delanoy, L. (2003). Gully Retreat in a Semi Urban Catchment in Saskatoon, Saskatchewan. *Applied Geography*, Vol. 23 (4), pp. 261– 279.

- Arulanandan, K. & Heinzen, R. T. (1977). Factors Influencing Erosion in Dispersive Clays and Methods of Identification. *Publication I.A.H.A* (International Association of Hydrological Sciences), Vol. 122, pp. 75–81.
- Arulanandan, K., and Perry, E. B. (1983). Erosion in Relation to Filter Design Criteria in Earth Dams. *J. Geotech. Eng.*, 109 (5), 682–698.
- Assouline, S. & Ben-Hur, M. (2006). Effects of Rainfall Intensity and Slope Gradient on the Dynamics of Interrill Erosion During Soil Surface Sealing. *Catena*, Vol. 66, pp. 211 – 220.
- ASTM 1979. *Standard Method for Direct Shear Test of Soils Under Consolidated Drained Conditions, Test Designation D 3080*, American Society for Testing and Materials, Philadelphia.
- Au, S.W.C. (1998). Rain-induced slope instability in Hong Kong. *Engineering Geology*. Vol. 51, pp. 1–36.
- Aysen, A. 2002. Soil Mechanics: Basic Concepts and Engineering Applications. Taylor & Francis, 468 p.
- Bara, J. P. (1976). Collapsible Soils. Presentation on the ASCE Annual Convention and Exposition, Philadelphia.
- Barradas, L. (1962). Esboço Agrológico do Sul de Moçambique. Serviços Agro Florestas, Investigação Científica de Moçambique, II.º Plano de Fomento, Lourenço Marques.
- Barata, A., Teles, M., Silva, R. P. (2001). Sistemas de Modelos Matemáticos Para a Gestão Integrada da Baía de Maputo. Iº Congresso Sobre Planeamento e Gestão das Zonas Costeiras dos Países de Expressão Portuguesa. 12 pp.
- Barden, L., McGown, A. & Collins, K. (1973). The Collapse Mechanism in Partly Saturated Soil. *Engineering Geology*. Amsterdam, The Netherlands, pp. 40-60.
- Bates, R. L. & Jackson, J. A. (1980). Glossary of Geology. 2nd ed. American Geological Institute, Falls Church Virginia, 751 p.
- Beckedahl, H. R. (1996). Subsurface Soil Erosion Phenomena in Transkei and Southern KwaZulu-Natal, South Africa. PhD Thesis, University of Natal. Pietermaritzburg, South Africa, 224 pp.
- Beernaert, F. (1987). Geomorphological-pedological Investigation of the Manangas in Southern Mozambique. PhD Thesis, University of Ghent, Belgium.
- Bell, F. G & Maud, R. R. (1994). Dispersive Soils: A Review from a South African Perspective. *Quarterly Journal of Engineering Geology*. Vol. 27, pp. 195-210.
- Bell, F. G. & Walker, D. J. H. (2000). A Further Examination of the Nature of Dispersive Soil in Natal, South Africa. *Quarterly Journal of Engineering Geology and Hydrogeology*.

- Vol. 33, pp. 187-199.
- Bell, F. G. (2000). Engineering Properties of Soils and Rocks. 4<sup>th</sup> Ed. illustrated, 482 p, Wiley-Blackwell.
  - Bennett, M. R. & Doyle, P. (1997). Environmental Geology: Geology and the Human Environment. Wiley 512 pp.
  - Berkey, C. P. (1939). Geology in Engineering. *Frontiers in Geology*, 31-34.
  - Birkeland, P. W. (1999). Soils and Geomorphology. 3<sup>rd</sup> Edition. New York: Oxford University Press, 430 p.
  - Bishop, A.W., 1955. The use of the slip circle in the stability analysis of slopes. *Geotechnique*, **5**, 7 – 17.
  - Boon kong, T., and Komoo, I. (1990). Urban Geology: Case Study of Kuala Lumpur, Malaysia. *Engineering Geology*, 28, 71-94.
  - Bradford, J. M., Ferris, J. E. & Remley, P. A. (1987). Interrill Soil Erosion Processes: I. Effect of Surface Sealing on Infiltration, Runoff, and Soil Splash Detachment. *Soil Sci Soc Am J*. Vol. 51, pp. 1566-1571.
  - Braja, M. D. (2006). Principles of Geotechnical Engineering. 6<sup>th</sup> Ed., Thomson, 686 p.
  - Brink, A. B. A & Bruin, R.M.H. (2002). Guidelines for Soil and Rock Logging in South Africa, 2<sup>nd</sup> Impression 2002. *Proceedings, Geoterminology Workshop organised by AEG, SAICE and SAIEG*, 1990, 45 p.
  - Brink, A. B. A., Partridge, T. C. & Williams, A. A. B. (1982). Soil Survey for Engineering: Monographs on Soil and Resources Survey. 378 pp, Oxford, Clarendon Press.
  - Brink, A.B.A., Partridge, T.C., & Williams, A.A.B., (1984). Soil Survey for Engineering: London, Oxford Science Publications, 364 p.
  - Bryan, R. B. (2000). Soil Erodibility and Processes of Water Erosion on Hillslope. *Geomorphology*, Vol. 32, pp. 385–415.
  - Bryan, R. B. (2004). Gully-Scale Implications of Rill Network and Confluence Processes. In: Li, Y., Poesen, J., Valentin, C. (Eds.), Gully Erosion Under Global Change. Sichuan Science and Technology Press, Chengdu, China, pp. 73–95.
  - Bryan, R. B.; Govers, G. & Poesen, J. (1989). The Concept of Soil Erodibility and Some Problems of Assessment and Application. *Catena*, Vol. 16, pp. 393-412.
  - BSI 1975. Methods of Testing Soils for Civil Engineering Purposes, BS 1377. British Standards Institute, London.
  - Camberato, J. J. (2001). Cation Exchange Capacity – Everything You Want to Know and Much More.

<http://virtual.clemson.edu/groups/turfornamental/tmi/fertlime/Cation%20exchange%20capacity.pdf> (Accessed 23 May 2009).

- Canda, E. S. (2007). Determinação da Influência do Fluxo da Água Subterrânea na Qualidade de Água da Cidade de Maputo. Licenciatura Dissertation, Eduardo Mondlane University, 79 p., Maputo.
- Canhanga, S. & Dias, J. M. (2005). Tidal Characteristics of Maputo Bay, Mozambique. *Journal of Marine Systems*. Vol. 58, pp. 83–97.
- Carey, B. (2006). Gully Erosion. Report Number QNRM05374. Queensland Government. The State of Queensland (Department of Natural Resources and Water). 4 p.
- Carman, P. C. ~1938!. “The determination of the specific surface of powders.” *J. Soc. Chem. Ind. Trans.*, 57, 225.
- Carman, P. C. ~1956!. Flow of gases through porous media, Butterworths Scientific Publications, London.
- Carrier, W. D. (2003). Goodbye, Hazen; Hello, Kozeny-Carman. *Journal of Geotechnical and Geoenvironmental Engineering*, Vol. 129, No. 11, pp. 1054–1056.
- Charlier, R.H. (2003). Hold the Sea Back – Is it Sustainable? Retrospective and Projection. *Journal of Coastal Research*, Vol. 19, pp. 875–883.
- Chmelová, R. & Šarapatka, B. (2002). Soil Erosion by Water: Contemporary Research Methods and Their Use. *Geographica*, Vol. 37, pp. 23-30.
- Chutumiá, I. I., (1987). Estudo de Águas Subterrâneas do Grande Maputo. Trabalho de Licenciatura. Universidade Eduardo Mondlane, Maputo.
- Clemence, S. P. & Finbarr, A. O. (1981). Design Considerations for Collapsible Soils. *Journal of the Geotechnical Division*, American Society of Civil Engineers, Vol. 107, No. GT3, March 1981, pp. 305-317.
- Coch, N. (1995). Geohazards: Natural and Human. Prentice Hall, New Jersey, 481 p.
- Coduto, D. P. (1999). Geotechnical Engineering: Principles and Practices. Prentice Hall, London, 759 p.
- Collison, A.J.C. (2001). The Cycle of Instability: Stress Release and Fissure Flow as Controls on Gully Head Retreat. *Hydrological Processes*. Vol. 15, pp. 3–12.
- Colosio, F., Abbiati, M. & Airolidi, L. (2007). Effects of Beach Nourishment on Sediments and Benthic Assemblages. *Marine Pollution Bulletin*, Vol. 54, pp. 1197–1206.
- Cooke, R. U. & Doornkamp (1990). Geomorphology in Environmental Management: A New Introduction. 2<sup>nd</sup> Ed. Claredon Press, Oxford, 410p.
- Cruden, D. M. & Varnes, D. J. (1996). Landslide Types and Processes (Chapter 3). In: Turner, A. K. & Shuster, R. L. (eds). Landslides: Investigation and Mitigation. National



- Research Council, Transportation Research Board, Special Report 247, National Academy of Sciences, Washington, pp. 36–75.
- Dahal, R. K. (2006). *Geology for Technical Students: A Text Book for Bachelor Level Students*. Brikuti Academic, Kathmandu, 748 p.
  - Davison, L. & Springman, S. (2000). *Soil Description and Classification*. University of the West of England. Bristol. Based on Atkinson, J. GeotechniCAL Reference Package. City University, London. URL: <http://www.uwe.ac.uk/geoal/geocal.htm>, on 22<sup>nd</sup>, October, 2008.
  - De Boer, W. F., Rydberg, L. & Saide, V. (2000). Tides, Tidal Currents and Their Effects on the Intertidal Ecosystem of the Southern Bay, Inhaca Island, Mozambique. *Hydrobiologia*. Vol. 428, Issue 1-3, pp. 187-196.
  - De Pippo, T., Donadio, C., Pennetta, M., Petrosino, C., Terlizzi, F. & Valente, A. (2007). Coastal Hazard Assessment and Mapping in Northern Campania, Italy. *Geomorphology*, doi: 10.1016/j.geomorph.2007.08.015.
  - Denisov, N. Y. (1951). *The Engineering Properties of Loess and Loess Loams*, Gosstroilzdat, Moscow, 136 p.
  - Dimande, A. A., Vicente, E. M. & Manuel, I. R. (2001). Geochemical Characterization of Groundwater from the Mavalane and Maxaquene Quarters, Maputo City, Mozambique. In: *Proceedings of 7<sup>th</sup> Geochemistry Congress of CPLP, Faro*, 740-742 (in Portuguese).
  - Doerge, T. (2001). Fitting Soil Electrical Conductivity Measurements into the Precision Farming Toolbox. Proceedings of the Wisconsin Fertilizer, Aglime and Pest Management Conference. Madison, WI, January 16-18.
  - Dolen, T. P., Fetzner, C. A., Jansen, R. B., Knodel, P. C., Schrader, E. K. & Timblin Jr., L. O. (1988) Materials. In Jansen, R. B. (Ed) (1988). *Advanced Dam Engineering for Design, Construction and Rehabilitation*. Springer, 811 p.
  - Duiker, S. W. (2009). Soil Management. In: (Ed.) Hall, M. H. (2009). *Crop and Soil Management (Part One) of The Penn State Agronomy Guide*. Penn State Univ. University Park. Pennsylvania.
  - EB (2009). Encyclopædia Britannica. Encyclopædia Britannica Online. <http://www.britannica.com/EBchecked/topic/708396/streambank-erosion> (Accessed 11 May 2009).
  - Eberhardt, E. (2003). *Rock Slope Stability Analysis: Utilization of Advanced Numerical Techniques*. Vancouver, Canada: Earth and Ocean Sciences, University of British Columbia. <http://www.eos.ubc.ca/personal/erik/e-papers/EE-SlopeStabilityAnalysis.pdf> (Accessed 30 October 2009)

- Ehsani, R. & Sullivan, M. (2002). Soil Electrical Conductivity (EC) Sensors. Ohio State University Fact Sheet AEX-565-02. <http://ohioline.osu.edu/aex-fact/pdf/0565.pdf> (Accessed 4 June 2009)
- Elges, H. F. W. K. (1985). Dispersive Soils. *The Civil Engineer in South Africa*. Transactions of SAICE, Vol. 27, No. 7, pp. 347-353.
- El-Ruwaih, I. A. & Touma, F. T. (1986). Assessment of the Engineering Properties of Some Collapsible Soils in Saudi Arabia. Proc. 5<sup>th</sup> Int. IAEG Cong. Theme 3.1.5, pp 685-693.
- Elsen, E.; Hessel, R. & Liu, B. (2003). Discharge and Sediment Measurements at the Outlet of a Watershed on the Loess Plateau of China. *Catena*, Vol. 54, pp. 147–160.
- Esteves, M., Descroix, L., Mathys, N. & Lapetite, J.M. (2005). Soil hydraulic properties in a marly gully catchment (Draix, France). *Catena*, Vol. 63, pp. 282– 298.
- Faria, J. M. R. & Gonçalves, C. A. (1968). Cartas das Isopletas dos valores Climáticos e da Classificação de Köppen em Moçambique. INAM, Maputo, 22 pp.
- Fedá, J. (1966). Structural stability of subsidant loess soil from Praha-Dejvice. *Engineering Geology*, Vol. 1(3), pp.201-219.
- Fedá, J. (1988). Collapse of Loess Upon Wetting. *Engineering Geology*, Vol. 25, pp. 263-269.
- Ferreira & Teixeira (1989). Collapsible Soil: A Practical Case in Construction (Pernambuco, Brazil). Proc. International Conference on Soil Mechanics and Foundation Engineering, Vol. 1, pp. 603-606.
- Fookes, P.G. (ed.) (1997). Tropical Residual Soils, Geological Society Professional Handbooks: London, The Geological Society of London, 184 p..
- Forster, A. (2001). An Investigation of Slope Instability and Building Damage in Maputo, Mozambique. British Geological Survey. Report CR/01/091.
- Fredlund, D. G. & Rahardjo, H. (1993). Soil Mechanics for Unsaturated Soils. Wiley-IEEE, New York, 517 p.
- French, P.W. (1997). Coastal and Estuarine Management. Routledge, London.
- Fu, B. & Gulinck, H. (1994). Land Evaluation in an Area of Severe Erosion: The Loess Plateau of China. *Land Degradation and Development*, Vol. 5, pp. 33–40.
- Futai, M. M., (1999). Comportamento Colapsável De Solos Tropicais Brasileiros. Proceedings of the 7th Congresso Nacional de Geotecnia, Vol. 1. Porto, pp. 193-201. (in Portuguese)
- Gerber, F.A. & Harmse, H. J. Von M. (1987). Proposed Procedure for Identification of Dispersive Soils by Chemical Testing. *The Civil Engineer in South Africa*. Transactions

- SAICE, Vol. 29, pp. 397–399.
- GESAMP (1994). Anthropogenic Influences on Sediment Discharge to the Coastal Zone and Environmental Consequences. UNESCO-TOC, Paris.
  - Gibbs, H. J. & Bara, J. P. (1962). Predicting Surface Subsidence From Basic Soil Tests. Special Technical Publication No. 322, ASTM, pp. 231-247.
  - GTK Consortium (2006). Map Explanation; Volume 1: Sheets 2032 – 2632. Geology of Degree Sheets, Espungabera/Chibabava, Nova/Mambone, Massangena, Chidoco, Save/Bazaruto, Chicualacuala, Machaila, Chigubo, Mabote/Vilanculos, Rio Singuédzi/Massingir, Rio Changana, Funhalouro/Inhambane, Chilembene, Chókwè, Zavala/Inharrime, Maputo, Xai-Xai/Zavala and Bela-Vista, Mozambique. *Ministério dos Recursos Minerais, Direcção Nacional de Geologia*, Maputo. 341 p.
  - GSEG (Geological Society Engineering Group Working Party) (1990). Tropical Residual Soils. *The Quarterly Journal of Engineering Geology*. Vol **23**, pp 1-101.
  - Guanglu L.; Klik, A., Wu, F. (2004). Gully Erosion Features and Its Causes of Formation on the (Yuan) Land in The Loess Plateau, China. In: Li, Y., Poesen, J., Valentin, C. (Eds.), *Gully Erosion Under Global Change*. Sichuan Science and Technology Press, Chengdu, China, pp. 131– 142.
  - Guerreiro, J., Freitas, S., Pereira, J., Paula, J., Macia, A. (1996). Sediment Macro-benthos of Mangrove Flats at Inhaca Island, Mozambique. *Cahiers de Biologie Marine*. Vol. 37, pp. 309–327.
  - Guillén, J., Stive, M. J. F. & Capobianco, M. (1999). Shoreline Evolution of the Holland Coast on a Decadal Scale. *Earth Surface Processes and Landforms*, Vol. 24, pp. 517-536.
  - Handy, R. L. (1973). Collapsible Loess in Iowa. *Proc. Soil. Sci. Soc. Amer.* Vol. 37(2). Pp. 281-284.
  - Harmse, H. J. Von M. (1980). Dispersive Soil and Their Origin, Identification and Stabilization. *Ground Profile*. Vol. 22, pp. 10-33.
  - Hazen, A. ~1892!. “Some Physical Properties Of Sands And Gravels, With Special Reference To Their Use In Filtration.” 24th Annual Rep., Massachusetts State Board of Health, Pub. Doc. No. 34, 539–556.
  - Head, K. H. (1984). *Manual of Soil Laboratory Testing: Soil Classification and Compaction Tests*. Vol. 1, pp. 1-339. Pentech Press: London,
  - Head, K. H. (1986). *Manual of Soil Laboratory Testing: Effective Stress Tests*. Vol. 3, pp. 743-1238. Pentech Press: London,
  - Head, K. H. (1988). *Manual of Soil Laboratory Testing: Permeability, Shear Strength and Compressibility Tests*. Vol. 2, pp. 335-747. Pentech Press: London,
  - Holtz, R. D. & Kovacs, W. D. (1981). *An Introduction to Geotechnical Engineering*.

- Prentice-Hall, 448 p.
- Houston, S. L., Houston, W. N., Zapata, C. E. & Lawrence, C. (2001). Geotechnical Engineering Practice for Collapsible Soils. *Geotechnical and Geological Engineering*, Vol. 19, pp. 333-355.
  - Huat, B. B. K., Mariappan, S. & Ali, F. Hj. (2005). Effect of Surface Cover on Water Infiltration Rate and Stability of Cut Slope in Residual Soils. <http://www.ejge.com/2005/Ppr0614/Ppr0614.htm>. (Accessed 6 February 2008).
  - INAM (2009). Climatic Data from 1974-2006. Courtesy of the National Institute of Meteorology.
  - INE (2007). III Censo Geral da População e Habitação: Resultados Definitivos de Cidade de Maputo. <http://www.ine.gov.mz/censo2007/rdcenso09/mc11/mcpop/q1>. (Accessed 28 November 2009)
  - Ismail, F., Mohamed, Z. & Mukri, M. (2008). A Study on the Mechanism of Internal Erosion Resistance to Soil Slope Instability. *Electronic Journal of Geotechnical Engineering*, Vol. 13, 12 pp.
  - IWACO B. V. 1986. Ground Water to Supply Maputo: Annex 1. Mozambican National Directorate of Water.
  - Jenkins, P. (1986). Estudo da Situação Habitacional da Cidade de Maputo — Variação do Stock Habitacional nos Anos 1980–85. Gabinete de Programas de Habitação, Ministerio de Construção e Aguas, Maputo.
  - Jenkins, P. (1999). *Housing and land markets in Maputo city*. Edinburgh College of Art/Heriot-Watt University, School of Planning & Housing, Edinburgh, Research Paper No. 72.
  - Jenkins, P. (2000). City profile: Maputo. *Cities*, Vol. 17, No. 3, pp. 207–218.
  - Jennings, J. E. & Knight, K. (1957). The additional Settlement of Foundations Due to Collapse of Sandy Soils on Wetting. *Proceedings Fourth International Conference on Soil Mechanics and Foundation Engineering*. Vol. 1, pp. 316-319.
  - Jennings, J. E. & Knight, K. (1975). A Guide to Construction on or With Materials Exhibiting Additional Settlement Due to Collapse of Grain Structure. *Proc. 6<sup>th</sup> Regional Conference for Africa on Soil Mechanics and Foundation Engineering*, pp. 99-105.
  - Jennings, J. E., Brink, A. B. A. & Williams, A. A. B. (1973). Revised Guide to Soil Profiling for Civil Engineering Purposes in Southern Africa. *Trans. S. Afr. Instn Civ. Engrs*, Vol. 15, pp. 3-12.
  - Kairu, K. & Nyandwi, N. (eds) (2000). Guidelines for the Study of Shoreline Change in the Western Indian Ocean Region. *IOC Manuals and Guides No. 40*. UNESCO. 55 pp.

- Kalk, M. (1995). A Natural History Of Inhaca Island, Mozambique. Third Edition. Witwatersrand University Press. Johannesburg. South Africa.
- Kassif, G., Henkin, E. N. (1967). Engineering and Physico-Chemical Properties Affecting Piping Failure of Loess Dams in the Negeve. Proc. 3<sup>th</sup> Asian Regional Conf. Soil Mech. Found. Eng., Haifa, Vol. 1, pp. 13 - 16.
- Khoshnavan, H. (2007). Beach sediments, morphodynamics, and risk assessment, Caspian Sea coast, Iran. *Quaternary International*, Vol. 167–168, pp. 35–39.
- Kinnell, P. I. A. (2005). Raindrop Impact Induced Erosion Processes and Prediction: A Review. *Hydrological Process*, Vol. 19, pp. 2815– 2844.
- Kozeny, J. ~1927!. “Ueber kapillare Leitung des Wassers im Boden.” Wien, Akad. Wiss., 136~2a!, 271.
- Lal, R. (1990). Soil Erosion in the Tropics: Principles and Management. McGraw-Hill, New York.
- Lal, R. (1992). Restoring Land Degraded by Gully Erosion in the Tropics. *Advances in Soil Science*, Vol. 17, pp 123–153.
- Lambe, T. W. & Whitman, R. V. (1979). Soil Mechanics. S.I. Version. Wiley, New York, 553 p.
- Lechman, J., Lu, N. & Wu, D. (2006). Hysteresis of Matric Suction and Capillary Stress in Monodisperse Disk-Shaped Particles. *Journal of Engineering Mechanics*, Vol. 132, No. 5, pp. 565–577.
- Lee, I. K., White, W. and Ingles, O. G. 1983, Geotechnical Engineering, Pitman, Boston, 508 p.
- Levy, G. J., Levin, J. & Shainberg, I. (1994). Seal Formation and Interrill Soil Erosion. *Soil Sci Soc Am J*. Vol. 58, pp. 203-209.
- Li, A. G., Yue, Z. Q., Tham, L. G., Lee, C. F. & Law, K. T. (2005). Field-Monitored Variations of Soil Moisture and Matric Suction in a Saprolite Slope. *Can. Geotech. J*. Vol. 42, pp. 13–26.
- Lumb, P., (1975). Slope Failures in Hong Kong. *Quarterly Journal of Engineering Geology*. Vol. 8, pp. 31-65.
- Lundin, C. & Linden, O. (eds) (1996). Integrated Coastal Zone Management in Mozambique. Proceedings of the National Workshop on Integrated Coastal Zone Management in Mozambique, Inhaca Island and Maputo, Mozambique, 5-10 May 1996. Sida/SAREC & the World Bank. 148 pp.
- Luttenegger, A. J.; Saber, R. T., (1988). Determination of Collapse Potential of Soil. *Geotechnical Testing Journal*, ASTM, Vol. 11, pp. 173-178.

- Maccarini, M. (1987). Laboratory Studies of a Weakly Bonded Artificial Soil. PhD Thesis, Imperial College of Science and Technology, London.
- Maccarini, M. (1993). A Comparison of Direct Shear Box Tests With Triaxial Compression Tests for a residual Soil. *Geotechnical and Geological Engineering*. Vol. 11, pp. 69-80.
- Maccarini, M.; Teixeira, V. H. & Trichês, G. (1989) Bonding Properties of a Residual Soil Derived from Diabase. 12<sup>th</sup> International Conference of Soil Mechanics and Foundation Engineering. Rio de Janeiro. Pp. 525-528.
- Macedo, M. J. A. (1971). Contribution for the Study of the “Red Soils” of the City of Lourenço Marques. 5<sup>th</sup> Regional Conference for Africa on Soil Mechanics and Foundation Engineering. Luanda. Pp 1.61-1.65.
- Manuel, I. R. & Vicente, E. M. (2002). Landslide Hazard in Maputo City: a Combination of Natural and Anthropogenic Causes. *Africa Geoscience Review*, Geohazards in Africa, Vol. 9 (4), pp. 413-418.
- Martínez-Casasnovas, J. A.; Ramos, M. C. & Poesen, J. (2004). Assessment Of Sidewall Erosion In Large Gullies Using Multi-Temporal DEMs And Logistic Regression Analysis. *Geomorphology*, Vol. 58, pp. 305–321.
- Mayhew, S. (2004). A Dictionary of Geography. 3<sup>rd</sup> Ed. 531 p. Oxford University Press
- McGraw-Hill (2003). McGraw-Hill Dictionary of Scientific and Technical Terms. 6<sup>th</sup> Ed, 2380 p. McGraw-Hill Companies, Inc.
- McKnight (2001). Av Julius Nyerere Dongas, Maputo: Geotechnical Investigation. Technical Report Prepared to Mozal-SARL, Report MGC262/5370/2000/G, 19 p.
- Momade, F. J; Ferrara, M. & Oliveira, J. T. (1996). Notícia Explicativa da Carta Geológica 2432 D3 Maputo: Escala 1/50.000. (*Explanation of 1:50.000 Geological Sheet 2432 D3 Maputo*. Mozambican National Directorate of Geology) 32 pp, Maputo, DNG.
- Morton, R. A., Gibeaut, J. C., Paine, J. G. (1995). Meso-scale Transfer of Sand During and After Storms: Implications for Prediction of Shoreline Movement. *Marine Geology*, Vol. 126, pp. 161-179.
- Mshana, N.S., Suzuki, A. & Kitazono, Y. (1993). Effects of Weathering on Stability of Natural Slopes in North-Central Kumamoto. *Soils Foundations*, Vol. 33, pp. 74-87.
- Mulder, F.J. De & Cordani, U.G. (1999). Geoscience Provide Assets for Sustainable Development. *Episodes*, 2(2), 78 – 82.
- Newmark, N. M. (1935). Simplified Computation of Vertical Pressures in Elastic Foundations. Engineering Experiment Station Circular No. 24, University of Illinois, Urbana.

- Nyssen, J., Poesen, J., Moeyersons, J., Luyten, E., Veyret Picot, M., Deckers, J., Mitiku, H. & Govers, G. (2002). Impact of Road Building on Gully Erosion Risk, a Case Study From the Northern Ethiopian Highlands. *Earth Surface Processes and Landforms*. Vol. 27 (12), pp. 1267– 1283.
- Odong, J. (2008). Evaluation of Empirical Formulae for Determination of Hydraulic Conductivity based on Grain-Size Analysis. *The Journal of American Science*, Vol. 4 (1), pp. 1-6.
- Oostwoud Wijdenes, D. J., Poesen, J., Vandekerckhove, L., Ghesquiere, M. (2000). Spatial Distribution of Gully Head Activity and Sediment Supply Along an Ephemeral Channel in a Mediterranean Environment. *Catena*. Vol. 39, pp. 147– 167.
- Øygarden, L. (2003). Rill and Gully Development During an Extreme Winter Runoff Event In Norway. *Catena* , Vol. 50, pp. 217–242.
- Paige-Green, P. (2004). The Geology and Engineering Geology of Roads in South Africa. *Proceedings of the 23<sup>rd</sup> Southern African Transport Conference (SATC 2004)*. pp. 216-225.
- Paige-Green, P. (2008). Dispersive and Erodible Soils - Fundamental Differences. Problem Soils in South Africa Conference, Midrand, Gauteng, South Africa, November 3-4, 2008, pp 7.
- Plummer, C. C.; Carlson, D. & McGeary D. (2007). *Physical Geology*. 12 ed., McGraw-Hill, 592 pp.
- Poesen, J.; Nachtergaele, J.; Verstraeten, G. & Valentin C. (2002a). Gully erosion and environmental change: importance and research needs. *Catena*, Vol. 50, pp 91– 133.
- Poesen, J., Vandekerckhove, L., Nachtergaele, J., Oostwoud Wijdenes, D., Verstraeten, G., Van Wesemael, B. (2002b). Gully Erosion in Dryland Environments. In: Bull, L. J., Kirkby, M. J. (Eds.). *Dryland Rivers: Hydrology and Geomorphology of Semi-Arid Channels*. Wiley, Chichester, England, pp. 229–262.
- Poesen, J., Nachtergaele, J., Verstraeten, G. & Valentin, C. (2003). Gully Erosion and Environmental Change: Importance and Research Needs. *Catena*, Vol. 50, pp. 91– 133.
- Poulos, S. J. (1989). *Advance Dam Engineering for Design, Construction, and Rehabilitation: Liquefaction Related Phenomena*. Ed. Jansen, R.B, Van Nostrand Reinhold, pp 292-297.
- Pradel, D. & Raad, G. (1993). Effect of permeability on surficial stability of homogeneous slopes. *Journal of Geotechnical Engineering*. Vol. 119, No. 2, pp. 315-332.
- Priklonskij, V. A. (1952). *Gruntovenedie - Utoraira Chast*. Gosgoelizdat, Moscow.
- Quartel, S., Kroo, A., Ruessink, B. G. (2007). Seasonal Accretion and Erosion Patterns of a

- Microtidal Sandy Beach. *Marine Geology*, doi: 10.1016/j.margeo.2007.11.003.
- Rao, S. M. (1996). Role of Apparent Cohesion in the Stability of Dominican Allophone Soil Slopes. *Engineering Geology*. Vol. 43, pp 265-279.
  - Ravens, T. M. & Jepsen, R. A. (2006). Computational Fluid Dynamics Analysis of Flow in a Straight Flume for Sediment Erodibility Testing. *Journal of Waterway, Port, Coastal, and Ocean Engineering*, Vol. 132 (6), pp. 457-461.
  - Ravens, T. M. & Gschwend, P. M. (1999). Flume Measurements of Sediment Erodibility in Boston Harbor. *Journal of Hydraulic Engineering*, Vol. 125 (10), pp. 998–1005.
  - Ravens, T. M. (2007). Comparison of Two Techniques to Measure Sediment Erodibility in the Fox River, Wisconsin. *Journal of Hydraulic Engineering*, Vol. 133 (1), pp. 111–115.
  - Ravens, T. M. & Sindelar, M. (2008). Flume Test Section Length and Sediment Erodibility. *Journal of Hydraulic Engineering*, Vol. 134 (10), pp. 1503–1506.
  - Renard, K. G. & Freidmund, J. R. (1994). Using Monthly Precipitation Data to Estimate the R-factor in the RUSLE. *Journal of Hydrology*. Vol. 157, pp. 287–306.
  - Renard, K. G.; Foster, G. R.; Yoder, D. C. & McCool, D. K. (1994). RUSLE Revisited: Status, questions, answers, and the future. *Journal of Soil and Water Conservation*. Vol. 49, pp. 213–220.
  - Renard, K. G.; Foster, G. R.; Weesies, G. A.; McCool, D. K. & Yoder, D. C. (1997). Predicting Soil Erosion by Water: A Guide to Conservation Planning with the Revised Soil Loss Equation (RUSLE). U.S. Dept. of Agriculture, Agric. Handbook No. 703, 404 p.
  - Riani, H. C. & Barbosa, M. C. (1989). Collapsible Sand and Its Treatment by Compaction. Proceedings of the 12<sup>th</sup> International Conference of Soil Mechanics and Foundation Engineering. Rio de Janeiro. Pp 643-646.
  - Rib, H. T. & Liang, T. (1978). Recognition and Identification (Chapter 3). In: Shuster, R. L. & Krizek, R. J. (eds). Landslides: Analysis and Control. National Research Council, Transportation Research Board, Special Report 176, National Academy of Sciences, Washington, pp. 34–79.
  - Rienks, S. M.; Botha, G. A. & Hughes, J. C. (2000). Some Physical and Chemical Properties of Sediments Exposed in a Gully (Donga) in Northern KwaZulu-Natal, South Africa and Their Relationship to the Erodibility of the Colluvial Layers. *Catena*. Vol. 39, pp. 11-31.
  - Rizkallah, V. & Keese, K. (1989). Geotechnical Properties of Collapsible Soils. Proc. International Conference on Soil Mechanics and Foundation Engineering, Vol. 1, pp. 101-104.
  - Rocscience, Inc. (2003). Slide: 2D Limit Equilibrium Slope Stability For Soil And Rock

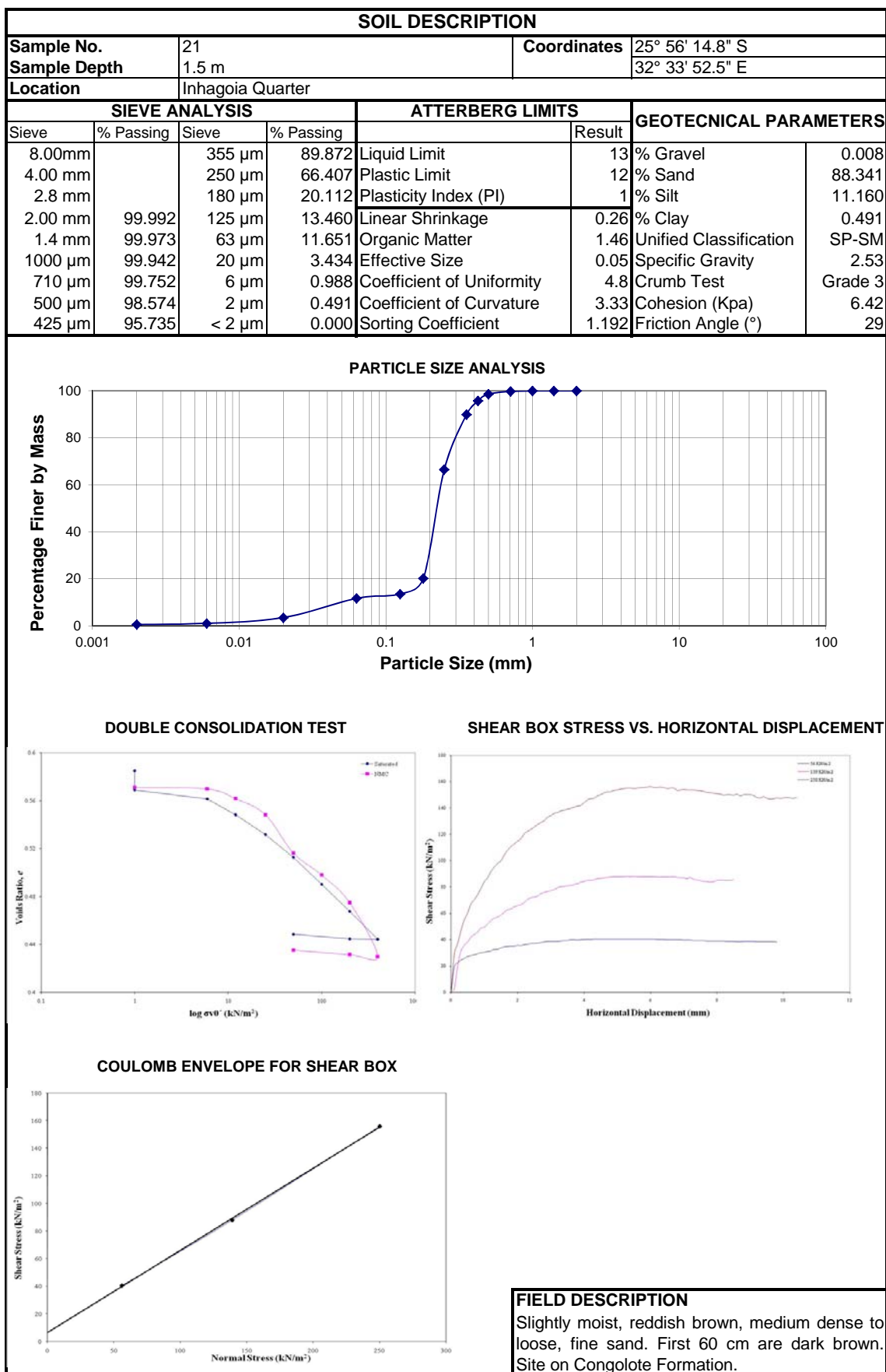


- Slopes, User's Guide, Part 2. 88 p. Rocscience Inc.
- Schmittner, K. E. & Giresse, P. (1999). The Impact of Atmospheric Sodium on Erodibility of Clay in a Coastal Mediterranean Region. *Environmental Geology*. Vol. 37, N. 3, pp 195-206.
  - Scholten, T. (1997). Hydrology and Erodibility of the Soils and Saprolite Cover of the Swaziland Middleveld. *Soil Technology*. Vol. 11, pp. 247-262.
  - Schwartz, K. (1985). Collapsible Soils. *The Civil Engineer in South Africa*. Transactions SAICE, Vol. 27, No. 7, pp. 379-393
  - Scott, A. J. (2008). *Introduction to Geology and Soil Mechanics*. University of Wisconsin-Stout Website. [http://physics.uw.ed/geo/perm\\_de\\_wat.htm](http://physics.uw.ed/geo/perm_de_wat.htm). (Accessed 25 October 2008).
  - Sherard, J. L., Dunnigan, L. P. & Decker, R. S. (1976b). Identification and Nature of Dispersive Soils. *J. Geo. Eng. Div.*, ASCE Paper 12052, pp. 287-301.
  - Sherard, J. L., Dunnigan, L. P., Decker, R. S. & Steele, E. F. (1976a). Pinhole Test for Identifying Dispersive Soils. *J. Geo. Eng. Div.*, ASCE Paper 11846, pp. 69-85.
  - Shroff, A. V. & Shah, D. L. (2003). *Soil Mechanics and Geotechnical Engineering*. 547 p. London: Taylor & Francis.
  - Signer, S.; Marinho, F. A. M.; Santos, N. B.; Andrade, C. M. M. (1989). Expansive and Collapsible Soils in Semi-Arid Region. In: 12th. International Congress of Soil Mechanics and Foundation Engineering, Rio de Janeiro, pp. 647-650.
  - Simon, A., Curini, A. Darby, S. E. & Langendoen, E. J. (2000). Bank and near-bank processes in an incised channel. *Geomorphology*, Vol. 35, pp. 193–217
  - Singha, R.; Tiwarib, K. N.; Malb, B.C. (2006). Hydrological Studies for Small Watershed in India Using the ANSWERS Model. *Journal of Hydrology*, Vol. 318, pp. 184–199.
  - Spigolon, S. J. (2001). *Geotechnical Engineering*. 1st edition, 350 p. New York: McGraw-Hill,
  - Sridharan, A. & Gurtug, Y. (2005). Compressibility characteristics of soils. *Geotechnical and Geological Engineering*. Vol. 23, pp. 615–634.
  - Terzaghi, K. (1943). *Theoretical Soil Mechanics*. John Wiley and Sons, New York
  - Terzaghi, K., Peck, R. B., and Mesri, G. (1996). *Soil Mechanics in Engineering Practice*. Third Edition, 412 p, New York: John Wiley & Sons.
  - Thorpe, G. S. (2002). *Barron's How to Prepare For the AP: Environmental Science, Advanced Placement Examination*. New York: Barron's Educational Series, 528 p.
  - UNDP 2002. *Human Development Report 2001*. UNDP, Maputo.
  - Valentin, C.; Poesen, J. & Li, Y. (2005). Gully Erosion: Impacts, Factors and Control. *Catena*, Vol. 63, pp. 132–153.

- Vandekerckhove, L., Poesen, J., Govers, G. (2003). Medium-Term Gully Headcut Retreat Rates in Southeast Spain Determined From Aerial Photographs and Ground Measurements. *Catena*. Vol. 50, pp. 329– 352.
- Vandekerckhove, L., Poesen, J., Oostwoud Wijdenes, D., de Figueiredo, T. (1998). Topographical Thresholds for Ephemeral Gully Initiation in Intensively Cultivated Areas of the Mediterranean. *Catena*, Vol. 33 (3–4), pp. 271–292.
- Vandekerckhove, L., Poesen, J., Oostwoud Wijdenes, D., Nachtergaele, J., Kosmas, C., Roxo, M.J., De Figueiredo, T. (2000). Thresholds for Gully Initiation and Sedimentation in Mediterranean Europe. *Earth Surface Processes and Landforms*. Vol. 25, pp. 1201–1220.
- Vaughan, P. R.; Macarini, M. & Mokhtar, S. M. (1988). Indexing the Engineering Properties of Residual Soil. *Quarterly Journal of Engineering Geology*. Vol. 21, pp. 69-84.
- Vaz. E.A. 1990. Construction of Two Buildings with Three Floors Close to Industrial Institute of Maputo: Geotechnical Studies. Engineering Laboratory of Mozambique. Report N° 18.328 (in Portuguese).
- Vicente, E. M.; Jermy, C. A. & Schreiner, H. D. (2006). Urban Geology of Maputo, Mozambique. Proceedings of the International Association of Engineering Geologists Congress. 8. Nottingham, 12 pp.
- Vicente, E. M.; Amurane, D. P. & Xerinda, L. (2006). Assessment of slope stability in Maputo City, Mozambique. I Proceedings of the International Association of Engineering Geologists Congress. 8. Nottingham, 9 pp.
- Walker, D. J. H. (1997). Dispersive Soils in KwaZulu-Natal. MSc Thesis, University of Natal, Durban, South Africa, 101 pp.
- Walker, D. J. H., Bell, F. G. & Jermy, C. A. (1997). Dispersive Soils in Natal, South Africa. In: Marinos, P. G. (1997). *Proceedings of the 22<sup>nd</sup> International Symposium on Engineering Geology and the Environment*. Pp. 437-444, Taylor & Francis.
- Wall, G.; Baldwin, C. S. & Shelton, I. J. (2003). Soil Erosion - Causes and Effects. OMAFRA Fact Sheet. Agdex # 572.  
<http://www.omafra.gov.on.ca/english/engineer/facts/87-040.htm> (Accessed 19 July 2009)
- Waltham, A.C. (1994). Foundations of Engineering Geology. Blackie Academic and Professional, London, 88p.
- Wan, C. F. & Fell, R. (2004). Investigation of Rate of Erosion of Soils in Embankment Dams. *Journal of Geotechnical and Geoenvironmental Engineering*, Vol. 130 (4), pp. 373-380.

- Watson, A. & Evans, R. (1991). A Comparison of Estimates of Soil-Erosion Made in The Field and From Photographs. *Soil and Tillage Research*, Vol. 19 (1), pp. 17– 27.
- Watson, D. A. & Laflen, J. M. (1986). Soil Strength, Slope and Rainfall Intensity Effects on Interrill Erosion. *Trans. ASAE*. Vol. 29, pp. 98– 102.
- Wei, W, Chen, L., Fu, B., Huang, Z., Wu, D., Gui, L. (2007). The Effect of Land Uses and Rainfall Regimes on Runoff and Soil Erosion in the Semi-Arid Loess Hilly Area, China. *Journal of Hydrology*, Vol. 335, pp. 247– 258.
- Westergaard, H. M. (1938). A Problem of Elasticity Suggested by a Problem of Soil Mechanics: Soft Material Reinforced by Numerous Strong Horizontal Sheets. Contribution to the Mechanics of Solids, MacMillan, New York.
- Wischmeier, W. H. & Smith, D. D. (1978): Predicting Rainfall Erosion Losses: A Guide to Conservation Planning. Agriculture Handbook No. 537. USDA, Hyatsville, Maryland.
- Wolle, C.M. (1985). Slope Stability. First International Conference on Geomechanics in Tropical Lateritic and Saprolitic Soils, Progress Report, Brazil, pp. 164--221.
- Yang, W., Wang, Z., Sui, G. & Ding, G. (2008). Quantitative determination of red-soil erosion by an Eu tracer method. *Soil & Tillage Research*, Vol. 101, pp. 52–56.
- Zhang, J., Jiao, J.J., and Yang, J. (2000). In Situ Rainfall Infiltration Studies at a Hillside in Hubei Province, China. *Engineering Geology*, 57(1): 31–38.
- Zhang, K. L.; Shu, A. P.; Xu, X. L.; Yang, Q. K. & Yu, B. (2008). Soil Erodibility and its Estimation for Agricultural Soils in China. *Journal of Arid Environments*. Vol. 72, pp. 1002-1011.
- Zhang, K.Q., Douglas, B.C., Leatherman, S.P. (2004). Global Warming and Coastal Erosion. *Climate Change*. Vol. 64, pp. 41–58.
- Zhang, L. L., Fredlund, D. G., Zhang, L. M. & Tang, W. H. (2004). Numerical Study of Soil Conditions Under Which Matric Suction Can Be Maintained. *Canadian Geotechnical Journal*. Vol. 41(4), pp. 569–582.
- Ziebell, D. (1999). Stream Bank Erosion. Note Number LC0096. State of Victoria, Department of Natural Resources and Environment.

## **APPENDIX A: Summary of the Engineering Geological Characteristics and Geotechnical Properties**



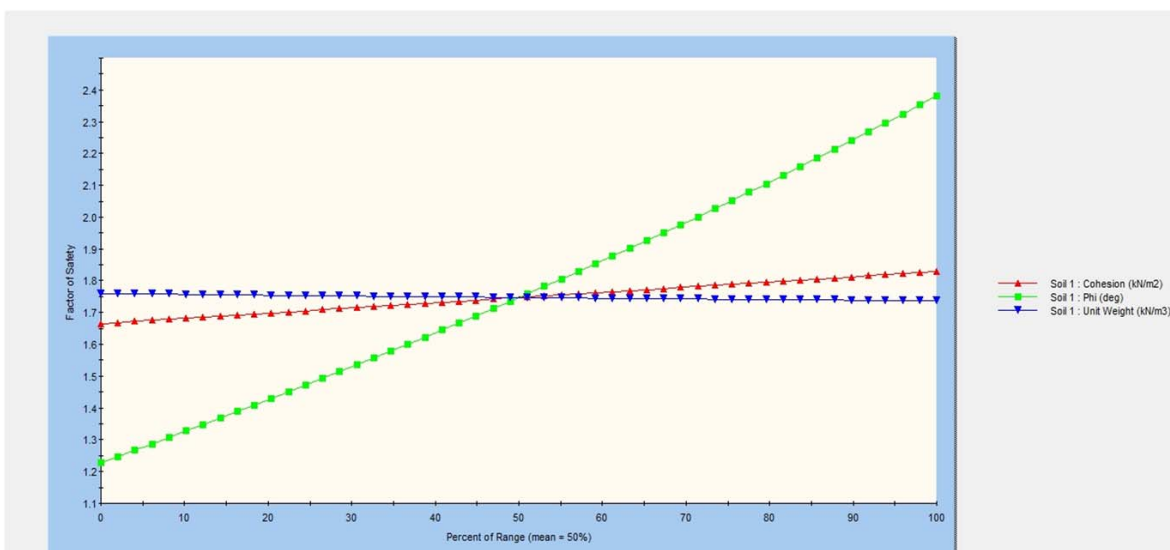
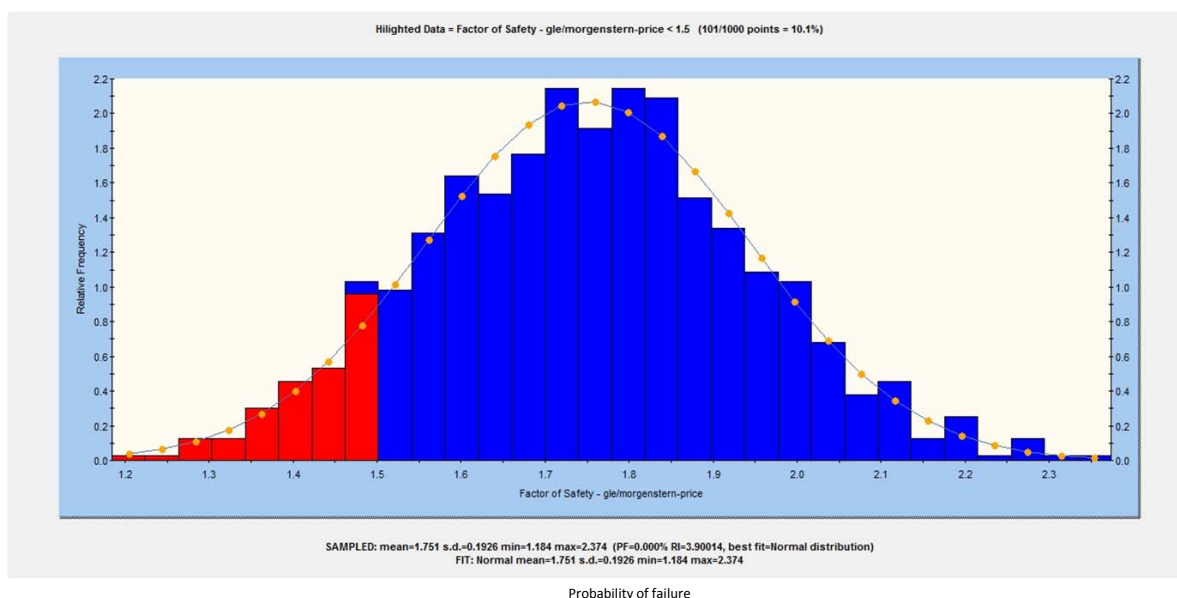
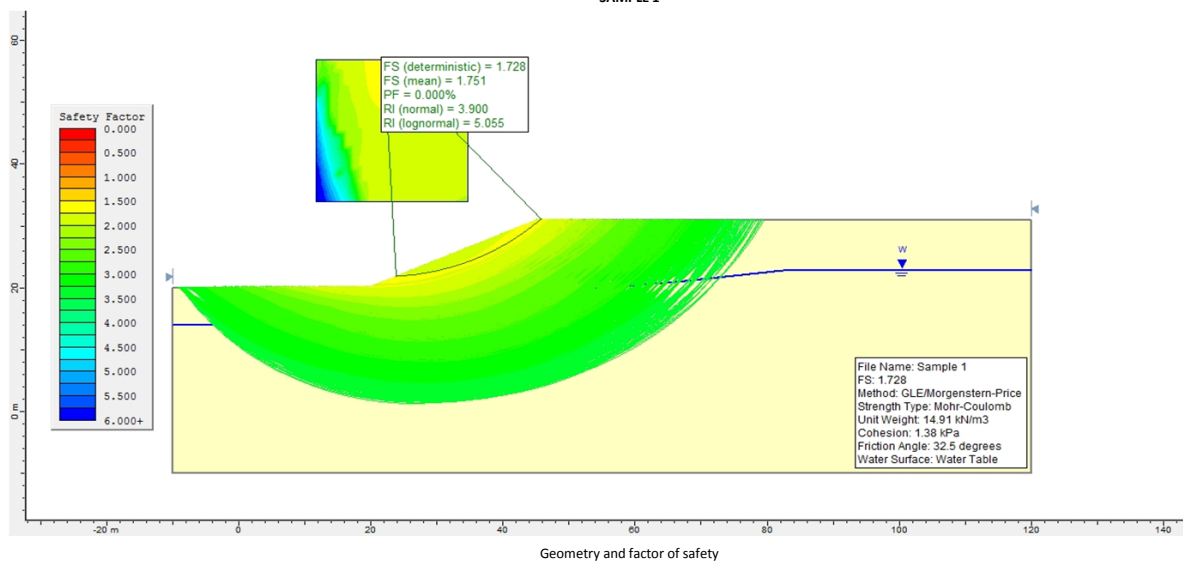
## **APPENDIX B: Raw Chemical Data**

| No. | pH   | Exchangeable Cations (meq/%) |      |      |      | CEC<br>(meq/l) | Saturated Extract (meq/l) |      |      | CE (Ms/m) |
|-----|------|------------------------------|------|------|------|----------------|---------------------------|------|------|-----------|
|     |      | K                            | Ca   | Mg   | Na   |                | Ca                        | Mg   | Na   |           |
| 1   | 7.73 | 0.16                         | 0.62 | 1.32 | 0.6  | 2.47           | 0.30                      | 0.20 | 7.00 | 101.00    |
| 2   | 8.17 | 0.48                         | 0.38 | 2.43 | 0.06 | 3.3            | 0.50                      | 0.60 | 0.60 | 22.00     |
| 3   | 7.81 | 0.35                         | 0.36 | 3.08 | 0.35 | 3.9            | 1.50                      | 1.20 | 4.30 | 89.00     |
| 4   | 5.93 | 0.14                         | 0.22 | 0.63 | 0.13 | 1.1            | 0.30                      | 0.10 | 0.70 | 10.00     |
| 5   | 7.96 | 0.05                         | 0.19 | 2.38 | 0.12 | 2.7            | 1.00                      | 0.30 | 1.10 | 32.00     |
| 6   | 9.21 | 0.49                         | 0.20 | 26.4 | 0.34 | 27.3           | 0.40                      | 0.60 | 2.00 | 29.00     |
| 7   | 8.71 | 0.50                         | 0.44 | 18.7 | 0.16 | 19.7           | 0.90                      | 0.90 | 0.80 | 30.00     |
| 8   | 8.19 | 0.12                         | 0.31 | 3.31 | 0.06 | 3.7            | 0.80                      | 0.30 | 0.70 | 20.00     |
| 9   | 5.81 | 0.36                         | 0.31 | 0.54 | 0.09 | 1.2            | 0.30                      | 0.30 | 0.50 | 11.00     |
| 10  | 6.18 | 0.28                         | 0.42 | 0.39 | 0.06 | 1.1            | 0.20                      | 0.10 | 0.40 | 8.00      |
| 11  | 5.39 | 0.19                         | 0.34 | 0.45 | 0.08 | 1              | 0.20                      | 2.00 | 0.80 | 15.00     |
| 12  | 5.18 | 0.18                         | 0.18 | 0.44 | 0.08 | 0.8            | 0.30                      | 0.20 | 0.50 | 8.00      |
| 13  | 5.52 | 0.01                         | 0.13 | 0.18 | 0.04 | 0.3            | 0.40                      | 0.10 | 0.40 | 8.00      |
| 14  | 5.47 | 0.02                         | 0.14 | 0.16 | 0.07 | 0.4            | 0.40                      | 0.10 | 0.30 | 4.00      |
| 15  | 6.26 | 0.01                         | 0.07 | 0.3  | 0.08 | 0.4            | 0.60                      | 0.10 | 0.50 | 7.00      |
| 16  | 4.74 | 0.03                         | 0.16 | 0.41 | 0.07 | 0.6            | 1.30                      | 0.60 | 1.30 | 53.00     |
| 17  | 5.15 | 0.02                         | 0.10 | 0.18 | 0.1  | 0.4            | 0.30                      | 0.10 | 1.00 | 16.00     |
| 18  | 6.12 | 0.04                         | 0.08 | 0.31 | 0.16 | 0.5            | 0.70                      | 0.40 | 2.90 | 46.00     |
| 19  | 7.08 | 0.03                         | 0.08 | 0.43 | 0.11 | 0.6            | 0.50                      | 0.20 | 1.10 | 19.00     |
| 20  | 7.23 | 0.07                         | 0.25 | 1.43 | 0.13 | 0              | 0.00                      | 0.00 | 0.00 | 0.00      |
| 21  | 5.09 | 0.05                         | 0.38 | 0.92 | 0.22 | 1.4            | 1.40                      | 0.50 | 3.80 | 75.00     |

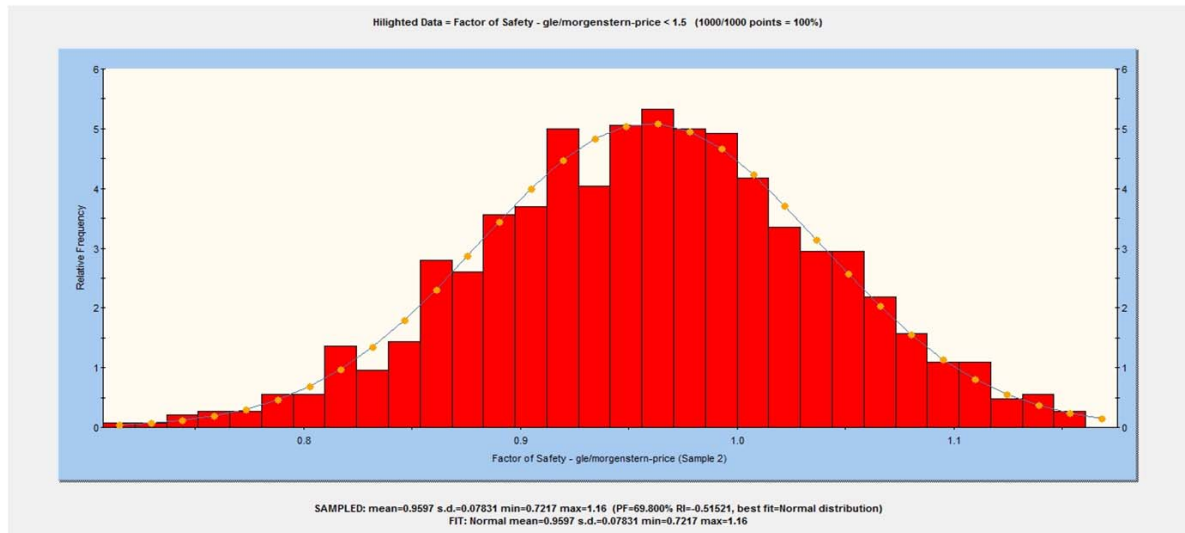
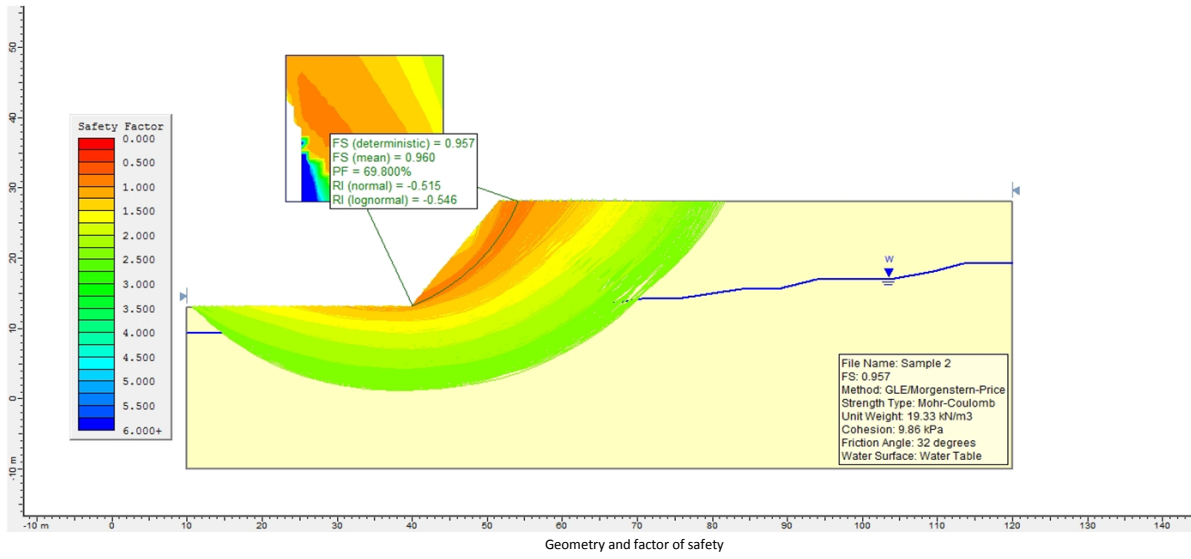
## **APPENDIX C: Graphs of Slope Stability Analysis**



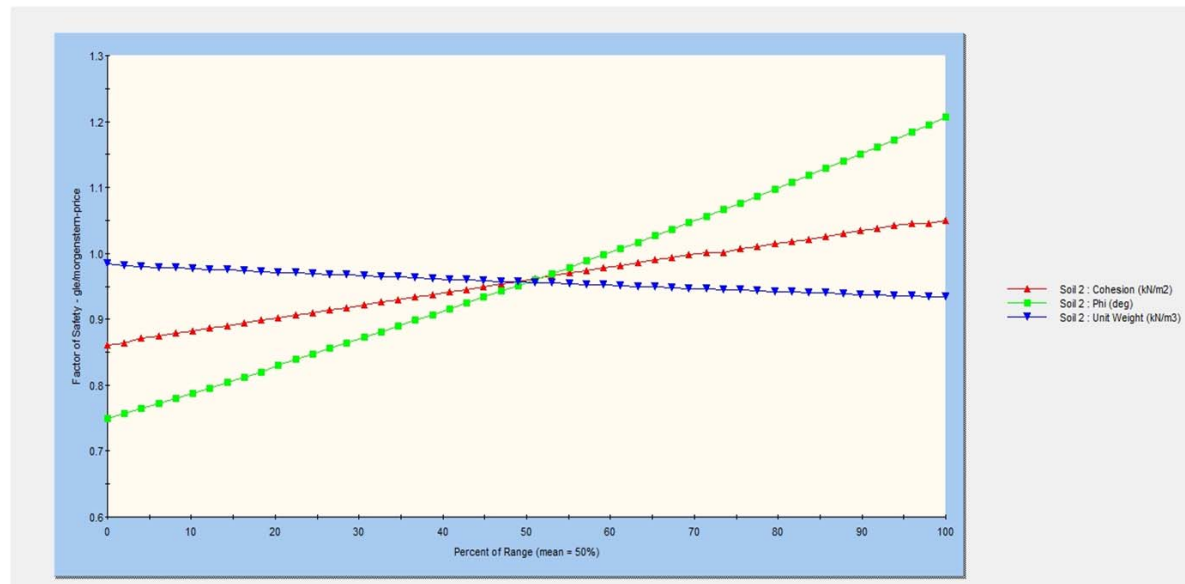
SAMPLE 1



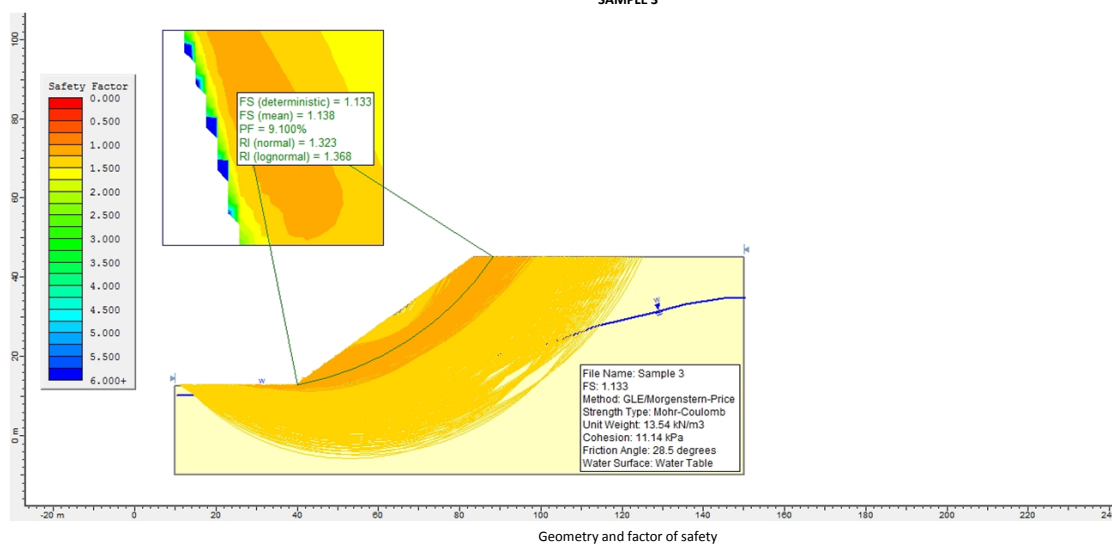
SAMPLE 2



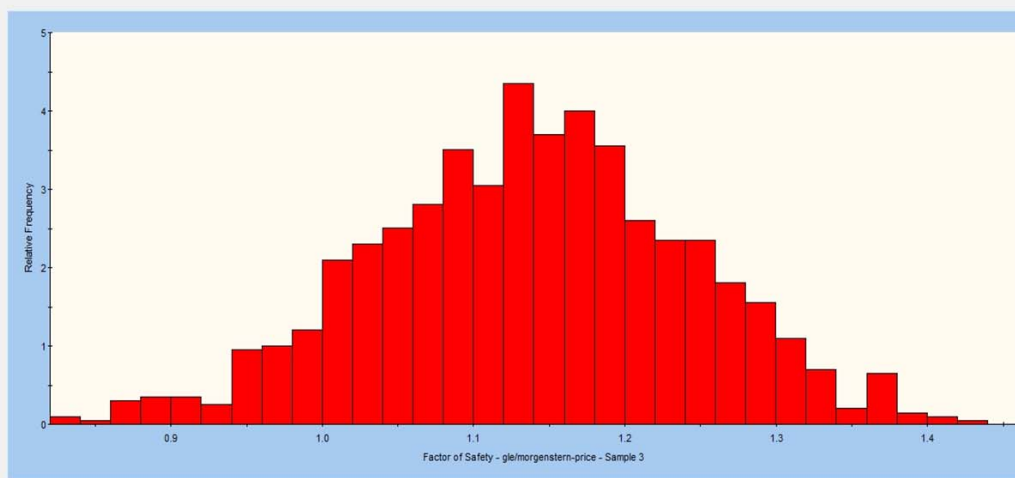
Probability of failure



SAMPLE 3

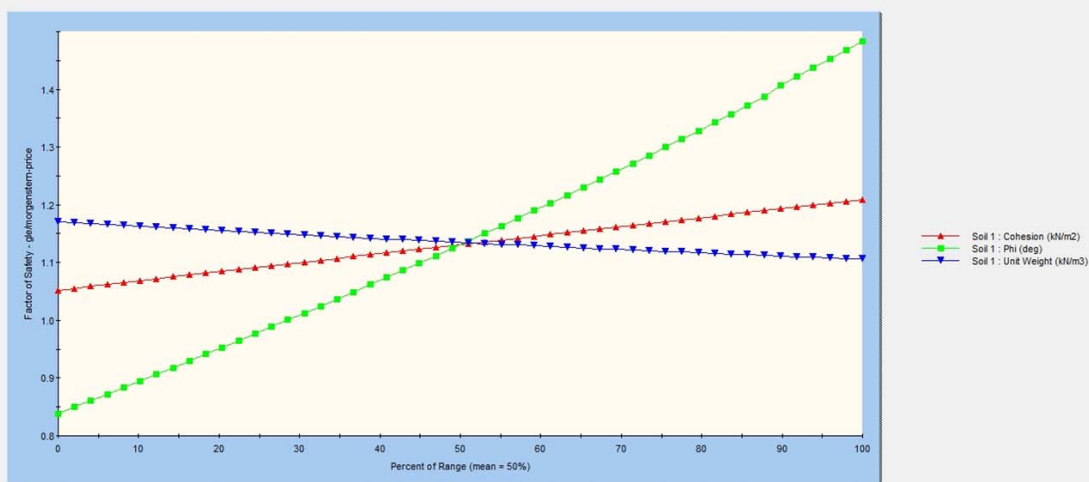


Highlighted Data = Factor of Safety - gle/morgenstern-price < 1.5 (1000/1000 points = 100%)



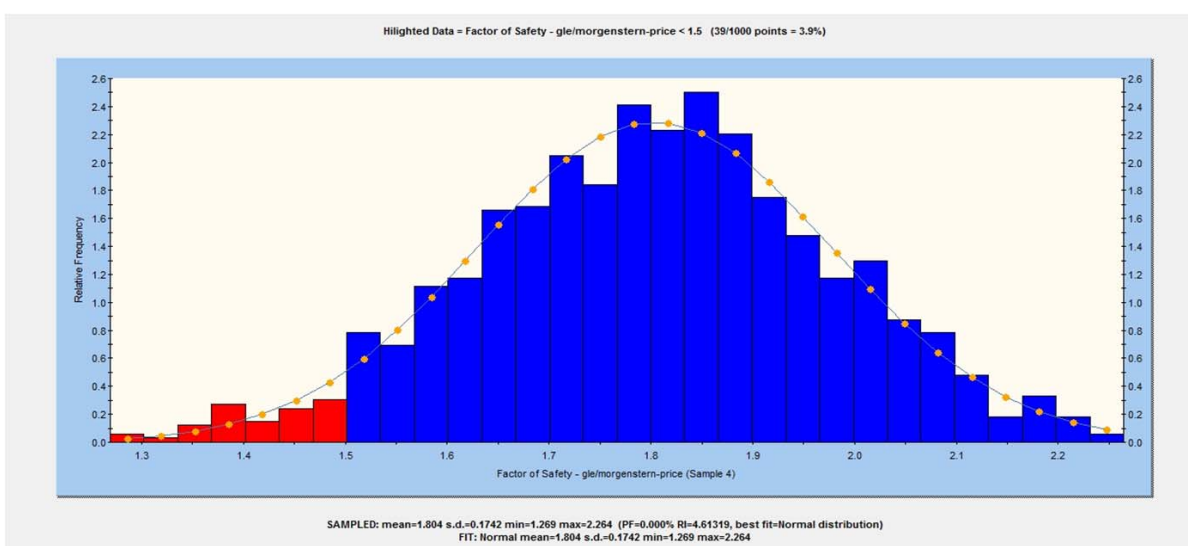
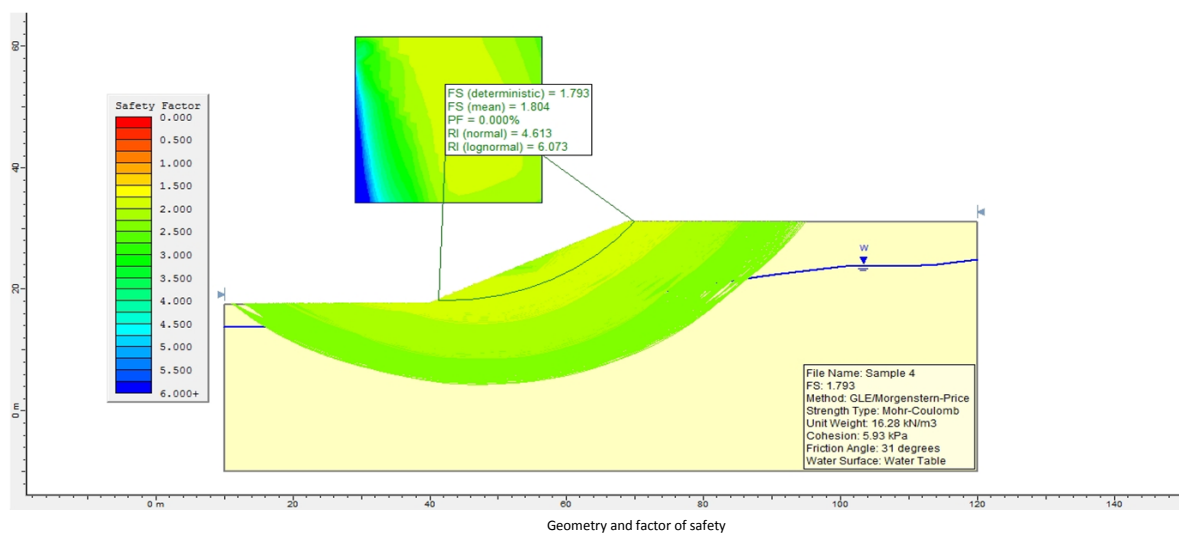
SAMPLED: mean=1.138 s.d.=0.1042 min=0.8258 max=1.425 (PF=9.100% RI=1.32306, best fit=Normal distribution)

Probability of failure

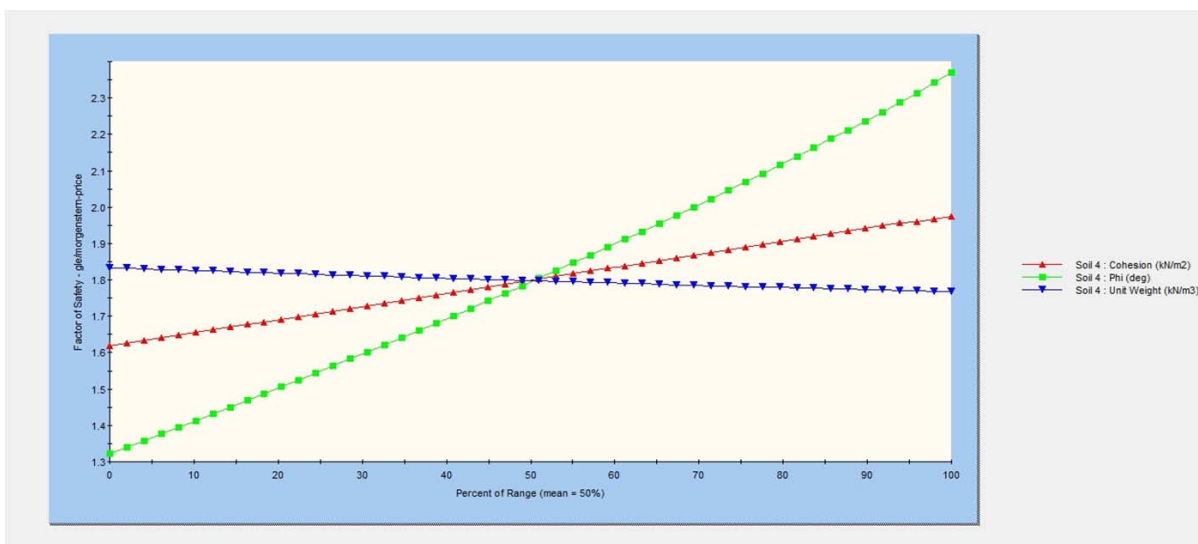


Sensitivity Analysis

SAMPLE 4

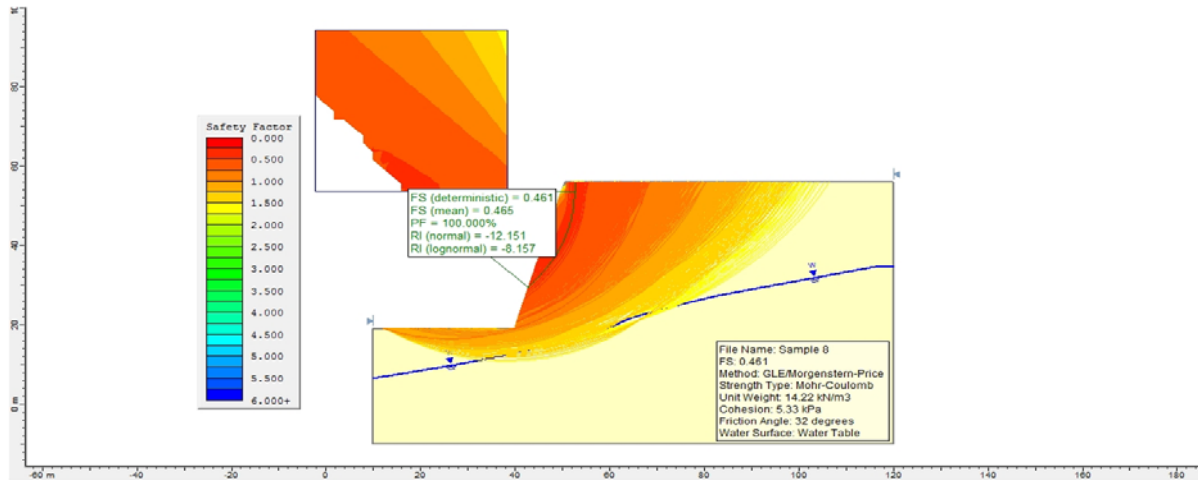


Probability of failure

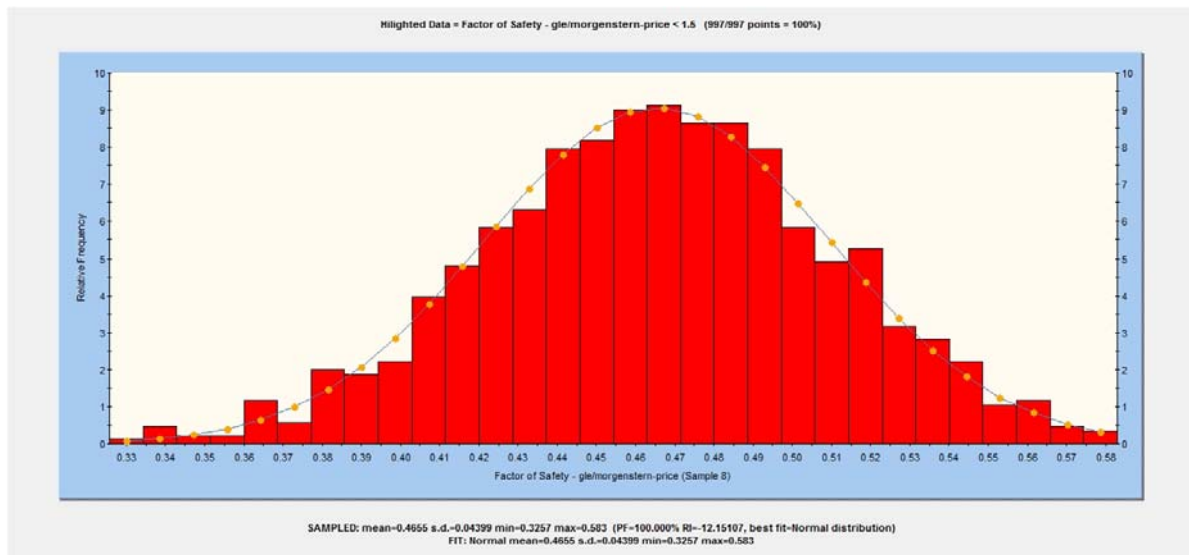




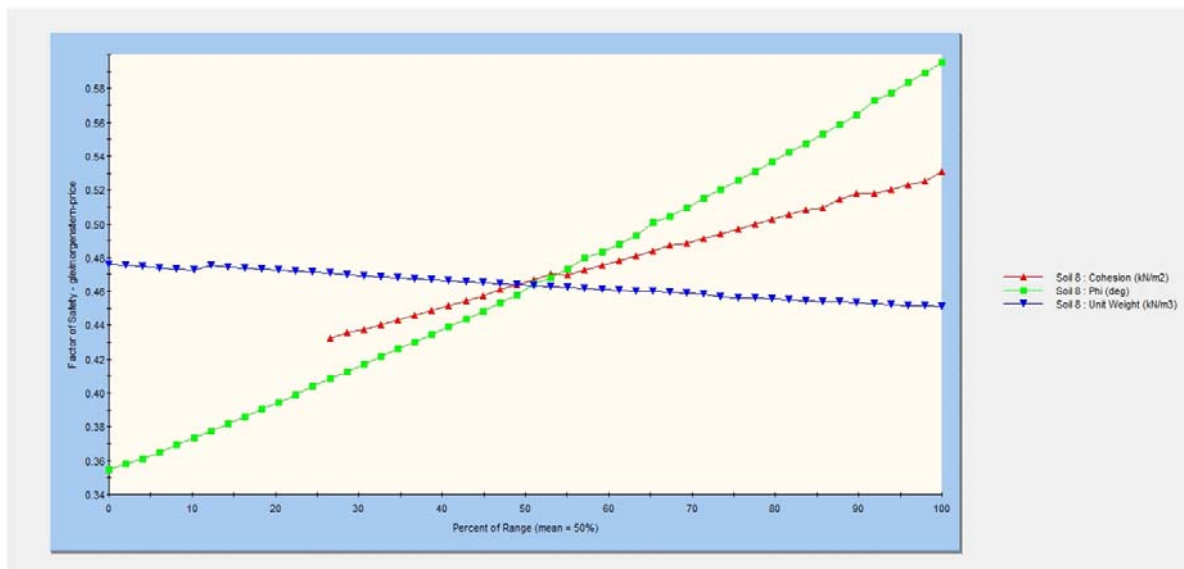
SAMPLE 8



Geometry and factor of safety

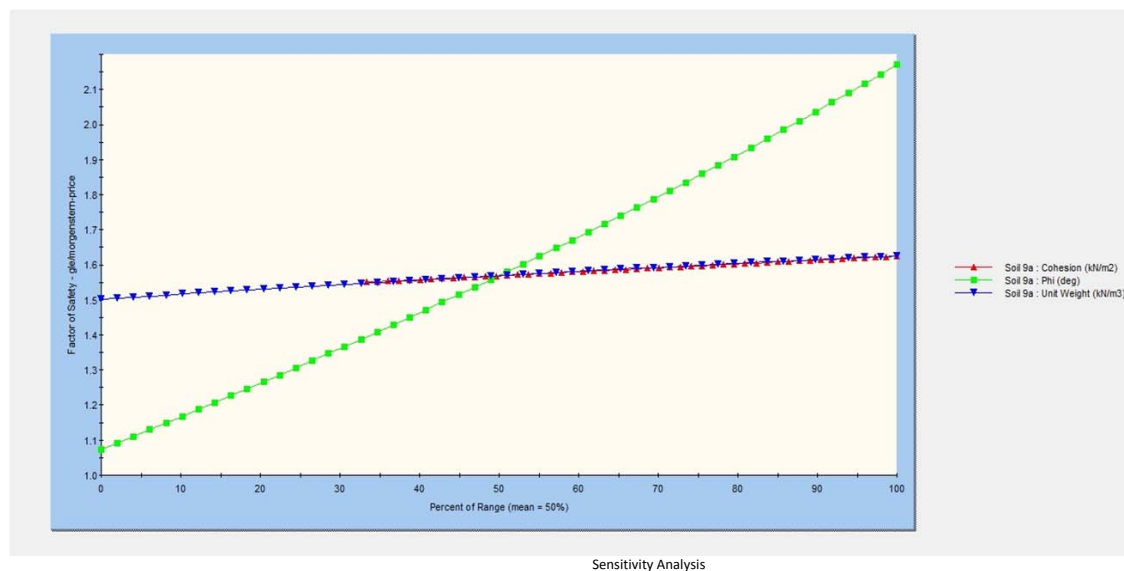
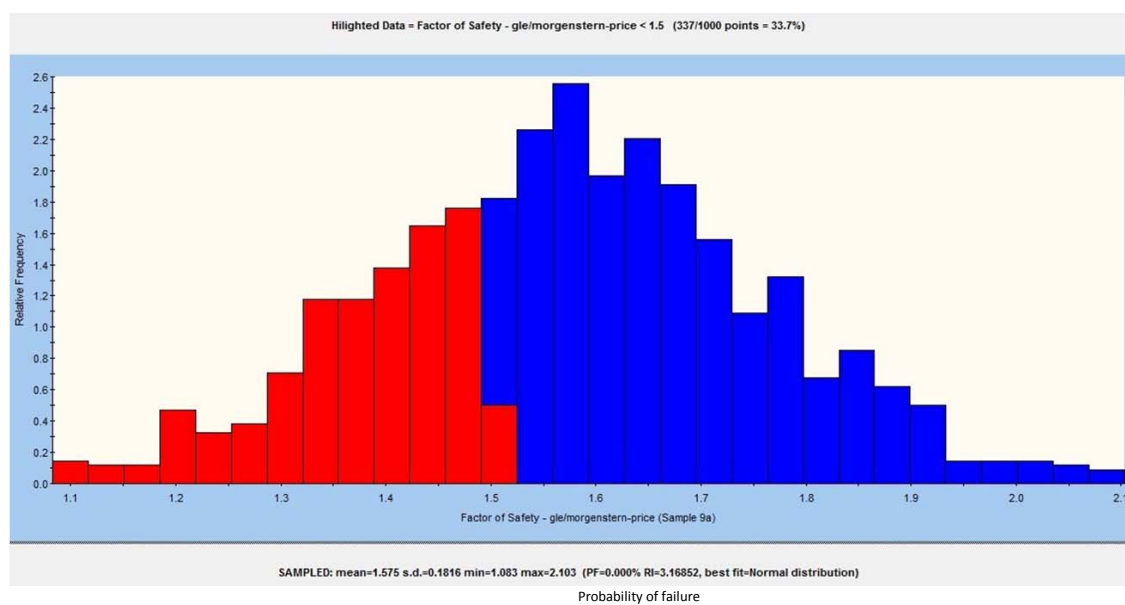
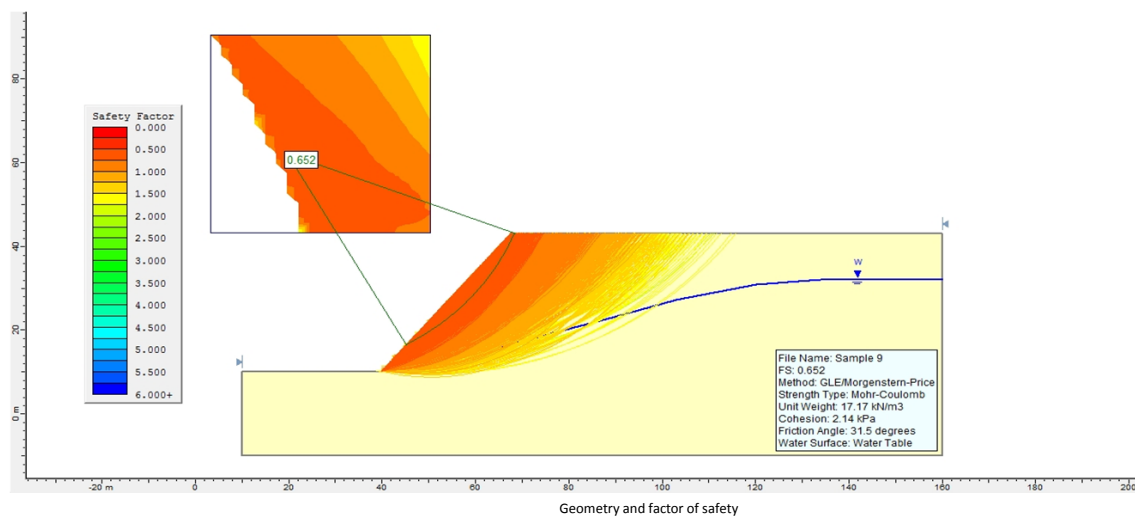


Probability of failure



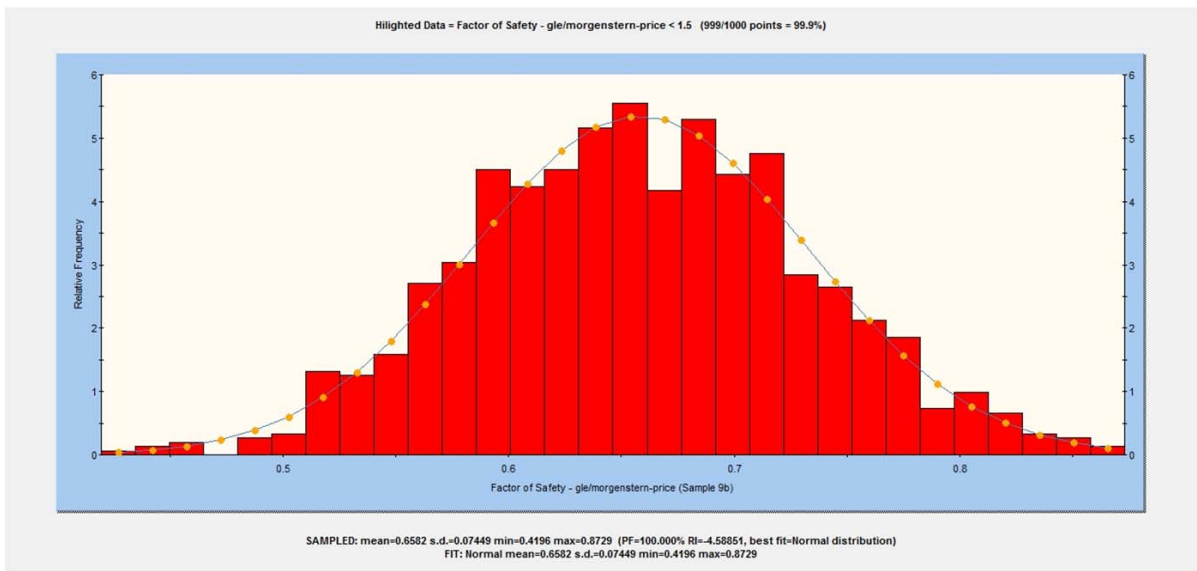
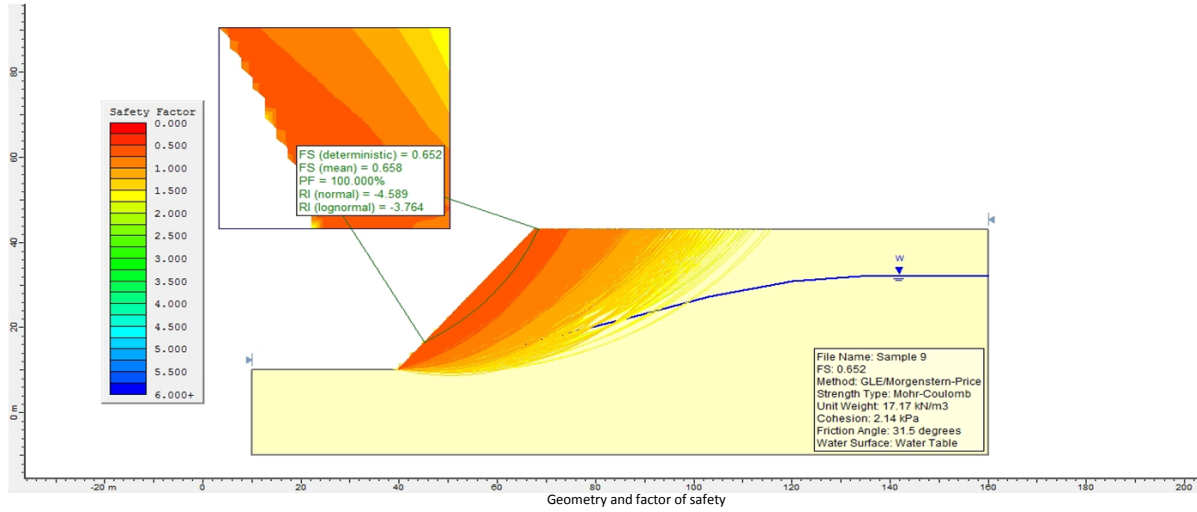
Sensitivity Analysis

SAMPLE 9a

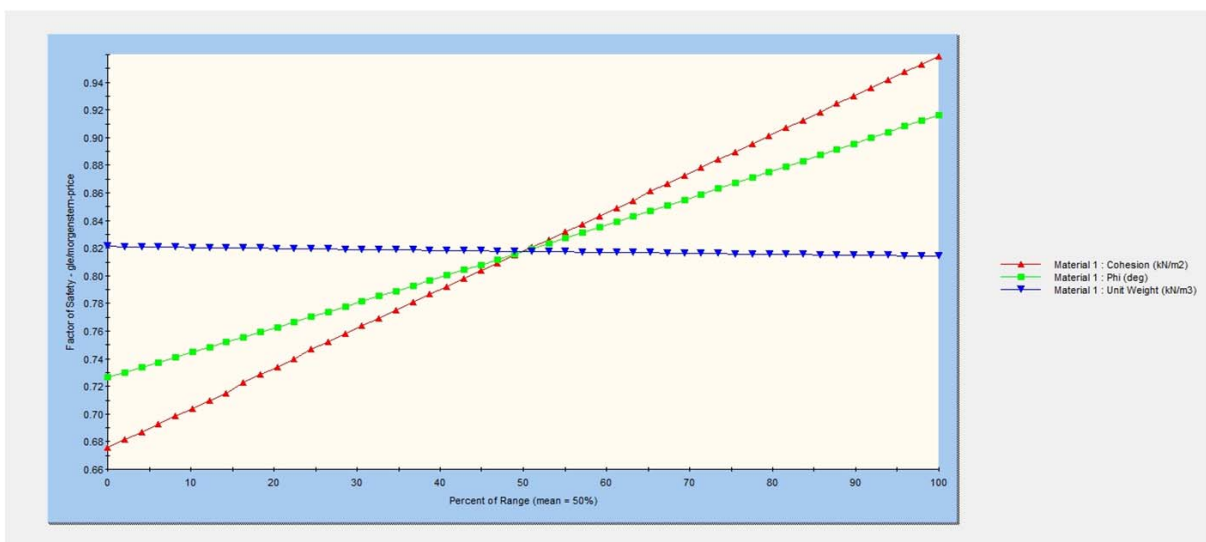




SAMPLE 9 b



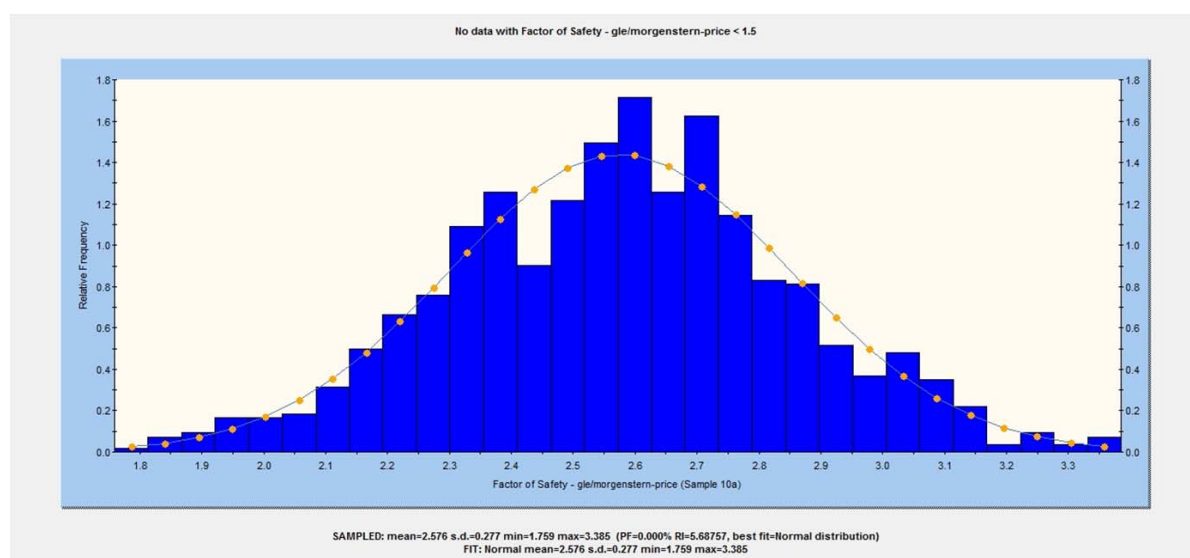
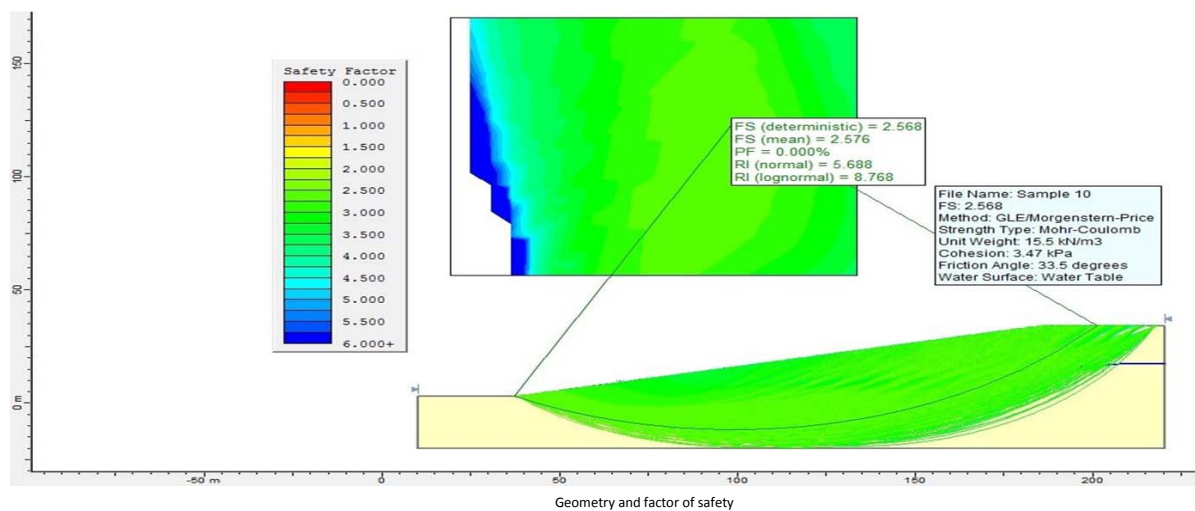
Probability of failure



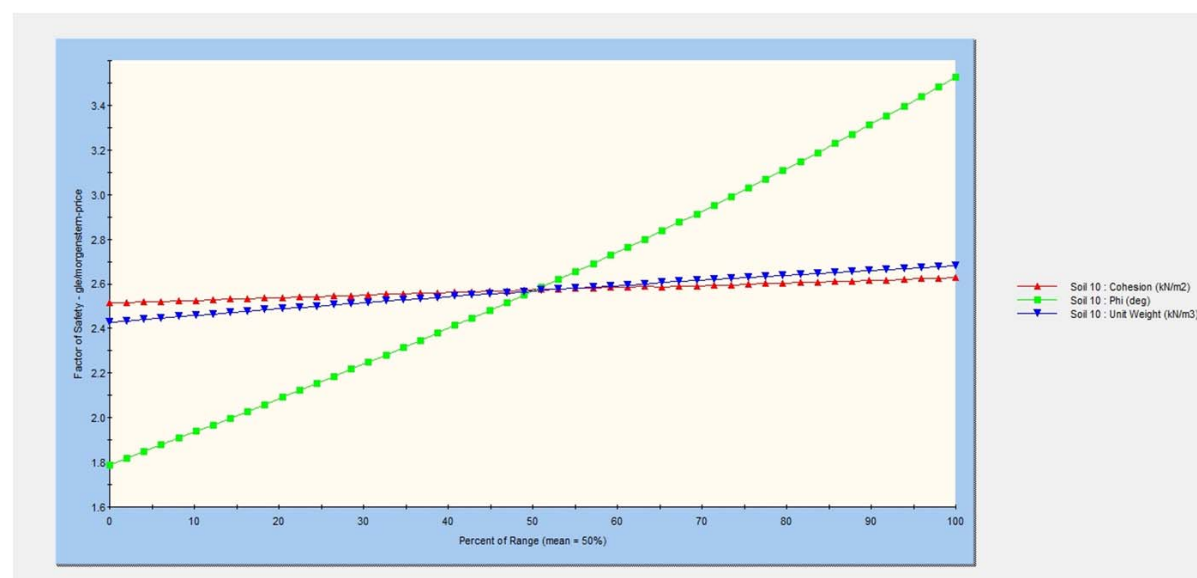
Sensitivity Analysis



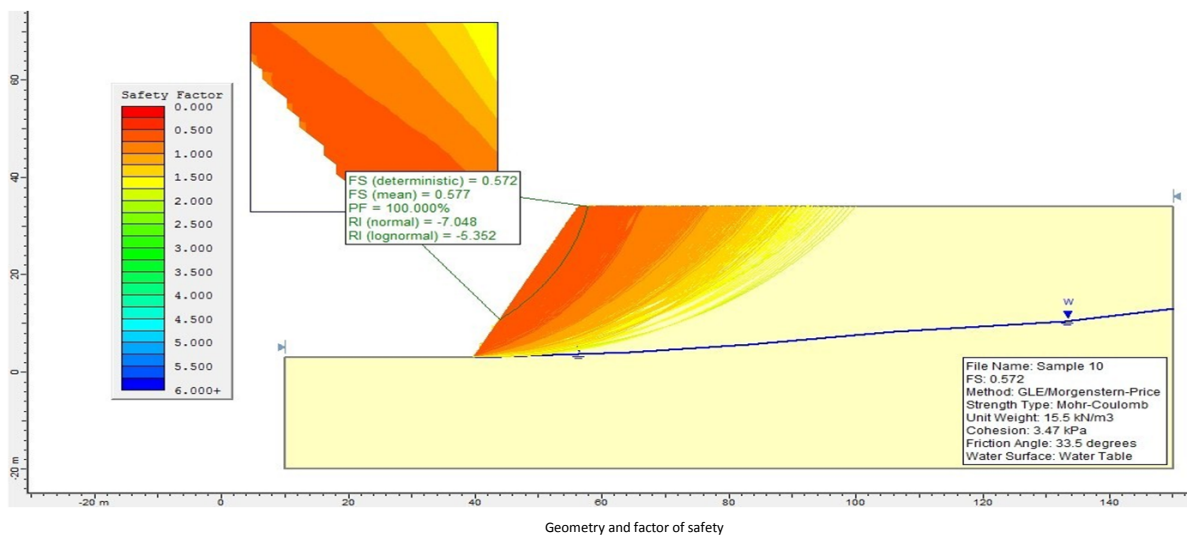
SAMPLE 10 a



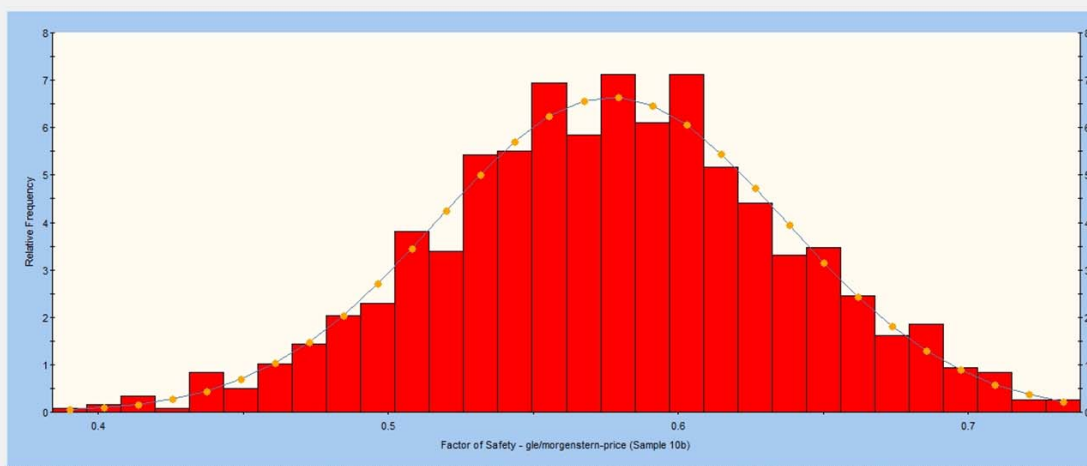
Probability of failure



SAMPLE 10 b

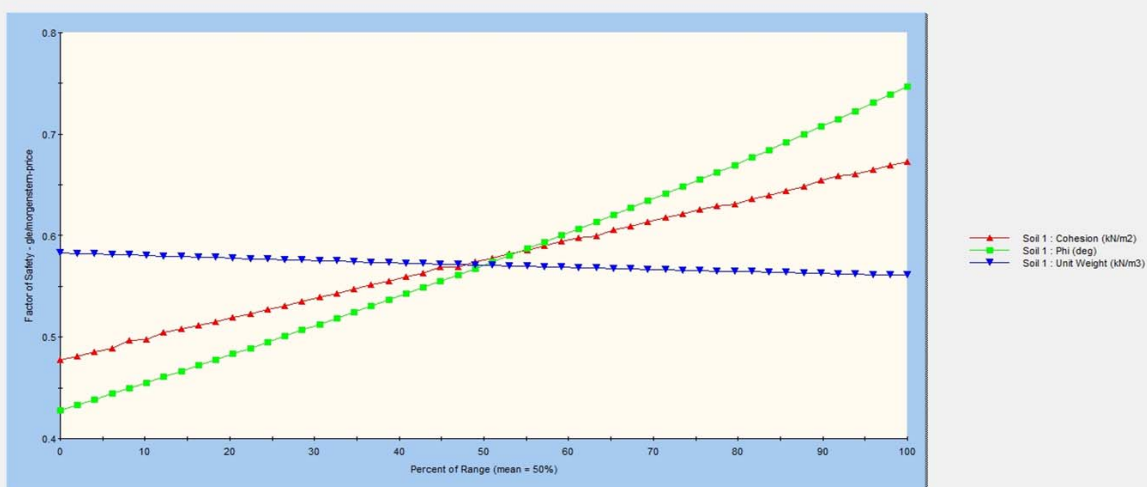


Highlighted Data = Factor of Safety - gle/morgenstern-price &lt; 1.5 (999/999 points = 100%)



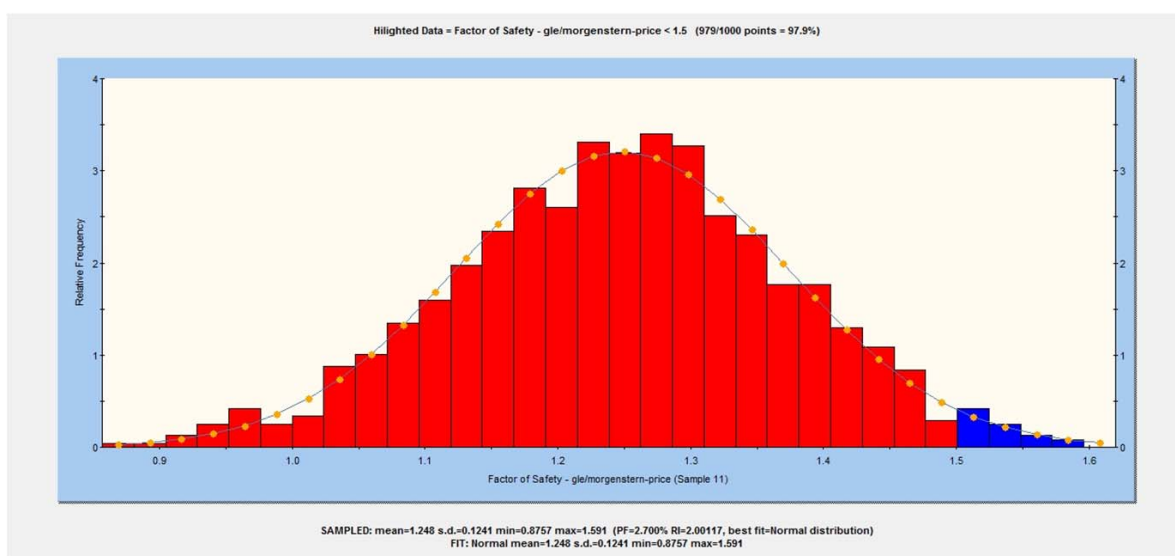
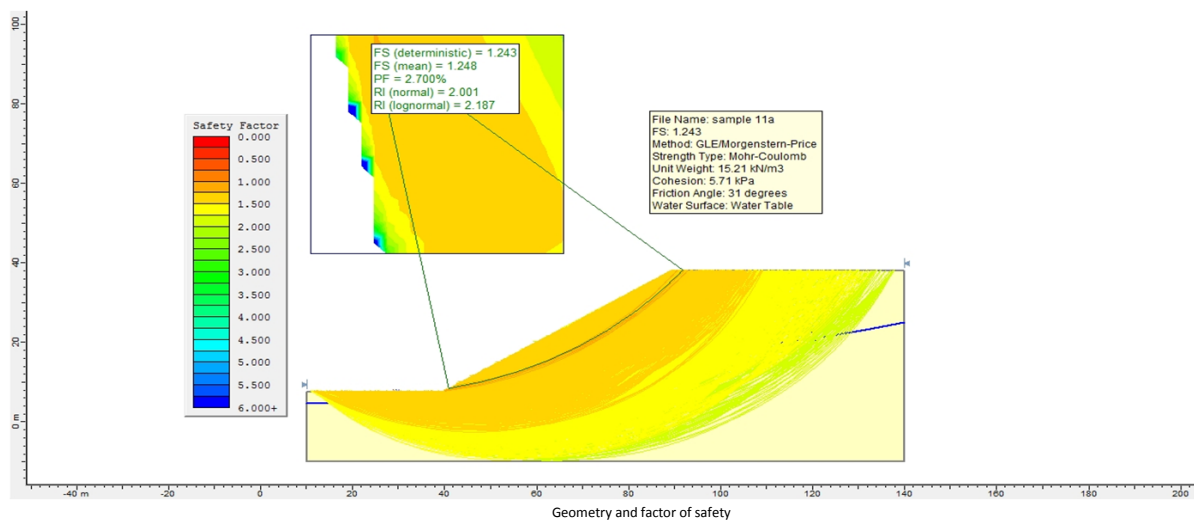
SAMPLED: mean=0.5769 s.d.=0.06003 min=0.3841 max=0.7387 (PF=100.000% RI=-7.04783, best fit=Normal distribution)  
 FIT: Normal mean=0.5769 s.d.=0.06003 min=0.3841 max=0.7387

Probability of failure

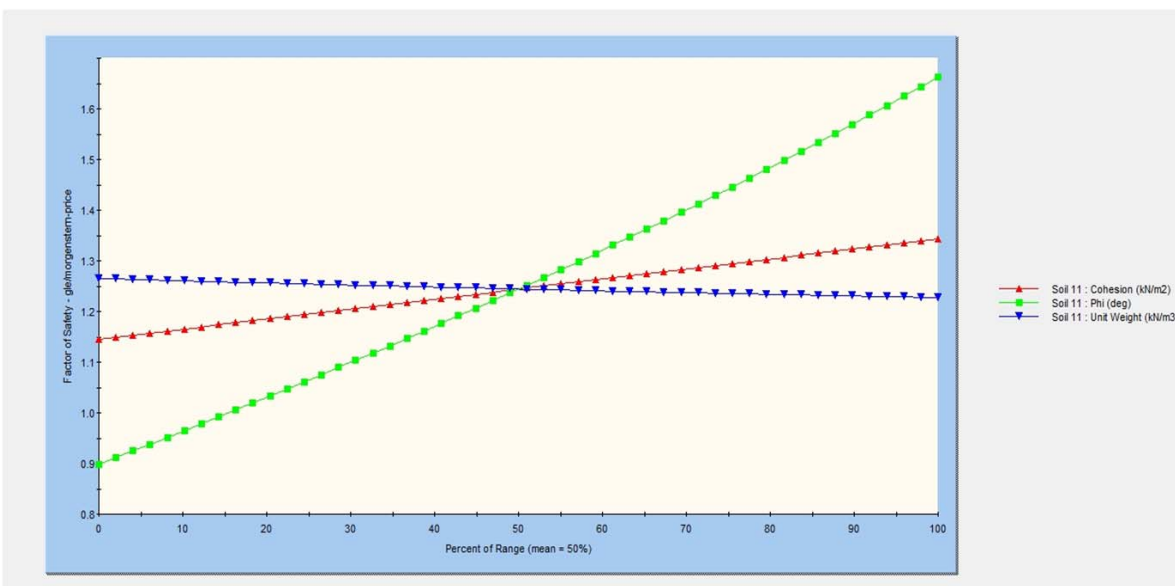


Sensitivity Analysis

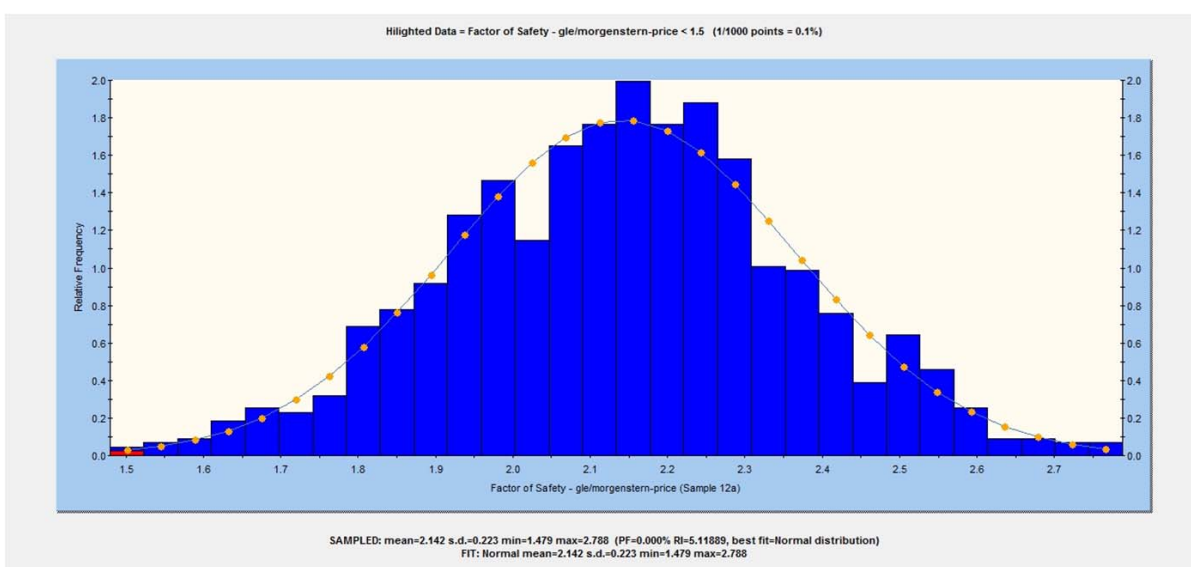
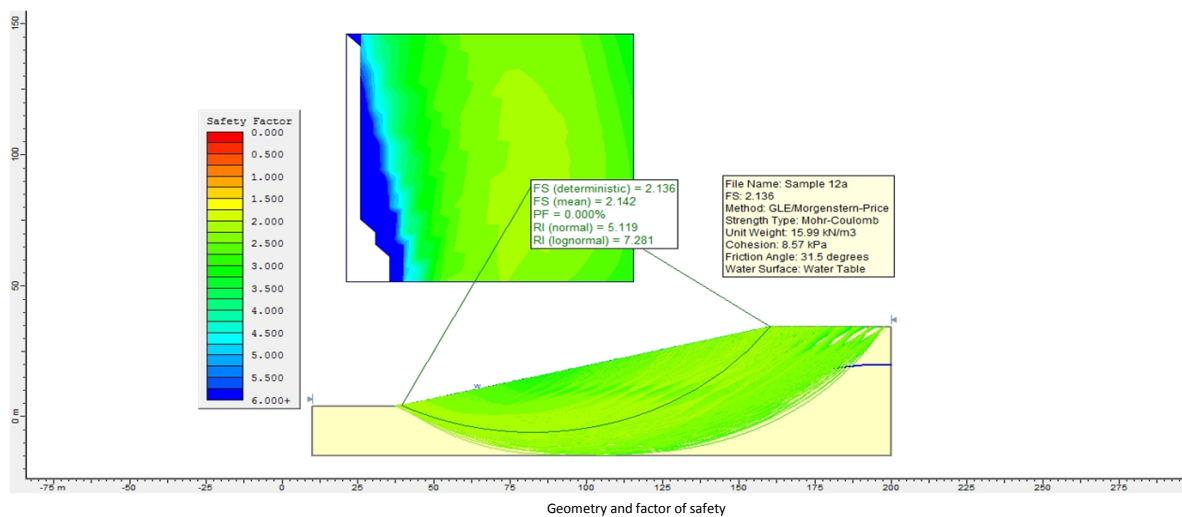
SAMPLE 11



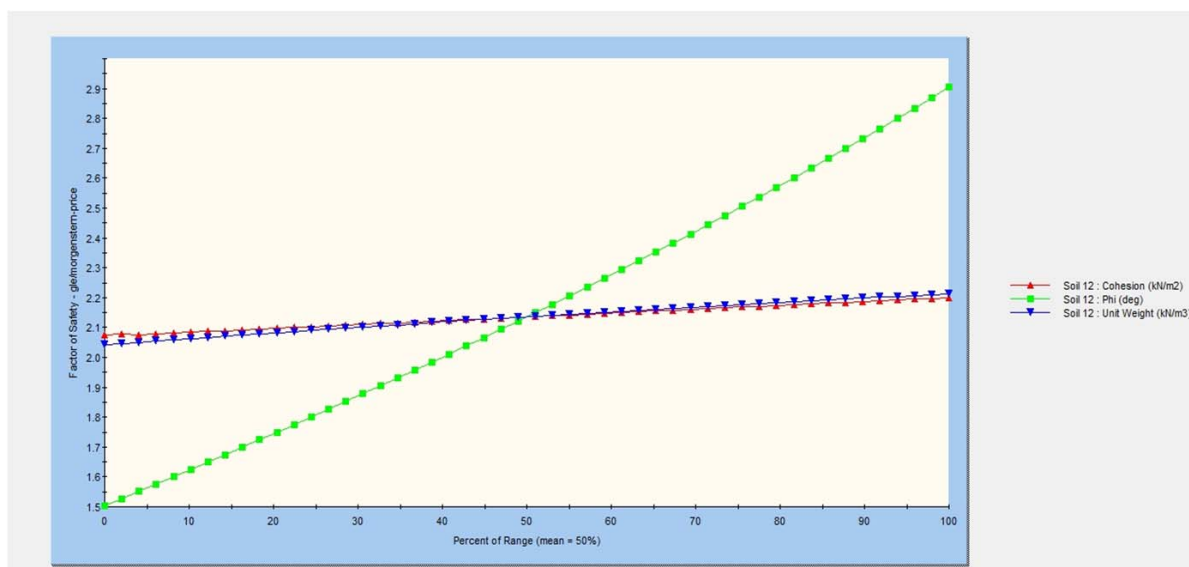
Probability of failure



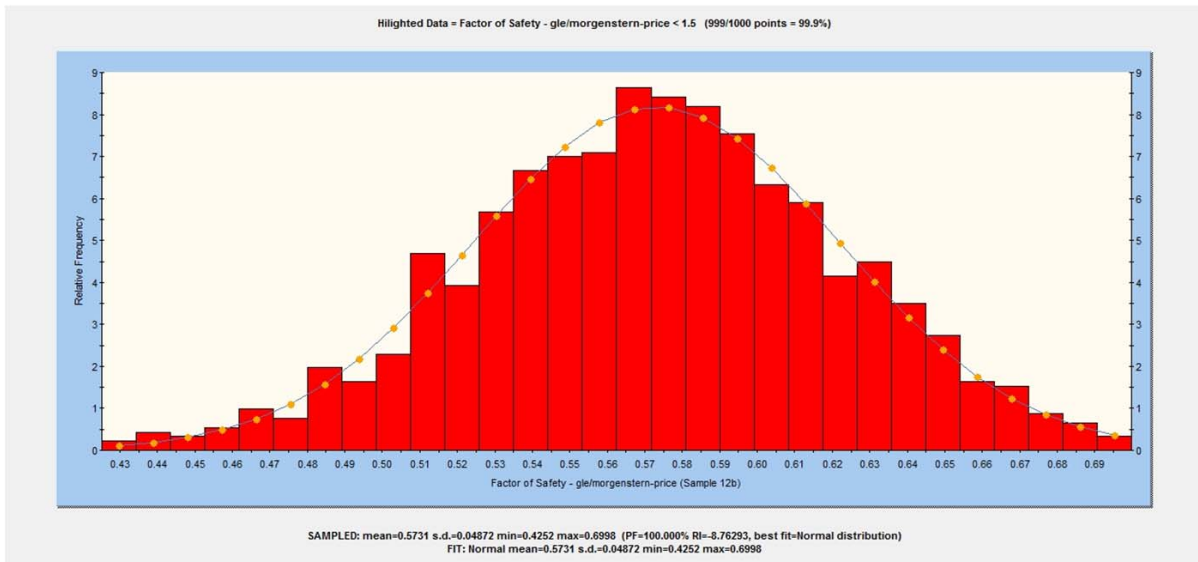
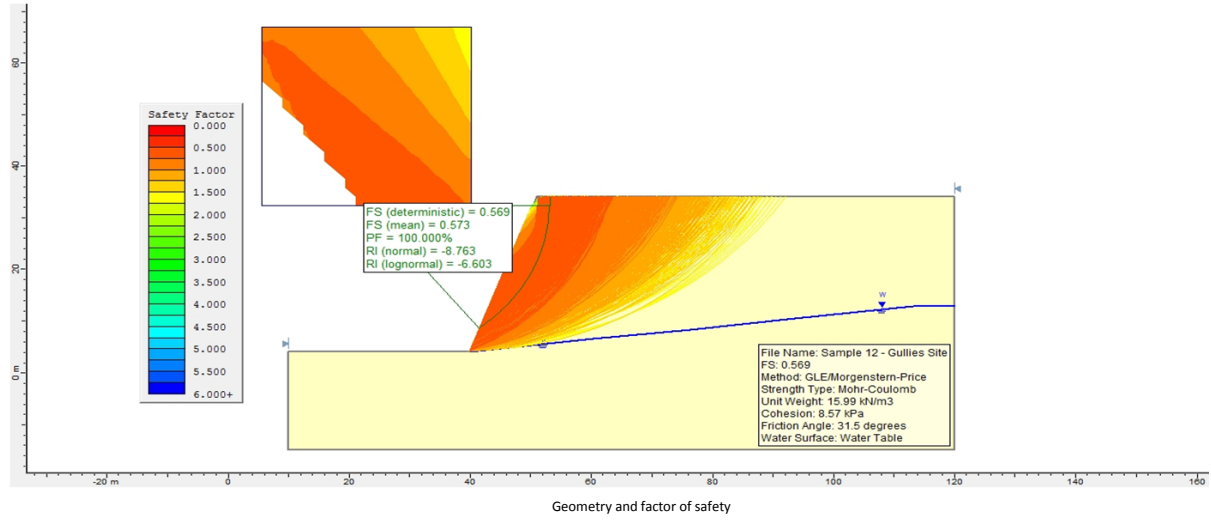
SAMPLE 12 a



Probability of failure



SAMPLE 12 b



Probability of failure

